Structural analysis of natural products focussing on the absolute configuration

Dissertation

zur

Erlangung des Doktorgrades

der Naturwissenschaften

(Dr. rer. nat.)

dem

Fachbereich Pharmazie der

Philipps-Universität Marburg

vorgelegt von

Frauke Reinscheid

aus **Siegen**

Göttingen **2016**

Erstgutachter: Prof. Dr. Michael Keusgen

Zweitgutachter: Prof. Dr. Martin Schlitzer

Eingereicht am 30.8.2016

Tag der mündlichen Prüfung am 13.10.2016

Hochschulkennziffer: 1180

1. Content

1.1 Abbreviations

AC	absolute configuration
aug	augmented
ax	axial
B3LYP	functional for DFT calculations
bzgl.	bezüglich
c	speed of light
calc.	calculated
cm	centimeter
CMAE	corrected mean absolute error
CS	chemical shift
DFT	density functional theory
deg	degrees
dm	decimeter
E	energy
ε	molar absorption coefficient
$\Delta\varepsilon$	difference between the molar absorption coeffients
ε_L	molar absorption coefficient of left circular polarized light
ε_R	molar absorption coefficient of right circular polarized light
E_{DFT}	energy calculated on the DFT level of theory
E_{Ne}	energy of the electron-nucleus interaction
E_{XC}	exchange-correlation energy
ECD	electronic circular dichroism
e.g.	exempli gratia
elec.	electric
eq	equatorial
ext.	external
exp.	experimental
ΔG	difference in free energies
g	*gauche*
g	gram
h	Planck`s constant
H	Hamilton operator
H_{CS}	operator of the chemical shift interaction
H_D	operator of the dipolar interaction
H_{ex}	operator of external interactions in NMR
H_{int}	operator of internal interactions in NMR
H_J	operator of the scalar coupling interaction
H_Q	operator of the quadrupolar interaction
HCl	hydrogen chloride
HF	Hartree-Fock
IEF-PCM	integral equation formalism-polarizable continuum model
int	internal
IR	infra-red
J	Joule
J-coupling	scalar coupling
K	Kelvin
K	equilibrium constant
λ_{max}	maximum wavelength of absorption
M	molar

$\hat{M}_{(elec.dipole)}$	electric dipole moment operator
$\hat{M}_{(mag.dipole)}$	magnetic dipole moment operator
mag.	magnetic
m_e	mass of an electron
mg	milligram
ml	milliliter
mpw1pw91	functional for DFT calculations
N_A	Avogadro number
nm	nanometer
NMR	nuclear magnetic resonance
NOE	Nuclear overhauser effect
N_{total}	total number of molecules
ORD	optical rotatory dispersion
Ψ	wavefunction
Ψ_e	excited state wavefunction
Ψ_g	ground state wavefunction
ρ_{non}	electron density of the non-interacting reference system
ρ_0	electron density of the interacting, real system
PCM	polarizable continuum model
ppm	parts per million
R	rectus
R	rotational strength
R	universal gas constant (8.31 Joule/mol^{-1} K^{-1})
rel	relative
ROA	Raman optical activity
s	second
S	sinister
t	*trans*
T	temperature
T_{non}	kinetic energy of the non-interacting reference system
TD-DFT	time-dependent-DFT
theo.	theoretical
UV/Vis	ultra-violet/visible
ν	wavenumber
ν_{xc}	exchange correlation potential
VCD	vibrational circular dichroism

1.2 Topic

The main topic of this thesis is the determination of the absolute configuration and the conformation of natural products in terms of an accurate and reliable stereochemical analysis. Experimental and calculated spectroscopic data by density functional theory (DFT) are used in an integrated approach to establish a structural model, which fulfills as much as possible the experimental restraints such as nuclear magnetic resonance (NMR) chemical shifts, J-couplings, optical rotatory dispersion (ORD), ultra-violet/visible (UV/Vis), electronic circular dichroism (ECD), infra-red (IR), and vibrational circular dichroism (VCD) data.

1.3 Motivation and Objectives

Despite the fact that a number of well-established methods for the structural analysis of dissolved compounds are available, misassignments and structure revisions are encountered in the literature. One reason is that faith is placed in only one structural analysis method. For example, even x-ray crystallography has led to an incorrect structure for the kinamycins (Omura et al., 1973; Gould et al., 1994; Mithani et al., 1994), and comparable misinterpretations occurred for the analysis of halipeptin A (Randazzo et al., 2001; Della Monico et al., 2002). A more recent example is that of the absolute configuration (AC) of *erythro*-mefloquine, which was incorrectly determined by asymmetric total synthesis, whereas the correct AC was assigned in a series of publications by spectroscopic and synthetic methods (Schmidt et al., 2012; Müller et al., 2013; Schützenmeister et al., 2013; Ding and Hall, 2013; Dassonville-Klimpt et al., 2013; Zhou et al., 2013).

Consequently, the main goal of the here presented work is the establishment of an integrated approach which combines a number of experimental and calculated spectroscopic data for structural analysis. This integrated approach should comprise of NMR chemical shifts and J-couplings, optical rotatory dispersion, ECD/UV-Vis, and VCD/IR data. The conformational analysis should give reliable information about the conformers and their populations in solution. A conformational analysis must be performed because different conformers might exhibit different spectroscopic values, and even the sign of chiroptical values can be inverted.

A guideline for the determination of the absolute configuration by the integrated approach should be established, and possibilities/limitations of this approach in the conformational and configurational analysis of natural products should be explored.

Most of the data should be easily available from literature data, in order that no extra measurements have to be conducted, and the integrated approach can be applied to already characterized compounds for which data are inconclusive and/or missing.

Natural products are the focus of this work since they (i) represent an important source of bio-active compounds for later pharmaceutical applications, (ii) display a large variety of chemical constitutions, a fact which allows conclusions to be drawn for a number of other compounds, and (iii) present the challenging situation that raw material for re-isolation may not be present and/or the isolated product readily decomposes so that only few spectroscopic data are available (e.g. specific optical rotation).

1.4 Outline

In order to reach the above mentioned goals, several steps have to be performed (Scheme 1). At first the structure of the molecule has to be constructed with a computational chemistry program (Gaussian^{TM}). Then a computational program searches for possible conformers of the molecule (Discovery Studio^{TM}, Gaussian^{TM}). The conformers lowest in energy are taken for a geometry optimization at a high level of theory. With these geometry optimized conformers a population analysis is performed. The calculations of the spectroscopic parameters can now be performed. The calculated NMR data, chemical shifts and J-couplings, are compared with experimental data to determine the conformations and their populations. The calculated chiroptical data are compared with experimental values to determine the absolute configuration.

Using a small, semi-rigid test molecule (limonene), a number of levels of theory are tested. Likewise, all experimental methods applied are evaluated. One level, with an appropriate cost-accuracy ratio, is evaluated for the structural analysis of a more complex compound (strychnine). Further structural aspects apart from conformational flexibility are investigated (e.g. protonation, solvent association). Lastly, a group of molecules (menthol/menthylamine and their isomers) are analysed to check the applicability of the proposed integrated approach.

Scheme 1: Overview of the integrated approach for the conformational and configurational analysis based on experimental and theoretical spectroscopic data

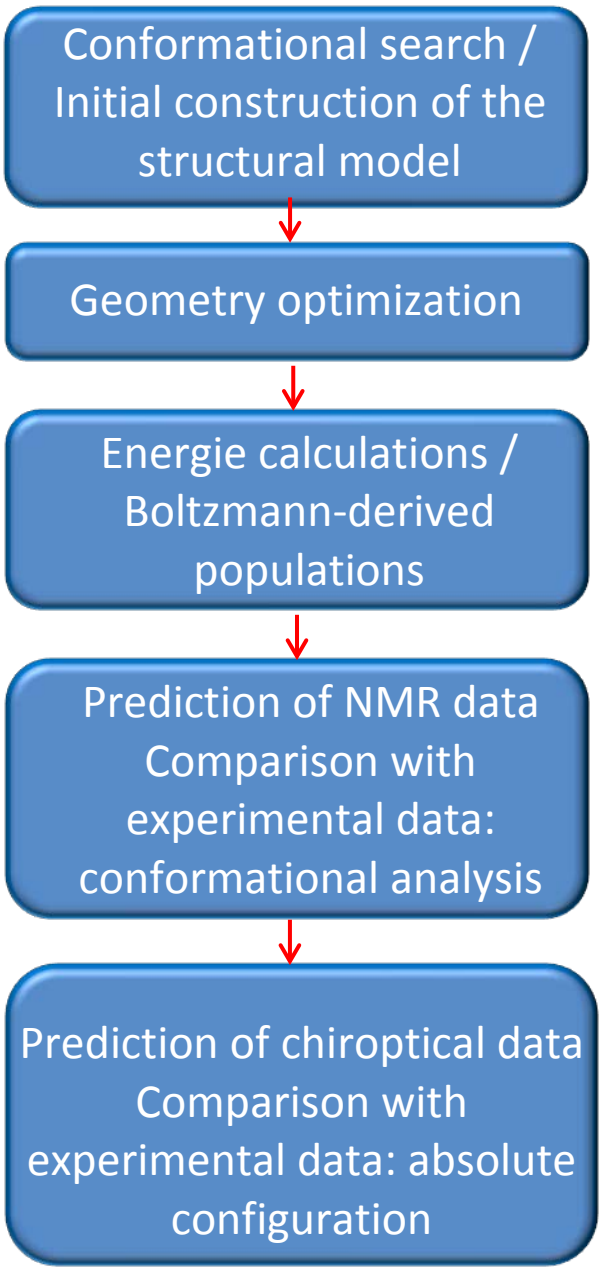

2. Historical overview

"Il y a trois périodes dans l`histoire de toute découverte.
Quand elle est annoncée pour la première fois, les gens pensent que ce n`est pas ***vrai****.*
Puis, un peu plus tard, quand son exactitude leur parait si flagrante qu`ils ne peuvent plus la nier, ils estiment que ce n`est pas ***important****.*
Après cela, si son importance devient assez manifeste, ils disent: en tout cas, ce n`est pas ***nouveau****."*

William James

According to the above mentioned citation taken from the Nobel Lecture of D. H. R. Barton in 1969, a typical evolution in the perception of new ideas or concepts in science follows three stages: it cannot be true; it seems to be unimportant; it is not new.

Structural analysis

If we adapt this classification to the field of structural analysis in chemistry comprising the constitutional, conformational and configurational determination of chemical structures, it can be stated that this research topic has reached the final stage: it is not new.

However, in the following it will become clear that recent delevopments allow a new approach to the structural analysis of molecules: The combination of calculated and experimental spectroscopic data allows the determination of the absolute configuration and conformation of compounds in solution.

The concept of conformation first appeared in the work of Sachse (1890, 1892) which did not get the deserved attention of the chemical community. It was re-discovered in 1918 and 1922 by Mohr, and confirmed by Hückel in 1925. The real breakthrough was the publication of Barton in 1950, in which he described conformational differences in terms of stability and reactivity.

In the view of Barton (1969), the research about conformation has already become a mature field in science, exemplified by the Nobel prize in 1969, and indicated by a review of Eliel about the conformational analysis of cyclohexanes more than 50 years ago (1965). However, the following decades have witnessed two methodological developments that clearly show that a research field can become new again due to new ideas/concepts and/or methods. On the experimental side, NMR spectroscopy has revolutionized structural analysis in solution and in the solid state, whereas on the theoretical side, molecular modelling has reached an unprecedented accuracy for medium sized molecules.

The concept of configuration can only be understood on the basis of the ideas of van't Hoff and Le Bel who introduced the concept of the tetravalent carbon atom independently in 1874 (see Meijer for a historical review, 2001). Many scientists remained sceptical, notably H.

Kolbe, who clearly classified this concept at that time to the first stage in the evolution of new ideas in science: it cannot be true. Interestingly, a later researcher of the van`t Hoff laboratories at Utrecht, Bijvoet, established in 1951 for the first time the absolute configuration of a compound using anomalous scattering of x-rays (Bijvoet et al., 1951). Up to this date, all configurational descriptions relied on the arbitrary assignment by Fischer (1896).

The review of Schlenk in 1965 already indicated, that configurational analysis will remain a vivid area of research, and in fact it has never reached the final stage of being “not new”.

The methods applied for determining configurations have been significantly expanded to include: (i) synthetic methods: total synthesis, degradation reactions, and conversion of the studied molecule into a compound with known configuration, (ii) anomalous X-ray diffraction (Bijvoet et al., 1951), (iii) chiroptical spectroscopy (Petrovic et al., 2010): optical rotatory dispersion, electronic circular dichroism, vibrational circular dichroism, and raman optical activity (ROA), (iv) empirical nuclear magnetic resonance based methods (Seco et al., 2004): e.g. Mosher ester analysis, (v) chromatographic methods, (vi) microwave spectroscopy (Shubert et al., 2014), (vii) Coulomb explosion imaging (Pitzer et al., 2013; Herwig et al., 2013). Each method has its own limitations, for example, monocrystals of good quality with at least an oxygen atom inside the molecules are required for anomalous X-ray crystallography, and Mosher ester analysis is only possible for molecules that have a functional group that can be derivatized (alcohols, amines, etc.).

Chiroptical methods

After the discovery of M. Arago of optical activity in 1811 (rotation of polarized light) and the early work of Biot, who studied the optical activity of organic compounds in 1815, W. Haidinger observed the phenomenon of electronic circular dichroism in the middle of the 19th century (for review: Laur, 2012). Cotton published two articles which described both effects showing their relationships (Cotton, 1895a (ORD), 1895b (ECD)).

From an experimental point of view, the electronic circular dichroism and optical rotatory dispersion measurements were in a mature state in the 1960’s of the last century, exemplified by a review of Snatzke in 1968. However, it was only empirically possible to assign the absolute configuration to measured ORD or ECD data. With some success, the octant rule could be applied for saturated cyclohexanones. However concerning limonene, in the course of the study presented here, it is shown by careful inspection of the literature, that this compound displays an anti-octant-rule behaviour, demonstrating the importance to use DFT calculation instead of empirical rules.

The quantum mechanical foundations of optical rotation were first laid down more than 80 years ago by Rosenfeld (1928). Since the Rosenfeld expression involves summation over all excited states, most quantum chemical calculations of the optical rotation avoid this approach in practice. Instead a linear response formalism (Jørgensen and Simons, 1981) is used, in which the perturbation of the ground-state wave function by the external electric and magnetic fields is the central quantity (see DFT chapter for further information).

To date, three main chiroptical methods are available: ORD, ECD, and VCD, the latter since the last 20 years. Only few applications exist for Raman optical activity, thus this method is not further discussed. The first complete theoretical description of ROA was given in 1971 by Barron and Buckingham.

3. Introduction

In the following chapters, the relevant concepts and methods are introduced.

3.1 Natural products

Chemical compounds produced by living organisms (e.g. by plants, fungi or bacteria) are called natural products (e.g. limonene and menthol by plants or penicillin by the fungi *Penicillium chrysogenum*). Rich sources of pharmacologically active natural products are terrestrial plants (e.g. the genus *Allium*; Kusterer et al., 2011; Martins et al., 2016) and marine organisms (Donia and Hamann, 2003; Molinski et al., 2009). Consequently, since decades natural products remain important targets of synthetic chemistry such as the alkaloid strychnine produced by the plant *Strychnos nux vomica*.

Quite often, biological activities render these compounds as interesting starting materials for medicinal drug development (Hanson, 2003). Based on their structural diversity, new pathways of drug actions have been discovered such as in the area of antibiotics. Almost 50% of the new drug molecules which were introduced from 1981 to 2006 originate from a natural product (Newman and Cragg, 2007).

3.2 Chirality

Chirality is a property of objects that are not identical to their mirror images, i.e. image and mirror image are non-superimposable. The term was first used by Lord Kelvin (1904), but was introduced into the chemical community, at a much later date in the 1960's according to Dunitz (2001). Numerous examples can be found as macroscopic objects in nature such as

Calystegia sepium (hedge bindweed, Convolvulaceae) (Figure 1). If an object can be distinguished from its mirror image it is called chiral. As a consequence, the two objects are not superimposable. When dealing with molecules, the chiral object and its mirror image are called enantiomers.

Figure 1: *Calystegia sepium* performing a helical growth (Bednarik, 2016)

The human hands can be regarded as classic example of chirality (Figure 2). In this figure, an enantiomeric pair of chiral α-amino acids is shown.

Figure 2: right and left hands as chiral objects; chiral α-amino acids (R≠ H, COOH, NH_2) (Wikipedia, chiral objects, 2016)

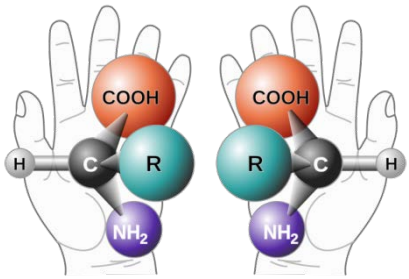

In the field of chemistry, chiral molecules belong to the group of stereoisomers (chiral amino acids: Figure 2; Scheme 2). Stereoisomers which do not form an enantiomeric pair are called diastereomers (Scheme 2). They have different physical and chemical properties and are often given different names, e.g. menthol and isomenthol. For the analysis of the relative configuration of organic molecules, the most frequently applied technique is that of NMR

spectroscopy. In contrast, stereoisomers forming a pair of enantiomers differ structurally only in their absolute configuration. Enantiomers are characterized by a unique three-dimensional handedness, and the individual enantiomer often exhibits distinct chemical activities when interacting with a chiral environment. There are a number of examples of chiral compounds whose enantiomers produce different odors, such as the naturally occurring limonene: while one enantiomer smells like oranges, the odor of the other resembles turpentine.

Scheme 2: Classification of isomers in chemistry

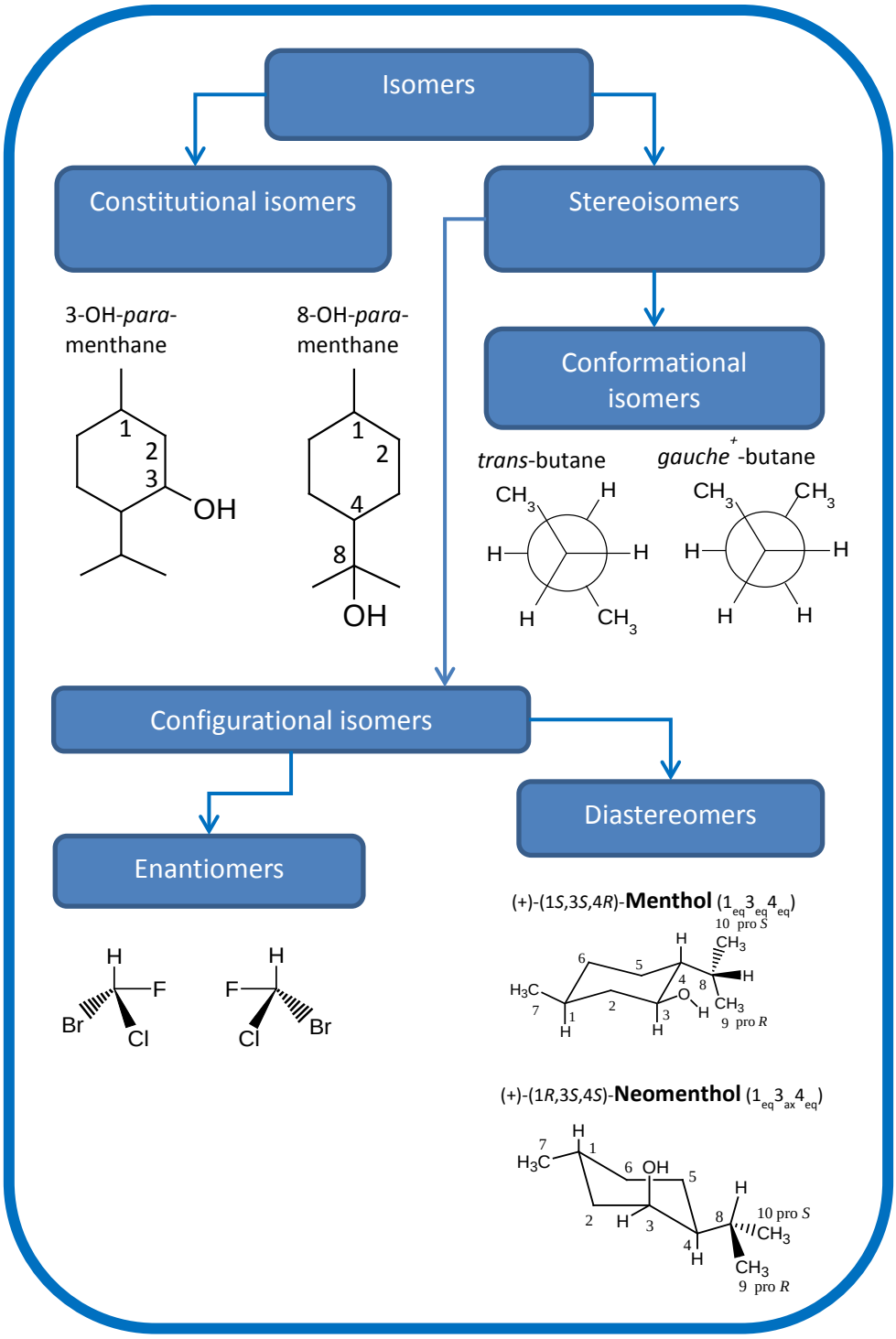

3.3 Configurational isomers

The configuration of a molecule results from the 3-dimensional positioning of its bonds/substituents (e.g. bromo-chloro-fluoro-methane, Figure 3). Configurational differences are based on differences in bond angles, in contrast to conformational differences which involve differences in torsional angles (Scheme 2) (Eliel, 2001).

Figure 3: Configurational isomers (enantiomers): Bromo-chloro-fluoro-methane

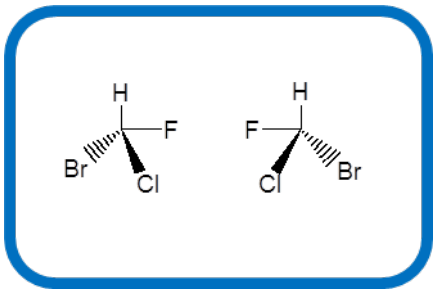

The absolute configuration refers to the 3-dimensional arrangement of the atoms of a chiral molecule itself, or to parts of it. As most important stereogenic element, the stereocenter is described by *R* or *S*, referring to rectus or sinister, respectively (Cahn–Ingold–Prelog priority rules) (Eliel, 2001).

3.4 Conformational isomers

The conformation of a molecule is defined by its torsional angles (Eliel, 2001). Conformational isomerism is a subgroup of stereoisomerism and occurs by rotation around single bonds. The isomers are generally referred to as conformational isomers or conformers (e.g. butane, Figure 4).

Figure 4: Conformational isomers

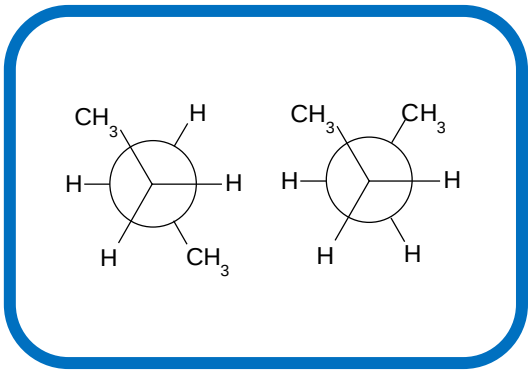

Conformational isomers occur if an almost free rotation about a single bond is possible. While configurational isomers can only interconvert by the breaking and reformation of chemical bonds, conformational isomers interconvert by rotations about single bonds.

Since the interconversion between conformers is often very fast, the separation of conformational isomers is in many cases impossible (Eliel, 2001).

Even with the help of computational chemistry programs, the search for conformers can be difficult since for a very fluxional molecule (very low barrier of interconversion between multiple conformers) a local minimum might not be found. On the other hand, a successful search can be hindered by the rigidity of a molecule, with strychnine as prominent example. For this molecule, standard molecular modelling programs do not find a second conformer which could be observed by low temperature NMR (Schmidt et al., 2014).

The relative free energy difference (ΔG) determines the population of each conformer in case of an equilibrium between two conformers (equation 1), whereas the energy barrier of single bond rotations determines the rate of interconversion (Eliel, 2001).

$$K = e^{-\Delta G / RT}$$ equation 1

(K as equilibrium constant, ΔG as difference in free energy between the two conformers in J/mol, R as universal gas constant (8.31 Joule/mol^{-1} K^{-1}), and T as the temperature in Kelvin)

As an example, the free energy difference of the two butane conformers (*gauche* and *trans*) in the gas phase is −0.9 kcal/mol, favoring the *trans* conformer (Scheme 2) (Eliel, 2001).

In case of multiple conformers, the Boltzmann distribution in equation 2 describes the fractional population of each conformer.

$$\frac{N_i}{N_{total}} = \frac{e^{-E_{rel} / RT}}{\sum_{k=1}^{N_{total}} e^{-E_k / RT}}$$ equation 2

(with N_i as number of molecules of the i-th conformer; N_{total} as total number of molecules; E_{rel} equals to the relative energy of the i-th conformer compared to the minimum energy conformer; E_k is the relative energy of the k-th conformer compared to the minimum energy conformer; R as universal gas constant (8.31 J/(mol·K)); T as the temperature in Kelvin).

Since the seminal work on cyclohexanes by Eliel (1965), six-membered rings remained the standard compounds for conformational analysis. Consequently, in this thesis, the well known cylcohexane derivative menthol together with some derivatives and isomers were taken for a detailed conformational and subsequent configurational analysis.

3.5 DFT calculations

The basic idea of DFT (density functional theory) is to substitute the complex N-electron Schrödinger equation by an equation that only contains electron density as parameter.
Hohenberg und Kohn showed in 1964, that the ground state electron density exactly determines the corresponding Hamilton operator, and thereby all other observables of the system. With the definition of a functional (the function of a function, in squared brackets [ ]), the ground state energy becomes a functional of the electron density, which explains the term „density functional theory", DFT. A subsequent publication introduced the orbital concept and allowed a successful implementation in quantum mechanical programs (Kohn, 1965). In short, the following procedure delivers the Kohn-Sham orbitals, the electron density, and subsequently the energy of the system:

1. A non-interacting reference system of N particles is defined with a density ρ_{non} that is by construction the same as for the real, interacting system, ρ_0.

2. The orbitals from the reference system allow the calculation of the non-interacting kinetic energy, T_{non}.

3. The energy of the interacting system is further partitioned into the kinetic energy (T_{non}) of the non-interacting system, the energy of the electron-nucleus interaction (E_{Ne}), the classical electrostatic electron-electron repulsion energy (J), and all other contributions as so-called exchange-correlation energy (E_{XC}). The latter contains contributions from the exchange energy, correlation energy and also kinetic energy, since there is a difference in kinetic energy between the non-interacting and interacting systems. This is the reason why the definition of correlation energy is different between the Hartree-Fock (HF) and DFT calculations.

4. The orbital coefficients for the energy expression are varied to obtain the lowest energy, and finally the sum of the squared orbitals gives the electron density.

One major obstacle is the unknown exchange-correlation energy functional (E_{XC}), or with respect to the electron density, its derivative the exchange-correlation potential (ν_{xc})(Lee et al., 1988). In effect, all the unknown exchange and correlation energies plus the difference of kinetic energy between the non-interacting system and the real, interacting system, are consequently included in the unknown energy functional (E_{XC}). The term is therefore

misleading. The exact energy (E_{DFT}) can be calculated by an apparently simple equation shown below (equation 3). However, due to the occurrence of the unknown energy functional E_{XC}, an exact solution can not be obtained.

$$E_{DFT} = T_{non} + E_{Ne} + J + E_{XC} \qquad \text{equation 3}$$

Although this procedure seems only to shift the problems instead of solving them, the successful applications in reproducing experimental data have proven the opposite. Consequently, Hartree-Fock methods which do not include electron correlation effects, were superseded in accuracy by modern DFT implementations. However, a drawback of DFT for the calculation of chiroptical properties is their dependence on exchange-correlation functionals that were not designed for such calculations. For example, the parameters of the popular “B3” exchange functional of Becke were obtained by a least-squares fit to the experimental data, excluding chiroptical values (atomization energies, ionization potentials, proton affinities, and atomic energies) for the G2 test set of molecules (Becke, 1993). Therefore, functionals such as B3LYP (Becke, 1993; Lee et al., 1988) often deliver accurate thermochemical predictions, but there is no fundamental physical reason why they should perform equally well for properties such as optical rotation. Furthermore, fundamental deficiencies in functionals still exist, such as self-interaction errors, lack of dispersion effects, and qualitatively incorrect descriptions of diffuse electronic states, and there is no systematic way to improve current DFT methods. In contrast, wave-function-based methods such as coupled cluster theory can be termed as “convergent” models since it is possible to systematically approach the exact (Born–Oppenheimer) solution. Unfortunately, the scaling with basis sets of such methods usually precludes their routine application to molecules containing more than 10 non-hydrogen atoms.

In this thesis a variety of E_{XC} functionals has been used, with the mpw1pw91 functional as the workhorse. In the case of basis sets, after evaluations with limonene as test compound, the Dunning’s series (Dunning, 1989) was preferred.

In the following, a description is given of how the experimentally observable properties are calculated with Gaussian09^{TM}. Since programming was not part of the thesis, a purely user based perspective was chosen. The actual code of the program is not part of the description.

Properties can be calculated by a derivative technique which is also conceptually the easiest to understand. The idea is to expand the energy in a Taylor series with a decreasing

perturbation strength λ. Then the corresponding terms of zeroth, first, second and higher order, with respect to the perturbation, are identified as observable properties.

In this way, the IR vibrational frequency within the harmonic approximation can be identified as second derivative of the energy with respect to the normal mode displacements. The IR intensity is proportional to a mixed derivative of the energy with respect to the normal mode displacement and the electric field.

The NMR shielding is proportional to the mixed derivative of the energy with respect to the external magnetic field and a nuclear magnetic field (the last originating from the nuclear spin), whereas the J-coupling is proportional to the derivative of the energy with respect to the two nuclear magnetic fields of the two coupled nuclei. The VCD intensities are proportional to the rotatory strength, which is defined as the scalar product of the electric and magnetic dipole transition moments. In a derivative formulation these transition moments can be derived from the second derivative of the electric dipole moment with respect to the normal mode displacement (electric transition moment), and from a scalar product between the derivative of the electric dipole moment with respect to the normal mode displacement, and from the derivative of the magnetic dipole moment with respect to the normal mode momentum.

This derivative approach is not suitable for time-dependent properties such as the UV/Vis absorption and interaction of light with matter resulting in ECD and ORD spectra. In this case, to the time-independent Hamiltonian, a time-dependent potential is added for simulating the perturbations due to oscillating electric and magnetic fields. This calculation follows a propagator approach as a variant of the response theory, which is also termed time-dependent-DFT (TD-DFT). In this formulation, poles of the mathematical expression corresponds to excitation energies, and the numerators at the poles deliver the transition moments between the ground and excited states, thereby allowing to calculate the intensity at the corresponding frequency.

Using Gaussian bandshapes with empirically adjusted widths at half height, the UV/Vis and ECD spectra can be simulated. Since the Kramers-Kronig transform relates the ECD curve to the ORD curve, the ORD can be calculated by the calculated ECD excitation frequencies and intensities described above (Polavarapu, 2005).

A major advantage of the TD-DFT methods is their relative simplicity and computational efficiency. They are easily applied to molecules containing >30 non-hydrogen atoms. However, they are incapable of describing charge-transfer states without inclusion of exact Hartree-Fock exchange (Tozer et al., 1999, Dreuw et al., 2003), and they can dramatically

underestimate excitation energies of diffuse Rydberg states due to self-interaction errors (Tozer and Handy, 2000).

3.6 NMR spectroscopy

Nuclear magnetic resonance spectroscopy is the most versatile and powerful technique for structural analysis in chemistry. NMR spectroscopy exploits the magnetic properties of atomic nuclei with a nuclear magnetic moment ≠ 0. It provides information about the structure and dynamics of molecules at an atomic level. Since the resonance condition is influenced by the interplay of electrons and nuclear magnetic moments, NMR spectroscopy gives also information about the electronic structure of a molecule (Günther, 2013).

In the presence of an external magnetic field, radiofrequency waves are able to interact with the nuclear magnetic moments. This interaction was discovered first in 1946 by the group of Bloch (Bloch et al., 1946) at Stanford University. It is the only method to get structural information with atomic resolution, if crystals cannot be obtained. In solution, the constitution and conformation is typically determined by NMR measurements. In favourable cases, the relative configuration can also be established by conventional NMR parameters such as J-coupling and NOE (nuclear overhauser effect; a relaxation-based parameter) contacts. However, the absolute configuration can only be determined by NMR after the formation of diastereomers (the traditional Mosher-method) (Hoye et al., 2007). This is clearly a drawback since it introduces a synthetic step with maybe undesired side products. The first examples of this empirical approach were given by Dale and Mosher in 1973 using a phenylacetic acid derivative as reagent.

Chemical shift

The chemical shift describes the resonance frequency of a nucleus relative to a standard in a magnetic field. NMR accessible atomic nuclei possess a magnetic moment (nuclear spin) ≠ 0, which leads to different energy levels and resonance frequencies in a magnetic field. The total magnetic field experienced by a nucleus is composed of the external magnetic field and local magnetic fields induced by currents of electrons. The electron distribution of the same type of nucleus varies according to its local surrounding (e.g. substiuents, bond types). This influences the energy levels, and hence the resonance frequencies. The chemical shift is measured with respect to a reference frequency or reference sample.

J-coupling

Scalar or J-couplings originate from an indirect interaction between two nuclei transferred by the electrons of the bonds between the two nuclei. It provides local information about dihedral angles along covalent bonds (Karplus, 1963), and in favourable cases hydrogen bonds (Kawahara et al., 2003).

In this thesis, only chemical shifts and J-couplings from NMR spectra have been used. The motivation for this was given above: for some natural products, only literature values are available which typically contain chemical shifts and J-couplings of the compound. Using these resources, the conformational and configurational analysis have been be performed by comparing the experimental values to calculated ones.

Calculation of NMR parameters by DFT

For the calculation of NMR parameters, the non-relativistic, time-independent Schrödinger equation can be applied, with a phenomenologically derived Hamilton operator describing the nuclear spin behaviour (equation 4).

$$H\Psi = E\Psi \qquad \text{equation 4}$$

In NMR spectroscopy, there are two components of the spin Hamiltonian that need to be considered (Benesi, 2015): one is based on the interaction between the spins and the external magnetic fields (H_{ex}), and the other is based on the internal interaction among the spins (H_{int}) (equation 5).

$$H = H_{ex} + H_{int} \qquad \text{equation 5}$$

The external Hamiltonian consists of H_{Zeeman}, which describes the interaction between the spins and the static magnetic field $B_{0,}$ that is essential for observations of NMR signals, and H_{RF} which is present when an oscillating radio frequency field is switched on.

The internal interactions of spins comprise the chemical shielding (H_{CS}), the J-coupling (H_J), the dipolar coupling (H_D), and the quadrupolar coupling (H_Q) (equation 6):

$$H_{int} = H_{CS} + H_J + H_D + H_Q \qquad \text{equation 6}$$

The chemical shift is the most important parameter in NMR spectroscopy for characterizing atoms in a molecule (Günther, 2013). The chemical shift difference of individual atoms with different electronic environments stems from the modification of the Zeeman interactions by the chemical shielding, and thus slightly changes the resonance frequency.

The shielding constants are calculated and can be referenced to calculated shieldings of reference molecules of which the experimental chemical shift is known, so that the calculated shieldings can be transformed into chemical shifts.

3.7 Chiroptical methods

ECD

Electronic circular dichroism spectra are derived from the different absorption of left- and right-circularly polarized light by a chiral sample. The theory of electronic circular dichroism spectra is closely related to that of optical rotation (Autschbach, 2006; Vaccaro, 2012).

Figure 5: Linearly (blue) and circularly (red) polarized electromagnetic radiation: electric field (E; red and blue) and magnetic field (B; green) vectors (Wikipedia, polarized light, 2016)

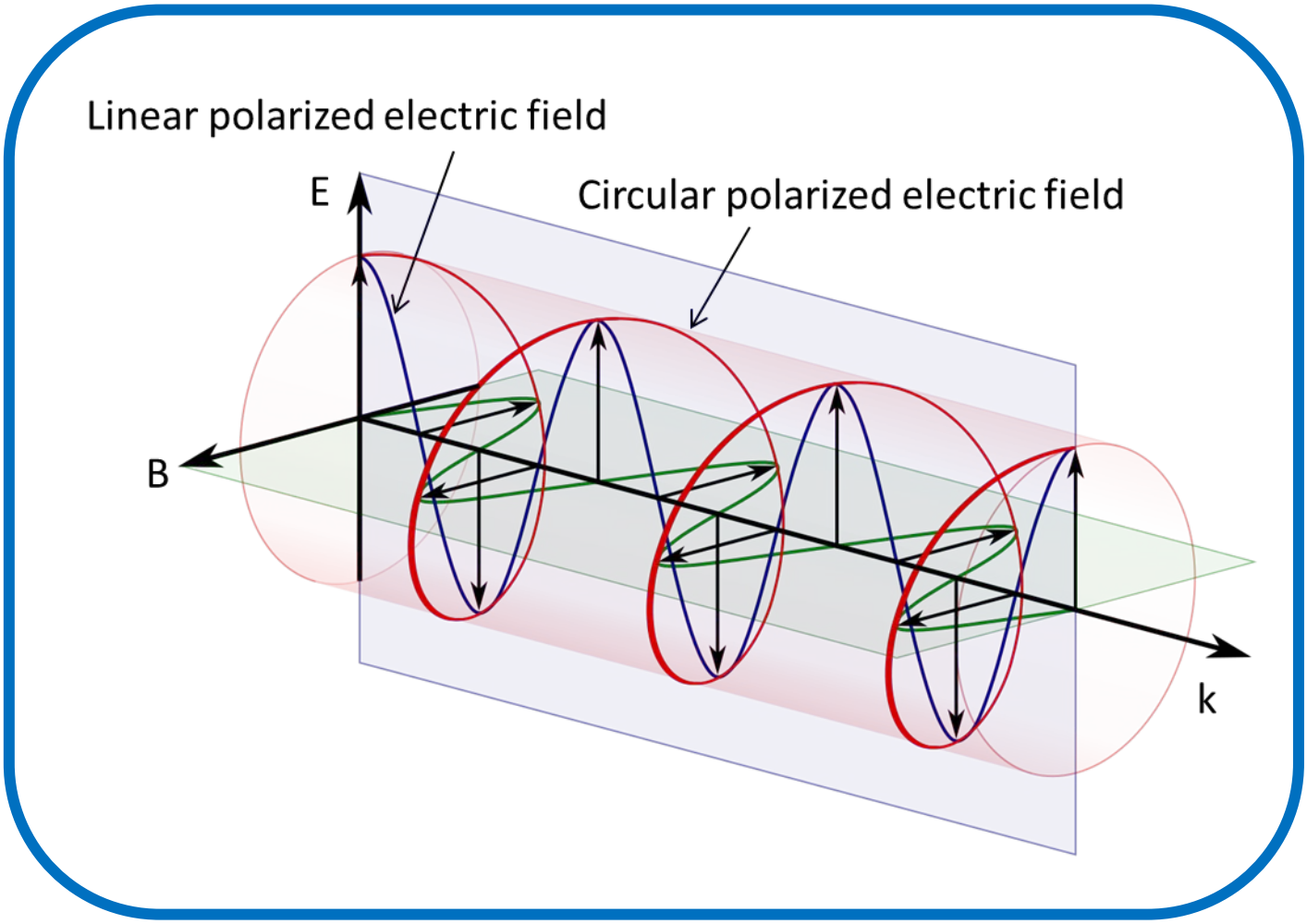

Light as electromagnetic radiation can be described as a transverse wave consisting of an electric (E; blue) and magnetic (B; green) field which oscillate perpendicular to one another, and to the propagating direction k (Figure 5). In linearly polarized light (blue line vertical in Figure 5), the electric field vector oscillates only in one plane. In circularly polarized light (red line in Figure 5), the direction of the electric field vector rotates about its propagation direction, but the magnitude of vector remains constant (Autschbach, 2006).

If the absorption coefficients for the right and left circularly polarized radiation differ ($\varepsilon_L \neq \varepsilon_R$), this phenomen is termed electronic circular dichroism, which is measured as the difference between the absorption coefficients: $\Delta\varepsilon \equiv \varepsilon_L - \varepsilon_R \neq 0$. As the differences in ε are a function of wavelength, the wavelength must be specified (Berova et al., 2000).

The interaction between light and an optically active molecule may be described schematically as follows: On a molecular level, the interaction between the electric field of the radiation and the electric dipole of the molecule, leads to a linear displacement of charge. The corresponding interaction between the magnetic field and the magnetic dipole of the molecule leads to a circulation of charge. The combined effect at the two motions leads to an excitation of an electron in a helical motion, quantified by its rotational strength (R_{exp}). Experimentally, the relationship between the rotational strength of a sample and the $\Delta\varepsilon$ is given by (Autschbach, 2006):

$$R_{\exp} = \frac{3hc10^3 \ln(10)}{32\pi^3 N_A} \int \frac{\Delta\varepsilon}{\upsilon} d\upsilon \qquad \text{equation 7}$$

With h as Planck`s constant, c as speed of light, N_A as Avogadro number, and ν as wavenumber. Theoretically, the rotational strength has also been described (Autschbach, 2006) as:

$$R_{theo} = \frac{1}{2m_e c} \mathrm{Im} \int \Psi_g \hat{M}_{(elec.dipole)} \Psi_e d\tau \bullet \int \Psi_g \hat{M}_{(mag.dipole)} \Psi_e d\tau \qquad \text{equation 8}$$

With m_e as mass of an electron, c as speed of light, Im indicating that the imaginary part of the dot product between the matrix elements should be taken, Ψ_g as ground state wavefunction, Ψ_e as exicited state wavefunction, $\hat{M}_{(elec.dipole)}$ as electric dipole moment operator, and $\hat{M}_{(mag.dipole)}$ as magnetic dipole moment operator.

ECD bands provide information about individual absorbing chromophores in the molecule. In contrast, the measured optical rotation principally relies on the interaction of all chromophores of the molecule with the polarized light. Therefore ECD bands are, in some cases, a better probe for the determination of the absolute configuration than the ORD values. However, many chiral molecules, such as the menthol series, do not allow an ECD analysis in solution because they lack experimentally accessible chromophores (in solution: absorption wavelength of solute > cut-off wavelength of the solvent). In addition, measurements of ECD spectra are not routinely performed, primarily because the experimental apparatus for optical rotation measurements is much simpler to use and costs nearly an order of magnitude less compared to an ECD spectrometer. In effect, literature concerning natural products contains many more ORD based studies than ECD based studies.

ORD

Optical rotatory dispersion refers to the wavelength dependent rotation of the plane of linearly polarized light as it passes through an enantiomerically enriched sample of a chiral species. The magnitude of this rotation is characteristic of the detailed molecular structure of the compound and varies with the wavelength of the incident light, the concentration of the compound, and the temperature (Snatzke, 1968).

It is also possible to derive conformational information from chiroptical data. This topic has been put forward in a review by Sandström in 1995. However, the information content relevant for conformational aspects is quite low, and NMR spectroscopy generally delivers better data in a shorter time. In two seminal publications, the calculation of ORD values based on DFT were investigated (Cheeseman et al., 2000; Stephens et al., 2001).

VCD

Like its ECD counterpart, vibrational circular dichroism refers to the different absorption of left and right-circularly polarized light by chiral molecules, but in this case, dependent on a vibrational transition. VCD provides even more information than either optical rotation or ECD, regarding the relationship between molecular structure and optical activity, owing to the fact that VCD rotational strengths may be measured even for molecules lacking a long-wavelength chromophore. However, experimental measurements of such spectra are carried out less often than their ORD and ECD counterparts due to the cost of the VCD apparatus and the high level of expertise required for its use. The current implementation of DFT calculations of

VCD spectra was reported by Cheeseman et al. in 1996. Apart from the need to consider higher levels of electron correlation in the electronic structure model, most of the remaining discrepancies between theory and experiment can likely be attributed to anharmonicity (especially in higher-frequency C−H stretching regions) (Bak et al., 1995) and solvent effects. Cappelli et al. (2002) have highlighted the latter working on PCM-based VCD simulations of 3-butyn-2-ol. In addition, two publications by He et al. (2004a, 2004) have indicated the need for improved quantitative accuracy in VCD calculations of the rotational strengths for the determination of conformer populations.

4. Thesis publications

1. F Reinscheid, UM Reinscheid, Stereochemical analysis of (+)-limonene using theoretical and experimental NMR and chiroptical data (2016a) J. Mol. Struct., 1106, 141-153

2. F Reinscheid, M Schmidt, H Abromeit, S Liening, GKE Scriba, UM Reinscheid, Structural and chiroptical analysis of naturally occurring (−)-strychnine (2016), J. Mol. Struct., 1106, 200-209

3. F Reinscheid, UM Reinscheid, Stereochemical analysis of menthol and menthylamine isomers using calculated and experimental optical rotation data (2016b) J. Mol. Struct., 1103, 166-176

5. Results

5.1 Limonene

The chiral monoterpene limonene is an important starting material in chemical synthesis (Mehta and Karra, 1991; Hansson and Wickberg, 1992; Pitsinos et al., 2012). Moreover, it is used in the fragrance and food industry, and is an important synthetic material (Thomas and Bessière, 1989). Limonene is biotransformed by a variety of organisms such as bacteria, fungi, and plants (Duetz et al., 2003). In this way, using the appropriate species, a number of synthetically important metabolites can be produced.

In this thesis, an integrated approach for the conformational and configurational analysis of limonene was established, together with an appropriate level of theory. The formula of (+)-*R*-limonene is shown (figure 6, left panel) alongside a schematic view of its application as test molecule for the calculation of spectroscopic parameters (NMR, ORD, ECD, VCD (figure 6, right panel).

Figure 6: Left panel: Formula of (+)-*R*-limonene; right panel: schematic overview of the spectroscopic data used for the conformational and configurational analysis

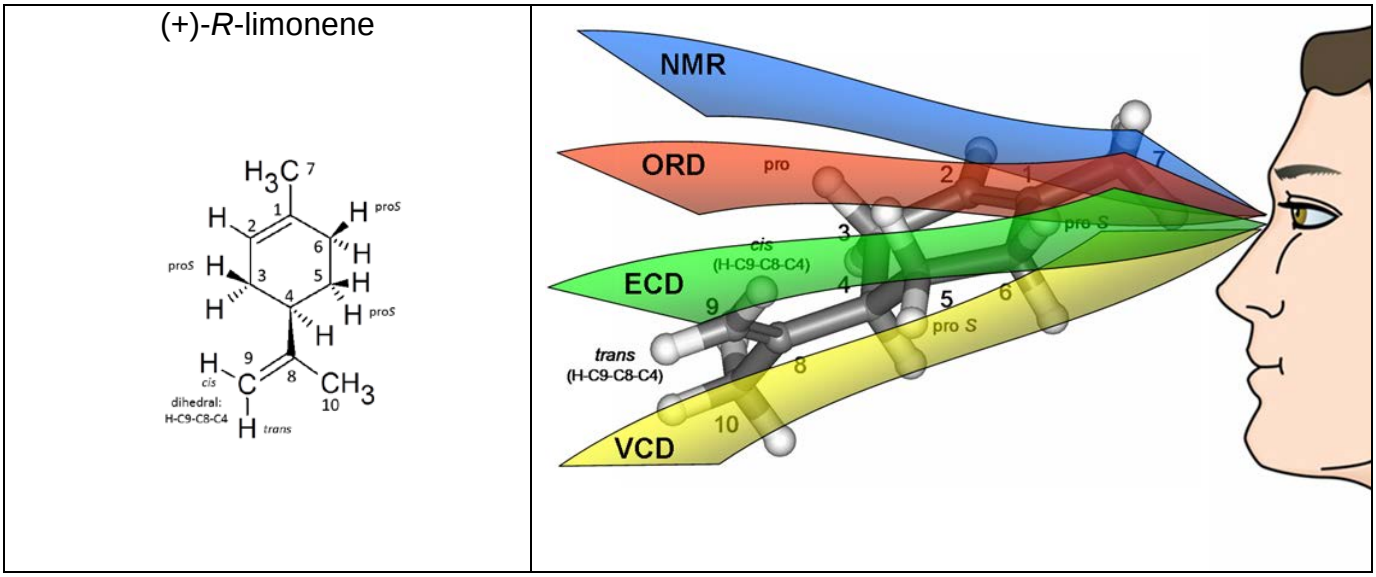

A conformational search and geometry optimization led to three conformers differing in the isopropenyl dihedral around the C4-C8 bond (Figures 7A-C). Two approaches to determine the conformer populations were taken: a pure computational, and the combination of experimental and calculated NMR chemical shifts. It turned out that the computational

approach results are heavily dependent on the level of theory used, and differ if enthalpies or free energies are used (Table 1). The second combinatorial approach resulted in a better match to experiment (Figure 8).

Figures 7A-C: Geometry-optimized conformational isomers of (+)-*R*-limonene with differing dihedral around C4-C8

A B C

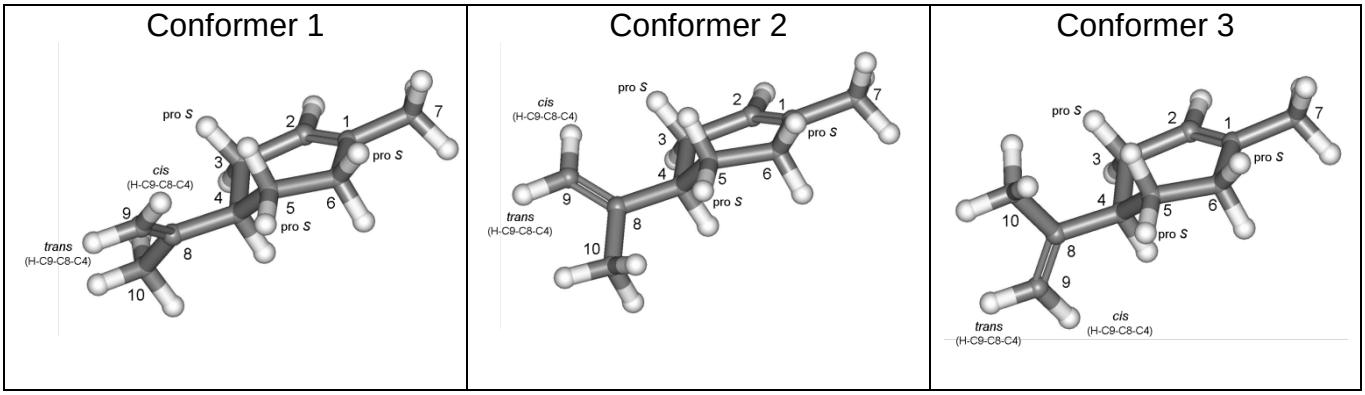

Table 1: Populations (in %) based on the Boltzmann equation using free energy differences, in brackets: enthalpy differences (integral equation formalism – polarizable continuum model (IEF-PCM) for solvent modelling)

theory level	**solvent**	**conformer 1**	**conformer 2**	**conformer 3**
mpw1pw91/cc-pvdz	$CHCl_3$	32 (34)	31 (23)	37 (43)
mpw1pw91/aug-cc-pvdz	$CHCl_3$	26 (34)	39 (23)	35 (43)
mpw1pw91/aug-cc-pvtz	$CHCl_3$	26 (34)	41 (23)	33 (43)
mpw1pw91/cc-pvdz	ethanol	31 (35)	32 (22)	37 (43)
mpw1pw91/aug-cc-pvdz	ethanol	25 (34)	44 (22)	31 (44)
mpw1pw91/aug-cc-pvtz	ethanol	25 (34)	43 (22)	32 (44)

Using the second combinatorial approach the best fit with experimental values was obtained with the following population mix: conformer 1, 2, and 3: 39 %, 31 %, and 30 %. The populations of the experimental based approach were within ±10 % of the populations derived from the pure computational approach. In the first approach, it is a must to use several levels of theory, and in our experience, this leads to populations differing up to ±10 %. The corrected mean absolute error (CMAE) which is the sum of the absolute differences between calculated (using the linear regression) and experimental values, divided by the number of data pairs, was lowest using the second approach: 0.47 ppm. With the calculated populations based on the first approach (free energies (28:38:34), enthalpies (34:23:43) and the arithmetic means of the data from Table 1) the CMAE increased to 0.52 ppm and 0.61ppm, respectively.

At the lowest level of theory (mpw1pw91/cc-pvdz, IEFPCM for solvent modelling) the experimental ORD values (in red) differed by less than 10 units from the calculated values using the experimentally derived populations (in black), whereas the match was worse when using the calculated population mixes of the first approach (Figure 8, orange and blue lines).

Figure 8: Experimental ORD values of (+)-limonene (chloroform, 22.4 mg/ml, 20.4°C) at four wavelengths and calculated ORD values (mpw1pw91/cc-pvdz, IEFPCM (methanol) In red: experimental; In black: mix 39:31:30 based on chemical shift prediction; In orange: mix 28:38:34 based on calculated free energies; In blue: mix 34:23:43 based on calculated enthalpies. Experimental ORD values were corrected using the chloroform $[\alpha]_D$ value (113.8) of Rule and Chambers (1937), which was itself corrected by a factor using the value of a homogenous sample of Wilson et al. (2005))

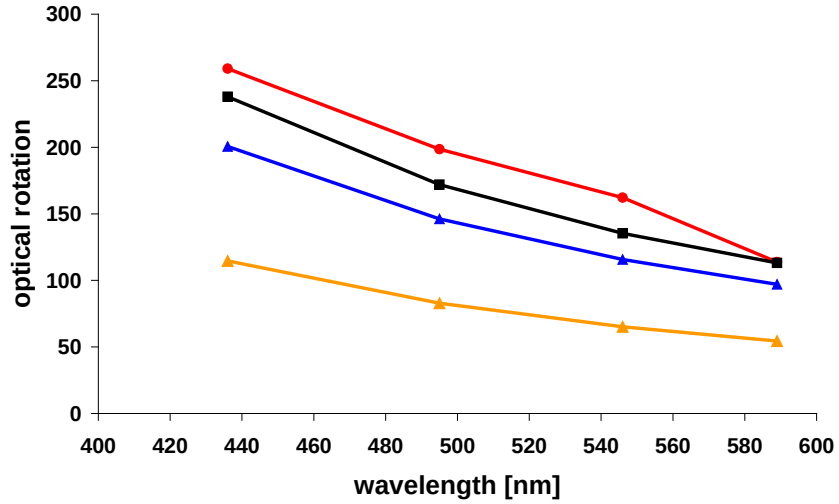

The ECD spectra prediction showed a decisive dependence on the basis set. Only augmented, in the case of Dunning`s basis sets, or diffuse in the case of Pople`s basis sets, predicted the position and shape of the ECD bands correctly (Figures 9A-C).

Figures 9 A-C: Calculated, population-weighted (39:31:30) ECD spectra of (+)-limonene for the different levels of theory: (A) mpw1pw91/cc-pvdz, (B) mpw1pw91/aug-cc-pvdz),and (C) experimental ECD spectra of (+)-limonene 0.1 mg/ml in methanol. Wavelengths in nm (x axis), and $\Delta\varepsilon$ [Mol*l^{-1}*cm^{-1}](y axis).

A B C

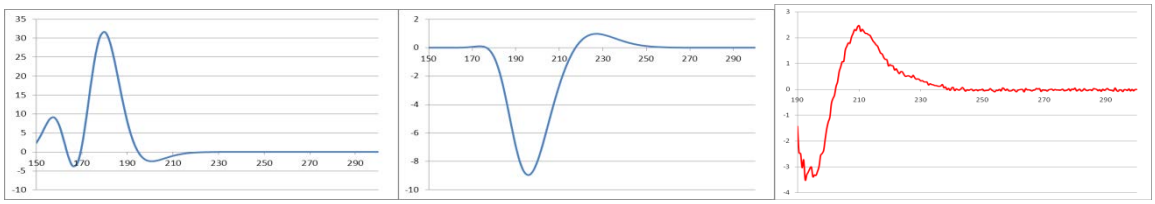

Several decades ago, Scott and Wrixon (1970) compiled ECD values of chiral olefins. However, an inappropriate application of the octant rule led to, by chance, a correct assignment of limonene which was later proven by Brint et al. (1984). The positive band of (+)-*R*-limonene (equals *D*-limonene) present at around 210 nm when measured in solution was assigned as π to π^* transition in agreement with the octant rule (Scott and Wrixon, 1970). However, gas-phase measurements revealed the presence of two positive bands at 218 nm and 210 nm which are assumed to belong to the same transition (Brint et al., 1984). These authors assigned this positive band to a π to 3s transition which is well known to show a blue-shift in solution. By chance, this positive band was taken erroneously by Scott and Wrixon (1970) as π to π^* transition, which followed the octant rule. However, limonene follows an anti-octant rule, and Brint et al. (1984) mention two other cases of this behaviour. Generally, the octant rule should no longer be applied for configurational purposes. However, it remains interesting to study this empirical rule, and especially the reasons why it fails.

Inspection of the experimental spectra obtained at different concentrations indicated no aggregation effects that would shift the position of the Cotton effect. In addition, methanol and ethanol as solvent gave similar spectra (Reischeid and Reinscheid, 2016a). From these results, it was concluded that the solvent modelling presents no problem for the structural models when calculating UV-Vis and ECD spectra. A negative band can be seen around 195 nm and a positive band around 210 nm (Reinscheid and Reinscheid, 2016a). These two decisive bands can be found in the calculated spectra (negative band at 196 nm, positive band at 228 nm) if Dunning's augmented basis sets or a Pople basis set with diffuse and polarization functions are applied. Importantly, spectra using the cc-pvdz and cc-pvtz basis sets would lead to an incorrect absolute configuration assignment if a red shift would be applied to the calculated data (+ 15 nm and + 25 nm for the shorter and the longer wavelengths, respectively).

VCD spectra were measured in the often used range of wavenumbers between 1800 cm^{-1} and 1000 cm^{-1}. Since pure limonene was used, the calculations used different solvents (chloroform and ethanol) to find a better mimic for limonene as solvent. In addition, different levels of theory were applied and the average of all calculated data was used to construct a VCD spectrum. The calculated and the experimental VCD spectra are shown in Figure 10. Here there is only a weak dependence on the level of theory (Reinscheid and Reinscheid, 2016a). It is important to note, that for these figures no shift in wavenumbers has been applied. Clearly, a 1:1 match between the spectra concerning the band position, shape and intensity was not observed. Therefore, the following guideline is proposed: one should concentrate on the most

significant stretch of bands in the experimental spectrum. Based on this stretch of bands one should decide if the calculated and experimental spectra match or if the inverted, calculated spectrum and the experimental spectrum matches. This depends on the correctness of a number of assumptions: the structural model represents one of the two enantiomers and no other molecule (e.g. diastereomer), the decisive bands are not inverted by matrix effects that have not been modelled and the position and sign of the decisive stretch of bands is correctly assigned. Although very strict, this is at present the only reliable means of interpretation since the matching of signs of a large number of bands, which are often found in the literature is questionable due to a shift in wavenumbers while inverting the calculated spectrum. Although this would also yield a good match with experiment, it gives an inverted, and thus incorrect, assignment of the absolute configuration.

Figure 10: Calculated VCD spectrum of (+)-limonene (theory level a) using a population-weighted mix of 39:31:30 (left); experimental VCD spectrum of pure (+)-limonene (right); wavelengths in nm (x axis), and $\Delta\varepsilon$ [Mol*l^{-1}*cm^{-1}](y axis)

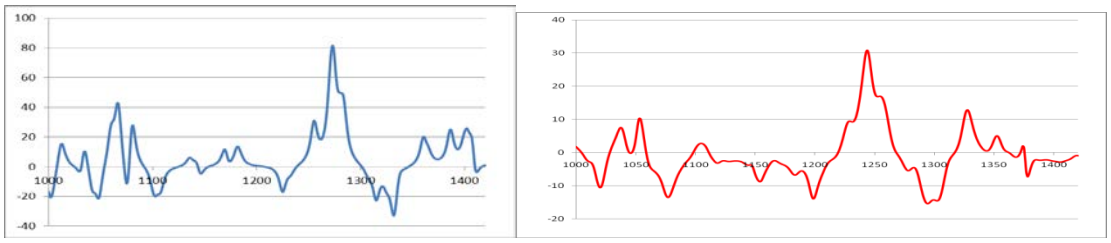

5.2 Strychnine

The formula of strychnine (Figure 11) has been established by Robinson (Robinson, 1946). Soon after it was confirmed by total synthesis (Woodward et al., 1954) and x-ray crystallography (Robertson and Beevers, 1950). The absolute configuration of naturally occurring (−)-strychnine was determined by Peerdeman in 1956 using x-ray crystallography (Peerdeman, 1956). Apart from the general chemical importance of strychnine, it serves as important test molecule for NMR method development (Berger, 2010).

Figure 11**:** Formula of (−)-strychnine HCl

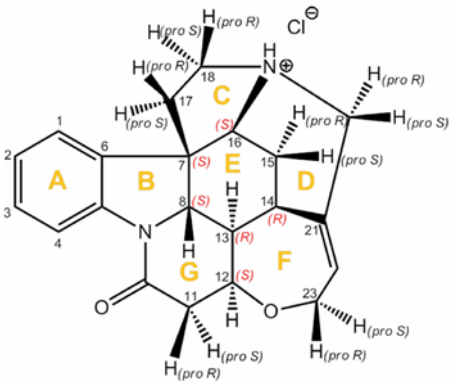

In a recent publication about the structure of strychnine, the first experimental and quantitative evidence of a minor conformer in solution using low-temperature NMR were presented (Figures 12A and B) (Schmidt et al., 2014).

Figure 12A: Geometry-optimized (mpw1pw91/cc-pvdz, IEFPCM: methanol) structure of protonated strychnine . Major and minor conformers are on the left and right-sides respectively.

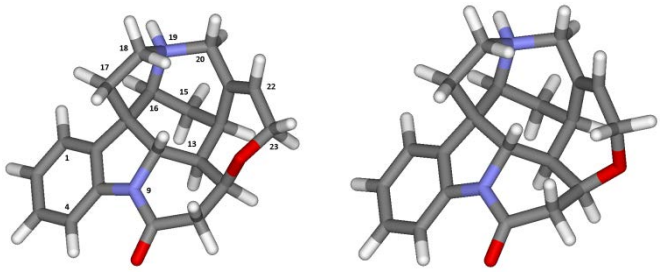

Figure 12B: Geometry-optimized (mpw1pw91/cc-pvdz, IEFPCM: methanol) structure of protonated strychnine with inverted aliphatic nitrogen. Major and minor conformers are on the left and right-sides respectively.

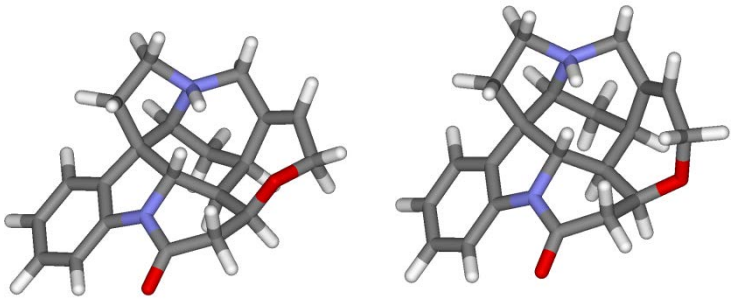

Earlier work by Butts et al. (2011) presented calculated quantitative information. In addition, a third low-populated conformer was predicted by computation (Bifulco et al., 2013). To date, there is no experimental evidence for its existence and so it hasnot been further investigated.

In the present study the question was adressed if the level of theory for the limonene investigations will also be appropriate for the structurally complex natural product strychnine. In particular, structural aspects such as protonation and solvent association were investigated in order to test if the integrated approach for the conformational and configurational analysis can be successfully applied (Figure 13) (Reinscheid et al., 2016).

Figure 13: Structural aspects of strychnine investigated by the integrated approach

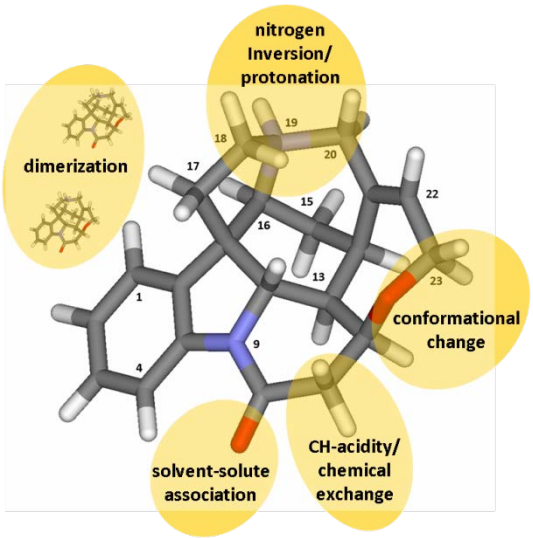

The structural analysis justified using a monomeric model of strychnine base and of the protonated form. Since experimental evidence for the existence of a second minor populated conformer of strychnine were presented (Schmidt et al., 2014), this minor conformer has to be taken into account for the population analysis and the interpretation of chiroptical data. Importantly, a typical level of theory for geometry optimization (B3LYP/6-31G(d)) delivered a structural model with which the calculated ^{13}C resonances did not match very well to the experiment. This was in contrast to the structural model obtained at the mpw1pw91/cc-pvdz level of theory (Schmidt et al., 2014). Therefore, this level of theory is often used for the limonene and menthol work.

It is shown that solvent association can be assumed in protic solvents such as methanol, and dimerization to a small extent in polar/protic solvents. However, the monomeric structural model neglecting explicit solvent molecules still allowed the correct prediction of the AC of base and hydrochloride using optical rotation and ECD data. The fit between experimental and calculated ECD spectra might be improved by using a higher level of theory.

The experimental optical rotation data of base and strychnine HCl were very well matched to the calculated values (Figures 14 and 15).

Figure 14: Calculated (mpw1pw91/aug-cc-pvdz, iefpcm: chloroform; in blue partly overlaid by the green curve: major conformer, in red: minor conformer, in green: 97.3/2.7 mix of the two conformers) and experimental (in orange, 2 % in chloroform) ORD curve of (−)-strychnine base based on four wavelengths (589, 546, 495, and 436 nm respectively)

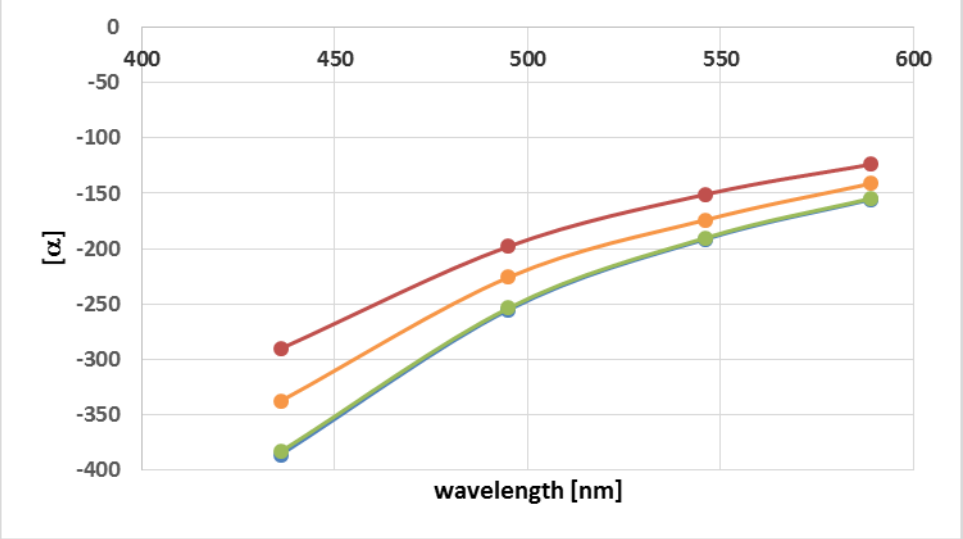

Figure 15: Calculated (mpw1pw91/aug-cc-pvdz, iefpcm: methanol; in blue: major conformer, in red: minor conformer, in green: 94.1/5.9 mix of the two conformers) and experimental (in purple, 2 % in methanol) ORD curve of (−)-strychnine HCl/protonated strychnine based on four wavelengths (589, 546, 495, and 436 nm respectively)

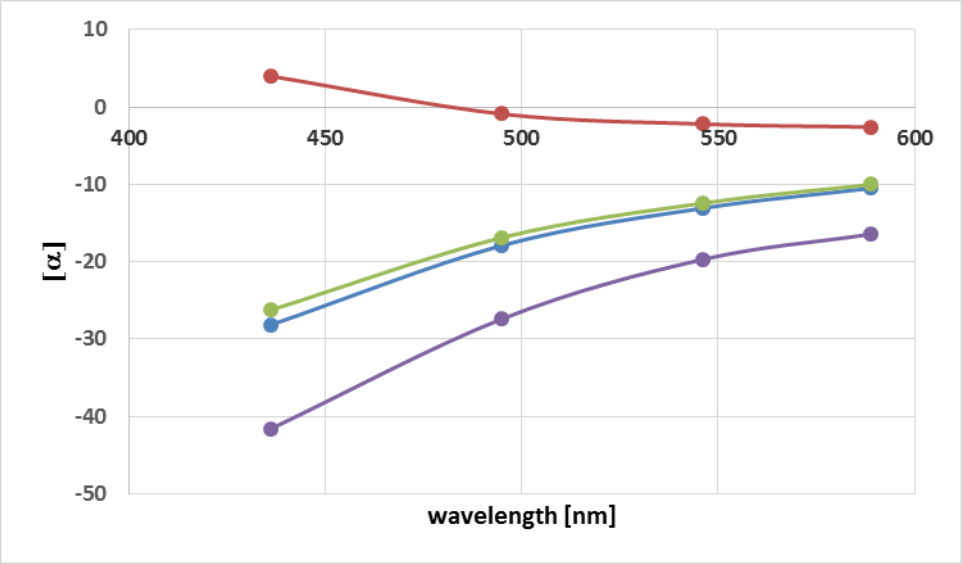

The calculations for (−)-strychnine base clearly showed a broad negative ECD band around 250 nm that correlates with the negative band around 235 nm in the experiment (acetonitrile) which is supported by comparison of the experimental and calculated UV spectra. The calculated ECD bands for protonated (−)-strychnine matched with the experiment without any wavelength shift. Interestingly, the calculated ECD bands among the major and minor conformers of strychnine base and protonated strychnine differ slightly. However, the decisive negative band at around 250 nm is always present and thus the AC assignment is reliable.

5.3 Menthol isomers and derivatives

Menthol is one of the best studied monoterpenes (Figure 16A). The development of structure determinations in the field of terpenes was described by Hanson (2003). Menthol isomers and its derivatives are of high commercial interest due to their unique properties such as cooling and flavouring agents (Croteau et al., 2005). Annually, several thousand tons of (–)-menthol are consumed. In addition, amino derivatives of the menthol series (the diastereomeric menthylamines (bases and hydrochloride salts)) have become important as chiral auxiliaries for asymmetric syntheses (Kulisch et al., 2011). Menthol (Fig. 16A) is the major constituent of the essential oil of the mint family (peppermint: *Mentha x piperita* and spearmint: *Mentha spicata*). Gladstone (1864) presented optical rotation values for crude oils. Without separation, the hydrocarbon from the oil of *Mentha viridis* was termed “menthol”.

Figures 16A-D: Menthol and the diastereomers neomenthol, isomenthol and neoisomenthol; conformers[a] of A) (+)-(1*S*,3*S*,4*R*)-menthol ($1_{eq}3_{eq}4_{eq}$); B) (+)-(1*R*,3*S*,4*S*)-neomenthol ($1_{eq}3_{ax}4_{eq}$); C) (–)-(1*S*,3*R*,4*S*)-isomenthol ($1_{ax}3_{eq}4_{eq}$); D) (–)-(1*S*,3*S*,4*S*)-neoisomenthol ($1_{ax}3_{ax}4_{eq}$)

A) (+)-(1*S*,3*S*,4*R*)-Menthol ($1_{eq}3_{eq}4_{eq}$)

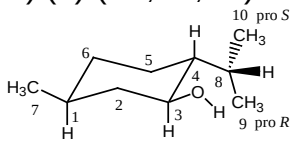

B) (+)-(1*R*,3*S*,4*S*)-Neomenthol ($1_{eq}3_{ax}4_{eq}$)

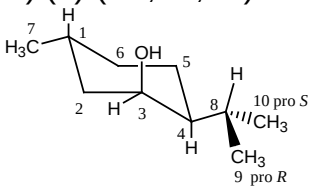

C) (–)-(1*S*,3*R*,4*S*)-Isomenthol ($1_{ax}3_{eq}4_{eq}$)

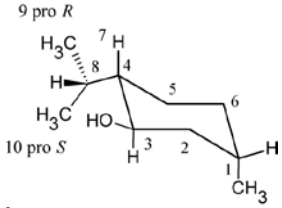

D) (–)-(1*S*,3*S*,4*S*)-Neoisomenthol ($1_{ax}3_{ax}4_{eq}$)

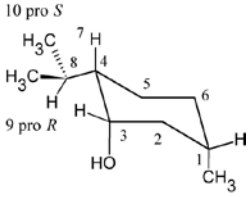

[a]:Nomenclature: chair with position of substituents: methyl / OH / isopropyl (eq: equatorial, ax: axial); isopropyl dihedral: H4-C4-C8-H8; OH dihedral: H-O-C3-H3; *trans* (t), *gauche*$^+$ (g^+) or *gauche*$^-$ (g^-)

This study adressed the question how reliable the integrated approach will be for a number of molecules that are: i) isomers (e.g. menthol series of diastereomers) and ii) closely related (menthols and menthylamines).

The full series of menthol diastereomers (menthol, isomenthol, neomenthol, neoisomenthol: Figures 16A-D) and their amino derivatives as base and as protonated/HCl forms were investigated.

Large discrepancies were found among the literature values concerning the calculated conformer population of even the best studied member of the series, i.e. menthol. It was shown that the correct determination of the population mix is a must for the correct prediction of the AC of neoisomenthol (Reinscheid and Reinscheid, 2016b). The neoiso forms are of special interest since a number of structural speculations can be found in the literature. Especially important is having the correct population ratio between the conformers with an equatorial or axial position of the isopropyl group (Figure 17). Using experimental ^{13}C chemical shifts, it was possible to correct the computationally derived populations.

Figure 17: Geometry optimized structures of (–)-(1*S*,3*S*,4*S*)-neoisomenthol: on the left side with an equatorial position of the isopropyl group; on the right side with an axial position of the isopropyl group

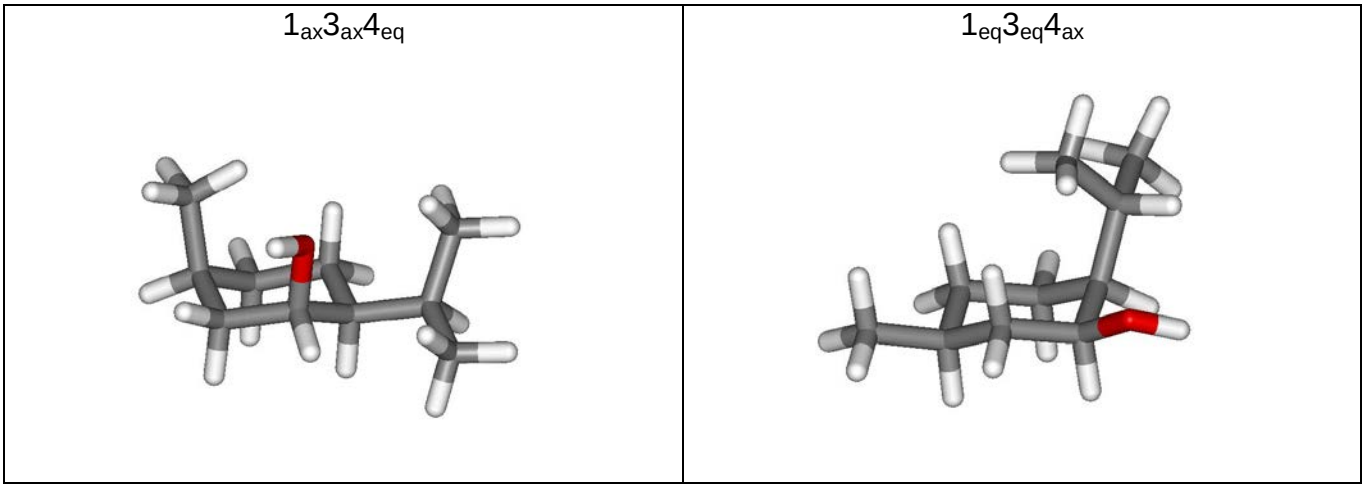

To the best of my knowledge, the AC of neoisomenthylamine is for the first time proven by comparison between experimental and calculated optical rotation data. A correction of a series of publications containing an important error in the assignment of (+)-menthylamine (correct: (+)-neomenthylamine) is presented.

The literature concerning VCD applications does not cover the challenging neoiso forms, and includes the questionable, pure computational population analysis. In fact, optical rotation data are the best choice for the AC determination of the menthol series and its amino derivatives. It was shown that the AC of all 12 compounds could be predicted correctly when experimental low-temperature NMR data were used for the most difficult neoiso forms. If experimental data with an optical rotation outside the range of $-10 < [\alpha] < +10$ were only taken, all 12 compounds were correctly assigned even without low-temperature NMR data as restraints.

All experimental and calculated ORD values of the (+)-menthol and (+)-menthylamine (base and HCl/protonated) isomers were collected, excluding data for wavelengths near excitations

for the amine derivatives (436 nm, 365 nm) (Table 2). This procedure was motivated by the inaccurate calculations near excitation wavelengths leading to substantial errors. The menthol isomers do not suffer from these shortcomings due to lower excitation wavelengths of the alcohols compared to that of the amines.

In Figure 18 the 26 data pairs together with the regression line (red) and the prediction bands (green) at a 99 % level of confidence are shown (experimental values were inverted if only values for the (−)-enantiomer were available. All calculated values belong to the (+)-enantiomer) and all data pairs are based on a correct AC assignment.

Figure 18: Left side: Experimental and calculated ORD values (26 in total) of the (+)-menthol and (+)-menthylamine (base and HCl/protonated) isomers; linear regression lines (red) and prediction bands at a 99 % level of confidence (green, Origin ^{R}); right side: close up in the region of small values; experimental values were inverted if only values for the (−)-enantiomer were available; all calculated values belong to the (+)-enantiomer, list of data pairs below the figure

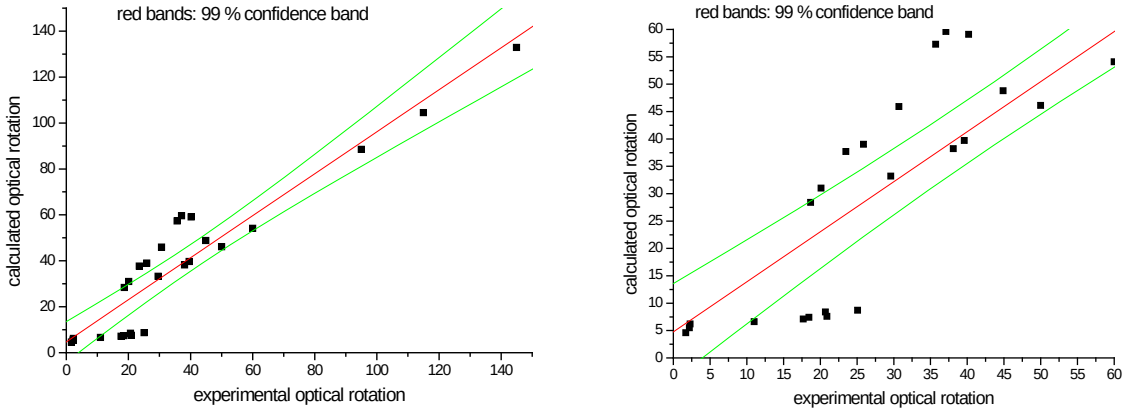

Experimental optical rotation values below 5 cannot be predicted reliably on a 99 % level of confidence. This is nicely demonstrated in Fig. 18 (right side: close-up of the left side of Figure 18) where the confidence interval intersects the x-axis near an optical rotation value of 5. The variation originating from different levels of theory used should be added. Based on work on limonene (Reinscheid and Reinscheid, 2016a), an additional range of uncertainty of 5 units can be assumed. A prediction of the absolute configuration of a compound is not recommended if it is solely based on the comparison of experimental and calculated ORD data, and the experimental values are within the range from -10 to +10. Overall, the calculated values for some neo and neoiso forms are systematically underestimated.

Table 2: Data pairs used for Figure 18

compound	λ in nm	[α]exp.	[α]calc.	compound	λ in nm	[α]exp.	[α]calc.
(+)-menthol	589	50.00	46.1	(+)-menthylamine	589	35.70	57.3
	546	60.00	54.1		578	37.10	59.6
	436	95.00	88.5	(+)-neomenthylamine	589	25.10	8.7
	405	115.00	104.5	(+)-isomenthylamine	589	29.60	33.2
	365	145.00	132.9	(+)-neoisomenthylamine	589	11.00	6.6
(+)-neomenthol	589	17.69	7.1	(+)-menthylamine (protonated/HCl	589	38.10	38.2
	578	18.47	7.4		578	39.60	39.7
	546	20.70	8.4		546	44.90	48.8
(+)-isomenthol	656	20.10	31.0	(+)-neomenthylamine (protonated/HCl)	589	18.70	28.4
	589	25.90	39.0	(+)-isomenthylamine (protonated/HCl)	589	23.50	37.7
	546	30.70	45.9	(+)-neoisomenthylamine (protonated/HCl)	589	20.90	7.6
	486	40.20	59.1				
(+)-neoisomenthol	656	1.70	4.6				
	589	2.20	5.5				
	546	2.30	6.2				

6. Discussion

The present work showed that it is possible to identify experimentally existing conformers in solution using currently available computer programs based on density functional theory. This was demonstrated by the good match between experimental and calculated NMR chemical shifts in case of the small monoterpene limonene (Reinscheid and Reinscheid, 2016a) and the complex alkaloid strychnine (Reinscheid et al., 2016). In addition, for most of the menthol/menthylamine isomers a computational conformational search determined the physically existing conformers in solution (Reinscheid and Reinscheid, 2016b). However, in case of the flexible neoiso forms of menthol and menthylamine further experimental constraints were needed, namely from low-temperature NMR experiments (Pehk et al., 1980), to narrow down the theoretically available conformational space.

I performed the calculations, analyzed the results, and assisted in writing the three publications which are part of this thesis. In addition, I performed the ECD/UV-Vis measurements of limonene and strychnine, and VCD/IR measurements of limonene.

The populations of the conformers of limonene were determined with a combination of experimental and calculated NMR chemical shifts, and with a pure computational approach using calculated energy differences. The most reliable results were obtained with the first approach. Multi-standard methodologies for chemical shift calculations has been reviewed (Lodewyk et al., 2012) and recently proposed (Sarotti and Pellegrinet, 2012). An early multiple regression analysis was presented by Sebag et al. (2001) for tertiary amines. We term our approach “internal referencing” since NMR resonances of the molecule itself are used for referencing. A similar approach has been presented by Andrews and Spivey (2013). They used reference molecules with known experimental chemical shifts which can be taken as fragments of the unknown molecule for which the shieldings are calculated. This approach differs from ours in that we directly take resonances of the unknown molecule for referencing. Clearly, our approach needs medium-sized molecules in order to have sufficient resonances for calibration/prediction. As an advantage, over-fitting can be easily identified and corrected.

In the following, the individual chiroptical methods and their applications are discussed.

ORD

Conformational analysis is very important in case of flexible molecules as ORD values can be highly dependent on conformation. Consequently, the correct conformers and their populations for limonene, strychnine, and the group of menthol/menthylamine isomers were determined by a pure computational method and a combination of calculated and experimental NMR data.

The importance of conformational effects on the ORD has been already described by Wiberg et al. (2003) for a number of 3-substituted 1-butenes. In the case of 3-chloro-1-butene, changing the temperature shifted the experimental ORD values which could be explained by a change in the conformer population. In a subsequent article, Wiberg et al. (2004) analysed 1-butene, butane and related hydrocarbons. They realized that the choice of basis set is very important to accurately calculate ORD values. Diffuse functions should be used (augmented basis sets in the case of Dunning`s correlation consistent basis sets such as cc-pvdz: aug-cc-pvdz). However, Rinderspacher and Schreiner (2004) emphasized that the balanced nature of the basis set is the important aspect. Concerning the basis set, in the recent study of Hedegård et al. (2012) it was shown that the aug-cc-pvdz basis set often led to significant

deviations from the basis set limit. This is in contrast to the study of Grimme et al. (2002). Since the more recent study used a larger number of molecules, it is likely that the often recommended usage of basis sets with diffuse functions must still be handled with caution.

Regarding the accuracy of ORD calculations, two studies are still valuable (Stephens et al., 2004; Stephens et al., 2005). From comparisons between experiment and calculation, the authors concluded that on a 95 % level of confidence, the correct absolute configuration could be predicted with confidence limits of ±60 deg /(dm*(g/cm^{-3})). In addition, Mennucci et al. (2002) presented the successful application of the IEF-PCM approach to account for solvent effects based on electrostatics.

Applying the mpw1pw91/cc-pvdz (IEF-PCM as solvent model) level of theory, the calculated ORD values of limonene at four wavelengths were closely matched to the experimental values obtained in solution, with relative differences less than 5 %, and absolute deviations less than 5. Therefore, this level of theory (using a non-augmented basis set) was chosen for the strychnine analysis. It again delivered accurate ORD data, and was consequently used for the group of menthol/menthylamine diastereomers. In this case it performed very well and the signs of all chosen experimental values were correctly predicted.

ECD

A clear advantage of the ECD based configurational analysis is the low amount of compound required for measurements. A further advantage for ECD is the possibility to use UV-Vis spectra as reference for the wavelength and intensity scale. At the same time, aggregation effects play a small role compared to the two other chiroptical methods, ORD and VCD. However, ORD offers a remarkable number of advantages. It is easy to measure and the reliability can be increased by using short or long wavelengths. Furthermore, ORD provides the only information regarding the absolute configuration of natural products isolated previously, which are meanwhile decomposed and cannot be isolated again.

For calibration of the ECD bands, the accuracy with which the UV-Vis spectrum can be calculated is very important. As a good starting point, the study of Perpète et al. (2007) can be used. They studied the λ_{max} values of dye molecules. Since focusing on a chemically related group of molecules will very often lead to bias, in this case, towards higher accuracy of the calculated data, one should be cautious and take the reported values as minimum error levels. A mean absolute error of 20.1 nm (0.113 eV) was found for a group of 86 naphtoquinone dyes in various solvents.

Autschbach et al. (2006) proposed to use an overall damping of 0.2 eV to simulate ECD spectra from calculated rotational strengths. In this thesis, several values were used, resulting in a broadening value that allows the best match between the experimental and calculated UV-Vis bands. The latter point is also related to the accuracy with which the rotational strengths are calculated. Based on recent results (Schmidt et al., 2012; Schmidt et al., 2014), we can assume differences of a factor of two between calculation and experiment concerning the rotational and dipolar strengths.

The main conclusion from my calculations is that non-augmented basis sets do not show the important positive band of limonene around 220 nm, and thus a reliable AC determination is not possible, whereas for strychnine the non-augmented basis set can be successfully applied. In contrast to the ORD results, for the ECD calculation it is imperative to use augmented Dunning's basis sets or Pople basis sets with diffuse functions for the correct prediction of the AC of limonene.

VCD

Vandenbussche et al. (2013) presented a statistical validation of absolute configuration assignment using VCD for a series of quinolizine molecules. Polavarapu and Covington (2014) introduced dissymmetry factors as similarity measures for the analysis of VCD, ECD, and Raman optical activity spectra. A systematic approach for assigning the absolute configuration using VCD has been proposed by Sherer et al. (2014). However, even ibuprofen was a difficult case since additional information i.e. dimerization, had to be taken into account and was not included in the systematic approach.

Overall, the scientific community has not reached a consensus procedure to obtain a similarity factor when comparing experimental and calculated chiroptical spectra. Therefore, in this thesis the use of so-called enantiodiscriminative bands was proposed for the analysis of limonene. This procedure cannot be automated and does not give a quantitative measure of uncertainty. Consequently, its use can only be recommended as a supporting method for the AC determination based on ORD/ECD.

Most often the harmonic approximation is used for calculations and the anharmonic contributions are neglected, and this is one of the reasons of mismatch between experiment and calculation. The importance of anharmonicity was shown by Cappelli et al. (2010) for the test molecule formaldehyde. Current computer resources often limit a full anharmonic treatment of molecules larger than 30 atoms.

Although VCD spectra can be much more difficult to interpret for assigning the absolute configuration, a number of studies have been published in the area of natural product analysis (e.g. Gordillo-Román et al., 2012). The research group of Avilés Moreno especially deals with the VCD analysis of natural products, such as limonene oxide (2009a) and carvone (2009b) Partal Ureña et al. (2009) studied limonene using the combination of IR, VCD and computations. However, using experimental and calculated chemical shifts for the populations, we have determined different populations. Intriguingly, with the incorporation of a solvent model, our populations based on enthalpies are very similar to the populations calculated by Partal Ureña et al. (2009) and Pedersen et al. (2009), both of which were calculated in vacuo.

As a result of the three publications from this thesis, the following requirements were formulated and should be fulfilled for a reliable AC determination based on the integrated approach:

1. The application of a number of reasonable levels of theory does not change the sign (plus or minus) of the calculated chiroptical values of the different methods (ORD, ECD, VCD).
2. Absolute values of the experimental specific optical rotation at 589 nm should be larger than 60, unless a detailed conformational analysis is performed based on the comparison between experimental and calculated NMR data.
3. The absolute configuration of a compound should not be predicted if this prediction is solely based on the comparison of experimental and calculated ORD data with experimental values that are within the range of ±10.
4. The experimental and calculated ORD curves show no zero crossing in a span of wavelengths of at least 100 nm.
5. The application of a reasonable wavelength shift (not more than 20 nm) does not change the AC assignment based on ECD spectra.
6. Two or more enantiodiscriminative stretches of VCD bands with opposite AC assignment should not be present

For limonene the specific optical rotation at 589, the ORD values and the VCD bands exhibit no sign change if a number of reasonable levels of theory are applied. However, the ECD data cannot be used successfully since the AC assignment depends on the basis sets applied. In addition, the absolute value of the experimental specific optical rotation is larger than 60, and

the ORD curve with 4 wavelengths spanning more than 100 nm shows no zero crossing so that all chiroptical methods except ECD can be used for a correct prediction of the AC.

For strychnine the specific optical rotation, ORD and ECD could be used for the AC determination. For the menthol series, only ORD values were used. A detailed conformational analysis enabled the determination of the AC based on small experimental values of all 12 investigated compounds.

In total, the integrated approach proved to be highly reliable for limonene, and decreased via strychnine to the menthol/menthylamine isomers. However, even the least reliable AC determinations (neoiso forms of menthol and menthylamine) fulfil some of the above proposed requirements.

ECD spectroscopy can be regarded as optimal chiroptical method for the AC determination if the requirements from above are fulfilled. The main disadvantage of this method (non-accessible excitations in solution as exemplified by the menthol series) restricts its use.

7. Summary

The absolute configuration (AC) of a variety of natural products was determined by an integrated approach: experimental spectroscopic data together with DFT calculated data of important bioactive molecules such as limonene, strychnine, and menthol-type compounds.

Using limonene as test molecule, the success and the limitations of three chiroptical methods, optical rotatory dispersion (ORD), electronic and vibrational circular dichroism (ECD and VCD respectively), could be demonstrated. At the mpw1pw91/cc-pvdz (IEFPCM for solvent modelling) level of theory, the experimental ORD values differ by less than 10 units from the calculated values.

Application of this level of theory allowed the correct prediction of the AC of strychnine base and hydrochloride based on the comparison between experimental and calculated ORD and ECD data. Structural aspects such as chemical exchange, dimerization, solvent association, nitrogen inversion and protonation status of strychnine were investigated using experimental and calculated data. The information was mainly interpreted in view of a successful AC determination with strychnine (base and salt) as test molecule due to its importance in chemistry and biology. By geometry optimization a stable isomer of protonated strychnine was found with an inverted nitrogen. However, it was 25 kcal/mole higher in energy than the non-inverted form, which suggests that its concentration will be very low under ambient conditions.

The complete series of menthol isomers and its corresponding amino derivatives, the latter as base and protonated/HCl forms, were investigated using experimental and theoretical data. Large discrepancies were found throughout the literature values concerning the calculated conformer population of even the best studied member of the series, i.e. menthol. It is shown that the correct determination of the population mix is a must for the correct prediction of the AC of neoisomenthol. The neoiso forms are of special interest since a number of structural speculations can be found in the literature. A stringent proof of the AC of neoisomenthol based on literature information using the gold standard (x-ray crystallography) as starting point was shown. To the best of my knowledge, the AC of neoisomenthylamine is for the first time proven by comparison between experimental and calculated optical rotation data. A correction of a series of publications containing an important error in the assignment of (+)-menthylamine (correct: (+)-neomenthylamine) is presented. With 26 data pairs (experimental versus calculated) of optical rotation a linear regression was performed. It was shown that the AC of all 12 compounds could be predicted correctly when experimental low-temperature NMR data were used for the most difficult neoiso forms. If only experimental data with an optical rotation outside the range of $-10 < [\alpha] < +10$ were taken, all 12 compounds would have been correctly assigned even without low-temperature NMR data as restraints.

7. Zusammenfassung

Die absolute Konfiguration (engl.: absolute configuration: AC) einer Reihe von Naturstoffen (Limonen, Strychnin und mentholartige Verbindungen) wurde mit einem integrierten Ansatz bestimmt (Kombination aus experimentellen und mittels Dichtefunktionaltheorie (DFT) berechneten spektroskopischen Daten).

Mit Limonen als Testmolekül wurden Möglichkeiten und Grenzen der drei chiroptischen Methoden (optische Rotationsdispersion (ORD), elektronischer- bzw. Schwingungs-Zirkulardichroismus, (engl.: electronic circular dichroism: ECD; engl.: vibrational circular dichroism: VCD) für die Bestimmung der absoluten Konfiguration gezeigt. Bei Anwendung des Theorieniveaus mpw1pw91/cc-pvdz und IEFPCM (integral equation formalism polarizable continuum model) als Lösungsmittel Modell weichen die berechneten ORD Werte weniger als 10 Einheiten von den experimentellen Werten ab.

Die Anwendung dieses Theorieniveaus erlaubte auch die korrekte Vorhersage der absoluten Konfiguration von Strychnin als Base und Hydrochlorid basierend auf dem Vergleich von

experimentellen und berechneten ORD- und ECD-Werten. Auf der Basis von experimentellen und berechneten Werten wurden strukturelle Aspekte, wie der chemische Austausch, Dimerisierung, Lösungsmitteleinflüsse, Stickstoffinversion und der Protonierungszustand von Strychnin untersucht.

Diese strukturellen Informationen wurden im Hinblick auf eine erfolgreiche AC Bestimmung mit Strychnin (Base und Salz) als Testmolekül interpretiert. Bei der Geometrie-Optimierung wurde ein stabiles Isomer eines protonierten Strychnins mit invertiertem Stickstoff gefunden, allerdings mit 25 kcal/ Mol höherer Energie als das nicht-invertierte Isomer, was bedeutet, dass seine Konzentration unter Standardbedingungen sehr gering ist.

Alle vier Diastereomere von Menthol und die dazugehörigen Aminoderivate wurden untersucht; die letzteren als Base und in protonierter/ HCl Form. Literaturwerte bezüglich der berechneten Konformerenpopulationen unterscheiden sich deutlich, sogar bei Menthol, dem bestuntersuchten Mitglied der Reihe. In der vorliegenden Arbeit wurde gezeigt, dass die korrekte Bestimmung der Populationen ein Muss für die korrekte Vorhersage der AC von Neoisomenthol ist.

Die Neoiso-Formen sind von besonderem Interesse, da in der Literatur eine Vielzahl von Spekulationen bzgl. der Struktur existieren. Daher wurde eine Beweisführung für die AC von Neoisomenthol basierend auf Literaturinformationen mit Daten aus Kristallstrukturanalysen als Ausgangspunkt vorgestellt. Nach bestem Wissen wurde die AC von Neoisomenthylamin zum ersten Mal durch den Vergleich von experimentellen und berechneten ORD Werten nachgewiesen.

Auf die Korrektur einer Reihe von Veröffentlichungen wurde hingewiesen, in denen ein wichtiger Fehler in der Konfigurationszuordnung enthalten ist. Ein Syntheseprodukt wurde als (+)-Menthylamin bezeichnet. Dabei handelt es sich jedoch vermutlich um (+)-Neomenthylamin.

Mit 26 Datenpaaren optischer Drehungen von Mentholderivaten (experimentell versus berechnet) wurde eine lineare Regression durchgeführt. Es wurde gezeigt, dass die AC von allen 12 Verbindungen richtig vorhergesagt werden konnte, wenn für die Neoiso-Formen experimentelle Tieftemperatur-NMR Daten verwendet werden.

Falls nur experimentelle Daten mit einer optischen Drehung außerhalb des Bereichs von $-10 < [\alpha] < +10$ verwendet worden wären, hätten alle 12 Verbindungen richtig bestimmt werden können, sogar ohne Tieftemperatur-NMR Daten.

8. Cited References

KG Andrews, AC Spivey, Improving the Accuracy of Computed C-13 NMR Shift Predictions by Specific Environment Error Correction: Fragment Referencing (2013) J. Org. Chem., 78, 11302

J Autschbach, L.Jensen, GC Schatz, YCE Tse, M Krykunov, Time-dependent density functional calculations of optical rotatory dispersion including resonance wavelengths as a potentially useful tool for determining absolute configurations of chiral molecules (2006) J. Phys. Chem. A, 110, 2461

JR Avilés Moreno, F Partal Ureña, JJ López González, Conformational preference of a chiral terpene: vibrational circular dichroism (VCD), infrared and Raman study of *S*-(-)-limonene oxide (2009a) PhysChemChemPhys, 11, 2459

JR Avilés Moreno, F Partal Ureña, JJ López González, Conformational landscape in chiral terpenes from vibrational spectroscopy and quantum chemical calculations: *S*-(+)-carvone (2009b) Vibr. Spectrosc., 51, 318

KL Bak, O Bludsky, P Jørgensen, Ab initio calculations of anharmonic vibrational circular dichroism intensities of *trans*-2,3-dideuteriooxirane (1995) J. Chem. Phys., 103, 10548

LD Barron, AD Buckingham, Rayleigh and Raman scattering from optically active molecules (1971) Mol. Phys., 20, 1111

DHR Barton, The conformation of the steroid nucleus (1950) Experientia, 6, 316

DHR Barton, The Principles of Conformational Analysis (1969) Nobel Lecture

AD Becke, Density-functional thermochemistry. III. The role of exact exchange (1993) J. Chem. Phys., 98, 5648

K Bednarik, 2016: https://de.wikipedia.org/wiki/Echte_Zaunwinde#/media/File:DSCM1934_Helix_Zaunwinde.jpg

AJ Benesi, Chapter 15 in: A primer of NMR theory with calculations in MathematicaR, 2015, First edition, John Wiley & Sons, New Jersey

S Berger, 200 and More NMR Experiments: A Practical Course, 2004, Wiley & Sons

N Berova, K Nakanishi, RW Woody (eds.), Circular dichroism: Principles and applications, second edition, 2000, Wiley-VCH

G Bifulco, R Riccio, GE Martin, AV Buevich, RT Williamson, Quantum Chemical Calculations of (1)J(CC) Coupling Constants for the Stereochemical Determination of Organic Compounds (2013) Org. Lett., 15, 654

JM Bijvoet, AF Peerdeman, AJ van Bommel, Determination of the Absolute Configuration of Optically Active Compounds by Means of X-Rays (1951) Nature, 168, 271

F Bloch, WW Hansen, M Packard, Nuclear Induction (1946) Phys. Rev., 69, 127

P Brint, E Meshulam, A Gedanken, Excited electronic steates of limonene: A circular dichroism and photoelectron spectroscopy study of d-limonene (1984), Chem. Phys. Lett., 109, 383

CP Butts, CR Jones, JN Harvey, High precision NOEs as a probe for low level conformers-a second conformation of strychnine (2011) Chem. Commun., 47, 1193

C Cappelli, S Corni, B Mennucci, R Cammi, J Tomasi, Vibrational Circular Dichroism within the Polarizable Continuum Model: A Theoretical Evidence of Conformation Effects and Hydrogen Bonding for (*S*)-(−)-3-Butyn-2-ol in CCl_4 Solution (2002) J. Phys. Chem. A, 106, 12331

C Cappelli, S Monti, G Scalmani, V Barone, On the Calculation of Vibrational Frequencies for Molecules in Solution Beyond the Harmonic Approximation (2010) J. Chem. Theory Comput., 6, 1660

JR Cheeseman, MJ Frisch, FJ Devlin, PJ Stephens, Ab initio calculation of atomic axial tensors and vibrational rotational strengths using density functional theory (1996) Chem. Phys. Lett., 252, 211

JR Cheeseman, MJ Frisch, FJ Devlin, PJ Stephens, Hartree−Fock and Density Functional Theory ab Initio Calculation of Optical Rotation Using GIAOs: Basis Set Dependence (2000) J. Phys. Chem. A, 104, 1039

A Cotton, Dispersion rotatoire anomale des corps absorbants (1895a), C. R. H. Acad. Sci, 120, 1044

A Cotton, Absorption inégale des rayons circulaires droit et gauche dans certain corps actifs (1895b), C. R. H. Acad. Sci, 120, 989

RB Croteau, EM Davis, KL Ringer, MR Wildung, (-)-Menthol biosynthesis and molecular genetics (2005) Naturwissenschaften, 92, 562

JA Dale, HS Mosher, Nuclear magnetic resonance enantiomer regents. Configurational correlations via nuclear magnetic resonance chemical shifts of diastereomeric mandelate, O-methylmandelate, and .alpha.-methoxy-.alpha.-trifluoromethylphenylacetate (MTPA) esters (1973) J. Am. Chem. Soc., 95, 512

A Dassonville-Klimpt, C Cézard, C Mullié, P Agnamey, A Jonet, S Da Nascimento, M Marchivie, J Guillon, P Sonnet, Absolute Configuration and Antimalarial Activity of erythro-Mefloquine Enantiomers (2013) ChemPlusChem, 79, 642

C Della Monico, A Randazzo, G Bifulco, P Cimino, M Aquino, I Izzo, F De Riccardis, L Gomez-Paloma, Structural revision of halipeptins: synthesis of the thiazoline unit and isolation of halipeptin C (2002) Tetrahedron Lett., 43, 5707

J Ding, DG Hall, Concise Synthesis and Antimalarial Activity of All Four Mefloquine Stereoisomers Using a Highly Enantioselective Catalytic Borylative Alkene Isomerization (2013) Angew. Chem. Int. Ed., 52, 8069

M Donia, MT Hamann, Marin natural products and their potential applications as anti-infective agents (2003) Lancet Infect. Dis., 3, 338

A Dreuw, JL Weisman, M Head-Gordon, Long-range charge-transfer excited states in time-dependent density functional theory require non-local exchange (2003) J. Chem. Phys., 119, 2943

WA Duetz, H Bouwmeester, JB van Beilen, B Witholt, Biotransformation of limonene by bacteria, fungi, yeasts, and plants (2003) Appl. Microbiol. Biotechnol., 61, 269

TH Dunning Jr., Gaussian basis sets for use in correlated molecular calculations. I. The atoms boron through neon and hydrogen (1989) J. Chem. Phys., 90, 1007

JD Dunitz, Pauling's Left-Handed α-Helix (2001) Angew. Chem. Int. Ed., 40, 4167

EL Eliel, Conformational Analysis in Mobile Cyclohexane Systems (1965) Angew. Chem. Int. Ed., 4, 761

EL Eliel, SH Wilen, MP Doyle (2001) Basic Organic Stereochemistry, p. 13-14, Wiley Interscience

E Fischer, Konfiguration der Weinsaurel (1896) Ber. Dtsch. Chem. Ges., 29, 1377

Gaussian09, MJ Frisch et al., Gaussian Inc., Wallingford CT, 2009

JH Gladstone, On essential oils. Part I (1864) J. Chem. Soc., 17, 1

B Gordillo-Román, J Camacho-Ruiz, MA Bucio, P Joseph-Nathan, Chiral recognition of diastereomeric 6-cedrols by vibrational circular dichroism (2012) Chirality, 24, 147

SJ Gould, N Tamayo, CR Melville, MC Cone, Revised Structures for the Kinamycin Antibiotics: 5-Diazobenzo[b]fluorenes Rather Than Benzo[b]carbazole Cyanamides (1994) J. Am. Chem. Soc., 116, 2207

S Grimme, F Furche, R Ahlrichs, An improved method for density functional calculations of the frequency-dependent optical rotation (2002) Chem. Phys. Lett., 361, 321

H Günther, NMR spectroscopy : basic principles, concepts and applications in chemistry, 2013, third edition, Wiley-VCH, Weinheim

JR Hanson (2003) Natural products: the secondary metabolites, Royal Society of Chemistry

T Hansson, B Wickberg, A short enantiospecific route to isodaucan sesquiterpenes from limonene: on the absolute configuration of (+)-aphanamol-I and (+)-aphanamol-II (1992) J. Org. Chem., 57, 5370

J He, A Petrovich, PL Polavarapu, Quantitative determination of conformer populations: Assessment of specific rotation, vibrational absorption, and vibrational circular dichroism in substituted butynes (2004a) J.Phys. Chem A, 108, 1671

J He, AG Petrovic, PL Polavarapu, Determining the conformer populations of (*R*)-(+)-3-methylcyclopentanone using vibrational absorption, vibrational circular dichroism, and specific rotation (2004b) J. Phys. Chem. A, 108, 20451

ED Hedegård, F Jensen, J Kongsted, Basis Set Recommendations for DFT Calculations of Gas-Phase Optical Rotation at Different Wavelengths (2012) J. Chem. Theory Comput., 8, 4425

P Herwig et al., Imaging the absolute configuration of a chiral epoxide in the gas phase (2013), Science, 342, 1084

P Hohenberg, W Kohn, Inhomogeneous electron gas (1964) Phys. Rev. B, 136, 864
TR Hoye, CS Jeffrey, F Shao, Mosher ester analysis for the determination of absolute configuration of stereogenic (chiral) carbinol carbons (2007) Nature Protocols, 2, 2451

W Hückel, Zur Stereochemie bicyclischer Ringsysteme. I. Die Stereoisomerie des Dekahydronaphthalins und seiner Derivate (1925) Liebigs Ann. Chem., 441, 1

P Jørgensen, J Simons (1981) Second quantization-based methods in quantum chemistry. Academic, NewYork

M Karplus, Vicinal Proton Coupling in Nuclear Magnetic Resonance (1963) J. Am. Chem. Soc., 85, 2870

S Kawahara, C Kojima, K Taira, T Uchimaru, A Theoretical Study of Correlation between Hydrogen-Bond Stability and J-Coupling through a Hydrogen Bond (2003) Helv. Chim. Acta, 86, 3265

Lord Kelvin (1904) Baltimore lectures on molecular dynamics and the wave theory of light, C. J. Clay and Sons, London

W Kohn, LJ Sham, Self-Consistent Equations Including Exchange and Correlation Effects (1965) Phys. Rev., 140, 1133

J Kulisch, M Nieger, F Stecker, A Fischer, SR Waldvogel, Efficient and Stereodivergent Electrochemical Synthesis of Optically Pure Menthylamines (2011) Angew. Chem. Int. Ed., 24, 5564

J Kusterer, RM Fritsch, M Keusgen, *Allium* species from central and southwest Asia are rich sources of Marasmin (2001) J. Agric. Food Chem., 59, 8289

P Laur, The first decades after the discovery of CD and ORD by Aimé Cotton in 1895 (2012) In: Comprehensive Chiroptical Spectroscopy, Volume 2: Applications in Stereochemical Analysis of Synthetic Compounds, Natural Products, and Biomolecules, First Edition, Eds.: N. Berova, P. L. Polavarapu, K. Nakanishi, and R. W. Woody, John Wiley & Sons, Inc.

CT Lee, WT Yang, RG Parr, Development of the Colle-Salvetti correlation-energy formula into a functional of the electron density (1988) Phys. Rev. B 37, 785

MW Lodewyk, MR Siebert, DJ Tantillo, Computational Prediction of H-1 and C-13 Chemical Shifts: A Useful Tool for Natural Product, Mechanistic, and Synthetic Organic Chemistry (2012) Chem. Rev., 112, 1839

N Martins, S Petropoulos, ICFR Ferreira, Chemical composition and bioactive compounds of garlic (*Allium sativum* L.) as affected by pre- and post-harvest conditions: A review (2016) Food chemistry, 211, 41

EW Meijer, Jacobus Henricus van 't Hoff; Hundred Years of Impact on Stereochemistry in the Netherlands (2001) Angew. Chem. Int. Ed., 40, 3783

B Mennucci, J Tomasi, R Cammi, JR Cheeseman, MJ Frisch, FJ Devlin, S Gabriel, PJ Stephens, Polarizable Continuum Model (PCM) Calculations of Solvent Effects on Optical Rotations of Chiral Molecules (2002) J. Phys. Chem. A, 106, 6102

G Mehta, SR Karra, Polyquinanes from (*R*)-(+)-limonene – enantioselective total synthesis of the novel tricyclic sesquiterpene (-)-ceratopicanol (1991) J. Chem. Soc. Commun., 1367
S Mithani, G Weeratunga, NJ Taylor, GI Dmitrienko, The Kinamycins are Diazofluorenes and Not Cyanocarbazoles (1994) J. Am. Chem. Soc., 116, 2209

E Mohr, Die Baeyersche Spannungstheorie und die Struktur des Diamanten (1918) J. prakt. Chem., 98, 315

E Mohr, Zur Theorie der cis-trans-Isomerie des Dekahydro-naphthalins (1922) Ber. Dtsch. Chem Ges., 55, 230

TF Molinski, DS Dalisay, SL Lievens, JP Saludes, Drug development from marine natural products (2009) Nature Rev. Drug Discovery, 8, 69

M Müller, CM Orben, N Schützenmeister, M Schmidt, A Leonov, UM Reinscheid, B Dittrich, C Griesinger, The Absolute Configuration of (+)- and (−)-*erythro*-Mefloquine (2013) Angew. Chem. Int. Ed., 52, 6047

DJ Newman, GM Cragg, Natural Products as Sources of New Drugs over the Last 25 Years (2007) J. Nat. Prod., 70, 461

S Omura, A Nakagawa, H Yamada, T Hata, A Furusaki, T Watanabe, Structures and Biological Properties of Kinamycin A, B, C, and D (1973) Chem. Pharm. Bull., 21, 931

F Partal Ureña, JR Avilés Moreno, JJ López González, Conformational study of (*R*)-(+)-limonene in the liquid phase using vibrational spectroscopy (IR, Raman, and VCD) and DFT calculations (2009) Tetrahedron: Asymmetry, *20*, 89

TB Pedersen, J Kongsted, TD Crawford, Gas Phase Optical Rotation Calculated from Coupled Cluster Theory with Zero-Point Vibrational Corrections from Density Funcional Theory (2009) Chirality, 21, E68

AF Peerdeman, The absolute configuration of natural strychnine (1956) Acta Cryst., 9, 824

TI Pehk, ET Lippmaa, VI Lysenko, II Bardyshev, ^{13}C NMR spectroscopy of terpenoids, related to menthane (1980) *Russ. J. Org. Chem.*, 1694

EA Perpète, C Lambert, V Wathelet, J Preat, D Jacqemin, Ab initio studies of the λ(max) of naphthoquinones dyes (2007) Spectrochim. Acta A, 68, 1326

AG Petrovic, A Navarro-Vazquez, JL Alonso-Gomez , From Relative to Absolute Configuration of Complex Natural Products: Interplay Between NMR, ECD, VCD, and ORD Assisted by ab initio Calculations (2010) Curr. Org. Chem., 14, 1612

EN Pitsinos, N Athinaios, VP Vidali, Enantioselective Total Synthesis of (-)-Laurenditerpenol (2012), Org. Lett., 14, 4666

M Pitzer et al., Direct determination of absolute molecular stereochemistry in gas phase by Coulomb explosion imaging (2013), Science, 341, 1096

PL Polavarapu, Kramers−Kronig Transformation for Optical Rotatory Dispersion Studies (2005) J. Phys. Chem. A, 109, 7013

PL Polavarapu, CL Covington, Comparison of Experimental and Calculated Chiroptical Spectra for Chiral Molecular Structure Determination (2014) Chirality, 26, 539

A Randazzo, G Bifulco, C Giannini, M Bucci, C Debitus, G Cirino, L Gomez-Paloma, Halipeptins A and B: Two Novel Potent Anti-inflammatory Cyclic Depsipeptides from the Vanuatu Marine Sponge *Haliclona* species (2001) J. Am. Chem. Soc., 123, 10870

F Reinscheid, UM Reinscheid, Stereochemical analysis of (+)-limonene using theoretical and experimental NMR and chiroptical data (2016a) J. Mol. Struct., 1106, 141

F Reinscheid, UM Reinscheid, Stereochemical analysis of menthol and menthylamine isomers using calculated and experimental optical rotation data (2016b) J. Mol. Struct., 1103, 166

F Reinscheid, M Schmidt, H Abromeit, S Liening, GKE Scriba, UM Reinscheid, Structural and chiroptical analysis of naturally occurring (−)-strychnine (2016) J. Mol. Struct., 1106, 200

BC Rinderspacher, PR Schreiner, Structure-property relationships of prototypical chiral compounds: Case studies (2004) J. Phys. Chem. A, 108, 2867

JH Robertson, CA Beevers, Crystal structure of strychnine hydrobromide (1950) Nature, 165, 690

R Robinson, The constitution of strychnine (1946) Experientia, 2, 28

L Rosenfeld, Quantenmechanische Theorien der natürlichen optischen Aktivität von Flüssigkeiten und Gasen (1928) Z. Physik, 52, 161

HG Rule, AR Chambers, Studies in solvent action. Part XIII. Optical rotatory power and the refractive index of the medium (1937) J. Chem. Soc., 145-153

H Sachse Ueber die geometrischen Isomerien der Hexamethylenderivate (1890) Ber. Dtsch. Chem. Ges., 23, 1363

H Sachse Über die Konfigurationen der Polymethylenringe (1892) Z. Physik. Chem., 10, 203

J Sandström, Chiroptical methods in conformational analysis (1995) Chirality, 7, 181

AM Sarotti, SC Pellegrinet, Application of the Multi-standard Methodology for Calculating 1H NMR Chemical Shifts (2012) J. Org. Chem., 77, 6059

W Schlenk, Recent Results of Configurational Research (1965) Angew. Chem. Int. Ed., 4, 139

M Schmidt, H Sun, P Rogne, GKE Scriba, C Griesinger, LT Kuhn, UM Reinscheid, Determining the Absolute Configuration of (+)-Mefloquine HCl, the Side-Effect-Reducing Enantiomer of the Antimalaria Drug Lariam (2012) J. Am. Chem. Soc.,134, 3080

M Schmidt, F Reinscheid, H Sun, H Abromeit, GKE Scriba, FD Sönnichsen, M John, UM Reinscheid, Hidden flexibility of strychnine (2014) Eur. J. Org. Chem., 6, 1147

N Schützenmeister, M Müller, UM Reinscheid, C Griesinger, A Leonov**,** Trapped in Misbelief for Almost 40 Years: Selective Synthesis of the Four Stereoisomers of Mefloquine (2013) Chem. Eur. J., 19, 17584

AI Scott, AD Wrixon, A symmetry rule for chiral olefins (1970), Tetrahedron, 3695

AB Sebag, DA Forsyth, MA Plante, Conformation and configuration of tertiary amines via GIAO-derived C-13 chemical shifts and a multiple independent variable regression analysis (2001) J. Org. Chem., 66, 7967

JM Seco, E Quinoa, R Riguera, The Assignment of Absolute Configuration by NMR (2004) Chem. Rev., 104, 17

EC Sherer, CH Lee, J Shpungin, JF Cuff, C Da, R Ball, R Bach, A Crespo, X Gong, CJ Welch, Systematic Approach to Conformational Sampling for Assigning Absolute Configuration Using Vibrational Circular Dichroism (2014) J. Med. Chem., 57, 477

VA Shubert, D Schmitz, D Patterson, JM Doyle, M Schnell, Identifying enantiomers in mixtures of chiral molecules with broadband microwave spectroscopy (2014), 53, 1152

G Snatzke, Circular Dichroism and Optical Rotatory Dispersion — Principles and Application to the Investigation of the Stereochemistry of Natural Products (1968) Angew. Chem. Int. Ed., 7, 14

PJ Stephens, FJ Devlin, JR Cheeseman, MJ Frisch, Calculation of Optical Rotation Using Density Functional Theory (2001) J. Phys. Chem. A, 105, 5356

PJ Stephens, DM McCann, E Butkus, E Stoncius, JR Cheeseman, MJ Frisch, Determination of absolute configuration using concerted ab initio DFT calculations of electronic circular dichroism and optical rotation: Bicyclo[3.3.1]nonane diones (2004) J. Org. Chem., 69, 1948

PJ Stephens, DM McCann, JR Cheeseman, MJ Frisch, Determination of absolute configurations of chiral molecules using ab initio time-dependent density functional theory calculations of optical rotation: How reliable are absolute configurations obtained for molecules with small rotations? (2005) Chirality, 17, S52

AF Thomas, Y Bessière, Limonene (1989) Nat. Prod. Rep., 291

DJ Tozer, RD Amos, NC Handy, BO Roos, L Serrano-Andres, Does density functional theory contribute to the understanding of excited states of unsaturated organic compounds? (1999) Mol. Phys., 97, 859

DJ Tozer, NC Handy, On the determination of excitation energies using density functional theory (2000) PhysChemChemPhys 2, 2117

PH Vaccaro, Chapter 11 in: Comprehensive Chiroptical Spectroscopy, Volume 1 (2012), First edition, Eds. N Berova, PL Polavarapu, K Nakanishi, RW Woody, John Wiley & Sons, New Jersey

J Vandenbussche, P Bultinck, AK Przybyl, WA Herrebout, Statistical Validation of Absolute Configuration Assignment in Vibrational Optical Activity (2013) J. Chem. Theory Comput., 9, 5504

KB Wiberg, PH Vaccaro, JR Cheeseman, Conformational Effects on Optical Rotation. 3-Substituted 1-Butenes (2003) J. Am. Chem. Soc., 125, 1888

KB Wiberg, Y-G Wang, PH Vaccaro, JR Cheeseman, G Trucks, MJ Frisch, Optical Activity of 1-Butene, Butane, and Related Hydrocarbons (2004) J. Phys. Chem. A, 108, 32

Wikipedia; chiral objects (2016):
https://upload.wikimedia.org/wikipedia/commons/thumb/e/e8/Chirality_with_hands.svg/300px-Chirality_with_hands.svg.png

Wikipedia; polarized light (2016):
https://upload.wikimedia.org/wikipedia/commons/thumb/7/77/Circular.Polarization.Circularly.Polarized.Light_With.Components_Right.Handed.svg/2000px-Circular.Polarization.Circularly.Polarized.Light_With.Components_Right.Handed.svg.png

SM Wilson, KB Wiberg, JR Cheeseman, MJ Frisch, PH Vaccaro, Nonresonant Optical Activity of Isolated Organic Molecules (2005) J. Phys. Chem. A, 109, 11752-11764

RB Woodward, MP Cava, WD Ollis, WD Hunger, HU Dabniker, K Schenker, The total synthesis of strychnine (1954) J. Am. Chem. Soc., 76, 4749

G Zhou, X Liu, X Liu, H Nie, S Zhang, W Chen, A Stereospecific Synthesis and Unambiguous Assignment of the Absolute Configuration of (−)-*erythro*-Mefloquine Hydrochloride (2013) Adv. Synth. Catal., 355, 3575

9. Own publication list

1. F Reinscheid, M Schmidt, H Abromeit, S Liening, GKE Scriba, UM Reinscheid (2014) Chiroptical analysis of the strychnine conformers derived from NMR data (Poster presentation), EUROMAR, Zürich, Switzerland

2. M Schmidt, F Reinscheid, H Sun, H Abromeit, GKE Scriba, FD Sönnichsen, M John, UM Reinscheid, Hidden flexibility of strychnine (2014) Eur. J. Org. Chem., 6, 1147-1150

3. F Reinscheid, UM Reinscheid, Stereochemical analysis of (+)-limonene using theoretical and experimental NMR and chiroptical data (2016a) J. Mol. Struct., 1106, 141-153

4. F Reinscheid, M Schmidt, H Abromeit, S Liening, GKE Scriba, UM Reinscheid, Structural and chiroptical analysis of naturally occurring (−)-strychnine (2016), J. Mol. Struct., 1106, 200-209

5. F Reinscheid, UM Reinscheid, Stereochemical analysis of menthol and menthylamine isomers using calculated and experimental optical rotation data (2016b) J. Mol. Struct., 1103, 166-176

6. F Reinscheid, UM Reinscheid (2016) Menthol and amino derivatives: configurational and conformational analysis (Poster presentation), EUROMAR, Aarhus, Denmark

9.1 Limonene publication

Stereochemical analysis of (+)-limonene using theoretical and experimental NMR and chiroptical data

F Reinscheid, UM Reinscheid (2016a)

J. Mol. Struct., 1106, 141-153

Stereochemical analysis of (+)-limonene using theoretical and experimental NMR and chiroptical data

F. Reinscheid[a], U.M. Reinscheid*[a]

Abstract: Using limonene as test molecule, the success and the limitations of three chiroptical methods (optical rotatory dispersion (ORD), electronic and vibrational circular dichroism, ECD and VCD) could be demonstrated. At quite low levels of theory (mpw1pw91/cc-pvdz, IEFPCM (integral equation formalism polarizable continuum model)) the experimental ORD values differ by less than 10 units from the calculated values. The modelling in the condensed phase still represents a challenge so that experimental NMR data were used to test for aggregation and solvent-solute interactions. After establishing a reasonable structural model, only the ECD spectra prediction showed a decisive dependence on the basis set: only augmented (in the case of Dunning`s basis sets) or diffuse (in the case of Pople`s basis sets) basis sets predicted the position and shape of the ECD bands correctly. Based on these result we propose a procedure to assign the absolute configuration (AC) of an unknown compound using the comparison between experimental and calculated chiroptical data.

Introduction

In the field of configurational analysis it is very important to use structural information since only then a reliable assignment of the absolute configuration of new molecules is possible.[1,2] Despite enormous progress in instrumentation and methods[3] structural analysis is still a challenge, illustrated by the review of Nicolaou and Snyder[4] who presented data based on which roughly 1000 articles published between 1990 and 2004 have to be revised because of structural reasons. Likewise, Maier[5] presented numerous recent examples of erroneous chemical formulas. One of the early configurational assignment strategies is based on the chiral recognition of unsaturated compounds with optically active lanthanide complexes measured by NMR. Offermann and Mannschreck[6] used limonene to demonstrate that the changes in chemical shifts by titrating

[a] F Reinscheid, UM Reinscheid *
NMR-based structural biology
Max-Planck-Institute of Biophysical Chemistry
Am Fassberg 11, 37077 Göttingen (Germany)
E-mail: urei@nmr.mpibpc.mpg.de

Supporting information for this article is given via a link at the end of the document.

the analyte with chiral lanthanide complexes can be used to determine the enantiomeric excess.

The chiral monoterpene limonene is an important starting material in chemical synthesis.[7-9] Moreover, it is used in the fragrance and food industry, and is an important synthetic material.[10] Limonene is biotransformed by a variety of organisms such as bacteria, fungi, and plants.[11] In this way, using appropriate species a number of synthetically important metabolites can be produced. One of the biosynthetic enzymes, limonene epoxide hydrolase, was recently used as test case for asymmetric biocatalysis.[12]

Limonene has served as chiral test molecule to investigate chiroptical methods such as vibrational circular dichroism (VCD), electronic circular dichroism (ECD), and optical rotatory dispersion (ORD), and even as inducer of chirality. After the early report of Noack[13] using the monoterpene menthol, Kobayashi et al.[14], Fukiji et al.[15a] and Aimi et al. [15b] were able to induce optical activity in achiral environments by limonene enantiomers. A review summarizes solvent chirality transfer in the field of supramolecular chemistry.[15c] In recent publications, the orientation of limonene enantiomers was measured by sum frequency vibrational spectroscopy, detecting surface chirality.[16]

In our report, we present a detailed analysis of spectroscopic data about (+)-limonene in order to (i) deliver detailed analytical data about the academically and industrially important monoterpene limonene and (ii) improve the methodology of chiral analysis. Based on the results for strychnine base and the protonated/HCl form,[17,18] we further explore the success and limitations of the absolute configuration (AC) determination using a comparison of experimental and calculated chiroptical data. Two recent publications nicely illustrate the importance of solvent modelling for the interpretation of chiroptical data.[19a] Consequently, we will discuss the influence of solvent models on the determination of the absolute configuration.

NMR and chiroptical data about limonene are combined, and all three major chiroptical methods (VCD, ECD, ORD) are applied. The importance to use more than one chiroptical method to determine the absolute configuration of a compound has been convincingly put forward by Polavarapu.[19b] As an example, the AC of two nonylphenols was determined by optical rotation and VCD analysis.[20] For one of the compounds (NP112) it is still unclear if the AC was correctly assigned due to impurity problems. The AC assignment of nonylphenol NP35[20] was confirmed by x-ray analysis.[21]

The present report is organized in the following way: First, the structural models of the relevant conformers are obtained together with their populations; second, population-weighted

chiroptical data are calculated for the structural models and compared to experimental values; third, conclusions derived from these comparisons are critically assessed.

Results

In order to develop a general procedure to analyse the configuration of compounds for which NMR data are available, limonene is a good choice since it serves as test molecule for NMR method development. For chemical shifts we used information from Skakovskii et al.[22] and Bohlmann et al.[23] In addition, deuterium NMR helped in assigning diastereotopic protons.[24] Assuming similar trends for both nuclei, protons and deuteriums, the calculations unambiguously assigned the methylene protons of limonene.

Structural models

Limonene represents a simple monoterpene (Figure 1). At first sight, it might be conformationally flexible in the six-membered ring. The conformational search (Discovery Studio, Accelrys,[25] Universal forcefield) of a model for *R*-limonene delivered two types of ring conformers which differed in the orientation of the isopropenyl substituent: equatorial or axial. However, the axial orientation of the isopropenyl substituent raises the computed energy substantially. Since the energy difference to the conformers with an equatorial isopropenyl substituent was larger than 2.5 kcal/mole, we can safely assume that almost exclusively the latter form exists in solution. Therefore, conformational averaging due to ring inversions cannot be taken as explanations in the course of spectrum interpretation.[24] It is more likely, that the rotation of the isopropenyl group is responsible for averaged signals in NMR spectra.

Figure 1: (+)-*R*-Limonene

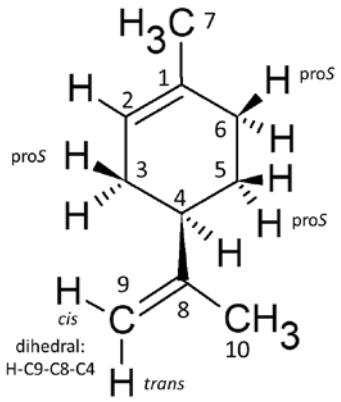

Having established the correct form with the isopropenyl group in the equatorial position, a full systematic conformational search was conducted using Discovery Studio. With the applied universial forcefield ten possible conformers were obtained with a cut-off of 2.5 kcal/mole higher than the lowest energy conformer. All ten were further geometry optimized with Gaussian09[26] (mpw1pw91/cc-pvdz; IEF-PCM: chloroform). During this step, only three optimized conformers remained (Figures 2A-D) indicating that most often non-stable conformations were generated in the forcefield search. Frequency calculations confirmed that all three are minimum structures due to the absence of vibrations with imaginary frequencies. The ring dihedrals only differ slightly among the isopropenyl rotamers, with differences smaller than 5 ° (Table 1). The isopropenyl dihedrals are similar (differences smaller than 4 °) to the dominant conformers calculated by Debie:[27] +132, -142, and -8 for conformer 1,2 and 3, respectively, which were obtained on the B3LYP/6-31g(d) level of theory in vacuo. For comparison, the axial conformer at lowest energy is also shown in Table 1. It is 1.9 kcal/mole higher in free energy compared to the highest in energy equatorial conformer (conformer 1) calculated at the mpw1pw91/cc-pvdz; IEF-PCM: chloroform level of theory.

Figures 2 A-D: Geometry-optimized (mpw1pw91/cc-pvdz, IEFPCM: chloroform) conformers

A: conformer 1

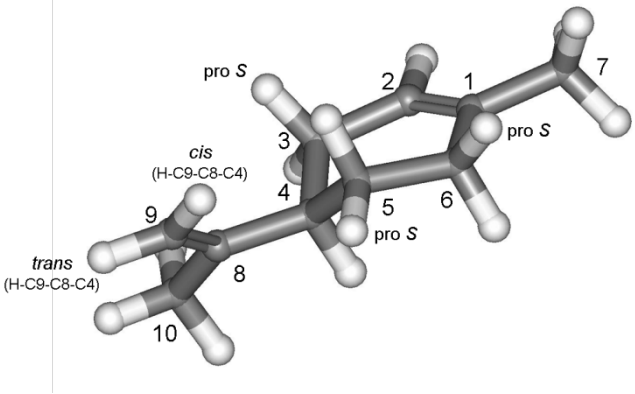

B: conformer 2

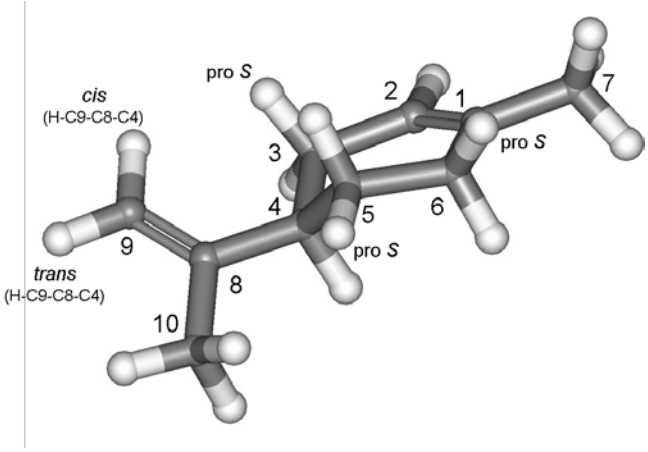

C: conformer 3

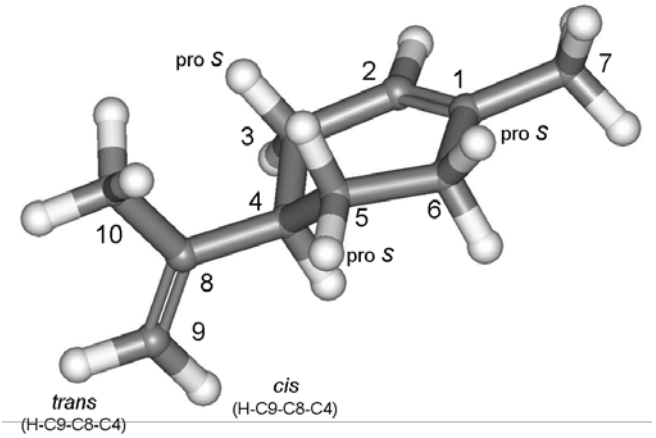

D: axial conformer

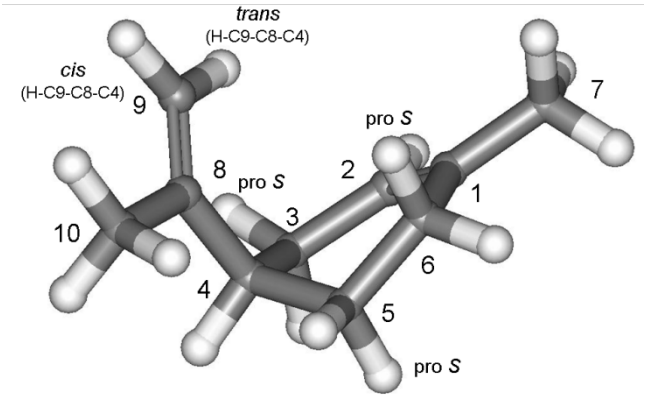

Table 1: (*R*)-Limonene dihedrals of the geometry optimized (mpw1pw91/cc-pvdz; IEF-PCM: chloroform) three conformers with an equatorial position of the isopropenyl group, and a geometry optimized conformer with an axial position of the isopropenyl group

dihedral	axial	equatorial conformer 1	Equatorial conformer 2	Equatorial conformer 3
C9-C8-C4-H4*	-134.16	129.52	-138.75	-8.03
H5pro*S*-C5-C6-H6pro*R*	-50.94	47.11	45.73	46.68
H5pro*R*-C5-C6-H6pro*R*	65.63	163.99	162.68	163.75
H5pro*R*-C5-C4-H4	-59.71	174.15	173.75	173.92
H5pro*S*-C5-C4-H4	56.51	-68.62	-69.47	-68.75
H3pro*R*-C3-C4-H4	78.29	166.02	170.99	166.95
H3pro*S*-C3-C4-H4	-36.23	50.62	55.16	51.54
H3pro*R*-C3-C2-H2	-43.25	-71.93	-74.95	-72.12
H3pro*S*-C3-C2-H2	71.21	43.07	40.06	42.86

*: isopropenyl dihedral

Population analysis

We followed two approaches for population analysis starting with the purely computational one. The three conformers differed in free energies depending on which level of theory and which solvent was used for modelling. Different levels of theory and two solvents (ethanol and chloroform) were used for frequency calculations and the free energy values are presented in Table 2. Using the Boltzmann equation we calculated the populations for the three conformers (Table 3). Since data with neat limonene have to be interpreted, it is important not to use only one solvent that might be an inappropriate substitute for limonene as solvent. So two largely different solvents and two different basis sets were used and the arithmetic mean for the calculated populations based on free energies were determined for conformer 1, 2, and 3 as 28 %, 38 %, and 34 %, respectively. The standard deviations of the calculated populations are 3 %, 6 %, and 3 %, respectively, which fits nicely to results from literature (e.g. glucose;[28] *endo*-borneol;[29] cylohexene oxides.[30] Interestingly, the calculated entropies are highest for conformer 2 at all levels of theory (Table 2).

Populations derived from calculated enthalpies differ (Table 2, Table 3) in that conformer 2 is less populated due to the neglect of entropic contributions (34:23:43). Since calculated entropies might be unreliable due to a large error associated with vibrations at low wavenumbers (< 200 cm^{-1}) it is not easy to decide if free energies or enthalpies deliver accurate energies for the population analysis. Applying a reasonable scaling factor in the thermochemical analysis does not solve the problem. Based on the literature[31-33] we can assume, that for the levels of theory in this study (mpw1pw91 as a functional, and the

Dunning`s basis sets) an average scaling factor of 0.97 can be assumed. Please note that Irikura et al.[34] suggested that only two digits are meaningful. As an example, using a scaling factor to zero-point vibrational energies and thermal corrections to enthalpies of 0.97, gives for the mpw1pw91/aug-cc-pvtz/IEFPCM (chloroform) level of theory the following populations for conformer 1, 2, and 3: 31%, 28%, and 41%, which differ to the values obtained using unscaled free energies or enthalpies.

Table 2: Calculated free energy differences in kcal/mole; in brackets: total entropy (in cal*mole^{-1}*K^{-1}); in bold: calculated enthalpy differences in kcal/mole(IEF-PCM for solvent modelling),

theory level	solvent	conformer 1	conformer 2	conformer 3
mpw1pw91/cc-pvdz	chloroform	0.097	0.113	0
		(100.5)	(101.3)	(100.3)
		0.135	**0.366**	**0**
mpw1pw91/aug-cc-pvdz	chloroform	0.246	0	0.078
		(100.0)	(101.8)	(100.1)
		0.136	**0.383**	**0**
mpw1pw91/aug-cc-pvtz	chloroform	0.284	0	0.134
		(100.3)	(102.0)	(100.3)
		0.142	**0.355**	**0**
mpw1pw91/cc-pvdz	ethanol	0.096	0.093	0
		(100.6)	(101.4)	(100.4)
		0.136	**0.403**	**0**
mpw1pw91/aug-cc-pvdz	ethanol	0.334	0	0.205
		(100.1)	(102.1)	(100.0)
		0.141	**0.405**	**0**
mpw1pw91/aug-cc-pvtz	ethanol	0.320	0	0.181
		(100.4)	(102.2)	(100.4)
		0.144	**0.423**	**0**

Table 3: Populations (in %) based on the Boltzmann equation using free energy differences, in brackets: enthalpy differences (IEF-PCM for solvent modelling)

theory level	solvent	conformer 1	conformer 2	conformer 3
mpw1pw91/cc-pvdz	chloroform	32 (34)	31 (23)	37 (43)
mpw1pw91/aug-cc-pvdz	chloroform	26 (34)	39 (23)	35 (43)
mpw1pw91/aug-cc-pvtz	chloroform	26 (34)	41 (23)	33 (43)
mpw1pw91/cc-pvdz	ethanol	31 (35)	32 (22)	37 (43)
mpw1pw91/aug-cc-pvdz	ethanol	25 (34)	44 (22)	31 (44)
mpw1pw91/aug-cc-pvtz	ethanol	25 (34)	43 (22)	32 (44)

The second approach for the population analysis represents a combination of experimental values and calculated data. Based on the three structural models for the conformers, we set out to calculate ^{13}C chemical shifts. Experimental data are readily available from literature

which is methodologically important since we want to draw conclusions from this study for the analysis of other molecules for which published values are available. In case of unstable molecules, or natural products for which no natural sources for re-isolation are available, it is then still possible to determine populations and to perform a configurational analysis.

The ^{13}C chemical shifts were used for the population analysis. There are three reasons for it: 1) it is an established parameter for discriminating isomers and conformers;[1] (2) The span between the different conformers is quite large for ^{13}C chemical shifts compared to proton chemical shifts; 3) For the following analysis it is very important to have enough data for calibration and prediction. If the two steps (calibration and prediction) are only based on few data, the results will become inaccurate. Three levels of theory were used, all three using the IEF-PCM solvent model with chloroform as solvent: theory level 1:mpw1pw91/cc-pvdz; theory level 2: B3LYP/6-311+g(d,p); theory level 3: PBEPBE*/*cc-pvtz.

Tables S1-3 (see supporting information) show the calculated data for the three conformers calculated on the three levels of theory. We first calibrated our calculated data in the following way: we selected resonances that did not differ much among the three conformers (cut-off value was ≤ 1.15 ppm). For the ^{13}C resonances fulfilling the requirement a linear regression with experimental values as x component was conducted. As y values the arithmetic mean of the shieldings of the three conformers were taken. The best fit to experiment was possible with theory level 1 (mpw1pw91/cc-pvdz) (Table 4) so that these calibration parameters (a and b from y = ax +b) were used (Fig. S4A and B, supporting information). The obtained parameters were then used to predict the experimental ^{13}C chemical shifts of the remaining nuclei which showed differences between the conformers larger than 3 ppm. From these predicted data, we obtained by a systematic variation of populations a best fit with experimental values with the following population mix: conformer 1, 2, and 3: 39 %, 31 %, and 30 %. The sum of CMAE (corrected mean absolute error; sum of absolute differences between calculated (using the linear regression) and experimental values, divided by the number of data pairs) and the variance was taken as indicator of the fit. The lowest sum of these values corresponds to the mentioned population mix which reproduced the experimental data at best. The populations of the experimental based approach are within ±10 % of the populations derived from the pure computational approach.

Table 4: Linear regression parameters

Level of theory	Slope/standard error	Intercept/ standard error	Regression coefficient R^2
mpw1pw91/cc-pvdz	-1.0092/0.002	195.27/0.23	0.99999
B3LYP/ 6-311+g(d,p)	-1.0759/0.015	182.45/1.54	0.99946
PBEPBE/ cc-pvtz	-1.0416/0.013	181.75/1.40	0.99522

Using the population mix of 39:31:30, the resonances with differences between the conformers of > 1.15 ppm were predicted and compared to experiment (Table 5). The very good match supports the view that the populations were accurately determined. All five resonances differ by less than 1 ppm between experimental and prediction. The corrected mean absolute error (CMAE) is 0.47 ppm. With the calculated populations (free energies, 28:38:34 and enthalpies 34:23:43) the CMAE is increased to 0.52 and 0.61, respectively. These values benefit from the internal referencing so that typical regression formulae based on a variety of compounds give much larger errors, e.g. 2.07 ppm of a mean unsigned error on the B3LYP/6-311+g(d,p)//6-31g(d) level of theory (van Eikema Hommes and Clark, 2005).[35]

Table 5: Predicted (mpw1pw91/cc-pvdz; IEF-PCM using chloroform as solvent), population-weighted (39:31:30) and experimental carbon chemical shifts

resonance	experimental	predicted
C3	31.5	31.8
C4	41.8	42.4
C5	28.6	29.1
C9	109.1	108.1
C10	21.5	20.9

Depending on the level of theory, calculated populations differ. Debie[27] reported 95.2 % equatorial and 4.8 % axial forms (B3LYP/6-31g(d), in vacuo) with respect to the isopropenyl group. Importantly, it was argued that the B3LYP functional gives unreliable energy differences for six-membered rings.[36] We did not find any axial conformer contributing substantially to the population mix, i.e. the lowest in energy was 1.9 kcal/mole higher in energy compared to the highest in energy of the three equatorial conformers.

The calculated populations of the equatorial conformers[27] differ from ours although the structures are quite similar (see above). For the corresponding equatorial conformers 1, 2, and 3 the populations were 31.1, 19.5, and 44.6. It was concluded that some bands in the IR and VCD spectra cannot be assigned, probably due to combination bands and overtones.[27] However, inaccurate populations could also be the reason since these were calculated in vacuo, but applied to simulate spectra obtained in solution. In addition, taking the populations from Debie[27] we obtained a worse match between experimental and predicted carbon resonances.

Under vacuum, reliable population predictions based on calculations might be easier. Śmiałek et al.[37] calculated a population mix for limonene of 55:29:16 (all with the equatorial position of the isopropenyl group; theory levels: geometry: MP2/cc-pvdz; energy: CCSD/cc-pvdz; all calculations in vacuo). Vacuum UV spectroscopy results agreed well with the calculated absorption frequencies.

We can conclude that literature data based on a pure computational approach differ significantly. Due to the importance of accurate and precise populations, we recommend a combined approach of experimental and computed data such as ^{13}C resonances.

Single point at 589 nm: $[\alpha]_D$

To assess the precision of the calculated ORD data, we applied several levels of theory for calculating the optical rotation of (+)-(*R*)-limonene assuming a 39:31:30 population mix. These values together with relative computational times are listed in Table 6. The arithmetic mean (seven levels of theory) of $[\alpha]_D$ is 119.5 with a standard deviation of 4.8 which matches very well to the experimental value of 113.8 (Table 7). On top of these uncertainties, the population mix might change up to ±5 % so that in extreme cases (34:36:30 and 44:26:30), the mean values are 96.8 and 142.8 and the standard deviations are 6.9 and 3.3. Using the populations based on free energies (28:38:34) the arithmetic mean and standard deviation amount to 71.2 (9.4), and with enthalpies (34:23:43) to 103.6 (5.5). Interestingly, only using the calculated optical rotation values, the best match with experiment ($[\alpha]_D$ of pure limonene: 122.8;[38]) is obtained with a population mix of 40:30:30, very close to the mix obtained using experimental carbon chemical shifts. It remains unclear why Leopold et al.[39] measured a $[\alpha]_D$ value of +96.6 for the neat compound at 21°C with a 98% purity assessed by GC.

It is important to look at the absolute values since we can assume from literature that low experimental $[\alpha]_D$ values in the range from -10 to +10 may have an incorrect sign. When analysing natural products with a low enantiomeric excess other optically active impurities might change the absolute value and sign of $[\alpha]_D$. In the case of limonene with absolute values in the range of 100, the experimentally determined sign is safe. The dependence of the calculated optical rotation on the population mix clearly limits the assignment of absolute configurations to cases with experimental absolute $[\alpha]_D$ values larger than roughly 10. This consists of (i) ± 5% population error which translates for $[\alpha]_D$ = 100 to ± Δ $[\alpha]_D$ = 5 and (ii) on top a computational error of ± 5 in calculating the specific optical rotation.

In order to compare the calculated uncertainties, experimental $[\alpha]_D$ data from literature[40] in different solvents are shown in Table 7. From these data a mean value of 113.5 and a standard deviation of 2.7 are calculated. In addition, using different solvents in the continuum model, similar differences are obtained (Table 8). The mean value is 114.4 and the standard deviation is 2.1. Therefore, it is reasonable to assume similar levels of precision for the solvent influence on $[\alpha]_D$ for the experimental and calculated data and the match between experiment and calculation is excellent. Consequently, the comparison between two different solvents is justified since this would introduce an error of 5% at maximum.

Table 6: Calculated $[\alpha]_D$ values of (+)-limonene (IEFPCM: chloroform) at different levels of theory using a population mix of 39:31:30 together with relative computational times

Number of theory level	Theory level	Relative Computational time	ORD at 589 nm with 39:31:30 population mix
1	mpw1pw91/cc-pvdz	1	111.4
2	mpw1pw91/aug-cc-pvdz	4	124.4
3	mpw1pw91/cc-pvtz	8	119.6
4	mpw1pw91/aug-cc-pvtz	60	126.2
5	b3lyp/6-311+g(d,p)	1	121.4
6	b3lyp/6-311++g(2d,2p)	4	115.1
7	b3lyp/aug-cc-pvdz	4	118.6

Table 7: Experimental $[\alpha]_D$ values of (+)-limonene in different solvents at 20°C ,[40] corrected by using the experimental value of Wilson et al.[38] for an homogenous sample (122.8) (experimental value for homogenous limonene was 124.2 by Rule and Chambers[40]

solvent	$[\alpha]_D$
methanol	108.5
acetonitrile	109.4
acetone	112.1
chloroform	113.8
cyclohexane	114.6
dichloromethane	114.7
homogenous	122.8

Table 8: Calculated (mpw1pw91/cc-pvdz) $[\alpha]_D$ values of (+)-limonene in different solvents (IEF-PCM solvent model)

solvents	conformer 1	conformer 2	conformer 3	with populations of 39:31:30
methanol	432.4	-141.3	-41.6	112.4
acetone	430.7	-136.5	-41.9	113.1
dichloro-methane	427.1	-126.5	-42.7	114.5
toluene	423.7	-117.0	-44.7	115.6
benzene	423.5	-116.3	-44.8	115.7
Chloroben-zene	422.2	-112.4	-43.3	116.8
aniline	419.4	-104.2	-43.0	118.4
ethanol (geo:eth)	431.1	-136.2	-42.0	113.3
ethanol (geo: $CHCl_3$)	430.7	-136.5	-42.3	113.0
$CHCl_3$ (geo: eth)	426.3	-124.0	-44.1	114.6
$CHCl_3$ (geo: $CHCl_3$)	426.6	-136.2	-42.5	111.4

Geo: geometry-optimization; eth: ethanol

In addition, we checked the influence of the solvent used in the geometry optimization in combination with a solvent change in the calculation of optical rotation at 589 nm of the three conformers (last four entries in Table 8). The specific optical rotation differed by 4.1 (4 %) at maximum.

To sum up, we can safely assume, that the structural models with a continuum model for solvent incorporation (IEF-PCM) are appropriate to be used for the prediction of optical rotation values of limonene.

To further broaden the applicability and to increase the reliability of the determination of the absolute configuration using ORD data, a multiple wavelength analysis was performed.

Multiple wavelengths ORD

The calculated values at different wavelengths (Table 9, Figure S5A supporting information) indicate a mono-signate curve down to 210 nm which can be easily and safely interpreted. The experimental values in chloroform as solvent are obtained at four wavelengths and are shown together with the population-weighted calculated values (Fig. 3). The experimental values can be used for comparison with the calculated values using methanol as solvent since we have demonstrated that the calculated values are quite insensitive for different solvents (see above), and the experimental values are only slightly affected by different solvents (see above). Calculated and experimental ORD values fit much better (Fig. 3) with the populations derived from experimental and calculated ^{13}C chemical shifts compared to the pure computationally derived populations.

Table 9: Calculated ORD values of (+)-limonene at different wavelengths using DFT (mpw1pw91/cc-pvdz, IEFPCM (methanol)

wavelength [nm]	conformer 1	conformer 2	conformer 3	Population mix 39:31:30
589	432.4	-141.3	-41.6	112.4
578	450.8	-152.9	-44.7	115.0
546	516.0	-161.7	-52.5	135.4
495	655.6	-202.2	-70.3	171.9
436	908.6	-272.9	-106.0	238.0
365	1501	-427.9	-206.3	391.2
300	2900	-754.9	-522.5	740.2
280	3815	-951.1	-782.7	958.5
265	4869	-1165	-1129	1199
254	5991	-1384	-1548	1443

235	9331	-1995	-3083	2095
220	15034	-2950	-6662	2950
210	23055	-4126	-13930	3533
200	43171	-5457	-52063	-473.9
190	89442	-26453	33285	36667
180	-5907213	-36973	631678	-2125771
170	1603338	-567424	-369051	338685
160	-154568	-1350916	101897	-448496

Figure 3: Experimental ORD values of (+)-limonene (chloroform, 22.4 mg/ml, 20.4°C) at four wavelengths (corrected by using the chloroform $[\alpha]_D$ value (113.8) of Rule and Chambers [40] which was itself corrected by a factor using the value of a homogenous sample of Wilson et al.[38]) and calculated ORD values (mpw1pw91/cc-pvdz, IEFPCM (methanol); In red: experimental; In black: mix 39:31:30 based on chemical shift prediction; In orange: mix 28:38:34 based on calculated free energies; In blue: mix 34:23:43 based on calculated enthalpies

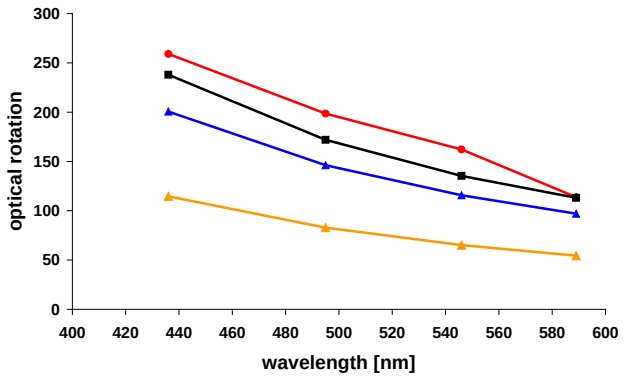

In addition, experimental values obtained from the gas phase at 365 nm and 633 nm, fit very well to the calculated data in vacuo (Table S5C, supporting information). The calculated data in Figure 3 directly follow the experimental values in magnitude and sign. If the wavelengths and/or the rotational strengths of the cotton effects are largely inaccurate and at the same time inverted, the assignment of the absolute configuration based on the optical rotation dispersion shown in Figure 3 would be incorrect. Since these conditions are very unlikely the AC of limonene can be derived from the ORD analysis. We can safely conclude that (+) limonene has *R*-configuration.

UV-Vis / ECD

A number of levels of theory were applied for the calculation of rotational strengths of cotton effects (Figures 4). Based on the calculated rotational strengths of the 10 excitations lowest in energy and a line broadening of 0.4 eV, the spectra in Figures S6 A-I for conformer 1, Figures S7 A-I for conformer 2, and Figures S8 A-I for conformer 3 were obtained (supporting information). In addition, the calculated UV spectra for the conformers at different levels of theory are shown in the supporting information (Figures S10-S12). It is important to note, that one level of theory was not able to deliver the longest wavelength absorption around 210 nm which was clearly observable in the experimental UV-Vis spectra. No wavelength shift was applied to allow an unbiased comparison. To obtain a robust computational result for comparison with experiment, we calculated the population average (39:31:30 for conformer 1, 2 and 3) of all levels of theory (Figures 4 A-I).

It is very important to measure samples with different concentrations since only then weak ECD signals can be observed (high concentration), and at the same time appropriately low noise levels are obtained (low concentration) for strong ECD signals. Two concentrations were measured in methanol and are depicted in Figure 5 A and B (UV: Figure S13 A and B) to illustrate the concentration effects. We want to emphasize that this is not related to concentration effects due to aggregation. It is an important technical requirement. An ECD spectrum measured in ethanol is also presented (Fig. 5 C; UV spectrum: Fig. S13 C). Inspection of the spectra obtained at different concentrations indicates no aggregation effects that would shift the position of the cotton effect. In addition, the same results were observed for methanol and ethanol as solvent. From these results, we conclude that the solvent modelling presents no problem for our structural models when calculating UV-Vis and ECD spectra. A negative band can be seen around 195 nm and a positive band around 210 nm. These two decisive bands can be found in the calculated spectra (negative band at 196 nm, positive band at 228 nm) if Dunning`s augmented basis sets or a Pople basis set with diffuse and polarization functions are applied (Figures 4: levels of theory: B, D, F, H, and I). Importantly, spectra using the cc-pvdz and cc-pvtz basis sets would lead to a wrong absolute configuration assignment if a red shift would be applied to the calculated data of the theory levels A, C and E. Without a red-shift, level G would lead to a wrong AC assignment. These conclusions also hold for the different population mixes based on calculated energies (Fig. S9, supporting information). Inspection of the rotational strength (and also dipolar strength) does

not help for the decision to apply a red-shift or not since similar ratios of the two bands were obtained for the different basis sets.

Applying basis sets with diffuse functions, we can safely assign the absolute configuration of (+)-limonene based on the comparison of the ECD bands.

Figures 4 A-I: Calculated, population-weighted (39:31:30) ECD spectra of (+)-limonene for the different levels of theory A-I; x-axis: wavelength [nm]; y-axis: $\Delta\varepsilon$ [Mol*l^{-1}*cm^{-1}] (IEFPCM using ethanol as solvent)

A: mpw1pw91/cc-pvdz, cost[a]: 1

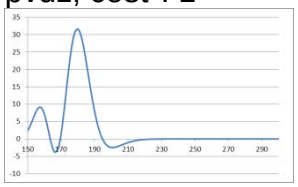

B: mpw1pw91/aug-cc-pvdz, cost[a]: 7

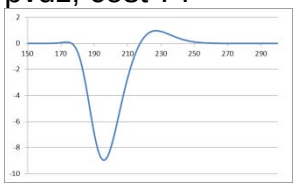

C: mpw1pw91/cc-pvtz, cost[a]: 14

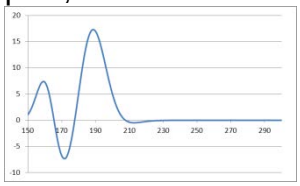

D: mpw1pw91/aug-cc-pvtz, cost[a]: 140

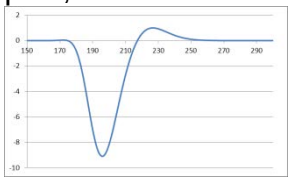

E: B3LYP/cc-pvdz, cost[a]: 1

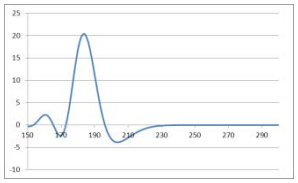

F: B3LYP/aug-cc-pvdz, cost[a]: 7

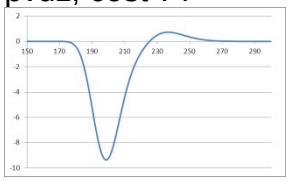

G: B3LYP/cc-pvtz, cost[a]: 14

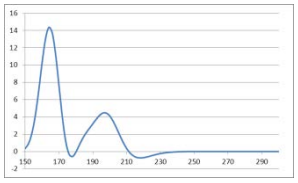

H: B3LYP/aug-cc-pvtz, cost[a]: 140

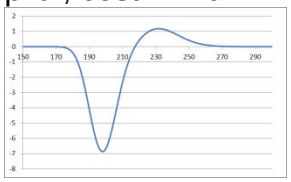

I: B3LYP/6-311++G(2d,2p),cost[a]: 7

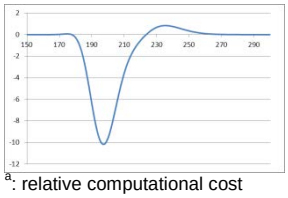

[a]: relative computational cost

Figures 5 A-C: Experimental ECD spectra of (+)-limonene in methanol or ethanol at different concentrations (on the x-axis: wavelengths in nm, on the y-axis $\Delta\varepsilon$ [Mol*l^{-1}*cm^{-1}]; A: 2.7 mg/ml in methanol; B: 0.1 mg/ml in methanol; C: 2.4 mg/ml in ethanol

A

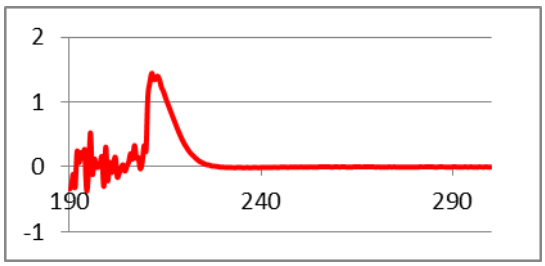

B

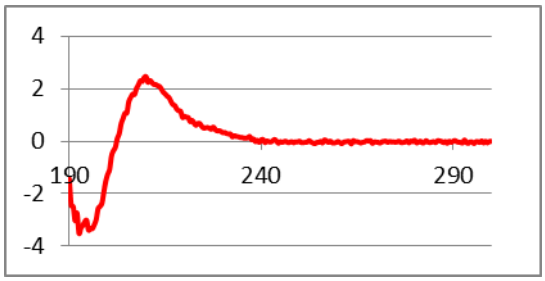

C

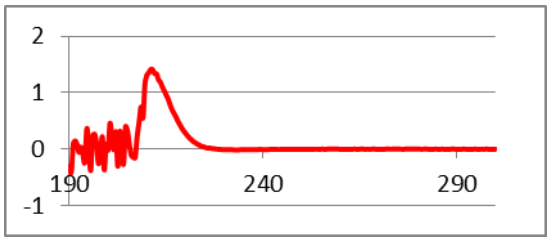

VCD

A number of reports presented VCD spectra of limonene in the past[27,41,42] also encompassing rarely measured areas of wavenumbers (near infrared, C-H stretching region). We measured the most often used range of wavenumbers between 1800 cm^{-1} and 1000 cm^{-1}. Since pure limonene was used, the calculations used different solvents (chloroform and ethanol) to find a better mimic for limonene as solvent. In addition, different levels of theory were applied (Table 10) and the average of all calculated data was used to construct a calculated VCD spectrum using lorentzian line shapes with a half width at half height of 4 cm^{-1}. The calculated and the experimental VCD spectra are shown in Figures 6 and 7. Calculated spectra for each conformer at different levels of theory can be found in the supporting information (Figures S14-

S17). It is important to note, that for these figures no shift in wavenumbers has been applied. It can be seen that there is no 1:1 match between the spectra concerning the band position, shape and intensity. Therefore, we propose the following qualitative analysis: we concentrate on the most significant stretch of bands in the experimental spectrum as being decisive for the conclusion if the calculated and experimental spectra match or if the inverted, calculated and the experimental spectrum matches, i.e. we focus only on the question of absolute configuration. This heavily depends on the correctness of a number of assumptions: the structural model represents one of the two enantiomers and no other molecule; the decisive bands are not inverted by matrix effects that have not been modelled; the position and sign of the decisive stretch of bands is correctly assigned.

In the case of limonene it is straightforward to select the decisive stretch of bands (i.e. large signal to noise ratio, at least 10; each band with a width of 10 cm^{-1} at minimum; peak to peak difference of 10 cm^{-1} at minimum; continues stretch of bands with isolated position): the bands around 1325 cm^{-1}, 1300 cm^{-1}, 1240 cm^{-1}, and 1200 cm^{-1} can be classified as decisive, giving the pattern +/-/+/- with intensities as medium /medium/strong/medium (Fig. 7 B). Although the last two are quite near, the shape renders them well separated: a width and separation of at least 10 cm^{-1}. However, since the accuracy of the calculated band positions is unknown and even sophisticated methods are not able to give precise answers,[27] it is important to compare the whole stretch of possible decisive bands.

In the case of limonene we are therefore left with a stretch of four bands that we then call enantiodiscriminative. They are robustly calculated (different levels of theory, different solvents), and can be found at 1360, 1320, 1280 and 1230 cm^{-1}, Fig. 7A). From the match with experiment we safely conclude that (+) limonene has *R*-configuration. All other interpretations of these bands do not fit with experiment (compare Fig. 7 B and 8, representing the calculated spectrum of (*S*)-limonene).

Table 10: Calculated VCD spectra of (+)-limonene of the three conformers at different levels of theory

short notation	theory level	solvent (IEF-PCM)
a	mpw1pw91/aug-cc-pvtz	chloroform
b	mpw1pw91/cc-pvdz	ethanol
c	mpw1pw91/aug-cc-pvtz	ethanol
d	mpw1pw91/cc-pvdz	chloroform
e	mpw1pw91/aug-cc-pvdz	chloroform

Figure 6: Calculated (level of theory a) VCD spectra of (+)-limonene of the three conformers and a population weighted mix 39:31:30 (on the x-axis: wavenumber in cm^{-1}, on the y-axis $\Delta\varepsilon$ [$Mol*l^{-1}*cm^{-1}$]

Conformer 1

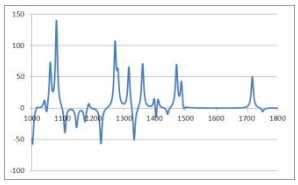

Conformer 2

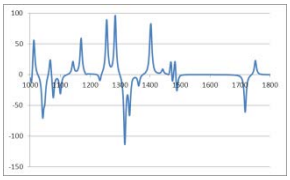

Conformer 3

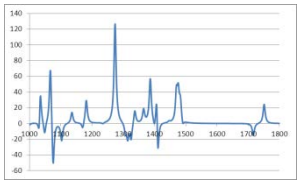

Population mix (39:31:30)

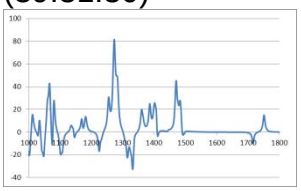

Figure 7A: Calculated VCD spectrum of (+)-limonene (theory level a) using a population-weighted mix of 39:31:30 from 1420 cm^{-1} to 1000 cm^{-1} (on the x-axis: wavenumber in cm^{-1}, on the y-axis $\Delta\varepsilon$ [$Mol*l^{-1}*cm^{-1}$]

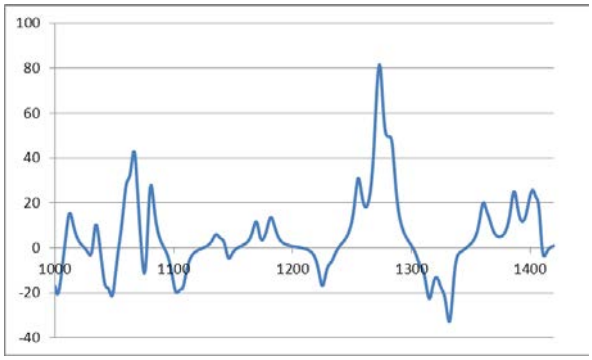

Figure 7B: Experimental VCD spectrum of pure (+)-limonene**:** Region 1420 cm^{-1} to 1000 cm^{-1}, on the x-axis: wavenumber in cm^{-1}, on the y-axis $\Delta\varepsilon$ [$Mol*l^{-1}*cm^{-1}$]

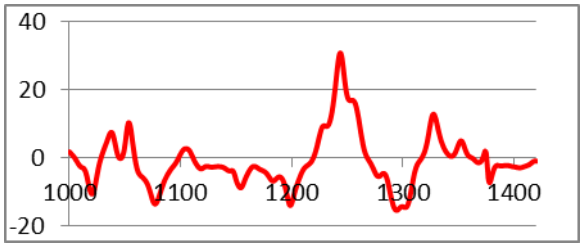

Figure 8: Calculated VCD spectrum of (−)-(*S*)-limonene (theory level a; population mix of 31:39:30, on the x-axis: wavenumber in cm^{-1}, on the y-axis $\Delta\varepsilon$ [$Mol*l^{-1}*cm^{-1}$]

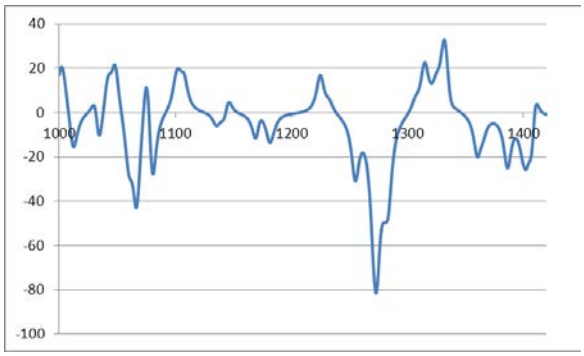

Discussion

ORD

Early attempts to correlate solvent effects on the optical rotation values with the refractive index[43] could already be rejected by Rule and Chambers.[40] Our results indicate that small solvent induced optical rotation changes could be explained by small population differences. However, an even likely explanation can be given based on the different calculated optical rotation values depending on the solvent used for modelling.

Lauricella et al.[44] tried to analyse the conformers of limonene by studying the temperature dependence of the optical rotation at 589 nm. Interestingly, the authors explained the variation of rotivity in vacuo (Ω_0; the rotivity is defined as $\Omega = [\alpha] / (n^2 + 2)$, with $[\alpha]$ as measured optical rotation, and n as refractive index of the sample) at different temperatures with a shift in the population mix: increasing the temperature resulted in decreased rotivities in vacuo. Using our population mix based on experimental ^{13}C resonances, we can support this view: increasing the temperature increases the populations of conformer 2 and 3 which have calculated negative optical rotation values so that the decrease of the experimental values with increased temperature is explained.

Pedersen et al.[45] investigated the temperature effects on ORD values of limonene using coupled cluster calculations. They compared the results for three conformers with experimental gas phase data at 355 nm and 633 nm. The conformers are the three equatorial conformers that we have found. The calculated ORD values (355 nm: 184.5; -1501.0; 543.2// 633 nm: 11.6, -340.4, 112.0) differ from ours indicating that the level of theory and the incorporation of solvent affects the results. Interestingly, after assessing vibrational effects, the

match with experiment was worse for CCSD compared to B3LYP: at 355 nm (-268.2 versus -311.1; exp: -315.5).[45] Likewise, the incorporation of vibrational averaging for six conformational rigid molecules did not improve the prediction of the optical rotation, maybe since the calculations were performed in vacuo and the experimental data were obtained in ethylcyclohexane.[46] Therefore, typical polarization effects of the solvent were neglected. In addition, Mort and Autschbach[46] concluded that the incorporation of vibrational effects on the ORD might not be sufficient to obtain accurate results as exemplified for methyloxirane and methylnorbornanone.

A publication on the gas phase optical rotation of limonene demonstrated that very small amounts of analyte can be measured: a detection limit of 20 ng was determined.[47] The cavity-ring-down polarimetry was applied in a more recent study to measure the optical rotation of limonene in the gas phase at 355 nm and 633 nm.[38] The value of this technology is the absence of complicating solvent effects since their modelling is one of the critical points in the determination of absolute configuration using the comparison between calculated and measured chiroptical data. The archetypical problematic molecule, methyloxirane, could be measured, and gas-phase values compared with the condensed phase values. Since methyloxirane is regarded as rigid, complicating solvent effects on the population mix of conformers cannot be the reason for unsuccessful modelling of optical rotation values. One possible explanation is the inappropriate modelling of static versus dynamic distribution of electron density, which might explain the solvent dependence of the optical rotation of methyloxirane. To date, explanations are not conclusive.

Regarding the possible accuracy, two studies about the accuracy of ORD calculations are still valuable.[48] From comparisons between experiment and calculation, the authors concluded that on a 95 % level of confidence, the correct absolute configuration could be predicted with confidence limits of ±60 deg /(dm*(g/cm^{-3})).[48] In addition, Mennucci et al.[49] presented the successful application of the IEF-PCM approach to account for solvent effects based on electrostatics.

Experimental optical rotation values for limonene[38] gave values that are very similar to our calculated data assuming a 39:31:30 population mix. This parallels the data of Wilson et al.[38] since they obtained (B3LYP/cc-pvdz) at 355 nm a specific ORD of 270.3, and at 633 a value of 76.3, similar to our calculated data and the experimental values. However, the authors did not give detailed information how they obtained the three conformers, and which data they

used for Boltzmann weighing of the conformers, nor they presented the individual ORD data for the conformers.

The importance of conformational effects on the ORD has been nicely described by Wiberg et al. [50] for a number of 3-substituted 1-butenes. Changing the temperature shifted the experimental ORD values which could be explained by a change in the conformer population, e.g. of 3-chloro-1-butene. However, the calculated ORD values of 3-chloro-1-butene were a factor of two larger compared to experiment, independent of the wavelength in the range from 589 nm to 250 nm. The reason for this large discrepancy (e.g. 589 nm: −188.1 (calc), −73.5 (exp)) is not yet known, effects of vibrations have been investigated and were found to be present, but no conclusive explanation could be made. In a subsequent article, Wiberg et al.[51] analysed 1-butene, butane and related hydrocarbons. They realized that the choice of basis set is very important to accurately calculate ORD values. Diffuse functions should be used (augmented basis sets in the case of Dunning`s correlation consistent basis sets such as cc-pvdz, aug-cc-pvdz). However, Rinderspacher and Schreiner[52] emphasized that the balanced nature of the basis set is the important aspect. Concerning the basis set, in the recent study of Hedegård et al.[53] it was shown that the aug-cc-pvdz basis set often led to significant deviations from the basis set limit. This is in contrast to the study of Grimme et al. .[54] Since the more recent study used a larger number of molecules, it is likely that the often recommended usage of basis sets with diffuse functions must still be handled with caution.

Concerning the level of theory, Crawford et al.[55] concluded that TD-DFT exhibits the cotton pole at higher wavelengths in the case of diffuse, Rydberg states when compared with CCSD calculation. Applying the mpw1pw91/cc-pvdz level of theory, the calculated ORD values of limonene at four wavelengths matched very well to the experimental values obtained in solution, with relative differences smaller than 5 %, and absolute deviations smaller than 5. In addition, previous work on a minor conformer of strychnine indicated that the mpw1pw91/cc-pvdz level of theory is superior to the “working horse” of geometry optimization, i.e. B3LYP/6-31G(d).[17]

ECD

Very early, Scott and Wrixon[56] compiled ECD values of chiral olefins. However, inappropriate application of the octant rule led to a by chance correct assignment of limonene which was proven by Brint et al. .[57] The positive band of (+)-*R*-limonene (equals *D*-limonene) around 210 nm measured in solution was assigned as π to π^* transition in agreement with the octant

rule.[56] However, gas-phase measurements revealed the presence of two positive bands at 218 nm and 210 nm which are assumed to belong to the same transition.[57] These authors assigned this positive band to a π to 3s transition which is well known to show a blue-shift in solution. By chance, this positive band was taken erroneously by Scott and Wrixon[56] as π to π^* transition, which followed the octant rule. However, limonene follows an anti-octant rule, and Brint et al.[57] mention two other cases of this behaviour. Generally, the octant rule should not be applied any more for configurational purposes. However, it remains interesting to study this empirical rule, especially the reasons why it fails.

For calibration of the ECD bands, the accuracy with which the UV-Vis spectrum can be calculated is very important. As a good starting point, the study of Perpète et al.[58] can be used. They studied the λ_{max} values of dye molecules. Since focusing on a chemically related group of molecules will very often lead to a bias towards, in this case, higher accuracy of the calculated data, we have to be cautious and take the reported values as minimum error levels. A mean absolute error of 20.1 nm (0.113 eV) was found for a group of 86 naphtoquinone dyes in various solvents. Calculations slightly overestimated the λ_{max} values (mean signed error of −7.2 nm (0.039 eV). Linear regression could not improve the prediction significantly which can be interpreted that systematic error is not the main reason for the errors. The equation of the regression was: λ_{max} (exp) = 36.687 + 0.9053 λ_{max} (calc). This led to a mean absolute error of 19.9 nm, not significantly improved compared to the non-fitted value from above.

Autschbach et al.[59] proposed to use an overall damping of 0.2 eV to simulate ECD spectra from calculated rotational strengths. In our work, we used several values, and decided to rely on a broadening value that allows the best match between the experimental and calculated UV-Vis bands. The latter point is also related to the accuracy with which the rotational strengths are calculated. Based on own results,[17,60] we can assume differences of a factor of two between calculation and experiment concerning the rotational and dipolar strengths.

Conformational flexibility in solution often complicates the analysis since all populated conformers have to be taken into account. In this case solid state ECD could offer the possibility to calculate only the conformer which is found in the crystal. From the crystal structure obtained by x-ray, the ECD spectrum can be calculated and compared with experiment to assign the AC. However, as stated by Pescitelli,[61] the influence of intermolecular interactions can hardly be predicted.

The main conclusion from our calculations is that non-diffuse basis sets do not show the important positive band around 220 nm so that a reliable AC determination is not possible. In

contrast to the ORD results, for the ECD calculation it is imperative to use augmented Dunning`s basis sets or Pople basis sets with diffuse functions for the correct prediction of the AC of limonene.

VCD

The importance of limonene as test molecule is demonstrated by a recent study of Rhee et al. .[62] They measured VCD spectra of 1.2 to 1.5 M solutions of limonene in CCl_4 on a femtosecond time scale. The authors mention that this method could deliver molecular motion pictures of chiral processes. However, the methodology is far from being established and the necessarily high concentrations of analyte will be an obstacle in the future. Furthermore, based on calculated energies in vacuo (not specified which ones) Rhee et al.[62] calculated populations (29:17:54; MP2/6-311++G**) that differ largely from the ones of the present article (39:31:30). Since Rhee et al.[62] used these populations to simulate VCD spectra, the comparison with experimental data obtained in CCl_4 as solvent is problematic. Surprisingly, QM/MM MD simulations with explicit solvent molecules gave similar VCD spectra with populations that resemble more the populations in the present article. Obviously, the good match to experiment was by chance with respect to the populations used.

A number of publications have used limonene as test molecule for VCD measurements (e.g. self-deconvolution of VCD spectra;[42] spectral standard).[63] In addition, limonene has been used as test molecule for Raman optical activity spectroscopy.[64] The mostly applied mid-IR spectral range used for VCD ranges from 1800 cm^{-1} to 1000 cm^{-1} since skeleton vibrations near to the stereocenters are typically in this area. Polavarapu et al.[41] and Abbate et al.[65] studied the CH stretching region which is not often used in VCD analysis. Likewise, Singh and Keiderling[66] studied limonene using VCD in the CH stretching region and in the region of the important skeleton vibrations. They also started an interpretation of the spectra but this was based on the assumption of only two conformers which can be rejected by our data and other literature studies. The VCD bands that we have identified as decisive for the determination of the absolute configuration were also measured by Singh and Keiderling.[66]

Although VCD spectra can be much more difficult to interpret for assigning the absolute configuration, a number of studies have been published in the area of natural product analysis (e.g. Gordillo-Román et al.).[67] The very active research group of Avilés Moreno especially deals with the VCD analysis of natural products, such as limonene oxide [68] and carvone.[69]

Partal Ureña et al.[70] studied limonene using the combination of IR, VCD and computations. Using experimental and calculated chemical shifts for the populations, we have determined different populations. Interestingly, with incorporation of a solvent model, our populations based on enthalpies are very similar to the populations calculated by Partal Ureña et al.[70] and Pedersen et al.,[45] both calculated in vacuo.

A systematic approach for assigning the absolute configuration using VCD has been proposed by Sherer et al. .[71] However, even ibuprofen was a difficult case since additional information i.e. dimerization, had to be taken into account, not included by the systematic approach.

Vandenbussche et al.[72] presented a statistical validation of absolute configuration assignment using VCD for a series of quinolizine molecules. Polavarapu and Covington[73] presented dissymmetry factors as similarity measures for the analysis of VCD, ECD, and Raman optical activity spectra. The scientific community has not reached consensus in using a protocol to obtain a similarity factor when comparing experimental and calculated chiroptical spectra. Most often the harmonic approximation is used for the calculations so that anharmonic contributions are neglected which will be one of the reasons of mismatch between experiment and calculation. The importance of anharmonicity was shown by Cappelli et al.[74] for the test molecule formaldehyde. Current computer resources often limit a full anharmonic treatment of molecules larger than 30 atoms.

Perspectives for chiroptical analysis

A clear advantage of the ECD based configurational analysis is the low amount of compound that is needed for measurements. At the same time, aggregation effects will play the smallest role compared to the two other chiroptical methods, ORD and VCD. In this respect, ORD is intermediate but offers a remarkable number of advantages: it is easy to measure; the reliability can be increased by using short or long wavelengths; it is the only information regarding the absolute configuration of natural products isolated in the past, which are meanwhile decomposed and cannot be isolated again.

A further advantage for ECD is the possibility to use UV-Vis spectra as reference for the wavelength and intensity scale. Of course, VCD benefits in the same way from the comparison with the IR spectrum. However, the large concentrations needed due to the 10-100 fold lower intensity compared to ECD, renders the interpretation of the VCD spectrum very complicated

due to low signal to noise ratios and possible aggregates. Especially the comparison with the calculated VCD spectrum for the assignment of the absolute configuration, will depend on the correct assumption of a single, solvated molecule since most often this represents the structural model for which the spectrum is calculated.

Conclusions

The present study about limonene gave important insights into the configurational analysis of small organic molecules using well known spectroscopic methods of NMR, VCD, UV-Vis, ECD, and ORD. To sum up, the main points are:

1. The current computational resources are able to identify the existing conformers in solution. However, in case of large and highly flexible compounds[75] experimental constraints are needed, mainly from NMR experiments, to narrow down the theoretical conformational space. In addition, the successful structural modelling of highly aggregating compounds depends on experimental information.

2. The populations should be determined with a combination of experimental and calculated data. Multi-standard methodologies for chemical shift calculations has been reviewed[76] and recently proposed.[77] Several systematic approaches in the field of structural analysis based on NMR data have been presented.[78] An early multiple regression analysis was presented by Sebag et al.[79] for tertiary amines. We term our approach “internal referencing” since resonances of the molecule itself are used for referencing. A similar approach has been presented by Andrews and Spivey.[80] They used reference molecules with known experimental chemical shifts which can be taken as fragments of the unknown molecule for which the shieldings are calculated. This approach differs from ours in that we directly take resonances of the unknown molecule for referencing. Obviously, our approach needs medium-sized molecules in order to have sufficient resonances for calibration/prediction. As an advantage, over-fitting can be easily discovered and corrected.

3. The chiroptical methods differ in a practical sense (amount needed, solubility etc.) but also in the response to the molecule under study leading to different signal to noise ratios.

4. Although all three chiroptical methods delivered the correct absolute configuration of limonene, it is a must to use at least two of them to assign the absolute configuration of an unknown compound.

The following procedure is proposed:
A. Achiral methods must agree on the same pair of enantiomers, i.e. all NMR and mass spectrometry data, as the two main methods, agree in the same structural model. In our experience, full assignment of resonances (including nitrogen), 2D NMR spectra fully interpreted (NOESY, COSY, HSQC, HMBC), proton and carbon 1D spectra with high resolution, homonuclear and heteronuclear scalar couplings (quantitative or qualitative), distances (qualitative from NOE intensities) are at present the complete requirements for a structural model of an unknown compound. In some cases, less information will also be sufficient. This is left to the NMR spectroscopist. Mass data must fit to the NMR derived structural model.

B. All single steps of absolute configuration assignment must fulfil basic requirements.

1. The application of a number of reasonable levels of theory does not change the sign of the specific optical rotation, ORD, ECD, and VCD data.

2. Absolute values of the experimental specific optical rotation at 589 nm should be larger than 60. This range of only unreliably predictable optical rotations (AC assignments) will be narrowed down in a current research project about menthol isomers.[81]

3. The experimental and calculated ORD curves at three or more wavelengths spanning at least 100 nm show no zero crossing.

4. The application of a reasonable wavelength shift (not more than 20 nm) does not change the AC assignment based on ECD spectra.

5. There are no two or more enantiodiscriminative stretches of VCD bands with opposite AC assignment.

For limonene we could show that for the specific optical rotation at 589, the ORD values and VCD bands no sign change occurs if a number of reasonable levels of theory are applied. However, the ECD data cannot be used successfully since the AC assignment depends on the basis sets applied. In addition, the absolute value of the experimental specific optical rotation is larger than 60, and the ORD curve with 4 wavelengths show no zero crossing so that all chiroptical methods except ECD (specific optical rotation > 60, ORD, and VCD) can be applied for the AC assignment.

Experimental Section

(*R*)-(+)-limonene was purchased from Aldrich (> 99.0 % purity).

IR and VCD spectroscopy
The VCD measurements were done with a VERTEX 80 FT-IR spectrometer equipped with a PMA 50 photoeleastic modulator and MCT-Detector (D313/B-A) (Bruker Optics). The VCD spectra were recorded with a 2-hour data collection time at 4 cm^{-1} resolution using a cell with BaF_2 windows. Spectra were measured at 22°C as a neat solution with a path length of 0.1 mm.

ORD measurements
Optical rotation measurements were performed using methanol and chloroform as solvents (22.4 mg/ml) at 20°C (Polartronic-E polarimeter, Schmidt+Haensch GmbH&Co).

ECD/UV-Vis spectroscopy
ECD spectra were obtained with a Jasco J-810 spectrometer at 25°C. A cell with a pathlength of 1 mm was used, five scans were accumulated with a scan speed of 50 nm/min, 0.5 nm pitch between 190 nm and 300 nm.

Computational details
A model of *R*-limonene was built in GaussView 5.0. A conformational search using the BEST algorithm with the universal force field was performed using DISCOVERY Studio (Accelrys, 2009).[25] DFT calculations were performed with Gaussian09 RevA.02[26] on various levels of theory for geometry optimization, energy calculations, and spectroscopic properties. The ten lowest in energy excitation wavelengths and corresponding dipolar and rotatory strengths were calculated. Energies were obtained at 298.15 K and 1 atmosphere of pressure. The lowest energy conformer was taken as reference, set to 0 kcal/mole and the resulting energy differences were used to calculate populations according to the Boltzmann distribution. In all calculations the Polarizable Continuum Model (PCM) using the integral equation formalism variant (IEFPCM) was used as solvent model.

Acknowledgements

We would like to thank Dr. Hans Abromeit for technical assistance and Prof. Gerhardt K. E. Scriba for helpful discussions. U.M.R. and F.R. would like to thank Prof. Griesinger (MPIBPC, NMR II), the Max-Planck-Society, and the DFG for support (FOR 934).

Keywords: limonene • ORD • ECD • VCD • NMR • conformation

References

[1] G. Bifulco, P. Dambruoso, L. Gomez-Paloma, R. Riccio, *Chem. Rev.* **2007**, *107*, 3744-3779.
[2] S. Qiu, E. De Gussem, K. A. Therani, S. Sergeyev, P. Bultinck, W. Herrebout, *J. Med. Chem*. **2013**, *56*, 8903-8914.
[3] M. Pitzer, M. Kunitski, A. S. Johnson, T. Jahnke, H. Sann, F. Sturm, L. P. H. Schmidt, H. Schmidt-Böcking, R. Dörner, J. Stohner, J. Kiedrowski, M. Reggelin, S. Marquardt, A. Schießer, R. Berger, M. S. Schöffler, *Science* **2013**, *341*, 1096-1100.
[4] K. C. Nicolaou, S. A. Snyder, *Angew. Chem. Int. Ed*. **2005**, *44*, 1012-1044.
[5] M. E. Maier, *Nat. Prod. Rep.* **2009**, *26*, 1105-1124.
[6] W. Offermann, A. Mannschreck, *Org. Magn. Reson*. **1984**, *22*, 355-363.
[7] G. Metha, S. R. Karra, *J. Chem. Soc. Commun.* **1991**, 1367-1368.
[8] T. Hansson, B. Wickberg, *J. Org. Chem.* **1992**, *57*, 5370-5376.
[9] E. N. Pitsinos, N. Athinaios, V. P. Vidali, *Org. Lett.* **2012**, *14*, 4666-4669.
[10] A. F. Thomas, Y. Bessière, *Nat. Prod. Rep.* **1989**, 291-309.
[11] W. A. Duetz, H. Bouwmeester, J. B. van Beilen, B. Witholt, *Appl. Microbiol. Biotechnol.* **2003**, *61*, 269-277.
[12] M. E. S. Lind, F. Himo, *Angew. Chem. Int. Ed*. **2013**, *52*, 4563-4567.
[13] K. Noack, *Helv. Chim. Acta* **1969**, *52*, 2501-2507.
[14] K. Kobayashi, Y. Asakawa, Y. Kikuchi, H. Toi, Y. Aoyama, *J. Am. Chem. Soc.* **1993**, *115*, 2648-2654.
[15] a: M. Fukuji, Y. Kawagoe, Y. Nakano, A. Nakao, *Molecules* **2013**, *18*, 7035- 7057; b: J. Aimi, K. Oya, A. Tsuda, T. Aida, *Angew. Chem. Int. Ed.* **2007**, *46*, 2031-2035; c: M. Fujiki, *Symmetry* **2014**, *6*, 677-703.
[16] a: L. Fu, Y. Zhang, Z.-H. Wei, H.-F. Wang, *Chirality* **2014**, *26*, 509-520; b: F. Wei, Y.-Y. Xu, Y. Guo, S.-L. Liu, H.-F. Wang, Chin. *J. Chem. Phys.* **2009**, *22*, 592-600; c: L. Velarde, X.-Y. Zhang, Z. Lu, A. G. Joly, Z. Wang, H.-F. Wang, *J. Chem. Phys.* **2011**, *135*, 241102.
[17] M. Schmidt, F. Reinscheid, H. Sun, H. Abromeit, G. K. E. Scriba, F. D. Sönnichsen, M. John, U. M. Reinscheid, *Eur. J. Org. Chem*. **2014**, 1147-1150.
[18] F. Reinscheid, M. Schmidt, H. Abromeit, S. Liening, G. K. E. Scriba, U. M. Reinscheid, *J. Mol. Struct.* **2015**, accepted
[19] a: F. Egidi, R. Russo, I. Carnimeo, A. D`Urso, G. Mancini, C. Cappelli, *J. Phys. Chem. A* **2015**, *119*, 5396-5404; E. C. Sherer, J. R. Cheeseman, R. T. Williamson, *Org. Biomol. Chem.* **2015**, *13*, 4169-4173. b: P. L. Polavarapu, *Chirality* **2008**, *20*, 664-672.
[20] U. M. Reinscheid, *J. Mol. Struct*. **2009**, *918*, 14-18.
[21] H. Zhang, I. M. Oppel, M. Spiteller, K. Günther, G. Böhmler, S. Zühlke, *Chirality* **2009**, *21*, 271-275.
[22] E. D. Skakovskii, W. P. Kiselev, L. Y. Tychinskaya, A. G. Schutova, L. W. Gonsharova, E. W. Spiridowish, N. A. Bovdey, P. A. Kiselev, O. A. Gaidukevich, *J. Appl. Spectrosc*. **2010**, *77*, 329-334.
[23] F. Bohlmann, R. Zeisberg, E. Klein, *Org. Magn. Reson*. **1975**, *7*, 426-432.
[24] P. Lesot, M. Sarfati, J. Courtieu, *Chem. Eur. J.* **2003**, *9*, 1724-1745.
[25] Accelrys, Discovery Studio, **2009**
[26] M. J. Frisch et al., **2009**, Gaussian 09 RevA.02, Gaussian Inc., Pittsburgh, PA
[27] E. Debie, PhD thesis, **2008**, Ghent University
[28] C. O. da Silva, B. Mennucci, T. Vreven, *J. Org. Chem*. **2004**, *69*, 8161-8164.
[29] F. J. Devlin, P. J. Stephens, P. Besse, *J. Org. Chem*. **2005**, *70*, 2980-2993.
[30] B. Mennucci, M. Claps, A. Evidente, C. Rosini, *J. Org. Chem*. **2007**, *72*, 6680-6691.

[31] A. P. Scott, L. Radom, *J. Phys. Chem*. **1996**, *100*, 16502-16513.
[32] J. P. Merrick, D. Moran, L. Radom, *J. Phys. Chem. A* **2007**, *111*, 11683-11700.
[33] M. L. Laury, S. E. Boesch, I. Haken, P. Sinha, R. A. Wheeler, A. K. Wilson, *J. Comput. Chem.* **2011**, *32*, 2339-2347.
[34] K. K. Irikura, R. D. Johnson III, R. N. Kacker, *J. Phys. Chem. A* **2005**, *109*, 8430-8437.
[35] N. J. R. van Eikema Hommes, T. Clark, *J. Mol. Model*. **2005**, *11*, 175-185.
[36] A. J. Weldon, T. L. Vickrey, G. S. Tschumper, *J. Phys. Chem. A* **2005**, *109*, 11073-11079.
[37] M. A. Śmiałek, M.-J. Hubin-Franskin, J. Delwiche, D. Duflot, N. J. Mason, S. Vronning-Hoffmann, G. G. B. de Souza, A. M. Ferreira Rodrigues, F. N. Rodrigues, P. Limão-Vieira, *PhysChemChemPhys* **2012**, *14*, 2056-2064.
[38] S. M. Wilson, K. B. Wiberg, J. R. Cheeseman, M. J. Frisch, P. H. Vaccaro, *J. Phys. Chem. A* **2005**, *109*, 11752-11764.
[39] M. F. Leopold, W. W. Epstein, D. M. Grant, *J. Am. Chem. Soc*. **1988**, *110*, 616-617.
[40] H. G. Rule, A. R. Chambers, *J. Chem. Soc*. **1937**, 145-153.
[41] P. L. Polavarapu, M. Diem, L. A. Nafie, *J. Am. Chem. Soc*. **1980**, *102*, 5449-5453.
[42] E. D. Lipp, L. A. Nafie, *Appl. Spectrosc*. **1984**, *38*, 774-778.
[43] K. L. Wolf, H. Volkmann, *Z. Physikal. Chemie B* **1929**, *3*, 139-148.
[44] R. Lauricella, J. Kechayan, H. Bodot, *J. Phys. Chem*. **1977**, *81*, 542-547.
[45] T. B. Pedersen, J. Kongsted, TD Crawford, *Chirality* **2009**, *21*, E68-E75.
[46] B. C. Mort, J. Autschbach, *ChemPhysChem* **2007**, *8*, 605-616.
[47] J. Poirson, M. Vallet, F. Bretenaker, A. Le Floch, J.-Y. Thépot, *Anal. Chem.* **1998**, *70*, 4636-4639.
[48] P. J. Stephens, D. M. McCann, E. Butkus, E. Stoncius, J. R. Cheeseman, M. J. Frisch, *J. Org. Chem.* **2004**, *69*, 1948-1958; P. J. Stephens, D. M. McCann, J. R. Cheeseman, M. J. Frisch, *Chirality* **2005**, *17*, S52-S64.
[49] B. Mennucci, J. Tomasi, R. Cammi, J. R. Cheeseman, M. J. Frisch, F. J. Devlin, S. Gabriel, P. J. Stephens, *J. Phys. Chem. A* **2002**, *106*, 6102-6113.
[50] K. B. Wiberg, P. H. Vaccaro, J. R. Cheeseman, *J. Am. Chem. Soc*., **2003** *125*, 1888-1896.
[51] K. B. Wiberg, Y.-G. Wang, P. H. Vaccaro, J. R. Cheeseman, G. Trucks, M. J. Frisch, *J. Phys. Chem. A*, **2004** *108*, 32-38.
[52] B. C. Rinderspacher, P. R. Schreiner, *J. Phys. Chem. A* **2004**, 108, 2867-2870.
[53] E. D. Hedegård, F. Jensen, J. Kongsted, *J. Chem. Theory Comput*. **2012**, *8*, 4425-4433.
[54] S. Grimme, F. Furche, R. Ahlrichs, *Chem. Phys. Lett*. **2002**, *361*, 321-328.
[55] T. D. Crawford, L. S. Owens, M. C. Tam, P. R. Schreiner, J. Koch, *J. Am. Chem. Soc*. **2005**, *127*, 1368-1369.
[56] A. I. Scott, A. D. Wrixon, *Tetrahedron* **1970**, 3695-3715.
[57] P. Brint, E. Meshulam, A. Gedanken, *Chem. Phys. Lett*. **1984**, *109*, 383-387.
[58] E. A. Perpète, C. Lambert, V. Wathelet, J .Preat, D. Jacqemin,*Spectrochim. Acta A* **2007**, *68*, 1326-1333.
[59] J. Autschbach, L. Jensen, G. C. Schatz, Y. C. E. Tse, M. Krykunov, *J. Phys. Chem. A* **2006**, *110*, 2461-2473.
[60] M. Schmidt, H. Sun, P. Rogne, G. K. E. Scriba, C. Griesinger, L. T. Kuhn, U. M. Reinscheid, *J. Am. Chem. Soc*. **2012**, *134*, 3080-3083.
[61] G. Pescitelli, *Chirality* **2012**, *24*, 718-724.
[62] J. Rhee, Y.-G. June, J.-S. Lee, K.-K. Lee, J.-H. Ha, Z. H. Kim, S.-J. Jeon, M. Cho, *Nature* **2009**, *458*, 310-313.
[63] C. Guo, R. D. Shah, R. K. Dukor, T. B. Freedman, X. Cao, L. A. Nafie, *Vibr. Spectrosc.* **2006**, *42*, 254-272.
[64] G.-S. Yu, T. B. Freedman, L. A. Nafie, *J. Raman Spectrosc.* **1995**, *26*, 733-743.

[65] S. Abbate, G. Longhi, L. Ricard, C. Bertucci, C. Rosini, P .Salvadori, A. Moscowitz, *J. Am. Chem. Soc*. **1989**, *111*, 836-840.
[66] R. D. Singh, T. A. Keiderling, *J. Am. Chem. Soc*. **1981**, *103*, 2387-2394.
[67] B. Gordillo-Román, J. Camacho-Ruiz, M. A. Bucio, P. Joseph-Nathan, *Chirality* **2012**, *24*, 147-154.
[68] J. R. Avilés Moreno, F. Partal Ureña, J. J. López González, *PhysChemChemPhys* **2009**, *11*, 2459-2467.
[69] J. R. Avilés Moreno, F. Partal Ureña, J. J. López González, *Vibr. Spectrosc*. **2009**, *51*, 318-325.
[70] F. Partal Ureña, J. R. Avilés Moreno, J. J. López González, *Tetrahedron: Asymmetry* **2009**, *20*, 89-97.
[71] E. C. Sherer, C. H. Lee, J. Shpungin, J. F. Cuff, C. Da, R. Ball, R. Bach, A. Crespo, X. Gong, C. J. Welch, *J. Med. Chem*. **2014**, *57*, 477-494.
[72] J. Vandenbussche, P. Bultinck, A. K. Przybyl, W. A. Herrebout, *J. Chem. Theory Comput*. **2013**, *9*, 5504-5512.
[73] P. L. Polavarapu, C. L. Covington, *Chirality* **2014**, *26*, 539-552.
[74] C. Cappelli, S. Monti, G. Scalmani, V. Barone, *J. Chem. Theory Comput*. **2010**, *6*, 1660-1669.
[75] a: H. Sun, E. J. d`Auvergne, U. M. Reinscheid, C. K. Z. Andrade, L. C. Dias, R. O. Rocha, C. Griesinger, *Chem. Eur. J.,* **2011**, *17*, 1811-1817; b: U. M. Reinscheid, J. Farjon, P. Haberz, M. Blackledge, C. Griesinger, *ChemBioChem* **2006**, *7*, 287-296.
[76] M. W. Lodewyk, M. R. Siebert, D. J. Tantillo, *Chem. Rev.* **2012**, *112*, 1839-1862.
[77] A. M. Sarotti, S. C. Pellegrinet, *J. Org. Chem.* **2012**, *77*, 6059-6065.
[78] M. Elyashberg, K. Blinov, A. Williams, *Magn. Reson. Chem*. **2009**, *47*, 371-389.
[79] A. B. Sebag, D. A. Forsyth, M. A. Plante, *J. Org. Chem*. **2001**, *66*, 7967-7973.
[80] K. G. Andrews, A. C. Spivey, *J. Org. Chem*. **2013**, *78*, 11302-11317.
[81] F. Reinscheid, U. M. Reinscheid, *J. Mol. Struct.* **2015**, accepted

Table of contents

limonene, conformation, configuration

On the basis of a comprehensive conformational and configurational analysis, the literature of the important mono-terpene limonene is critically assessed. The main chiroptical methods (ORD, ECD, and VCD) are experimentally applied, together with DFT calculations showing success and limits of the assignment of the absolute configuration based on chiroptical spectroscopy.

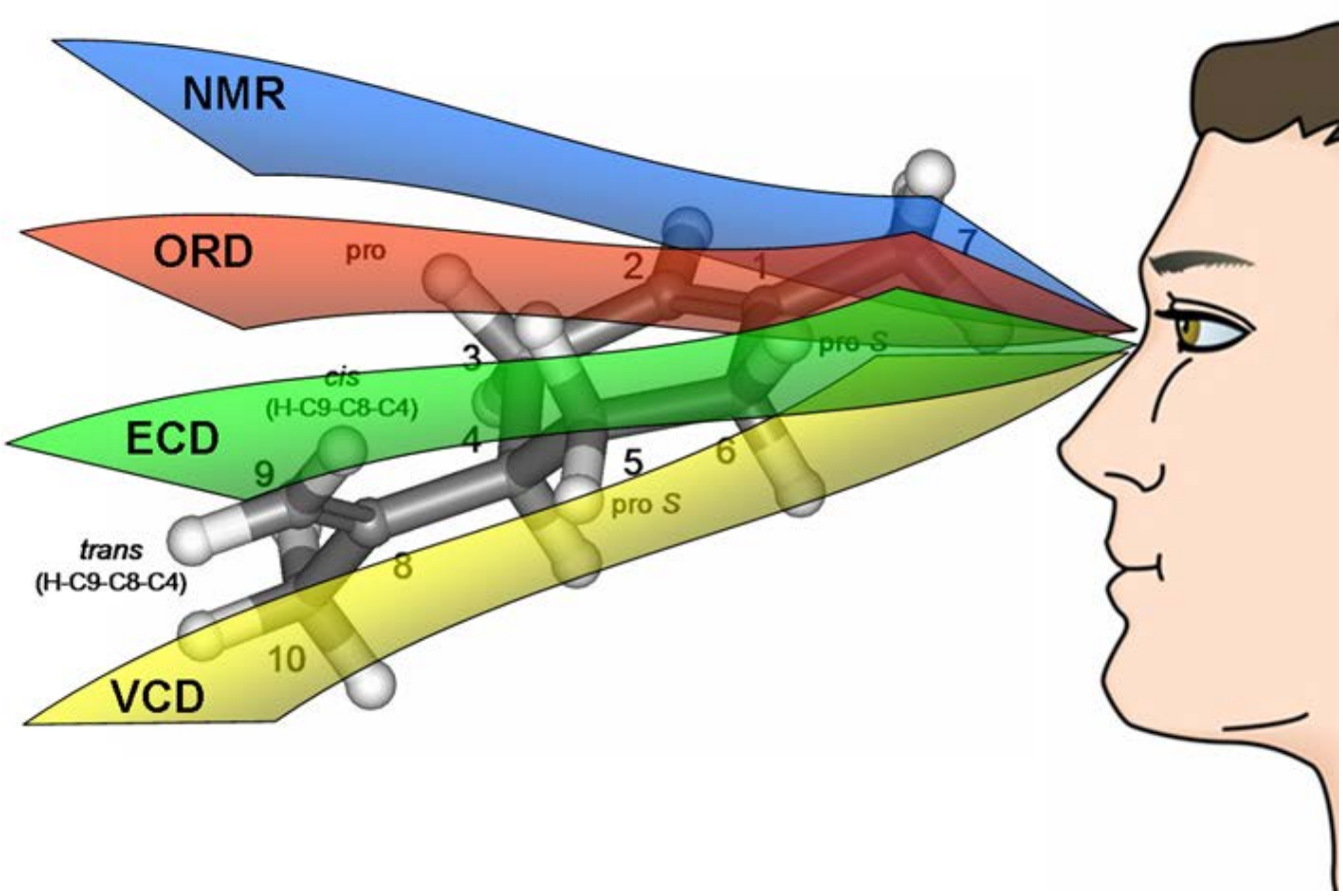

9.2 Strychnine publication

Structural and chiroptical analysis of naturally occurring (−)-strychnine

F Reinscheid, M Schmidt, H Abromeit, S Liening, GKE Scriba, UM Reinscheid (2016)

J. Mol. Struct., 1106, 200-209

Structural and chiroptical analysis of naturally occurring (−)-strychnine

F. Reinscheid[a], M. Schmidt[a], H. Abromeit[b], S. Liening[b], G. K. E. Scriba[b], U.M. Reinscheid*[a]

Abstract: Structural aspects such as chemical exchange, dimerization, solvent association, nitrogen inversion and protonation status of strychnine were investigated using experimental and calculated data. The information was mainly interpreted in view of a successful determination of the absolute configuration (AC) with strychnine (base and salt) as test molecule due to its importance in chemistry. By geometry optimization a stable isomer of protonated strychnine was found with an inverted nitrogen, however, 25 kcal/mole higher in energy. It is shown that solvent association can be assumed in protic solvents such as methanol and dimerization to a small extent in polar/protic solvents. However, the monomeric structural model neglecting explicit solvent molecules still allows the correct prediction of the AC of base and hydrochloride using optical rotation and ECD data.

Introduction

Recently, it was stated that “today the focus of chemical research is much more on function than on structure.”[1] Although it is still more difficult to give answers to functional questions on the same scientific level as has been achieved for structural research, it is important to push the limits in structural descriptions even further. Since a number of stereochemical misassignments of natural products can be found in the literature (for reviews),[2-5] studying the structure of known molecules may give surprising results. Two recent examples are the correct determination of the absolute configuration (AC) of the antimalarial

[a] F Reinscheid, M Schmidt, UM Reinscheid *
NMR-based structural biology
Max-Planck-Institute of Biophysical Chemistry
Am Fassberg 11, 37077 Göttingen (Germany)
E-mail: urei@nmr.mpibpc.mpg.de
[b] H Abromeit, S Liening, GKE Scriba
Pharmaceutical Chemistry
Friedrich-Schiller Universität
Philosophenweg 14, 07743 Jena (Germany)

Supporting information for this article is given via a link at the end of the document.

drug mefloquine,[6] and the discovery of the yet hidden structural flexibility of strychnine.[7] Even this extremely well studied (first isolation in 1818 by Pelletier and Caventou)[8] prototypic molecule of rigidity turned out to exist as two conformers in solution. Consequently, all functional effects due to the presence of a minor conformer will be neglected if only the crystal structure of strychnine[9,10] is considered.

The structure of strychnine (Scheme 1) has been established by Robinson.[11] Soon after it was confirmed by total synthesis[12] and x-ray crystallography.[13] The absolute configuration of naturally occurring (−)-strychnine was determined by Peerdeman in 1956 using x-ray crystallography.[14] Apart from the general chemical importance of strychnine, there is an astonishing funnel effect in all synthetic schemes published so far: either the Wieland-Gumlich aldehyde is prepared, or isostrychnine.[15,16] From these intermediates known conversions lead to strychnine, but are quite often not performed. In addition, comparing the IR spectra presented as proof for the successful synthesis of strychnine[17] leads to the conclusion that two identical spectra are shown.

Scheme 1: Stereochemical formula of (−)-strychnine HCl

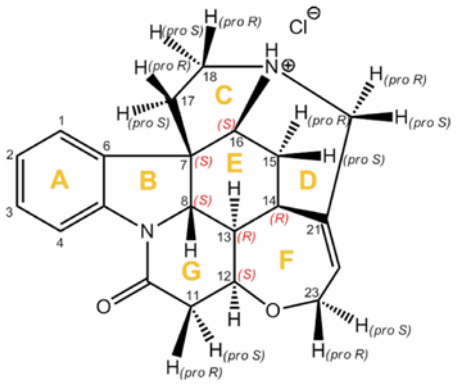

To the best of our knowledge, the only further structural information concerning the conversion of isostrychnine into strychnine[18] was given by Magnus et al.[19] in their introduction to the second total synthesis of strychnine, more than 30 years after Woodward`s first total synthesis. Magnus et al.[19] mentioned without giving experimental details, that by using different reaction conditions as Prelog et al.,[18] i.e. ethanolic potassium hydroxide at 80 °C, almost no conversion into strychnine was observed, and in case of cesium carbonate in *tert*-butyl alcohol

as solvent 13-*epi*-isostrychnine was formed. In conclusion, the strychnine chemistry is far from being well understood. This motivated us to further analyse experimentally and computationally the structural model of strychnine, followed by a chiroptical analysis. Insofar serves strychnine as a test molecule to explore the success and limitations of the purely chiroptical approach to determine the AC of a chiral compound.

Results and Discussion

Structural model

In our first publication about the structure of strychnine, we showed the first experimental and quantitative evidence of a minor conformer in solution using low-temperature NMR (Fig. 1).[7a] Structure calculation of this low-populated conformer is successful on the mpw1pw91/cc-pvdz level of theory, but not on the often used B3LYP/6-31G(d) level of theory.[7a] Earlier work by Butts et al. (2011)[7b] presented calculated quantitative information. In addition, a third low-populated conformer was predicted by computation.[52] To date, there is no experimental evidence for its existence so it was not further investigated.

In the present study we investigate structural aspects in order to explore the success and limitations of the determination of the absolute configuration by comparing experimental and calculated chiroptical data. Strychnine represents an excellent test molecule for the structural work since it is still a challenging synthetic target and a typically complex natural product. From our analysis we want to derive limits that can be further tested and maybe pushed even further by using smaller natural products such as limonene.[20]

Chemical exchange in ring G

The protons at C11 of strychnine are acidic. It is known that under alkaline conditions these protons can be exchanged by tritiated water.[21] At a hydroxide concentration of 0.1 M, the exchange rate amounts to 4.32×10^4 s^{-1}. However, without using a large excess of hydroxide

anions the rate rapidly drops to very small values so that under the conditions of our NMR measurements (measurement times of hours, strychnine at low concentrations of < 20 mM, 25°C (pH of 9.5 (base in water) and pH of 5.5 (strychnine sulphate in water) as saturated solutions) [22] almost no exchange will take place so that the experimental, structural data are not contaminated by fast exchange of the H11 protons. However, this reaction is important for the isostrychnine-strychnine conversion.[18] Likewise, a lactamization reaction is much too slow to produce ring-opened derivatives during the measurements,[23] but could be relevant for the isostrychnine-strychnine conversion.

Dimerization, ion-pairing

Mostad[9] analyzed strychnine base by x-ray crystallography. He concluded that the amide oxygen is mostly involved in the intermolecular interactions in the crystal. In order to test the dimerization of (−)-strychnine base, two samples with different concentrations were compared: 2 mg/mL (6 mM) and 100 mg/mL (300 mM) in $CDCl_3$ at 298 K. The proton spectra showed concentration dependent resonances affecting the protons near the aliphatic amine with an upfield shift of more than 0.1 ppm for the high concentration compared to the low concentration, i.e. H16, H18 pro*S*, H20 pro*R* and pro*S*, and H22, located on one side of the 3D-model (Figure 1; see supporting information). These data indicate aggregation**.** In contrast with our results, Metaxas and Cort [24] did not observe concentration dependent effects for the base in chloroform. However, the concentration range studied might be too small so that weak associations were not detected. Assuming a low association constant of 1 $[M]^{-1}$, 6 % of the strychnine base molecules would exist as dimer in our high concentration sample (100 mg/mL, 300 mM). For comparison, with an association constant of 100 M^{-1}, 12 % of the strychnine base molecules would exist as dimers in our low concentration sample.

For salts of strychnine a concentration dependent change of proton chemical shifts of protons near the protonated tertiary amine were observed (maximum of -8.7 ppb/mM for one of the H20 protons of (−)-strychnine nitrate in $CDCl_3$).[24] Interestingly, in the same solvent counter-ion dependent proton chemical shifts near the aliphatic nitrogen varied up to 0.3 ppm which can be explained by different ion-pairs formed. Since we have measured strychnine HCl in

much more polar and H-bond accepting solvents (DMSO-*d6* and methanol-*d3*), ion-pair formation should be decreased compared to $CDCl_3$, and concomitantly the tendency to form ionic aggregates would be reduced. In agreement, Moreno et al.[25] observed ion-pairing for brucine BF_4 in chloroform which decreased in acetone-*d6* at a 2 mM concentration. With larger anions, strong ion-pairing was observed even in acetone as polar solvent so that we can assume that for strychnine HCl a reduced ion-pairing is reasonable due to the smaller size of the chloride anion compared to $BF4^-$. In agreement, by comparing two samples 2 mg/mL (5 mM) and 65 mg/mL (163 mM) in methanol-*d3* at 298 K, we observed that the protons surrounding the aliphatic nitrogen are mostly affected but to a lower extent compared to the base in chloroform, i.e. H15 pro*R*, H16, H17 pro*R*, H18 pro*S* by more than 0.03 ppm (see supporting information). In this case, up- and downfield shifts were observed. Interestingly, H1 at the aromatic ring is shifted by 0.04 ppm downfield at the higher concentration. These concentration dependent differences in chemical shifts are smaller than the values observed by Metaxas and Cort[24] due to the different solvent effect on the aggregation/ion-pairing process. The latter is much more pronounced in apolar solvents such as chloroform used by Metaxas and Cort [24] compared to the polar solvent methanol-*d3* in our study. In conclusion, there are clear indications of aggregation of strychnine base (in $CDCl_3$) and strychnine HCl (in methanol-*d3*) at very high concentrations. It is therefore reasonable to use a monomer as structural model if the chiroptical analysis is performed at sufficiently low concentrations, i.e. <20 mM. In polar solvents and at low concentrations of strychnine HCl, the effect of ion-pairing on the chiroptical analysis can be neglected.

Figure 1: Geometry-optimized (mpw1pw91/cc-pvdz, IEFPCM: methanol) structure of protonated strychnine (major conformer on the left, minor conformer on the right with a population of 5.9 % of strychnine HCl in methanol at 298 K)[7]

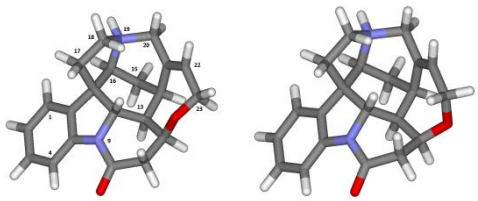

Figure 2: Geometry-optimized (mpw1pw91/cc-pvdz, IEFPCM: methanol) structure of protonated strychnine with inverted aliphatic nitrogen (major conformer on the left, minor conformer on the right with a population of 2.7 % of strychnine base in chloroform at 298 K)[7]

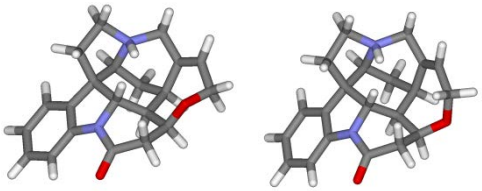

Solvent-association

Strychnine contains six potential H-bond accepting (HBA) sites: the amine and amide nitrogens, the amide and ether oxygens, and the ethylene and benzene moieties.[26] The authors analysed IR spectra of 4-fluorophenol as H-bond donor together with strychnine and observed 3 OH bands. This indicated that three sites are preferred, in the following order of decreasing basicity: aliphatic amine (N19), O-amide, and O-ether. To study such solvent-associations ^{15}N chemical shifts are very important parameters. In addition, they might indicate the protonation state ,[27] dimerization, and the presence of ion-pairs. The latter information was already utilized for the determination of the absolute configuration of mefloquine HCl in DMSO.[6]

In addition, the comparison between calculated and experimental ^{15}N resonances is a valuable tool to construct the structural model.[28-30] Ramalho and Bühl[29] showed that the ^{15}N chemical shifts of the references such as nitromethane are highly dependent on the level of theory. We propose to use an internal referencing to circumvent this dependence on the level of theory. As an example, taking the calculated data for 5-nitroimidazole using DFT and the PCM approach to model solvent effects, the absolute difference between the two nitrogen resonances was 97 ppm (BP86 functional, DMSO as solvent for geometry optimization and NMR calculation) which is very close to the experimental difference of 96.8 ppm.[29] A different approach used empirical solvent scales such as the normalized solvent polarity scale of Reichardt in order to obtain a good correlation for the ^{15}N chemical shifts of pyrimidine.[31] In

addition, by scaling of the spheres (standard value of 1.2) used within the PCM approach to define the cavity a better match to experiment for pyrimidine in water was achieved using a value of 1.1.[32]

Solvent effects on tertiary amine resonances are dominated by hydrogen bonding to the lone pair of the nitrogen, resulting in downfield shifts.[30,33] For *N*-methylpiperidine, the nitrogen resonance was shifted downfield in chloroform as solvent by 3 ppm and 2.4 ppm compared to cyclohexane for chloroform and methanol, respectively.[33] In addition, H-bonding of chloroform to acetamide was measured.[34] Association constants of 0.46 M^{-1} for *N*-methylacetamide and 0.99 M^{-1} for *N,N*-dimethylacetamide were found at 16 °C. Similar values were determined by Wong and Ng[35] for tertiary amines and ethers (e.g. 0.45 M^{-1} for tetrahydrofurane at 34 °C) as H-bond acceptors with chloroform as proton donor so that solvent association with strychnine is expected for the tertiary aliphatic N19, the amide group and the ether linkage in ring F.

From these literature values one would expect downfield shifts when going from DMSO-*d6* to $CDCl_3$ for the two nitrogen resonances of strychnine base due to H-bonding, in contrast to the experiment (Table 1). Obviously, other effects such as solvent polarity and/or H-bonding to other parts of the molecule are relevant. In addition, using the referencing between the two nitrogen resonances, the experimental (DMSO-*d6* / $CDCl_3$) and calculated differences (113 ppm / 115 ppm and 119.8 ppm, respectively, Table 1) differ by almost 7 ppm. This indicates that the structural model of isolated strychnine base does not fully represent the measurement conditions and/or that the calculations are erroneous. The difference between the two nitrogen resonances changed dependent on the level of theory by 3.9 ppm (mpw1pw91/cc-pvdz vs. mpw1pw91/6-311+g(d,p)) and by 1.7 ppm (B3LYP/cc-pvdz vs. mpw1pw91/cc-pvdz) so that computational errors are one of the reasons for the large discrepancies between experiment and calculation.

Similar to strychnine base, the experimental (DMSO-*d6* / methanol-*d3*) and calculated differences for strychnine HCl/protonated strychnine differ (87 ppm /89.2 ppm and 92.2 ppm, respectively, Table 1) which might also be related to a systematic error in the calculations.

Table 1: Experimental and calculated ^{15}N resonances in ppm for strychnine base and strychnine HCl/protonated strychnine in different solvents at 298 K

^{15}N resonance/ Exp. or calc.	N9 [a] (δ or σ)	N19 [b] (δ or σ)	Absolute difference Δ (N9-N19)
Exp. strychnine HCl in DMSO-*d6* (36 mg /mL)	$\delta = 150$	$\delta = 63$	87
Exp. strychnine HCl in methanol-*d3* (65 mg /mL)	$\delta = 151.4$	$\delta = 62.2$	89.2
Calc. protonated strychnine, DMSO as solvent [c]	$\sigma = 78.6$	$\sigma = 170.8$	92.2
Exp. strychnine base in DMSO-*d6*[d] (5 mg /mL)	$\delta = 152$	$\delta = 37$	115
Exp. strychnine base in $CDCl_3$ (33 mg/mL)	$\delta = 148$	$\delta = 35$	113
Calc. strychnine base, chloroform as solvent [c]	$\sigma = 101.9$	$\sigma = 221.7$	119.8

[a] N9: amide nitrogen, [b] N19: aliphatic nitrogen, [c] All calculations using DFT on the mpw1pw91/cc-pvdz level of theory, with IEFPCM as solvent model and solvents indicated in the table, [d] taken from Hilton and Martin[36]

The proton resonances of strychnine HCl are all shifted downfield in methanol compared to DMSO as solvent for similar concentrations (65 mg/mL in methanol-*d3* and 36 mg/mL in DMSO-*d6*), except the NH proton which is shifted upfield by 1.31 ppm. The interaction area around the aliphatic nitrogen is mostly affected, i.e. H17 pro*S*, H18 pro*S* and pro*R*, and H20 pro*R* are shifted by more than 0.15 ppm (Figure 1). The ^{13}C resonances follow the same solvent dependence found for the proton values. The chemical shifts appear always downfield in methanol compared to DMSO, with C4, C13, C16, C18, and C20 mostly affected by more than 1.5 ppm chemical shift differences. Apart from the obvious interaction area around the aliphatic nitrogen, there is a downfield shift difference of 1.9 ppm for the carbonyl ^{13}C resonance in methanol compared to DMSO.

In conclusion, it is clear that a substantial fraction of strychnine should exist as solute-solvent complex via the amine, amide and ether functionalities. Without further structural and quantitative information it is not reasonable to construct a static model so that we decided to use an isolated strychnine molecule for the subsequent chiroptical analysis.

Protonation

The structural model for protonation of tertiary amines may be more complicated than expected. Nagy et al.[37] analyzed theoretically and experimentally the prototypic *N*-

methylpiperazine hydrochloride in aqueous solution. Modelling as a monomer could not reproduce the proton NMR-based experimental population analysis. However, as an ionic aggregate composed of one or two chloride anion(s) H-bonded to the organic molecule the calculated results fit very well to the experimental results. In addition, the protonation of the neurotransmitter serotonin reduced the number of low-energy conformers determined by IR spectroscopy and DFT calculations[38] similar to the results of mefloquine HCl.[6]

Protonation of tertiary amines typically leads to a downfield shift of ^{15}N resonances (*N*-methylpiperidine HCl in DMSO: 8 ppm downfield of the base in cyclohexane).[33] This is exactly what was measured for strychnine: protonation of the aliphatic nitrogen shifts the ^{15}N resonance 25-30 ppm downfield (Table 1). The much larger difference between the two ^{15}N resonances for the basic compared to the protonated state (115/113 ppm to 89.2/87 ppm) is correctly reproduced by the calculations (119.8 to 92.2 ppm). The difference (N9-N19) upon protonation is 28 ppm for experiment (DMSO-*d6*, base-HCl: 115 ppm – 87 ppm) matching very well the calculated value of 27.6 ppm (base/chloroform – protonated/DMSO: 119.8 ppm – 92.2 ppm). To conclude, a reasonable model for samples of strychnine HCl in DMSO or methanol shows a protonation at N19.

Nitrogen inversion

Nitrogen pyramidal inversion means moving the lone pair from one side of the tetrahedral amine to the other. The energy barriers for nitrogen inversion in acyclic amines are in the order of 6-7 kcal/mole.[39] The barrier is increased by hydrogen-bonding,[40] protonation,[41] and ring formation. Well studied examples are the aziridines for which the barriers of inversion increase up to 18-20 kcal/mole. Substitutions by aromatic rings lower the barrier. As recent example, an aziridine derivative with a cyanophenyl *N*-substitution showed a free energy barrier of 11.3 kcal/mole.[42] The barrier of inversion for *N*-methylpiperidine as example of a larger *N*-heterocyle amounts to 12.0 kcal/mole, which can be further lowererd by α,α-dimethyl substitution. In this case, the crowding is responsible for an increased inversion rate. Belostotskii et al.[43] have analysed the pathways for conformational exchange of piperidines. Following these schemes it appears that literature values must be cautiously interpreted. The authors concluded that the isolated C-N rotation analysed by Anderson et al.[44] is in fact a

combination of ring-inversion/nitrogen-inversion, ring-inversion, and isolated C-N rotation. However, a forcefield (MM3) based scheme was applied so that shortcomings due to the low level of theory were not taken into account.[43]

Two interconverting species separated by a barrier larger than 23 kcal/mole corresponding to a transition rate of less than 10^{-4} s^{-1} can be separated.[45] This means that very often nitrogen-inverted isomers cannot be separated and explains how scarce data about these isomers are, although a large number of bioactive compounds and pharmaceuticals contains tetrahedral amines. The speed of the inversion process often hinders the direct measurement in solution by NMR. Quite often, enantiotopic groups in α position to the nitrogen are used for the analysis. An interesting example for slowing down the process is the complexation by supramolecular host molecules.[46]

Among the most fascinating natural products, cocaine plays a special role since it is the most abused bioactive compound worldwide. Interestingly, Poupaert et al.[47] reported a nitrogen inversion of the tertiary amine of cocaine that is highly dependent on the solvent: the form with an intramolecular H-bond is favoured in CD_2Cl_2 whereas in water the form with a solvent-directed proton is dominating.[48] However, the inversion barrier was calculated on quite low levels of theory so that the two energies (AM1: 7.9 kcal/mole; PM3: 6.7 kcal/mole) can only be taken as rough estimates.[47] Furthermore, experiments are needed with specified concentrations and pH conditions since these parameters are also relevant for the observed inversion rate. The latter point seems to be relevant for the investigation about trimipramine maleate.[49] The authors interpreted the results as nitrogen inversion with a barrier of 16.3 kcal/mole. This value is very high for an aliphatic dimethylamino group. Since also concentration effects were observed, a careful interpretation of the low temperature spectra is very important. Increasing the concentration led to an apparent increase of the inversion rate. This can be an artifact if aggregates with smaller chemical shift differences are formed. In addition, the pH influences heavily the apparent inversion rate since only the basic form can exhibit nitrogen inversion.

Protonation further slows down the inversion since deprotonated forms are the only species that are able to invert.[50] Therefore, the protonation state is very important since it influences the observed rate of inversion. The aliphatic nitrogen of strychnine is more basic compared to the amide nitrogen so that strychnine salts will have a protonated aliphatic nitrogen (pK_A

values of 6.0 and 11.7 at 20°C; pH of a saturated solution of strychnine base: 9.5; pH of a saturated strychnine sulphate solution: 5.5.[22] In their analysis, Morgan and Leyden[50] could show that the concentration of the base might also influence the inversion rate. However, in the case of strychnine, the concentrations in the NMR measurements were quite low (< 20 mM). This means that too few strychnine molecules were available as base to assist the deprotonation of a protonated strychnine molecule. Consequently, in methanol and DMSO we expect that solvent assisted deprotonation is the major process, maybe with the counter-ions as acceptors as illustrated in the following.

Rates of proton exchange for the hydrochloride of *N*,*N*-dibenzylaniline were measured in $CDCl_3$ and acetonitrile-*d3*.[51] Importantly, small amounts of water in $CDCl_3$ with an at least 30-fold excess of test compound did not change the exchange rates. Likewise, the concentration of the test compound did not affect the proton exchange rate. Very similar free energies of activation were obtained for acetonitrile. However, this appeared to be caused by an enthalpy-entropy compensation. Interestingly, the authors conclude that the chloride anion acts as proton acceptor since water and amine as base could be excluded. This is in agreement with the observations of Metaxas and Cort[24] who found strong influences of the counter-ions on the proton resonances of strychnine salts.

By geometry optimizations we detected a second minimum for the protonated (−)-strychnine conformers belonging to an inverted aliphatic nitrogen stereoisomer (Figure 2). The free energy difference on the mpw1pw91/cc-pvdz (IEFPCM with methanol) level of theory was quite large (25.1 kcal/mole for the major conformer and 29.2 kcal/mole for the minor conformer) which can be explained by the highly strained ring systems in which the amine is involved. The envelope of the five-membered ring C is changed (*endo* position of C7 in the non-inverted forms of Figure 1; *endo* position of N19 in the inverted forms in Figure 2). Interestingly, the boat form of ring D remains very similar. We could not find a minimum for the nitrogen-inverted strychnine base. From the Boltzmann-derived populations it is clear that the nitrogen inversion of the aliphatic amine in protonated strychnine was not detected at low temperatures (210 K, methanol-*d3*)[7] due to the low population of the inverted form.

However, synthetic reactions might create conditions under which nitrogen inversion occurs much faster and/or the inverted isomer dominates. One prominent example could be the isostrychnine-strychnine conversion performed at high pH. This leads to a high concentration

of strychnine as base. In addition, it would be interesting to analyze nitrogen-inversion for strychnine isomers. Bifulco et al.[52] showed that it is possible to determine the relative configuration of naturally occurring strychnine by comparing the experimental $^{1}J_{CC}$ couplings with calculated ones of all possible diastereomers. However, isomers with inverted nitrogen were not yet taken into account.

Optical rotatory dispersion

The Sigma-Aldrich product information about the specific optical rotation of (−)-strychnine base is [α] = -139.0 at 22 °C, c=1 in chloroform (1.0 g compound dissolved in 100 mL of solvent which equals 10 mg/mL) at a wavelength of 589 nm. The sulphate showed a specific optical rotation at 25°C and 589 nm of -25.1.[22] For the hydrochloride (7 mg/mL in water at 25°C) a specific rotation of -28.3 at 589 nm is reported.[53] We measured in chloroform at 24.5 °C a specific optical rotation [α] = -141 for strychnine base (589 nm, c = 20 mg/mL, i.e. c=2) which differs by less than 2 % from the Sigma-Aldrich product information. The strychnine HCl measurement of [α] at 24.5°C (c=2, methanol as solvent) gave -15 at 589 nm. The difference to the literature value might be explained by a solvent dependence of [α].
Using the aug-cc-pvdz basis set, we achieved to predict correctly the AC of strychnine base (Figure 3) and strychnine HCl (Figure 4) by comparing calculated with experimental values. Values of (−)-strychnine HCl were corrected for a protonated form for comparison with the calculated values obtained with a protonated structural model. Figures 3 and 4 show that the minor conformer[7a] only slightly contributes to the calculated ORD values (mpw1pw91/aug-cc-pvdz, IEFPCM solvent model with methanol (protonated strychnine) or chloroform (strychnine base) as solvent) since the ORD values are quite small or similar compared to the major conformer.
The experimental values shown are measured at a quite high concentration (2 %) but are still low enough to be modelled by a monomeric isolated molecule. Values obtained for a concentration of 0.2 % together with the values for 2 % are shown in Table 2. A dependence on the concentration was observed which was ascribed to the limited precision of the

polarimeter (α +/- 0.01) which translates to [α] changes of +/- 20 in our measurements using the lowest concentration of 0.2 %. In addition, from our structural analysis it is clear that aggregation and solvent-solute interactions are present at high concentrations but are neglected in our structural model. However, since no sign changes occurred at all concentrations and wavelengths measured, a monosignate behaviour of the ORD curve was safely determined for which a much better AC prediction can be obtained compared to the single value optical rotation at 589 nm.[54]

Figure 3: Calculated (mpw1pw91/aug-cc-pvdz, iefpcm: chloroform; in blue partly overlaid by the green curve: major conformer, in red: minor conformer, in green: 97.3/2.7 mix of the two conformers) and experimental (in orange, 2 % in chloroform) ORD curve of (−)-strychnine base based on four wavelengths (589, 546, 495, and 436 nm respectively)

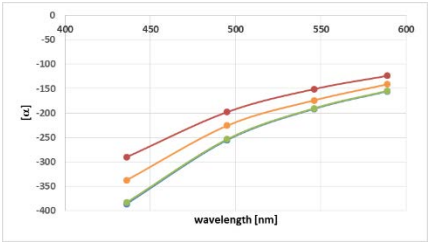

Figure 4: Calculated (mpw1pw91/aug-cc-pvdz, iefpcm: methanol; in blue: major conformer, in red: minor conformer, in green: 94.1/5.9 mix of the two conformers) and experimental (in purple, 2 % in methanol) ORD curve of (−)-strychnine HCl/protonated strychnine based on four wavelengths (589, 546, 495, and 436 nm respectively)

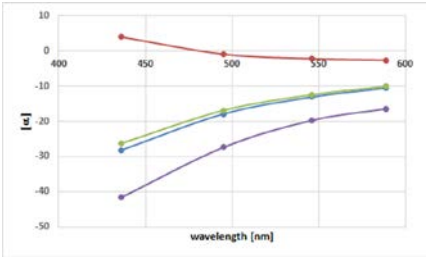

Table 2: Experimental specific optical rotation at different wavelengths at two concentrations for (−)-strychnine base (in chloroform) and (−)-strychnine HCl (in methanol)

wavelength [nm]	[α] of strychnine base 2 %	[α] of strychnine base 0.2 %	[α] of strychnine HCl 2 %	[α] of strychnine HCl 0.2 %
589	-141	-110	-15	-40
546	-174	-160	-18	-30
495	-226	-210	-25	-50
436	-338	-310	-38	-40

In view of an uncertainty of roughly +/- 60 for the calculation of $[\alpha]_D$,[55] the AC prediction of strychnine (base and hydrochloride) should be based on several wavelengths. It is important to note that even with the inclusion of solvent effects and zero-point vibrational corrections, a number of signs of the optical rotation of (*S*)-propylene oxide were not predicted correctly so that further shortcomings of the procedure (e.g. level of theory, dynamic effects in condensed phases) must exist.[56] However, we expect a higher precision than the above mentioned range of values due to the improvement achieved in the calculations of chiroptical properties. Especially, inclusion of solvents as dielectric continuum typically improves the match with experiment.[57] Furthermore, the better the structural model, the better the agreement. Only notoriously problematic molecules such as the above mentioned (*S*)-propylene oxide still pose severe problems for the AC assignment.

UV-Vis and ECD

In Tables 3 and 4 the experimental molar extinction coefficients are listed for (−)-strychnine base and (−)-strychnine HCl, respectively. There are discrepancies between the experimental and calculated extinction coefficients (Table 5). In principle, the level of theory and the modelling by gaussian bandshapes are two factors that can be responsible for the differences. However, it is clear that there are substantial solvent effects if the strychnine base data in methanol are compared with acetonitrile at similar concentrations. Based on the above mentioned analysis we assume that specific solute-solvent interactions might be responsible for the solvent dependent ECD spectra.

The experimental λ_{max} values all appear at 255 nm for strychnine base (except for methanol: 254 nm) which is quite similar to the calculated values (Table 5). For strychnine base in chloroform, a concentration dependent extinction coefficient was determined which might be explained by aggregation and/or solute-solvent interactions. This effect was not observed for strychnine base in acetonitrile and strychnine HCl in methanol, two solvents with much higher polarity.

We concentrate on the comparison between calculated and experimental excitation energies useful for the interpretation of the ECD bands. It is important to note, that we did not apply any

scaling to neither wavelengths nor intensities to allow for own interpretations of the reader. In our opinion, the interpretation and comparison of calculated and experimental ECD spectra is problematic if scalings of the wavelength and intensity axis are used. As an example, Shimizu et al.[58] scaled the intensities by a factor of 0.5, fixed the broadening at 0.4 eV, and used different shifts for the wavelength axis (0.3 eV, 0.7 eV red shift, 1.0 eV blue shift) depending on the level of theory. For all three measures, no explicit reasoning was indicated. With respect to our scientific goal to explore the success and the limitations of the prediction of the absolute configuration based on chiroptical data, we cannot recommend this procedure. Especially n−π* transitions are notoriously difficult to predict in solution (see supporting information for some literature examples).

Table 3: Experimental molar extinction coefficients ε [l M^{-1} cm^{-1}] for (−)-strychnine base in different solvents and different concentrations, all at 25 °C and λ_{max} = 255 nm, except in methanol (λ_{max} = 254 nm)

	$CHCl_3$ (0.049 mg/mL)	$CHCl_3$ (0.47 mg/mL)	Methanol (0.12 mg/mL)	Acetonitrile (0.029 mg/mL)	acetonitrile (0.145 mg/mL)
ε	7590	11070	12420	28640	28410

Table 4: Experimental molar extinction coefficients ε [l M^{-1} cm^{-1}] of strychnine HCl in methanol at different concentrations, all at 25 °C and λ_{max} = 255 nm

	0.378 mg/mL	1.3 mg/mL
ε	9950	11610

Table 5: Calculated molar extinction coefficients ε [l M^{-1} cm^{-1}] for (−)-strychnine base in chloroform and protonated (−)-strychnine in methanol (mpw1pw91/cc-pvdz, IEFPCM)

	strychnine base, conformer 1	strychnine base, conformer 2	protonated strychnine, conformer 1	protonated strychnine, conformer 2
ε	14459	14571	12741	12402
λ_{max} [nm]	247	246	244	244

Figures 5A-H: Experimental ECD and UV/Vis spectra of (−)-strychnine base and (−)-strychnine HCl in different solvents and at different concentrations at 25°C

A: ECD spectrum of strychnine base in $CHCl_3$ (0.47 mg/mL) 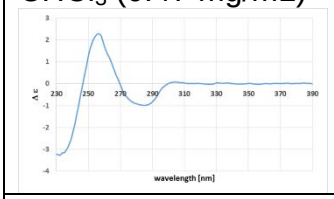	B: UV/Vis spectrum of strychnine base in $CHCl_3$ (0.47 mg/mL) 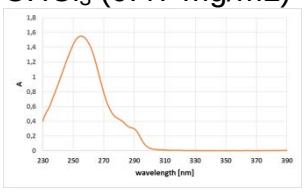
C: ECD spectrum of strychnine base in methanol (0.12 mg/mL) 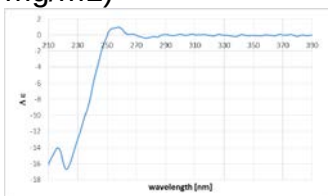	D: UV/Vis spectrum of strychnine base in methanol (0.12 mg/mL) 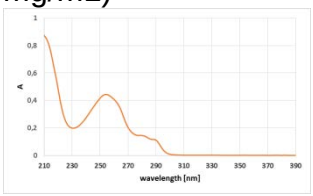
E: ECD spectrum of strychnine base in acetonitrile (0.145 mg/mL) 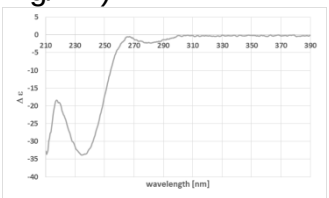	F: UV/Vis spectrum of strychnine base in acetonitrile (0.145 mg/mL) 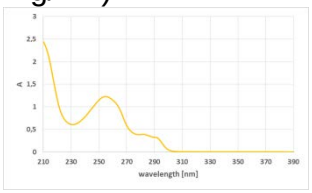
G: ECD spectrum of strychnine HCl (0.378 mg/mL) in methanol-*d3* 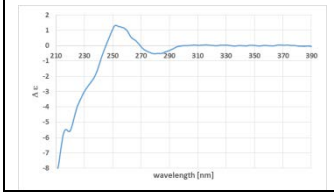	H: UV/Vis spectrum of strychnine HCl (0.378 mg/mL) in methanol-*d3* 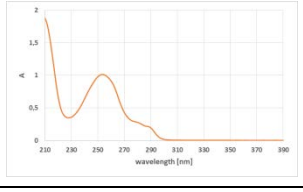

Snow and Hooker [59] have measured (−)-strychnine in aqueous acidic solution and as a base in triethylphosphate (TEP). Unfortunately, no information was given about the acidifiying agent

so that it remains unknown which salt has been formed. Likewise, an aqueous neutral sample was measured but no information was given about its preparation. Additionally, an apparent aggregation at alkaline pH was mentioned but no further information given. In the UV spectrum of (−)-strychnine two shoulders (287 nm and 277 nm) were identified in the aqueous neutral sample. The following ECD bands together with their signs were measured for aqueous strychnine at pH 3:[59] 210 nm (−), 250 nm (+); for strychnine in TEP: 205 nm (−), 230 nm shoulder (-), 260 nm (+), 280 nm (−). All bands also appear in our spectra except the band at 205 in TEP, since we have used solvents with a higher wavelength cut-off. The shoulder at 230 nm was tentatively assigned to the n−π* transition of the carbonyl oxygen lone pairs.[59] Two arguments were put forward: 1. the transition seems to be electrically forbidden since no corresponding UV absorption band was detected; 2. such transitions are very sensitive to the environment which was shown for this ECD band for strychnine and five related compounds: it shifts dependent on the solvent and pH. We also detected solvent dependent shifts, notably in acetonitrile strychnine base (Figure 5 E) does not show a positive ECD band around 255 nm which is present in all other solvents (chloroform and methanol) for (−)-strychnine base and in methanol for (−)-strychnine HCl. Calculations indicate that protonation increases the intensity of the positive ECD band around 255 nm. The list of rotational strengths can be found in the supporting information.

The calculations for (−)-strychnine base clearly show a broad negative ECD band around 250 nm that correlates with the negative band around 235 nm in the experiment (acetonitrile) which is supported by comparison of the experimental and calculated UV spectra (Figures 5 and 6). Since an incorrect modelling of n−π* transitions is likely, it is important to explore different levels of theory for smaller test molecules.[20] The calculated ECD bands for protonated (−)-strychnine match with experiment without any wavelength shift (Fig. 5 F and G; Fig. 6 E-H). Interestingly, the calculated ECD bands for the major and minor conformers of strychnine base and protonated strychnine differ slightly. However, the decisive negative band around 250 nm is always present so that the AC assignment is reliable. In conclusion, the good match between experiment and calculation proves that the naturally occurring (−)-strychnine HCl is assigned 13*R* since this was the configuration of the structural model used (Scheme 1). In the case of (−)-strychnine base, higher levels of theory might improve the fit with experiment.

Figures 6 A-H: Calculated ECD and UV/Vis spectra of (−)-strychnine base and protonated (−)-strychnine of the major and minor conformer[7a] at the mpw1pw91/cc-pvdz level of theory using the IEFPCM approach and chloroform (strychnine base) or methanol (protonated strychnine) as solvent

A: ECD spectrum for strychnine base of the major conformer 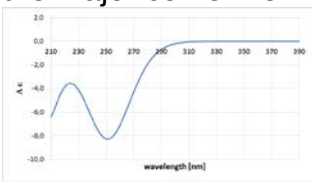	B: UV/Vis spectrum for strychnine base of the major conformer 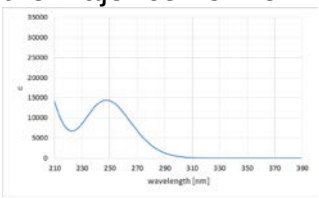
C: ECD spectrum for strychnine base of the minor conformer 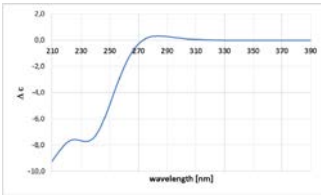	D: UV/Vis spectrum for strychnine base of the minor conformer 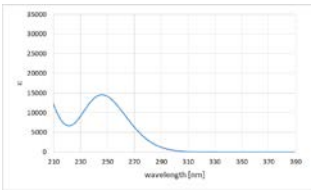
E: ECD spectrum for protonated strychnine of the major conformer 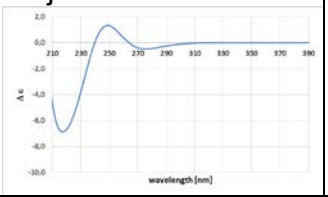	F: UV/Vis spectrum for protonated strychnine of the major conformer 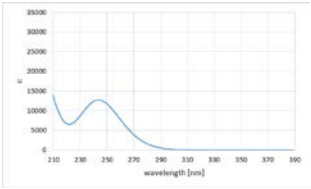
G: ECD spectrum for protonated strychnine of the minor conformer 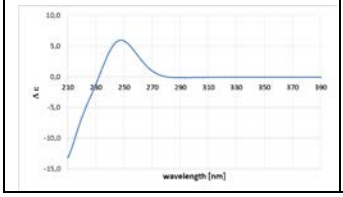	H: UV/Vis spectrum for protonated strychnine of the minor conformer 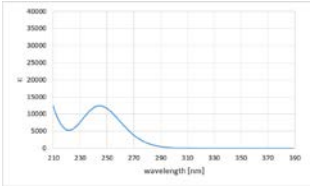

IR and VCD

Setnička et al.[60] presented IR and VCD spectra of (−)-brucine in three different solvents: $CDCl_3$, methanol-*d3*, and DMSO-*d6*. Under the experimental conditions the AC determination is problematic since very high concentrations (> 0.16 M) were used and aggregation has to be taken into account for the structural modelling. Neglecting aggregation effect and assuming that the two methoxy groups of brucine only slightly influence the two selected VCD bands (1660 cm^{-1} and 1500 cm^{-1}), we took the (−)-brucine information for comparison with our calculated (−)-strychnine VCD data. The corresponding IR bands appear in strychnine crystals at 1667 cm^{-1} and 1476 cm^{-1}, judged by the intense intensities[61] so that the band identification should be correct. Only the IR band at higher wavenumbers shows a solvent dependent shift of roughly 20 cm^{-1} at most. Since this band appears isolated in the spectrum, it can be safely assigned as amide stretch. In addition, the corresponding VCD band at 1660 cm^{-1} shows almost no shift in wavenumbers depending on the solvent due to the quite broad absorption bands. The VCD bands have a negative (1660 cm^{-1}; amide stretch) and a positive sign (1500 cm^{-1}). The calculated IR amide band of (−)-strychnine base (major conformer) is shifted by ca. 115 cm^{-1} to higher wavenumbers (1775 cm^{-1}, Figure 7, left), and the calculated VCD band (major conformer) has a negative sign (Figure 7, right), matching with experiment. The experimental VCD band at 1500 cm^{-1} cannot be reliably assigned in the calculated spectrum. We conclude that applying the VCD amide band of (−)-brucine for (−)-strychnine gives the correct AC assignment for (−)-strychnine (calculated spectra of the minor conformer and of protonated (−)-strychnine can be found in the supporting information).

Figure 7: Calculated spectra of (−)-strychnine base of the major conformer (mpw1pw91/cc-pvdz, IEFPCM: chloroform; IR on the right, VCD on the left)

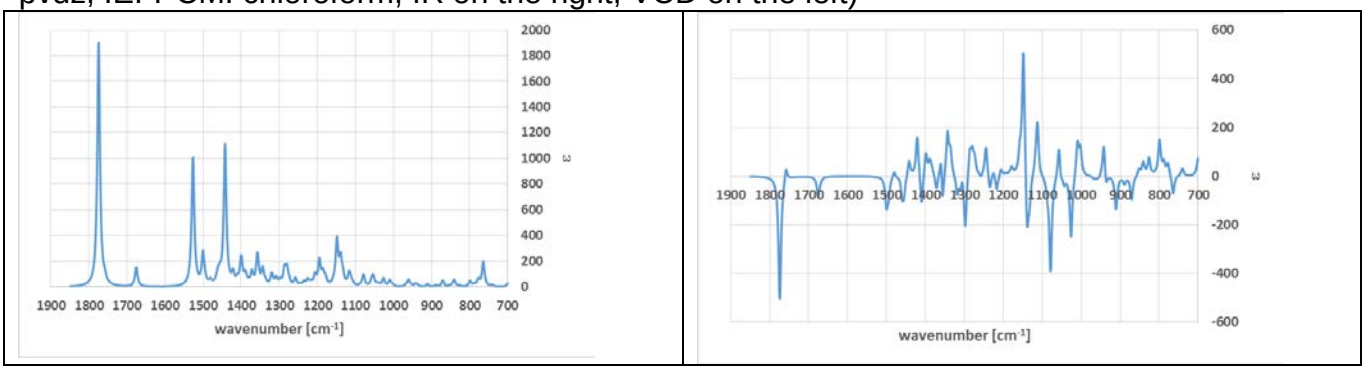

Conclusions

The structural analysis based on the comparison between experimental and calculated NMR data justified using a monomeric model of strychnine base and as protonated form. The experimental optical rotation data of both forms matched very well to the calculated values whereas the comparison between the experimental and calculated ECD spectrum of strychnine base showed larger discrepancies compared to the protonated/hydrochloride data pair. Application of the mpw1pw91/cc-pvdz (IEFPCM for solvent modelling) level of theory allowed the correct prediction of the AC of strychnine base and hydrochloride based on the comparison between experimental and calculated ORD and ECD data.

Experimental Section

(−)-Strychnine base and all other chemicals were obtained from Sigma Aldrich Laborchemikalien GmbH (Germany) and were used without further purification. The purity of (−)-strychnine base was corrected for 100 % for all measured values assuming that the strychnine content has an enantiomeric excess of 100 %. Solvents had p.a. grade. (−)-Strychnine HCl was formed by dissolving the free base in hydrochloric acid (gas) in ethyl acetate (1.3 M). After precipitation of the strychnine salt the solvent was removed under reduced pressure. The purity was determined by proton NMR and adjusted to 100 % for all measured values.
NMR measurements were performed at 298 K using a Bruker Avance 400 MHz NMR spectrometer (400.13 MHz for ^{1}H) equipped with a TXI probe head and a Bruker Avance III 600 MHz NMR spectrometer (600.25 MHz for ^{1}H) equipped with a QXI probe head. The proton spectra were measured for samples of the indicated concentrations with the following parameters: time domain = 32k points, number of scans = 16, apodization with an exponential window function with 0.3 Hz line width, relaxation delay between scans of 2 s.
The UV/Vis and ECD spectra were measured using a JASCO J-815 spectrometer and quartz cuvettes with 1 mm path length at 25 °C. Measurement parameter were: scanning speed: 200 nm/min, pitch: 0.5 nm, and band width: 1 nm. All spectra were solvent corrected and represent an average of three consecutive scans. For the ECD spectra values of $\Delta\varepsilon$ [$lM^{-1}cm^{-1}$] are used. The experimental UV/Vis spectra are shown with absorption units.
Optical rotation measurements were performed with methanol or chloroform as solvent at the indicated concentrations using a Polartronic-E polarimeter (Schmidt+Haensch GmbH&Co) at 24.5 °C. The unit of [α] is [degrees*$(dm*g/cm^3)^{-1}$].

Computations

For computations G09 and GaussView were used (Gaussian09, RevA.02).[62] The mpw1pw91 functional[63] was used together with Dunning`s correlation consistent basis sets[64,65] for geometry optimization, frequency and IR/VCD calculations, oscillator and rotational strength, specific optical rotation, and chemical shifts. Minima were indicated by the absence of

imaginary frequencies. Other levels of theory are indicated in the text. For solvent modelling, the IEFPCM (integral equation formalism polarizable continuum model) approach was applied with the appropriate solvent.[57] IR and VCD spectra were simulated using a broadening of 4 cm^{-1}. The oscillator strengths and rotational strengths were calculated using the velocity representation for the 30 excitations lowest in energy. The calculated UV/Vis and ECD spectra were simulated with gaussian bandshapes with a broadening of 0.33 eV. The calculated UV/Vis spectra are shown with extinction coefficients ε [$lM^{-1}cm^{-1}$] on the y-axis.

Acknowledgements

We gratefully acknowledge support by the DFG (FOR 934 to F.R. and U.M.R), the Max-Planck-Society, and by Prof. Griesinger (NMR II, MPIBPC, Göttingen).

Keywords: strychnine • structure • NMR • optical rotation • electronic circular dichroism • conformation

References

[1] Royal Swedish Academy of Sciences, 9. October **2013**, Scientific background on the Nobel Prize in chemistry 2013, Development of multiscale models for complex chemical systems
[2] K. C. Nicolaou, S. A. Snyder, *Angew. Chem. Int. Ed.* **2005**, *44*, 1012-1044.
[3] M. E. Maier, *Nat. Prod. Rep.* **2009**, *26*, 1105-1124.
[4] M. Elyashberg, A. J. Williams, K. Blinov, *Nat. Prod. Rep.* **2010**, *27*, 1296-1328.
[5] T. L. Suyama, W. H. Gerwick, K. L. McPhail, *Bioorg. Med. Chem.* **2011**, *19*, 6675-6701.
[6] M. Schmidt, H. Sun, P. Rogne, C. Griesinger, L. Kuhn, U. M. Reinscheid, *J. Am. Chem. Soc.* **2012**, *134*, 3080-3083.
[7] a: M. Schmidt, F. Reinscheid, H. Sun, H. Abromeit, G. K. E. Scriba, F. D. Sönnichsen, M. John, U. M. Reinscheid, *Eur. J. Org. Chem.* **2014**, 1147-1150; b: C. P. Butts, C. R. Jones, J. N. Harvey, *Chem. Commun*. **2011**, *47*, 1193-1195.
[8] P. J. Pelletier, J. B. Caventou, *Ann. Chim. Phys.* **1818**, *8*, 323.
[9] A. Mostad, *Acta Chem. Scand*. **1985**, *B39*, 705-716.
[10] M. Messerschmidt, S. Scheins, P. Luger, *Acta Cryst.* **2005**, *B61*, 115-121.
[11] R. Robinson, *Experientia* **1946**, *2*, 28-29.
[12] R. B. Woodward, M. P. Cava, W. D. Ollis, W. D. Hunger, H. U. Dabniker, K. Schenker, *J. Am. Chem. Soc.* **1954**, *76*, 4749-4751.
[13] J. H. Robertson, C. A. Beevers, *Nature* **1950**, *165*, 690-691.
[14] A. F. Peerdeman, *Acta Cryst.* **1956**, *9*, 824.
[15] J. Bonjoch, D. Solé, *Chem. Rev.* **2000**, *100*, 3455-3482.
[16] J. S. Overman, L. E. Cannon, *Angew. Chem. Int. Ed.* **2012**, *51*, 4288-4311.
[17] R. B. Woodward, M. P. Cava, W. D. Ollis, W. D. Hunger, H. U. Dabniker, K .Schenker, *Tetrahedron* **1963**, *19*, 247-288.
[18] V. Prelog, J. Battegay, W. I. Taylor, *Helv. Chim. Acta* **1948**, *30*, 2244-2246.

[19] P. Magnus, M. Giles, R. Bonnert, G. Johnson, L. McQuire, M. Deluca, A. Merritt, C. S. Kim N. Vicker, *J. Am. Chem. Soc.* **1993**, *115*, 8116-8129.
[20] F. Reinscheid, U. M. Reinscheid, *J. Mol. Struct..* **2015**, accepted
[21] J. T. Edward, S. C. Wong, A. J. Kresge, MF Powell, *Can. J. Chem.* **1984**, *62*, 2448-2450.
[22] Muthadi and Hifnawy, Strychnine, Analytical Profiles of Drug substances, Vol.15, **1986**, p. 563-646.
[23] J. T. Edward, S. C. Wong, R. A. McClelland, *Can. J. Chem.* **1984**, *62*, 144-146.
[24] A. E. Metaxas, J. R. Cort, *Magn. Reson. Chem.* **2013**, *51*, 292-298.
[25] A. Moreno, P. S. Pregosin, L. F. Veiros, A. Albinati, S. Rizzato, *Chem. Eur. J.* **2009**, *15*, 6848-6862.
[26] C. Laurence, M. Berthelot, Perspect. *Drug Discov. Design* **2000**, *18*, 39- 60.
[27] U. M. Reinscheid, C. Cychon, M. Köck, V. Schmidts, C. Thiele, C. Griesinger, *Eur. J. Org. Chem.* **2010**, *36*, 6900-6903.
[28] S. Chimichi, M. Boccalini, A. Matteucci, S. V. Kharlamov, S. Latypov, O. G. Sinyashin, *Magn. Reson. Chem.* **2010**, *48*, 607-613.
[29] T. C. Ramalho, M. Bühl, *Magn. Reson. Chem.* **2005**, *43*, 136-146.
[30] G. A. Webb, M. Witanowski, *Proc. Indian Acad. Sci (Chem. Sci.)* **1985**, *94*, 241-290.
[31] V. Manzoni, M. L. Lyra, R. M. Gester, K. Coutinho, S. Canuto, *PhysChemChemPhys* **2010**, *12*, 14023-14033.
[32] B. Mennucci, **2008**, Ed. S. Canuto, Solvation effects on molecules and biomolecules,1-21, Springer
[33] R. O. Duthaler, J. D. Roberts, *J. Magn. Reson.* **1979**, *34*, 129-139.
[34] F. Takahashi, N. C. Li, *J. Phys. Chem.* **1965**, *69*, 2950-2954.
[35] K. F. Wong, S. Ng, *J. Chem. Soc. Faraday Trans. II* **1975**, *71*, 622-630.
[36] B. Hilton, G. E. Martin, *J. Nat. Prod.* **2010**, *73*, 1465-1469.
[37] P. I. Nagy, A. Maheshwari, Y.-W. Kim, W. S. Messer Jr., *J. Phys. Chem. B* **2010**, *114*, 349-360.
[38] A. Lagutschenkov, J. Langer, G. Berden, J. Oomens, O. Dopfer, *J. Phys. Chem. A* **2010**, *114*, 13268-13276.
[39] F. A. L. Anet, I. Yavari, *Org. Magn. Reson.* **1979**, *12*, 362-364.
[40] A. T. Bottini, J. D. Roberts, *J. Am. Chem. Soc.* **1956**, *78*, 5126.
[41] M. Saunders, F. Yamada, *J. Am. Chem. Soc.* **1963**, *85*, 1882.
[42] D. de Loera, F. Liu, K. N. Houk, M. A. Garcia-Garibay, *J. Org. Chem.* **2013**, *78*, 11623-11626.
[43] A. M. Belostotskii, H. E. Gottlieb, P. Aped, A. Hassner, *Chem. Eur. J.* **1999**, *5*, 449-455.
[44] J. E. Anderson, D. Cazarini, J. E. T. Corrie, L. Lunazzi, *J. Chem. Soc. Perkin Trans. 2* **1993**, 1299-1304.
[45] H. Kessler, *Angew. Chem.* **1970**, 82, 237-253.
[46] M. D. Pluth, R. G. Bergman, K. N. Raymond, *J. Am. Chem. Soc.* **2008**, *130*, 6362-6366.
[47] J. H. Poupaert, F. A. Gbaguidi, C. N. Kapanda, H. Aichaoui, C. R. McCurdy, *Med. Chem. Res.* **2013**, *22*, 247-252.
[48] R .Glaser, Q.-J. Peng, A. S. Perlin, *J. Org. Chem.* **1988**, *53*, 2172-2180.
[49] J. C. Wilson, S. L. A. Munro, D. J .Craik, *Magn. Reson. Chem.* **1995**, *33*, 367-374.
[50] W. R. Morgan, D. E. Leyden, *J. Am. Chem. Soc.* **1970**, *92*, 4527-4531.
[51] M. Ōki, M. Ohira, Y. Yoshioka, T. Morita, H. Kihara, N. Nakamura, *Bull. Chem. Soc. Jpn.* **1984**, *57*, 2224-2229.

[52] G. Bifulco, R. Riccio, G. E. Martin, A. V. Buevich, R. T. Williamson, *Org. Lett.* **2013**, *15*, 654-657.
[53] CRC Handbook of chemistry and physics, 69th ed., DR Lide (ed.), CRC press(Boca Raton, Fl: **1988**), p. C-498
[54] P. L. Polavarapu, A. Petrovic, F. Wang, *Chirality* **2003**, *15*, S143-S149.
[55] P. J. Stephens, D. M. McCann, J. R. Cheeseman, M. J. Frisch, *Chirality* **2005**, *17*, S52-S64.
[56] J. Kongsted, K. Ruud, *Chem. Phys. Lett.* **2008**, *451*, 226-232.
[57] B. Mennucci, C. Cappelli, R. Cammi, J. Tomasi, *Chirality* **2011**, *23*, 717-729.
[58] A. Shimizu, T. Mori, Y. Inoue, S. Yamada, *J. Phys. Chem. A* **2009**, *113*, 8754-8764.
[59] J. W. Snow, T. M. Hooker, *Can. J. Chem.* **1978**, *56*, 1222-1230.
[60] V. Setnička, M. Urbanová, S. Pataridis, V. Král, K. Volka, *Tetrahedron: Asymmetry* **2002**, *13*, 2661-2666.
[61] V. A. Narayanan, N. A. Stump, G. D. Del Cul, T. Vo-Dinh, *J. Raman Spectrosc.* **1999**, *30*, 435-439.
62] Gaussian09: M. J. Frisch et al., Gaussian 09, Gaussian, Inc., Wallingford CT, **2009** RevA.02
[63] C. Adamo, V. Barone, *J. Chem. Phys.* **1998**, *108*, 664-675.
[65] E. R. Davidson, *Chem. Phys. Lett.,***1996**, *260*, 514-18.
[64] T. H.Dunning Jr., *J.Chem.Phys.* **1989**, *90*, 1007-1023.

Table of contents

Strychnine, structure, configuration

A detailed analysis of experimental and calculated data approved a monomeric structural model of strychnine (base and protonated/HCl) which could successfully be used for the assignment of the absolute configuration on the basis of chiroptical data (ORD, ECD, VCD). A number of dynamic processes such as solvent-solute association and nitrogen inversion/protonation could be identified.

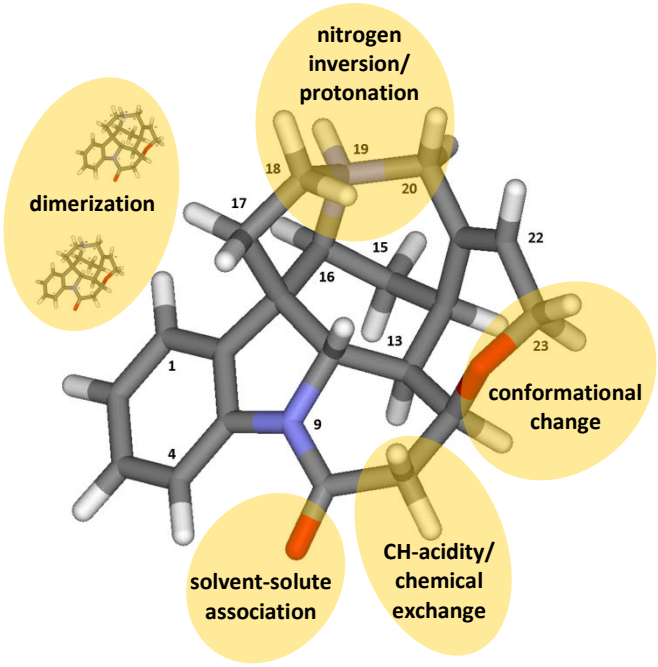

9.3 Menthol isomers and derivatives publication

Stereochemical analysis of menthol and menthylamine isomers using calculated and experimental optical rotation data

F Reinscheid, UM Reinscheid, (2016b)

J. Mol. Struct., 1103, 166-176

Stereochemical analysis of menthol and menthylamine isomers using calculated and experimental optical rotation data

F. Reinscheid[a], U.M. Reinscheid*[a]

Abstract: The complete series of menthol isomers and their corresponding amino derivatives (base and protonated/HCl forms), were investigated using experimental and theoretical data. Our study focused on the conformational and configurational analysis, and revealed that experimental data should be used in combination with calculated data. Furthermore, even in the case of the highly studied member, menthol, discrepancies were found among previously published literature values. We show that the correct determination of the population mix is a must for the correct prediction of the absolute configuration (AC) of neoisomenthol. The neoiso forms are of special interest since a number of structural inconsistences can be found in the literature. We present a stringent proof of the AC of neoisomenthol based on literature information. To the best of our knowledge, the AC of neoisomenthylamine is for the first time shown using experimental and calculated optical rotation data. A correction of a series of publications containing an important error in the assignment of (+)-menthylamine (correct: (+)-neomenthylamine) is presented. With 26 data pairs (experimental versus calculated) of optical rotation values a regression is performed. The AC of all 12 compounds, even the most difficult neoiso forms, could be predicted correctly using experimental low-temperature NMR data. Furthermore, if only experimental data with an optical rotation outside the range of $-10 < [\alpha] < +10$ are used, all 12 compounds would have been correctly assigned without low-temperature NMR data as restraints.

[a] F Reinscheid, UM Reinscheid *
NMR-based structural biology
Max-Planck-Institute of Biophysical Chemistry
Am Fassberg 11, 37077 Göttingen (Germany)
E-mail: urei@nmr.mpibpc.mpg.de

Supporting information for this article is given via a link at the end of the document.

Introduction

Menthol represents the most highly studied monoterpene. The development of structure determinations in the field of terpenes was described by Hanson.[1] Menthol and its derivatives are of high commercial interest due to their unique properties such as cooling and flavouring agents.[2] In addition, amino derivatives of the menthol series-the diastereomeric menthylamines (bases and HCl), have become important as chiral auxiliaries for asymmetric syntheses.[3]

Menthol (Fig. 1a) is the major constituent of the essential oil of the mint family (peppermint: *Mentha x piperita* and spearmint: *Mentha spicata*). Gladstone[4] presented optical rotation values for crude oils. Without separation, the hydrocarbon from the oil of *Mentha viridis* was termed “menthol”. Annually, several thousand tons of (–)-menthol are consumed. Its biosynthesis starts with geranyldiphosphate, which is converted by the limonene synthase to (–)-limonene. (–)-Limonene itself is also a very important monoterpene used for many pharmaceutical, cosmetic and health care products. Via (+)-pulegone, two carbonyl terpenes ((–)-menthone and (+)-isomenthone) are enzymatically produced. With (–)-menthone as a starting point, menthol reductase forms (–)-menthol, and a neomenthol reductase (+)-neomenthol. Likewise, with (+)-isomenthone as the substrate, neomenthol reductase produces (+)-isomenthol, and the menthol reductase (+)-neoisomenthol.[2] (–)-Menthol is able to activate the TRPM (transient receptor potential cation channel subfamily M member 8) receptor, which can also be activated by temperatures between 8 and 28°C. This receptor is also known as cold and menthol receptor 1 (CMR1).[5] Derivatives of the menthol isomers are patented as cooling agents.[6] The effective concentration (EC50) is 4.1 μM for (–)-menthol and almost 4 times higher for (+)-menthol (EC50 = 14.4 μM).[5]

Overall, published literature concerning the stereochemical analysis of the menthol isomers mostly focuses on menthol. The first report available based on the x-ray analysis of the menthol isomers dates back to 1999.[7] The authors presented data for (–)-menthol and emphasized the difficulties in obtaining suitable crystals. We believe this hindered the x-ray analysis of the other three isomers. Bombicz et al.[7] could not derive the absolute configuration due to very weak anomalous scattering. Menthol is also used as a test molecule for structure elucidation by NMR (nuclear magnetic resonance).[8] As a cyclohexane derivative, its stereochemical analysis has been the focus of research since decades.[9] Although computational chemistry has contributed a lot to our present knowledge, it is still mandatory to use experimental information for an accurate conformational analysis of cyclohexanes.[10] This

is also nicely illustrated by the report of Basso et al.[11] which revealed that, even for the deceptively simple *cis*-2-halocyclohexanols, it is difficult to correctly predict conformer populations. Therefore, low-temperature NMR data has turned out to be indispensable.

In this report we focus on the stereochemistry in solution of the complete series of menthol stereoisomers (Fig. 1a-e), together with their amino derivatives, both in their base form and protonated. A detailed structural analysis is presented for the parent molecule menthol, the neoiso forms, and menthylamine (base). Our comprehensive analysis aims at providing reliable information concerning the structure and configuration of 12 (four diastereomers of each series) compounds. In conclusion, we present limits of the applied procedure for the AC assignment based on the comparison between calculated and experimental optical rotation values.

Results and Discussion

Nomenclature is highly important in the field of stereochemical analysis. Enantiomers differ in the *gauche*$^+$/*gauche*$^-$ descriptors. A dihedral of *gauche*$^-$ in (–)-menthol, is *gauche*$^+$ in (+)-menthol. Many misconceptions have arisen as the definition of the dihedral varies among published reports. In a recent publication, the dihedral was without definition since the cited report did not contain the relevant information.[12]

We used the following short hand notation (Fig. 1a-e): chair with the position of substituents in the following order: methyl / OH / isopropyl (e.g. $1_{eq}3_{eq}4_{eq}$ equals eq/eq/eq) (eq: equatorial, ax: axial); isopropyl dihedral: H8-C8-C4-H4, OH dihedral: H-O-C-H; *trans* (t), *gauche*$^+$ (g^+), *gauche*$^-$ (g^-). Alongside the schematic drawings, geometry optimized representative conformers of the menthol isomers are shown in Figure 1.Throughout the text the units [degrees*(dm*g/cm^3)$^{-1}$] for [α] and Hz for J-couplings are used. Relative conformer populations refer to 298 K unless otherwise stated.

Figures 1a-e: Menthol and the diastereomers neomenthol, isomenthol and neoisomenthol; calculated conformers[a] of (+)-(1*S*,3*S*,4*R*)-menthol ($1_{eq}3_{eq}4_{eq}$), (+)-(1*R*,3*S*,4*S*)-Neomenthol ($1_{eq}3_{ax}4_{eq}$), (–)-(1*S*,3*R*,4*S*)-Isomenthol ($1_{ax}3_{eq}4_{eq}$) and ($1_{eq}3_{ax}4_{ax}$), (–)-(1*S*,3*S*,4*S*)-Neoisomenthol ($1_{eq}3_{eq}4_{ax}$) and ($1_{ax}3_{ax}4_{eq}$) obtained by DFT (density functional theory) optimization at the mpw1pw91/cc-pvdz level of theory with a continuum solvent model using acetonitrile as solvent[13]

a) (+)-(1*S*,3*S*,4*R*)-Menthol ($1_{eq}3_{eq}4_{eq}$)

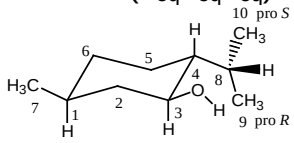

(+)-Menthol: eq/eq/eq; g^+/*trans*

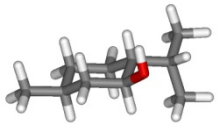

b) (+)-(1*R*,3*S*,4*S*)-Neomenthol ($1_{eq}3_{ax}4_{eq}$)

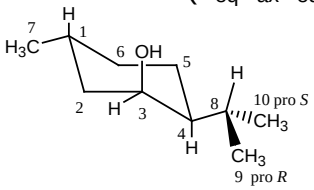

(+)-Neomenthol: eq/ax/eq; *trans*/ g^-

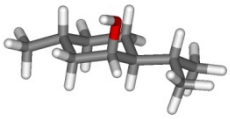

c) (–)-(1*S*,3*R*,4*S*)-Isomenthol ($1_{ax}3_{eq}4_{eq}$)

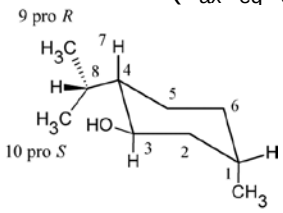

(–)-Isomenthol: ax/eq/eq; g^-/ g^-

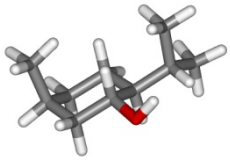

(–)-Isomenthol: eq/ax/ax; *trans*/ *trans*

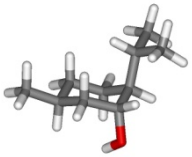

d) (–)-(1*S*,3*S*,4*S*)-Neoisomenthol ($1_{ax}3_{ax}4_{eq}$)

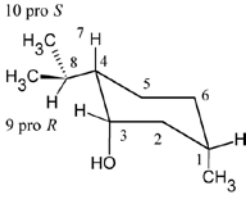

(–)-Neoisomenthol: eq/eq/ax; *trans*/g^-

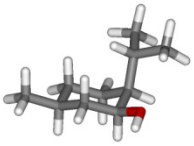

(–)-Neoisomenthol: ax/ax/eq; g^+/g^-

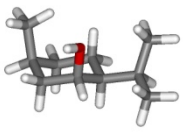

[a]:Nomenclature: chair with position of substituents: methyl / OH / isopropyl (eq: equatorial, ax: axial); isopropyl dihedral: H4-C4-C8-H8; OH dihedral: H-O-C3-H3; *trans* (t), *gauche*$^+$ (g^+) or *gauche*$^-$ (g^-)

Structural restraints from NMR $^{3}J_{HH}$ coupling constants and ^{13}C chemical shifts

An important structural parameter for the menthol series is the $^{3}J_{OH}$ ($^{3}J_{HOCH}$) coupling constant, which indicates the rotamer population. Overall, measured values show that averaging around the C-O bond should be performed so that the experimental values represent a mixture of *gauche* and *trans* rotamers. The $^{3}J_{OH}$ coupling constants in DMSO (dimethyl sulfoxide) were determined as 5.6 Hz, 4.9 Hz, overlap, and 3.5 Hz for menthol, isomenthol, neomenthol, and neoisomenthol, respectively.[14] For a detailed analysis refer to the individual compound sections.

Two other stereochemical aspects are important: the chair type and the isopropyl dihedral. We analysed the experimental and calculated $^{3}J_{H4H8}$ coupling constants to derive an average value for the isopropyl dihedral.

The $^{3}J_{H4H8}$ coupling constants were measured in $CDCl_3$.[15] The $^{3}J_{H4H8}$ coupling constants of menthol (2.5 Hz), neomenthol (9.1 Hz), and isomenthol (4.2 Hz) indicate dominant isopropyl rotamers for menthol and neomenthol, and substantial conformational averaging of the isopropyl rotamers of isomenthol. The $^{3}J_{H4H8}$ coupling constant of neoisomenthol could not be measured due to severe overlap.

Low-temperature ^{13}C chemical shifts in CD_2Cl_2[16] could be applied for the population analysis based on room temperature data in $CDCl_3$[17] since the experimental optical rotation is similar between the two solvents.[18] Clearly, the direct influence of the solvent on the ^{13}C chemical shift is quite small and the solvent dependent conformer populations are the major determinant for the chemical shifts under conditions of fast exchange, which is valid for room temperature for isomenthol and neoisomenthol. Since a very good fit between experimental ^{13}C resonances in chloroform and the calculated resonances with acetonitrile as solvent was observed, we regard acetonitrile as being a good representative even for more apolar solvents. Taking the solvent parameters used into account,[19] acetonitrile seems to be a good compromise for simulating experimental solvents such as chloroform, ethanol, and pure solute, in the case of menthol isomers, a secondary alcohol.

Structural analysis of the menthol-type isomers

With all 12 menthol-type isomers (menthols, menthylamines as base and protonated) a conformational search with Discovery Studio (Accelrys,[20] Charmm force field, BEST search algorithm, in vacuo) and subsequent DFT calculations (Gaussian09,[21] level of theory:

mpw1pw91/cc-pvdz, IEFPCM (integral equation formalism polarizable continuum model): acetonitrile as solvent) with the conformers lowest in energy (cut-off: 2 kcal/mole) were conducted. The DFT calculations comprised geometry optimization, frequency calculations to obtain free energies to calculate the Boltzmann-weighted populations, calculations of NMR parameters such as ^{13}C chemical shifts and J-coupling constants, and optical rotation calculations.

During the analysis of the menthol conformers, it became clear that the OH rotamers have to be calculated. Therefore, for menthol, neomenthol and isomenthol, all OH rotamers of the dominant conformers obtained by the conformational search using a forcefield and subsequent DFT optimization were calculated. For neoisomenthol and neoisomenthylamine, all 18 combinations (2 chairs, 3 OH rotamers, 3 isopropyl rotamers) were calculated.

The OH rotamers are a very important factor in the configurational analysis using chiroptical methods. In the near IR region, the experimental ECD (electronic circular dichroism) spectra of *endo*-borneol enantiomers more successfully matched with calculations if equal populations of the three OH rotamers are assumed, in contrast to the energy calculation which indicates one predominant (51.5 %) conformer.[22] In a recent study, Qiu et al.[23] investigated the tadalafil isomers by chiroptical and NMR methods. The authors showed that the population mixes differ if different levels of theory are used for energy calculations. Rottmannová et al.[24] investigated 1,2,4-trihydroxy-*para*-menthane using calculated and experimental NMR data. In the case of this compound, an intramolecular H-bond is possible, which will restrict at least two OH dihedrals, facilitating the analysis. In biomolecular NMR $^{1}J_{C1'H1'}$ coupling constants have been used for structural modelling of RNA (ribonucleic acid), as these coupling constants depend on the OH dihedral, and therefore can be used to determine this important dihedral.[25,26]

In the present report we used ORD data obtained in solution, meaning that solvent effects had to be modelled in both the configurational and conformational analyses. Several factors had to be taken into account at different stages of the analysis: geometry optimization (structural model), energies (population mix), NMR parameters such as chemical shift and J coupling constants (structural model, population mix), and chiroptical data such as ORD (optical rotation dispersion, ECD (electronic circular dichroism), VCD (vibrational circular dichroism) (absolute configuration).

In the field of configurational analysis, the modelling of solvent effects on chiroptical properties is of great importance (see the review of Mennucci et al.).[13] The continuum models often

account for large parts of the solvent effects. They have been applied often successfully for the prediction of NMR chemical shifts.[27] Polavarapu [28] presented important points for consideration for incorporation of solvent effects into the configurational analysis. A detailed study of limonene has shown that the mpw1pw91/cc-pvdz level of theory delivers reliable results for the calculation of ^{13}C chemical shifts.[29] In addition, this level of theory was successful in the geometry optimization of a low-populated conformer of strychnine, base and HCl.[30,31]

However, specific, local effects such as H-bonding are neglected. Generally, two procedures are applied to take these effects into account: 1. the formation of supermolecules consisting of solute and a sufficient large layer of solvent molecules; 2. calculation and averaging of MD (molecular dynamics)/Monte Carlo snapshots. However, both procedures are difficult to use for chiroptical property prediction. One very important point to consider, for both approaches, is the system definition. Depending on the choice, the predicted value may differ rendering the experimental comparison unreliable. Furthermore, the solvent shell can become chiral and thus experiments are needed to decide if this induced chirality is a computational artefact, or real.[13] If an aggregation is proven, the supermolecule approach should be the best choice.

2.2.1 (+)-(1*S*,3*S*,4*R*)-menthol

Using a conformational search and subsequent DFT optimization we found a dominant chair with all three substituents in the equatorial position for menthol (Figure 1a, Table 1), in agreement with a crystal structure for (–)-menthol.[7] Likewise, at low temperature (-193 °C) Pekh et al. observed only one chair in dichloromethane [22]. With the assumption that all three OH rotamers of the dominant conformer are populated, we calculated the *trans*, g^+ and g^- rotamers of the OH eq chair of (+)-menthol with the isopropyl group in the g^+ position (Table 1). In agreement of our analysis, Lomas[32] investigated (–)-menthol and found the g^- rotamer of the isopropyl group as dominant conformer, with the crystal structure revealing the isopropyl group in the *gauche* position.[7] However, pure computational results differ even between similar levels of theory (Table 2). Therefore, we propose to use experimental data for supporting or revising the calculated data.

With the conformers of Table 1, we calculated a $^3J_{OH}$ coupling constant of 4.9 Hz, which fits the experimental value of 5.6 HZ in DMSO.[14] Likewise, the calculated $^3J_{isopropyl}$ coupling

constant of 1.7 Hz fits the experimental value of 2.5 Hz in $CDCl_3$. The calculated ^{13}C population-weighted shieldings gave a good fit with the experimental chemical shifts (y = 193.8 ppm – 0.97*chemical shift [ppm] of experiment; standard error of intercept and slope, 0.83 ppm and 0.022 ppm, respectively, R^2 = 0.9959, n = 10) (see Table S1 in the supporting information). A CMAE (corrected mean absolute error, defined as sum of the absolute differences between calculated (using the linear regression) and experimental values, divided by the number of data pairs) of 0.62 ppm resulted, if the alcoholic C3 was excluded. Since we calculated an isolated molecule, H-bonding in chloroform is neglected as it might heavily influence the chemical shift of C3. For neoisomenthol, the regression parameters were later used for transforming calculated shieldings into chemical shifts.

Table 1: Calculated parameters of the OH rotamers of the OHeq chair with a g^+ isopropyl dihedral of (+)-(1*S*,3*S*,4*R*)-menthol (eq/eq/eq) (mpw1pw91/cc-pvdz, IEFPCM: acetonitrile)

Isopropyl/OH dihedral	g^+/*trans*	g^+/g^+	g^+/g^-
H8-C8-C4-H4	+69.8	+64.5	+67.2
H-O-C3-H3	-178.8	+50.2	-80.5
$[\alpha]_{589}$	+43.3	+3.8	+80.5
$[\alpha]_{578}$	+44.9	+3.85	+83.9
$[\alpha]_{546}$	+50.7	+4.08	+94.9
$[\alpha]_{436}$	+82.9	+4.14	+157.3
$[\alpha]_{405}$	+97.8	+3.43	+186.9
$[\alpha]_{366}$	+124.2	+0.98	+240.3
rel. free energy (kcal/mole)	0	0.30	0.12
population (%)	41.2	24.9	33.9
$^3J_{OH}$ [Hz]	9.85	2.13	0.83
$^3J_{isopropyl}$ [Hz]	1.55	1.85	1.75

In agreement with our results in the solution phase, Albrecht et al.[33] found by IR (infra-red) spectroscopy in the gas phase, a chair conformation in which the OH group is equatorial in menthol. Although the OH group positions differ with respect to the cyclohexane chair (equatorial to axial), the OH wavenumber of the stretching mode is similar: 3654 cm^{-1} and 3655 cm^{-1} for menthol and neomenthol, respectively. The dominant OH dihedral was determined as g^+ for (–)-menthol and the isopropyl dihedral as g^- for (–)-menthol. This is partly in agreement with our results for (+)-menthol: a *gauche*$^+$ isopropyl dihedral but a *trans* OH dihedral in solution.

Table 2: Own results and literature data converted to (+)-menthol with calculated energy differences among the conformers (chair: eq/eq/eq; isopropyl and OH dihedrals indicated, energies in kcal/mole)

Isopropyl/ OH dihedral	g^+/ *trans*	g^+/g^+	g^+/g^-	g^-/ *trans*	g^- /g^-	*trans*/ *trans*	*trans*/ g^-
this study mpw1pw91/cc-pvdz (IEFPCM: acetonitrile)	0	0.3	0.12	-	-	-	-
RHF/6-31G* In vacuo [35]	-	-	0	-	0.76	-	2.4
B3LYP/6-31G* in vacuo [35]	-	-	0	-	0.5	-	-
B3LYP/cc-pvdz in vacuo [34]	0	0.84	0.33	0.53	0.74	1.72	2.11
B3LYP/6-31+G* in vacuo [34]	0.22	0.57	0	1.20	1.03	2.61	2.30
B3LYP/cc-pvdz/ PCM CCl_4 [34]	0.10	0.36	0	1.20	1.08	2.58	2.39
B3LYP/6-31G** In vacuo [36]	0	0.71	0.25	0.59	0.93	1.86	2.29
B3LYP/aug-cc-pvtz in vacuo [37]	0.24	0.45	0	1.27	1.08	-	-
B3LYP/6-311++ G(d,p) in vacuo [37]	0.22	0.48	0	1.20	1.00	-	-
MP2/6-311++G (d,p) in vacuo [37]	0.33	0.50	0	1.20	0.79	-	-
B3LYP/6-311+G* in vacuo [33]	0.31	-	0	1.22	0.96	-	-
MP2/6-311+G* in vacuo [33]	0.45	-	0	-	-	-	-

Importantly, Albrecht et al.[33] described several levels of theories which did not give reliable relative energies, and thus a population analysis could not be performed. Based on experimental data it was concluded that the B97D functional provided qualitatively incorrect

results. From the experimental $^3J_{OH}$ coupling constant, however, it is clear that a mix of OH rotamers exist in solution, with balanced *trans* and *gauche* populations. Therefore we believe that our calculated populations are close to the real values. Furthermore, similar to our findings, Senda and Imaizumi[38] predicted 100 % of the equatorial OH group for menthol based on free energy estimates for the different substituents being equatorial or axial. Likewise, Jensen[39] assumed 100 % of the equatorial OH group for menthol based on the bandwidth measurements of the H3 resonance, presumably in CCl_4 as solvent.

Based on the free energy derived populations of Table 1 we predicted a $[\alpha]_{589}$ value of +46.1 which fits very well to the experimental value of +48.13 in toluene (c=10.05, +20.0 °C, Paine III).[40] The three rotamers with a g^+ isopropyl group (Table 2) were used for the calculation of the ORD curve (Table 3). The calculated and experimental ORD data from a Jasco application note[40a] show that in the wavelength range from 589 nm to 365 nm, the ORD curves for menthol are monosignate (Table 3). This allows a more reliable prediction of the AC when compared to a bisignate curve[41] since the zero crossing prediction is not required. The crossing is related to a correct prediction of amplitudes and excitation wavelengths. The latter are quite often associated with a large error. Since it is not clear which electronic excitation, to what extent is affected, there is no systematic way to correct it. In contrast, this can easily be done with ECD spectra, since the predicted UV (ultra-violet) spectra can be used as a guide to adjust the x-axis of the calculated ECD spectra to the experimental one. This procedure is not possible for the ORD curve.

Table 3: Calculated (acetonitrile) and experimental ORD values of (–)-(1*S*,3*S*,4*R*)-menthol taken from Ref. [40] for (+)-menthol at 578 nm, and a JASCO application note (ethanol, 20°C, 1 % solution)[40a]

wavelength [nm]	$[\alpha]_{exp}$	$[\alpha]_{calc}$
589	-50	-46.1
578	+50.39[a]	-47.9
546	-60	-54.1
436	-95	-88.5
405	-115	-104.5
365	-145	-132.9

[a]: 20.0°C, toluene, c=10.05, (+)-menthol enantiomer [40]

The electronic excitations of the menthol and menthylamine isomers lie in the UV region that is not accessible with typical ECD instruments and solvents. An interesting investigation by Grigor`ev et al.[42] presented data about an induced CD of menthol complexes with ketones such as acetone as solvents. This would allow the assignment of the absolute configuration

even for the difficult case of neoisomenthol (vide infra). However, this publication lacks some experimental information (e.g. wavelength), and thus a reproduction of the results is impossible to obtain

In the following section, we focus on the difficult to analyse neoiso forms, and menthylamine for which an important correction has to be made in the literature. A detailed description of all other compounds can be found in the supporting information.

2.2.2 (–)-(1*S*,3*S*,4*S*)-neoisomenthol

It is important to assign the sign of the $[\alpha]_{589}$ value of neoisomenthol to a specific solvent since a solvent-dependent sign change occurs. Our reference solvent is ethanol.

A full conformational search encompassing all possible conformers was performed, motivated by three reasons: (i) Neoisomenthol shows the smallest optical rotation value among the menthol isomers. Only a highly accurate conformational analysis has the ability to reproduce this value; (ii) Hückel et al.[43] mentioned a higher tendency for aggregation of neomenthol and neoisomenthol compared to menthol and isomenthol. The authors concluded that neoisomenthol differed markedly from the other three isomers with respect to conformation and reactivity, and hypothesized that a high flexibility could be responsible for the characteristic behaviour of neoisomenthol, with the possible existence of a non-chair form, e.g. twisted boat; (iii) the $[\alpha]$ of neoisomenthol exhibits a strong solvent dependence. Interestingly, also the *O*-methyl derivative shows strong solvent dependent optical rotations.[44]

Consequently, we built, and geometry optimized 18 chair conformers of (–)-neoisomenthol with ethanol as a solvent as it is the reference solvent for the optical rotation of neoisomenthol (2 chairs, 3 rotamers of the OH group, 3 rotamers of the isopropyl group). All data of Tables 4A (OHeq chair) and B (OHax chair) were obtained with ethanol as solvent, with the four dominant conformers selected for further analysis indicated in bold, and the optical rotations calculated on three levels of theory.

The OHax:OHeq ratio was found to be 87:13. With the populations and $[\alpha]_{589}$ values of Tables 4A and B, the incorrect sign is predicted: +15.4, +24.3, and +20.8 for the three levels of theory for (–)-(1*S*,3*S*,4*S*)-neoisomenthol (experimental $[\alpha]_{589}$ value in ethanol: +1.98 for (+)-1*R*,3*R*,4*R*)-neoisomenthol (c=4.028, 20°C).[18]

Calculated enthalphies instead of the free energies in Table 4A and B were used. This procedure is justified due to the large error in the calculated entropic term, but did not change the result: a slightly increased OHeq chair population of 19.8 %, but still the incorrect sign of the specific optical rotation: +9.3 for the (*S*)-enantiomer of neoisomenthol (IEFPCM: ethanol) (see supporting information, Tables S9C and D).

Interestingly, if a factor is applied to the data of Tables 4A and B that calibrates the two chair forms to a ratio of 60:40 (OHax:OHeq) using ethanol as solvent, the $[\alpha]_{589}$ values of the three levels are found to be: –2.2/+2.9/+0.2. Although this ratio gives at least with one basis set the correct sign of the optical rotation, it is not clear if the individual OH and isopropyl rotamers can be scaled in this way since we do not have an experimental value for $^{3}J_{isopropyl}$, and the $^{3}J_{OH}$ indicates averaging (3.5 Hz). Furthermore, for a population analysis with all 18 conformers too few parameters are available: at best 10 ^{13}C resonances, and 2 ^{3}J coupling constants. The inclusion of other parameters such as proton chemical shifts is currently not possible due to heavy overlap and strong coupling constant artefacts. Therefore, a full proton assignment has yet to be performed. In addition, a fraction of resonances showed only small differences among the conformers.

One solution is to analyse a smaller number of conformers which are selected to represent a large fraction of molecules based on the calculated energies. As a first step we used the experimentally determined chair ratio by Pekh et al. .[16] At 193 K in CD_2Cl_2 two sets of signals were obtained which were assumed to belong to the two chair forms. Using the ^{13}C resonances at low temperatures and fitting to the values obtained at room temperature in $CDCl_3$[17] resulted in a 67:33 (OHax:OHeq) ratio with the lowest CMAE.[16] This is justified since the optical rotation in chloroform is very similar to the value in ethanol, indicating that the chair ratio in these two solvents is similar. The room temperature chemical shifts in CCl_4[16] differ less than 0.5 ppm to the room temperature data in $CDCl_3$.[17] This means that solvent induced changes in the conformer populations are relatively small, or masked by a concomitantly changed chemical shift due to direct interactions, and/or magnetic susceptibility differences which are not perfectly removed by using TMS as reference.

Table 4A: Calculated dihedrals and populations based on free energy differences weighted by the Boltzmann equation (mpw1pw91/cc-pvdz, IEFPCM: ethanol), $[\alpha]_{589}$ at three different levels of theory (level 1: mp1pw91/cc-pvdz, IEFPCM: ethanol; level 2: mp1pw91/aug-cc-pvdz, IEFPCM: ethanol; level 3: mp1pw91/cc-pvtz, IEFPCM: ethanol) of the OHeq chair of (–)-(1*S*,3*S*,4*S*)-neoisomenthol

Isopropyl dihedral	g^+	g^-	t	g^+	g^-	t
OH dihedral	g^+	g^+	g^+	g^-	g^-	g^-
Isopropyl dihedral	82.0	-78.2	-166.4	84.3	-76.5	161.1
OH dihedral	56.3	59.1	61.7	-63.6	-63.3	-63.7
dipole moment [D]	1.87	1.78	1.77	1.95	1.82	2.11
population [%]	0.05	0.44	6.44	0.05	0.34	4.10
$[\alpha]_{589}$ level 1	-38.2	-93.2	-63.1	+45.4	-10.4	+4.1
$[\alpha]_{589}$ level 2	-28.4	-90.1	-64.6	+47.8	-12.8	-11.9
$[\alpha]_{589}$ level 3	-35.4	-88.6	-68.1	+42.1	-7.9	-6.4

Isopropyl dihedral	g^+	g^-	t
OH dihedral	t	t	t
Isopropyl dihedral	81.6	-73.2	162.5
OH dihedral	-167.4	-168.0	-173.9
dipole moment [D]	1.98	1.76	2.10
population [%]	0.02	0.32	1.02
$[\alpha]_{589}$ level 1	-41.9	-64.8	-69.3
$[\alpha]_{589}$ level 2	-42.9	-64.5	-34.9
$[\alpha]_{589}$ level 3	-43.6	-59.5	-47.9

Next we selected the five mostly populated conformers (2 OHeq, 3 OHax) based on calculated energies, calculated the ^{13}C shieldings and used ^{13}C data obtained by low-temperature measurements representing the individual two chairs[16] for multiple regression. Using the

calculated values of the three dominant conformers tg^+, tg^- and tt of the OHax chair, a population mix of 34:3:63 was obtained. Since the ^{13}C resonances of the latter two differ only slightly (max. difference: 1.62 ppm, only two resonance differences bigger than 1.0 ppm), we selected tg^- as representative conformer. The predicted energy for the tg^- conformer was lower than that for conformer tt. We repeated the regression using only two conformers of the OHax chair: tg^+ and tg^-. With these two conformers we obtained a good fit (R^2=0.993, n=10) and a low corrected mean absolute error (CMAE) of 0.41 ppm with all 10 resonances using the population mix of 46:54 for tg^+:tg^-.

Likewise, the ^{13}C data for the OHeq chair were analysed with the tg^+ and tg^- conformers. A CMAE of 0.85 ppm was obtained for a population mix of 55/45 for tg^+/tg^- with all 10 resonances (R^2=0.998). The combination of the four conformers of the two chair forms with a chair ratio of 67:33 (OHax:OHeq) as restraint, gave a population mix of 30.8:36.2:18.2:14.8 (OHax,tg^+/OHax,tg^-/OHeq,tg^+/OHeq,tg^-) which was regressed versus the experimental values at room temperature in $CDCl_3$[17] using the menthol regression parameters (intercept: 193.8 ppm, slope: -0.97 ppm). The CMAE amounts to 0.92 ppm using all ten ^{13}C resonances. Based on this good fit between experimental and calculated values based on chair forms, the existence of reasonably populated twisted boat form can be excluded.[45]

The predicted $^3J_{OH}$ coupling constant of 0.7 Hz which is much smaller than the experimental value (3.5 Hz in $CDCl_3$), indicates that the predicted OH *gauche*/*trans* ratio is too low. This discrepancy can be explained due to the fact that we exclusively selected the tg^- conformer for the OHax chair instead of the tt conformer. Using a mix of 6 % tg^- and 30 % tt, the predicted coupling constant would exactly match the experiment: 3.5 Hz. Of course, this population mix would change the predicted optical rotation: +0.7 for the *S*-enantiomer instead of –5.5 approaching the experimental value of +2.2 for (+)-(1*R*,3*R*,4*R*)-neoisomenthol, however, with the wrong sign (Table 5). The experimental $^3J_{H4,H8}$ coupling constant for neoisomenthol could not be determined due to overlapping resonances. Thus, a comparison with a calculated value is not possible.

Table 4B: Calculated dihedrals and populations based on free energy differences weighted by the Boltzmann equation (mpw1pw91/cc-pvdz, IEFPCM: ethanol), $[\alpha]_{589}$ at three different levels of theory (level 1: mp1pw91/cc-pvdz, IEFPCM: ethanol; level 2: mp1pw91/aug-cc-pvdz, IEFPCM: ethanol; level 3: mp1pw91/cc-pvtz, IEFPCM: ethanol) of the OHax chair of (–)-(1*S*,3*S*,4*S*)-neoisomenthol

Isopropyl dihedral	g^+	g^-	t	g^+	g^-	t
OH dihedral	g^+	g^+	g^+	g^-	g^-	g^-
Isopropyl dihedral	64.4	-81.0	175.0	54.0	-75.7	172.9
OH dihedral	63.9	45.7	59.2	-66.2	-66.5	-65.8
dipole moment [D]	2.18	1.88	1.97	1.88	1.96	1.73
population [%]	1.13	1.38	20.10	2.70	4.57	39.46
$[\alpha]_{589}$ level 1	+49.1	-56.4	-20.5	+78.2	+11.9	+32.2
$[\alpha]_{589}$ level 2	+32.9	-19.9	-15.7	+96.8	+26.8	+45.7
$[\alpha]_{589}$ level 3	+41.7	-37.9	-15.3	+92.7	+23.9	+40.4

Isopropyl dihedral	g^+	g^-	t
OH dihedral	t	t	t
Isopropyl dihedral	56.1	-75.2	174.1
OH dihedral	169.8	-178.4	169.6
dipole moment [D]	2.12	2.13	2.02
population [%]	1.04	0.97	15.87
$[\alpha]_{589}$ level 1	+88.7	+27.7	+53.2
$[\alpha]_{589}$ level 2	+102.5	+34.3	+61.5
$[\alpha]_{589}$ level 3	+94.6	+30.8	+55.6

Based on the four conformers, the $[\alpha]_{589}$ values of (–)-(1*S*,3*S*,4*S*)-neoisomenthol are -5.5, -1.8, -3.4 for the basis sets cc-pvdz, aug-cc-pvdz and cc-pvtz, respectively (experiment: +1.98 for (+)-1*R*,3*R*,4*R*)-neoisomenthol, c=4.028, ethanol, 20°C;[18] +2.2 for (+)-1*R*,3*R*,4*R*)-

neoisomenthol, c=2.0, ethanol, 16°C).[46] Magnitude and sign of the experimental ORD data were correctly predicted (Table 5).

Table 5: Calculated ORD values based on four conformers of (–)-(1S,3S,4S)-neoisomenthol (mpw1pw91/cc-pvdz, IEFPCM: ethanol) and experimental ORD values of (+)-(1*R*,3*R*,4*R*)-neoisomenthol

	$[\alpha]_{656}$	$[\alpha]_{589}$	$[\alpha]_{578}$	$[\alpha]_{546}$
(+)-(1*R*,3*R*,4*R*)-neoisomenthol[a]	-	+0.406[d]	+0.425[d]	+0.473[d]
(+)-(1*R*,3*R*,4*R*)-neoisomenthol[a]	+1.7[c]	+2.2[c]	-	+2.3[c]
(–)-(1*S*,3*S*,4*S*)-neoisomenthol[b]	–4.6	–5.5	–5.6	–6.2

[a]: experimental; [b]: calculated with the four selected conformers from above; [c]: c=2.0, ethanol, 16°C;[46] [d]: neat, 99.3% pure by GC, at 20.0°C[40]

The most probable explanation for the solvent dependent optical rotation is a solvent dependent conformational equilibrium for neoisomenthol. Hückel and Gupté[47] hypothesized that the chair with the OH in an axial position is responsible for the negative value in diethylether this appears to be correct for the (+)-(1*R*,3*R*,4*R*)-neoisomenthol enantiomer. Starting from negative $[\alpha]_{589}$ values for diethylether and cyclohexane (–12.36 and –8.69), the specific optical rotation becomes positive in more dipolar and H-bond donating solvents such as ethanol (+1.98). This behaviour indicates a strong solvent dependence and probably the H-bond assisted stabilization of conformers and/or stabilization of conformers by solvent polarity. Our data confirm this assumption since the OHax conformers contribute +20.7 to the total calculated $[\alpha]_{589}$ value of +15.4 for (–)-(1*S*,3*S*,4*S*)-neoisomenthol with a incorrect sign (mpw1pw91/cc-pvdz, IEFPCM: ethanol) (Tables 4A and B). The OHeq conformers contribute –5.3 units with the correct sign. The OHax:OHeq ratio is 87:13. This indicates a too low population of the OHeq conformers. All solvents increasing the contribution of the OHeq chair such as ethanol would shift the $[\alpha]_{589}$ value of (–)-(1*S*,3*S*,4*S*)-neoisomenthol towards a negative sign. In more apolar, especially non-H-bond donating solvents such as CCl_4 and cyclohexane, the OHax:OHeq ratio is better modelled with a dominant OHax form. Likewise, Cole and Jefferies[48] concluded based on IR spectroscopy of a diol of neoisomenthol that a ratio of at least 80:20 (OHax:OHeq) is present for neoisomenthol in CCl_4. In fact, the $[\alpha]_{589}$ values from Table 6 indicate that in this solvent the population of OHax is higher than in ethanol. For a correct sign prediction in ethanol without selecting individual conformers a OHax:OHeq ratio of 60:40 was necessary (vide supra).

Interestingly, using the acidity and dipolarity parameters of Catalán[19] a relatively good regression was obtained using the optical rotation values at 546 nm neglecting *tert*-butanol and diethylether (y = -9.047 + 17.16 * SA + 5.97 * SdP, R^2=0.853, n=10; SA: solvent acidity;

SdP: solvent dipolarity). With increasing solvent acidity and dipolarity, the OHeq is more stabilized than the OHax form due to the formation of 2 instead of 1 H-bond.[49,50] As an explanation, the following should be considered: the size of an OH group increases from apolar/aprotic via polar to protic solvents due to the formation of solvent-solute interactions, rendering the OH group larger in space. Concomitantly, the population of the equatorial form increases.[49] A study of the diffusion of cyclohexanol in different solvent supports this explanation.[51] Importantly, in the apolar/aprotic solvent decane, the diffusion is slowed down compared to acetonitrile which can be explained by the formation of cyclohexanol aggregates (concentration: 10 mg/ml).

A selective chair stabilization, due to very different dipole moments among the conformers, can be ruled out as the calculated dipole moments of the conformers (Tables 4A and B) are similar for both chairs: on average the OH eq conformers have a population weighted dipole moment of 1.91, whereas the OH ax conformers of 1.87. Even the dominant populations show evenly distributed dipole moments among the two chairs.

Neglecting *tert*-butanol in the analysis can be rationalized as a too small SA value was obtained in the reference reaction due to steric hindrance. Therefore, the SA value of *tert*-butanol appears to be too low for the stabilizing interaction with the OHeq form of neoisomenthol. Diethylether cannot stabilize the OHeq chair by dipolar interactions because of accessibility problems, so the SdP value appears to be too large for the interaction with the OHeq form of neoisomenthol.

A similar chair ratio was determined by Feltkamp and Franklin[52] who investigated the solution conformations of the menthol isomers. Based on NMR coupling constants analysed as sum (bandwidth), they determined a 71:29 (OHax:OHeq) ratio for neoisomenthol. Unfortunately, we could not find information concerning the solvent, and we speculate that chloroform or CCl_4 was used. Likewise, Jensen[39] obtained a 62:38 ratio (OHax:OHeq), presumably using CCl_4 as solvent. These results match the 62:38 (OHax:OHeq) ratio obtained by the analysis of the $^3J_{H2H3}$ coupling constant in $CDCl_3$.[15]

However, the Boltzmann-weighted energy differences of all 18 conformers led to a 87:13 (OHax:OHeq) ratio which overestimates the axial OH conformers compared to the experimentally based ratios. This might be due to the fact that intermolecular H-bonding to appropriate solvents was not modelled. The equatorial OH group should be more stabilized in H-bond donor and/or acceptor solvents compared to the axial OH group which might be extra stabilized in the calculations by an intramolecular H-bond.[50] In addition, this stabilizing effect

may be temperature-dependent as has been shown for 3-substituted cyclohexanols.[53] Interestingly, based on empirical energy estimates an inverted ratio of 30:70 (OHax:OHeq) was calculated by Feltkamp and Franklin.[59] Likewise, the dominant chair of neoisomenthol was predicted to bear the OH in the equatorial position with an OHax/OHeq ratio of 9:91 based on free energy estimates,[38] but this conclusion was reached using an incorrect assignment and has to be discarded.

Table 6: [α] values of (+)-(1*R*,3*R*,4*R*)-neoisomenthol at 20°C in different solvents,[18] solvent acidity (SA) and dipolarity (SdP)[19]

solvent	conc.[a]	$[\alpha]_{656}$	$[\alpha]_{589}$	$[\alpha]_{546}$	SA	SdP	$[\alpha]_{546}$ [c]
diethyl-ether	4.044	-9.89	-12.36[b]	-14.21	0	0.385	-
cyclo-hexane	4.024	-7.45	-8.69	-9.94	0	0	-9.05
hexane	4.034	-7.43	-8.67	-9.91	0	0	-9.05
chloro-ben-zene	4.056	-5.17	-6.53	-7.64	0	0.537	-5.84
CCl_4	4.072	-5.03	-6.38	-7.49	0	0	-9.05
ben-zene	4.022	-4.97	-6.34	-7.45	0	0.27	-7.43
ben-zene	8.028	-4.98	-6.35	-7.47	0	0.27	-7.44
dioxane	4.038	-4.95	-6.31	-7.42	0	0.312	-7.18
benzo-nitrile	4.054	-3.21	-3.94	-4.56	0	0.852	-3.96
aceto-nitrile	4.036	-2.10	-2.47	-2.84	0.044	0.974	-2.48
chloro-form	4.080	-0.37	-0.61	-0.98	0.047	0.614	-4.57
ethanol	4.028	+1.49	+1.98[b]	+2.11	0.4	0.783	+2.49
ethanol	8.008	+1.56	+2.00[b]	+2.18	0.4	0.783	+2.49
acetic acid	4.076	+1.96	+2.70	+3.18	0.689	0.676	-
t-butanol	4.060	+2.96	+3.83	+4.80	0.145	0.732	-

[a]: g/100 ml; [b]: at higher concentrations: $[\alpha]_{589}$: +2.2 (c=12.8, ethanol), $[\alpha]_{589}$: -12.2 (c=14.3, diethylether;[43] [c]: by linear regression: y = -9.047 + 17.16*SA + 5.97*SdP, R^2 = 0.853, n=10

Geometry optimization and energy calculations of a twist-boat form (favourable isoclinal (IC) position: isopropyl group; OH and CH_3 substituents in favourable pseudo-equatorial positions) in three solvents resulted in much higher free energies than the lowest in energy chair conformer in ethanol (ax/ax/eq; *trans*/g^-): 6.99, 6.94 and 7.74 kcal/mole in ethanol, acetonitrile, and diethylether (IEFPCM) with *trans*/g^+ dihedrals (isopropyl/OH). The energy difference is reduced in ethanol to 6.2 kcal/mole at maximum for the g^+/*trans* conformer (isopropyl/OH). The low temperature NMR data and the calculated data clearly indicate that only negligible populations of twist-boat forms might exist in solution. A convincing example of a twist-boat cyclohexane derivative was presented by Gill et al.[54] using *cis*-1,4-di-*tert*-butylcyclohexane in propane.

To conclude, the energy calculations of Feltkamp and Franklin[52] and Senda et al.[38] erroneously indicated that the equatorial OH chair dominates for neoisomenthol. Based on

DFT energies, the axial OH chair dominates (87:13, OHax:OHeq) but this has to be corrected to 67:33 using low-temperature NMR ^{13}C data.[16] The 67:33 ratio is further supported by the analysis of experimental $^{3}J_{H2H3}$ coupling constants in $CDCl_3$[15] and bandwidth measurements of H3.[39]

2.2.3 (+)-(1*S*,3*S*,4*R*)-menthylamine base

For all amino derivatives, experimental J-coupling constants are not available in the literature. The conformational search resulted in a chair with all substituents in the equatorial position, with a highly dominant g^+/*trans* conformer with respect to the isopropyl and NH_2 group. The NH_2 dihedral is defined by Hpro*R*-N-C3-H3. Firl et al. [55] estimated for (+)-menthylamine the g^+ rotamer of the isopropyl group as the dominant conformer. This estimate was based on empirical rules for the dependence of ^{13}C chemical shifts on the position of substituents. This is in agreement with our populations based on calculated energies (Table 7).

As with the menthol series, we additionally calculated all three NH_2 rotamers of this dominant conformer with a g^+ isopropyl group (Table 7). With the populations based on free energies, we predicted a $[\alpha]_{589}$ value of +57.3 for the (+) enantiomer (Table 8) which fits roughly to the experimental value of –35.70 (c=1.39, chloroform, 20 °C) for (–)-menthylamine.[56] De Vekki et al.[57] reported a $[\alpha]_{589}$ value of -24.0 at 20°C for the neat compound. The calculated and experimental ORD values are shown in Table 8. A population-weighted $^{3}J_{isopropyl}$ coupling constant of 1.8 Hz is predicted.

Table 7: Calculated parameters of the NH_2 rotamers of the NH_2eq chair with a g^+ isopropyl dihedral of (+)-(1*S*,3*S*,4*R*)-menthylamine (mpw1pw91/cc-pvdz, IEFPCM: acetonitrile)

	eq/eq/eq; g^+/*trans*	eq/eq/eq; g^+/g^+	eq/eq/eq; g^+/g^-
H8-C8-C4-H4	68.0	65.0	60.6
Hpro*R*-N-C3-H3	-175.2	58.5	-66.2
$[\alpha]_{589}$	+75.5	-13.6	+28.3
rel. free energy (kcal/mole)	0	0.66	1.31
population (%)	69.4	22.9	7.7
$^{3}J_{isopropyl}$ [Hz]	1.8	1.9	2.3

Table 8: Calculated ORD values of (+)-menthylamine (mpw1pw91/cc-pvdz, IEFPCM: acetonitrile) and experimental ORD values of (–)-menthylamine, c=1.39, $CHCl_3$, 20°C)[56]

Wavelength in nm	$[\alpha]_{exp}$	$[\alpha]_{calc}$
589	-35.7	+57.3
578	-37.1	+59.6
546	-41.9	+67.4
436	-67.6	+110.9
365	-98.9	+167.6

Importantly, in a series of recent publications [58,59] the authors claimed to have synthesized (+)-menthylamine. In the first article, the experimental section contains several typing errors which indicate (–) instead of (+).[58] In addition, the formula which is shown represents (+)-neomenthylamine, yet in fact, the presented experimental data in chloroform (not assigned ^{13}C and $[\alpha]_{589}$) clearly shows that (+)-neomenthylamine has been prepared. In comparison with the experimental values of Firl et al.[55] in the same solvent, the MAE (mean absolute error) was found to be 1.9 ppm for menthylamine and 0.07 ppm for neomenthylamine, clearly indicating that neomenthylamine has been synthesized. The data of Firl et al.[55] are similar to Schopohl et al. [56] with differences less than 1 ppm. In addition, the experimental $[\alpha]_{589}$ of Zhou et al.[58] for the (+)-enantiomer was found to be +5.4 (c=0.6, $CHCl_3$ at 25°C) and –35.7 for the (–) enantiomer of menthylamine (c=1.39, chloroform, 20 °C)[56] but +11.6 (c=1.0, chloroform, 20 °C) for the (+) enantiomer of neomenthylamine.[3] Interestingly, in the crucial synthetic step of the reduction of the oxime, apart from (+)-(1*R*,3*S*,4*S*)-neomenthylamine, (–)-(1*R*,3*R*,4*S*)-menthylamine was obtained. With an incomplete purification, the presence of the last compound as impurity could explain the reduced specific optical rotation obtained compared to the data of Kulisch et al. .[3] Furthermore, the literature cited to justify the assignment ($[\alpha]_{589}$: +6.5, c=0.54, $CHCl_3$ at 20°C) is incorrect[60] , as the synthetic schemes contain clear mistakes: the depicted formulas of the intermediates represent neomenthylamine instead of menthylamine, and the final products show erroneously two different substituents for the urea and isocyanate derivatives. In summary, the aforementioned series of articles all contain the incorrect name of the chiral ligand for asymmetric synthesis: (+)-neomenthylamine has been prepared instead of (+)-menthylamine.

2.2.4 (–)-(1*S*,3*S*,4*S*)-neoisomenthylamine base

Notably, the assignment of neoisomenthylamine as base uses chloroform as solvent. To the best of our knowledge, only a synthetic approach was used for assignment of the absolute configuration, starting with enantiomerically pure and known isomenthone.[61] With respect to the date of publication, it is important to re-assign the AC of this compound. We could only find an ad hoc assignment without referring to valid experimental data.[62] In the present report we demonstrate the first spectroscopical assignment of the AC of neoisomenthylamine base, likewise of the protonated form, or experimentally, the hydrochloride (vide infra).

Similar to neoisomenthol, the full series of conformers were geometry optimized. Structural parameters and populations based on calculated free energies and $[\alpha]_{589}$ values are presented in Tables 9A and B.

Table 9A: Calculated dihedrals and populations based on free energy differences weighted by the Boltzmann equation (mpw1pw91/cc-pvdz, IEFPCM: acetonitrile) and $[\alpha]_{589}$ values (mp1pw91/cc-pvdz, IEFPCM: acetonitrile) of the NH_2eq chair of (–)-(1*S*,3*S*,4*S*)-neoisomenthylamine

Isopropyl dihedral	g^+	g^-	t	g^+	g^-	t
NH_2 dihedral	g^+	g^+	g^+	g^-	g^-	g^-
isopropyl dihedral	66.0	–73.2	–151.3	82.6	–77.7	–161.3
NH_2 dihedral	81.0	69.0	67.4	–59.07	–58.0	–56.6
population [%]	0.1	4.4	8.7	0.2	3.0	18.8
$[\alpha]_{589}$	–79.1	–107.4	–105.9	+1.9	–45.4	–26.1

Isopropyl dihedral	g^+	g^-	t
NH_2 dihedral	t	t	t
isopropyl dihedral	82.3	–70.0	162.4
NH_2 dihedral	–168.9	–165.9	–164.7
population [%]	0.1	2.1	1.8
$[\alpha]_{589}$	+14.0	+0.2	–6.2

To date low temperature ^{13}C experimental NMR data for neoisomenthylamine has not been reported. With the calculated populations based on free energies a specific optical rotation of +7.2 for (1*S*,3*S*,4*S*)-neoisomenthylamine was obtained with an NH_2ax:NH_2eq ratio of 61:39. Based on calculated energies, the amino group stabilizes the NH_2eq chair more than the OH group in neoisomenthol. The sign of the $[\alpha]_{589}$ value does not fit the experimental value of +11.0 in chloroform for the (1*R*,3*R*,4*R*)-enantiomer (c=between 2 and 4).[63] This prompted us to reproduce the experimental conditions and repeat the calculations with chloroform as solvent (geometry optimization, population analysis based on free energy differences, optical rotation calculations: supporting info, Tables S14A and B). A value of +10.2 was calculated for $[\alpha]_{589}$ using the population mix based on calculated free energies and this still has an incorrect sign compared to the experimental data.

Table 9B: Calculated dihedrals and populations based on free energy differences weighted by the Boltzmann equation (mpw1pw91/cc-pvdz, IEFPCM: acetonitrile) and $[\alpha]_{589}$ values (mp1pw91/cc-pvdz, IEFPCM: acetonitrile) of the NH_2ax chair of (–)-(1*S*,3*S*,4*S*)-neoisomenthylamine

Isopropyl dihedral	g^+	g^-	t	g^+	g^-	t
NH_2 dihedral	g^+	g^+	g^+	g^-	g^-	g^-
isopropyl dihedral	51.2	–83.6	179.6	49.0	–82.9	175.5
NH_2 dihedral	48.8	54.2	52.2	–70.0	–69.7	–65.0
population [%]	0.2	0.6	9.8	0.8	1.9	30.2
$[\alpha]_{589}$	+47.83	–26.91	+18.44	+63.49	–22.48	+23.19

Isopropyl dihedral	g^+	g^-	t
NH_2 dihedral	t	t	t
isopropyl dihedral	50.9	–79.7	174.9
NH_2 dihedral	174.3	–179.0	175.0
population [%]	0.6	1.0	15.8
$[\alpha]_{589}$	+129.1	+63.76	+109.47

As a second approach to obtain a better fit with experimental conditions, we selected the same four conformers as for neoisomenthol, and adjusted the populations based on calculated

free energies in order that they represent 100% of the conformers (12.8:27.9:14.5:44.8; NH_2eq,tg$^+$/NH_2eq,tg$^-$/NH_2ax,tg$^+$/NH_2ax,tg$^-$) (Table 10). Using these we calculated the ORD data (Table 11) that match quite well to the experiment. In fact, the analysis of the protonated form (experimentally: the HCl salt) shows that the NH_2eq forms are more highly populated in the experiment than in the calculations. We therefore hypothesize that the same reasoning applies as for neoisomenthol (vide supra).

Table 10: Calculated dihedrals and populations of four conformers (mpw1pw91/cc-pvdz, IEFPCM: acetonitrile) and $[\alpha]_{589}$ values (mp1pw91/cc-pvdz, IEFPCM: acetonitrile) of (–)-(1*S*,3*S*,4*S*)-neoisomenthylamine

Isopropyl dihedral	NH_2eq t	NH_2eq t	NH_2ax t	NH_2ax t
NH_2 dihedral	g$^+$	g$^-$	g$^+$	g$^-$
isopropyl dihedral	-151.3	-161.3	179.6	175.5
NH_2 dihedral	67.4	-56.6	52.2	-65.0
population [%]	12.9	27.9	14.5	44.8
$[\alpha]_{589}$	-105.88	-26.08	+18.44	+23.19
$[\alpha]_{578}$	-110.38	-27.10	+19.13	+24.08
$[\alpha]_{365}$	-327.37	-69.53	+45.68	+59.12

Table 11: Calculated optical rotational values of (–)-(1*S*,3*S*,4*S*)-neoisomenthylamine base using the four conformers of Table 10 and experimental ORD values of (+)-(1*R*,3*R*,4*R*)-neoisomenthylamine

Wavelength in nm	$[\alpha]_{exp}$	$[\alpha]_{calc}$
589	+11.0[a]	-7.8
578	+15.4[b]	-8.1
365	+24.1[b]	-28.2

[a]: c=between 2 and 4, $CHCl_3$;[63] [b]: 20°C[64]

2.2.5 (–)-(1*S*,3*S*,4*S*)-neoisomenthylamine protonated

Calculations with all six staggered conformations were performed (Table 12). Interestingly, the protonation inverts the chair ratio and now favours the equatorial form with respect to the NH_2 group based on calculated free energies: NH_2ax:NH_2eq, 38.7:61.3. This ratio should be compared to 61:39 (NH_2ax:NH_2eq) of (–)-neoisomenthylamin as base. Using all six

conformers, the predicted $[\alpha]_{589}$ value was –9.4 for the (1*S*,3*S*,4*S*) enantiomer which fits the experimental value of +20.9 for the (1*R*,3*R*,4*R*) enantiomer (c=2, water).[63] The absolute calculated value changed to –4.8 at 546 nm.

Table 12: Calculated dihedrals, populations based on free energy differences weighted by the Boltzmann equation (mpw1pw91/cc-pvdz, IEFPCM: acetonitrile), and $[\alpha]_{589}$ values of the NH_2eq and NH_2ax chair of protonated (–)-(1*S*,3*S*,4*S*)-neoisomenthylamine adjusted for comparison with the experimental values of the hydrochloride

Isopropyl dihedral	eq/eq/ ax g^+	eq/eq/ ax g^-	eq/eq/ ax t	ax/ax/ eq g^+	ax/ax/ eq g^-	ax/ax/ eq t
isopropyl dihedral	80.9	–73.3	–151.3	51.1	–83.6	179.6
Population [%]	0.4	13.0	47.9	1.0	1.8	35.9
$[\alpha]_{589}$	–17.8	–54.5	–39.6	+84.7	+4.9	+44.0
$[\alpha]_{546}$	–20.9	–64.0	–46.4	+99.2	+5.6	+51.4

For the protonated neoisomenthylamine, all NH_2eq conformers contribute with a negative sign, and all NH_2ax conformers contribute with a positive sign to the optical rotation. The NH_2ax forms contributes +16.7 and the NH_2eq forms –26.1 to the $[\alpha]_{589}$ value. In this case, a clear decision can be made which chair is dominant.

2.3 Linear Regression of experimental and calculated optical rotation values

Experimental and calculated ORD values of the (+)-menthol and (+)-menthylamine (base and HCl/protonated) isomers were collected and a linear regression performed (Figure 2).

Data pairs at shorter wavelengths for the amino isomers (base and HCl/protonated) were excluded as incorrect calculations near excitation wavelengths can lead to substantial error. The menthol isomers do not suffer from this shortcoming due to lower excitation wavelengths of the alcohols compared to the amines.

In Figure 2, the data pairs together with the regression line (in red) and the prediction bands (in green) at a 99 % level of confidence (Origin ^{R})[65] are shown (experimental values were inverted if only values for the (−)-enantiomer were available; all calculated values belong to the (+)-enantiomer). The regression parameters are as follows: slope (0.885; standard error: 0.063 ppm), intercept (7.0, standard error: 3.12), $R^2 = 0.892$.

Experimental optical rotation values below 5 cannot be predicted reliably at a 99 % level of confidence. This is nicely demonstrated on the left side of Fig. 2 (close-up of the right side of Figure 2) where the lower confidence interval intersects the x-axis near an optical rotation value of 5. On top of the range of unreliably predictable ORD data we added the variation originating from the different levels of theory used. Based on our work on limonene,[29] we assumed an additional range of uncertainty of 5 units. Adding these two contributions, we propose not to predict the absolute configuration of a compound if this prediction is solely based on the comparison of experimental and calculated ORD data with experimental values that are within the range of ±10. This parallels the mean absolute error of 9.5 (sum of the absolute differences between experimental and calculated values, divided by the number of data pairs). Systematically underestimated are the calculated values for some neo and neoiso forms.

Figure 2: Top: Experimental and calculated ORD values (in total: 26) of the (+)-menthol and (+)-menthylamine (base and HCl/protonated) isomers; linear regression lines (in red) and prediction bands at a 99 % level of confidence (in green, Origin ™);[65] bottom: close up in the region of small values; experimental values were inverted if only values for the (−)-enantiomer were available; all calculated values belong to the (+)-enantiomer, the list of data pairs can be found below the figure

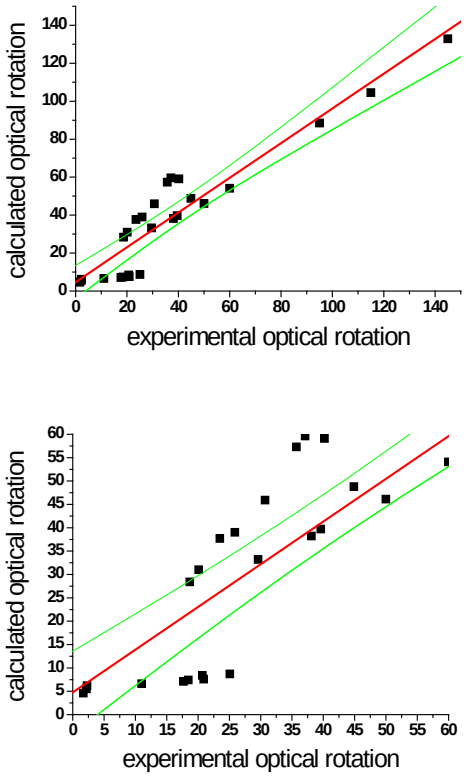

List of data pairs for Figure 2 (taken from the tables of the main text and supporting information)

compound	wavelength	[α]exp.	[α]calc.
(+)-menthol	589	50.0	46.1
	546	60.0	54.1
	436	95.0	88.5
	405	115.0	104.5
	365	145.0	132.9
(+)-neomenthol	589	17.7	7.1
	578	18.5	7.4
	546	20.7	8.4
(+)-isomenthol	656	20.1	31.0
	589	25.9	39.0
	546	30.7	45.9
	486	40.2	59.1
(+)-neoisomenthol	656	1.7	4.6
	589	2.2	5.5
	546	2.3	6.2
(+)-menthylamine	589	35.7	57.3
	578	37.1	59.6
(+)-neomenthylamine	589	8.7	25.1
(+)-isomenthylamine	589	29.6	33.2
(+)-neoisomenthylamine	589	11.0	7.8
(+)-menthylamine (protonated/HCl	589	38.1	38.1
	578	39.6	39.7
	546	44.9	48.8
(+)-neomenthylamine (protonated/HCl)	589	18.7	28.4
(+)-isomenthylamine (protonated/HCl)	589	23.5	37.7
(+)-neoisomenthylamine (protonated/HCl)	589	20.9	9.4

3. Discussion

Kondru et al.[66] investigated the conformational dependence of optical rotation with menthol as one of the test molecules. Without presenting further information concerning population and geometry, two conformers were used and a value of 33.3 for the specific optical rotation predicted. This resembles our value when the three conformers lowest in energy were taken, together with Boltzmann-based populations. It might be argued that MD modelling together with high level ORD calculations should be used as gold standard. However, even this approach has clear shortcomings as illustrated by Kundrat and Autschbach[67] by use of extensive MD modelling for the prediction of specific optical rotation values. The experimental values for the two test molecules (proline and phenylalanine) in water (−99.2 and −57) were

most accurately predicted by an older study using static geometries and the COSMO solvent model (-101.5 and -36.8).[67] In contrast, the MD simulation with COSMO as solvent model delivered values of −63.3 and −16.1 for proline and phenylalanine, respectively. One crucial point in MD modelling is the force field. Especially H-bonding is a difficult property to predict.[68] In the very early study of Polavarapu and Chakraborty[69] the dependence of the optical rotation of chiral 3-butyn-2-ol for different conformers was investigated. The optical rotation was highly dependent on the OH rotamer (−80.8, −30.0, and +69.7 for the three staggered conformers).

Galisteo et al.[62] investigated the empirical relationship between structure and optical rotation of the menthol and menthylamine (as bases) stereoisomers. A forcefield (MM2) was used for the conformational search and the population analysis, whereas a purely empirical approach was used to assign contributions of molecular fragments to the overall optical rotation. For all 8 enantiomeric menthol isomers the optical rotation sign was successfully predicted. A follow-up study[70] indicated that other calculation schemes (MM3, semiempirical AM1) predicted the incorrect sign for neoisomenthol.

Menthol has also been used as model compound for the development of chiroptical methods such as VCD and Raman optical activity (ROA).[71] The conformational flexibility of the other isomers leads to complex data that are much more difficult to interpret. A recent study selected (−)-menthol to analyse the hydrogen bonding network using IR, Raman, and VCD as experimental techniques, together with DFT calculations.[34] Even for menthol, the most rigid isomer within the series, different levels of theory delivered different orderings of energies, which subsequently leads to different population mixes. Depending on the level of theory, two conformers were at lowest energy: the g^-/*trans* and g^-/g^- (isopropyl / OH dihedral). With the B3LYP/cc-pVDZ level of theory the second conformer was 0.3 kcal/mole higher in energy, whereas on the B3LYP/6-31+G* level of theory the first conformer was 0.2 kcal/mole higher in energy. In the group of five conformers with lowest energy, the maximum deviation between the two levels of theory was 1.0 kcal/mole. Such large differences might affect the calculated spectra. Even with the use of a set of scaling factors, a comparison between experimental and calculated IR and VCD spectra showed large discrepancies. This is not surprising if errors in calculating anharmonic effects are taken into account.[72]

Neoisomenthol presents a special configurational problem due to its very low specific optical rotation, lack of ECD bands in the UV/Vis region, and a high conformational flexibility. Even at shorter wavelengths the ORD values do not increase much, however, indicate a monosignate

curve like all other menthol isomers.[40] Likewise, neoisomenthylamine as base appears to be sensitive towards temperature and impurities. It is therefore a difficult task to reliably assign the sign of the optical rotation which is conventionally taken from ethanol solution to the *R*/*S* nomenclature. Therefore, we present a line of arguments proofing that the original assignment (1*R,*3*R,*4*R*) for (+), and (1*S,*3*S,*4*S*) for (–) is correct. It is important to note that the four menthol diastereomers can be separated by various methods, one being gas chromatography.[73]

Paine III[40] synthesized neoisomenthol from isomenthone with a known absolute configuration (1*R*,4*R*), so that the (1*R,*3*R,*4*R*) form of neoisomenthol was obtained. Then, a *di*-terephtalate derivative was prepared, and following ester cleavage, (1*R,*3*R,*4*R*)-neoisomenthol was formed (purity of 99.3 % by gas chromatography). The optical rotation of the neat compound at 20.0 °C (variation of less than 0.2 °C) with 10 cm path length was +0.406, +0,425, and +0.473 for 589 nm, 578 nm, and 546 nm respectively. A synthetic route via the 2,6-naphtalenedicarboxylate gave values of +0.137, +0.140, and +0.148. From this we can assign a (+) sign of the $[\alpha]_{589}$ value for the neat compound with the (1*R,*3*R,*4*R*) form. Since Read and Grubb[46] (Table S21 in the supporting information) presented data of a (+) $[\alpha]_{589}$ value for the neat compound which also showed a (+) sign when measured in ethanol, we can assign the same sign of the neat compound to the solution in ethanol.

Next, it was important to derive the isomenthone configuration. It was synthesized from (+)-(1*R*,3*S*,4*R*) isomenthol. The proof that this is the correct assignment can be taken from the publication of Kartha et al. . [14] They determined by the heavy atom method and anomalous x-ray dispersion, the absolute configuration of the isomenthyl derivative together with the chiroptical information Putting the pieces together, from assigned isomenthol, and via isomenthone, a neoisomenthyl derivative was synthesized which corresponds to the (1*R,*3*R,*4*R*) form. This form, following ester cleavage, resulted in neoisomenthol with a (+) $[\alpha]_{589}$ value in ethanol. The correct assignment is therefore (+)-(1*R,*3*R,*4*R*)-neoisomenthol using ethanol as solvent, as can be found in the literature.

Taking into account the difficulties in the AC assignment of neoisomenthol, it is not surprising that some configurational information in the literature of the amino derivative must be revised. Bose et al.[74] claimed to have assigned the AC of isomenthol and neoisomenthylamine. However, both assignments are incorrect. Similarly, Kozlov et al.[75] assigned the AC of isomenthylamine incorrectly. In their report, the optical rotation was measured in ethanol as solvent which might explain the error since other optical rotation data with this solvent are not

available for isomenthylamine and neoisomenthylamine. For the latter compound, it is still possible that Kozlov et al.[75] by chance assigned the AC correctly. The correct assignment was presented by Read and Robertson.[61] Starting from *d*-(+)-isomenthone, the dextrorotatory (in chloroform as solvent) neoisomenthylamine base was prepared. Experimental data for the pure compound were presented in in the year 1930 by Read and Storey.[76] In contrast to (1*R*,3*R*,4*R*)-neoisomenthol, a sign change did not occur, thus (1*R*,3*R*,4*R*)-neoisomenthylamine base remains dextrorotatory when measured as a homogenous sample.

4. Conclusion

We have shown that the AC of all 12 compounds, even in the case of the most difficult neoiso forms, can be predicted correctly using experimental NMR data. If only experimental data with an optical rotation outside the range of $-10 < [\alpha] < 10$ are used, all 12 compounds were correctly assigned even without low-temperature NMR data as restraints for the conformational analysis.

5. Computational Section

Models of the menthol and menthylamine (base and protonated) isomers were built in GaussView 5.0. A conformational search using the BEST algorithm with the CHARMm force field and a cut-off of 2 kcal/mole was performed using DISCOVERY Studio (Accelrys, 2009).[20] DFT calculations were performed with Gaussian09 [21] RevA.02 (Frisch et al., 2009) on the mpw1pw91/cc-pvdz (IEFPCM: acetonitrile as solvent) level of theory (unless other solvents are indicated) for geometry optimization, energy calculations, and spectroscopic properties. For the calculation of the specific optical rotation of neoisomenthol, two additional levels of theory were used as indicated: mpw1pw91/aug-cc-pvdz and mpw1pw91/cc-pvtz. Energies were obtained at 298.15 K and 1 atm of pressure. The lowest energy conformer was taken as reference, set to 0 kcal/mole (conversions used: 1 Hartree = 627.5 kcal; 1 cal = 4.18 J) and the resulting energy differences were used to calculate populations according to the Boltzmann distribution. In all calculations the Polarizable Continuum Model (PCM) using the integral equation formalism variant (IEFPCM) implemented in G09 was used as solvent model. The unit of $[\alpha]$ is [degrees*(dm*g/cm^3)$^{-1}$]. Experimental ORD values from literature are listed in the supporting information.

Acknowledgements

We want to thank the DFG (FOR 934) and the MPG (MPIBPC: Department for NMR-based structural biology, Prof. Griesinger) for support. We gratefully acknowledge the careful reading of the manuscript by Dr. T. Schweizer.

Keywords: menthol isomers • menthylamine isomers • chiral analysis • optical rotation • conformation

References

[1] J. R. Hanson, *Nat. Prod. Rep.* **2001**, *18*, 607-617.
[2] R. B. Croteau, E. M. Davis, K. L. Ringer, M. R. Wildung, *Naturwissenschaften* **2005**, *92*, 562-577.
[3] J. Kulisch, M. Nieger, F. Stecker, A. Fischer, S. R. Waldvogel, *Angew. Chem. Int. Ed*. **2011**, *24*, 5564-5567.
[4] J. H. Gladstone, *J. Chem. Soc.* **1864**, *17*, 1-21.
[5] B. Schäfer, *Chem. Unserer Zeit* **2013**, *47*, 174-182.
[6] M. B. Erman, P. J. Whelan, US patent **2007**, 7,189,760 B2
[7] P. Bombicz, J. Buschmann, P. Luger, N. Xuan Dung, C. Ba Nam, *Z. Kristallogr.* **1999**, *214*, 420-423.
[8] E. E. Kwan, S. G. Huang, *Eur. J. Org. Chem.* **2008,** 2671-2688.
[9] H. D. Orloff, *Chem. Rev.* **1954**, *54*, 347-447.
[10] M. Marianski, A. Asensio, J. J. Dannenberg, *J. Chem. Phys*. **2012**, *137*, 044109
[11] E. A. Basso, C. A. Abiko, G. F. Gauze, R. M. Pontes, *J. Org. Chem.* **2011**, *76*, 145-153.
[12] J. Shen, Y. Li, R. Vaz, H. Izumi, *J. Chem. Theory Comput.* **2012**, *8*, 2762-2768.
[13] B. Mennucci, C. Cappelli, R. Cammi, J. Tomasi, *Chirality*, **2011**, *23*, 717-729.
[14] G. Kartha, K. T. Go, A. K. Bose, M. S. Tibbetts, *J. Chem. Soc. Perkin* II **1976**, 717-723.
[15] J. Härtner, U. M. Reinscheid, *J. Mol. Struct*. **2008**, *872*, 145-149.
[16] T. I. Pehk, E. T. Lippmaa, V. I. Lysenko, I. I. Bardyshev, *Russ. J. Org. Chem.* **1980**, 1694-1703.
[17] D. A. Lanfranchi, M.-C. Blanc, M. Vellutini, P. Bradesi, J. Casanova, F. Tomi, *Magn. Reson. Chem.* **2008**, *46*, 1188-1194.
[18] W. Hückel, H. Niggemeyer, *Ber. Dtsch. Chem. Ges.* **1939**, *72*, 1354-1358.
[19] J. Catalán, *J. Phys. Chem. B* **2009**, *113*, 5951-5960.
[20] Accelrys, Discovery Studio, **2009**
[21] GaussianG09, Revision A.02, M. J. Frisch et al., Gaussian, Inc., Wallingford CT, **2009**
[22] F. Gangemi, R. Gangemi, G. Longhi, S. Abbate, *Phys. Chem. Chem. Phys.* **2009**, *11*, 2683-2689.
[23] S. Qiu, E. De Gussem, K. A. Therani, S. Sergeyev, P. Bultinck, W. Herrebout, *J. Med. Chem.* **2013**, *56*, 8903-8914.
[24] L. Rottmannová, V. Lukeš, M. IlčP Fodran, P. Herich, J. Kožišek, T. Liptaj, E. Klein, *J. Mol. Struct.* **2013**, *1049*, 494-501.
[25] J. Fohrer, U. Reinscheid, M. Hennig, T. Carlomagno, *Angew. Chem. Int. Ed*. **2006**, *45*, 7033-7036.
[26] S. Nozinovic, P. Gupta, B. Fürtig, C. Richter, S .Tüllmann, E. Duchardt-Ferner, M. C. Holthausen, H. Schwalbe, *Angew. Chem. Int. Ed.* **2011**, *50*, 5397-5400.
[27] C. Benzi, O. Crescenzi, M. Pavone, V. Barone, *Magn. Reson. Chem.* **2004**, *42*, S57-S67.
[28] P. L. Polavarapu, *Chirality* **2012**, *24*, 909-920.
[29] F. Reinscheid, U. M. Reinscheid, *J. Mol. Struct.* **2015**, submitted
[30] M. Schmidt, F. Reinscheid, H. Sun, H. Abromeit, G. K. E. Scriba, F. D. Sönnichsen, M .John, U. M. Reinscheid, *Eur. J. Org. Chem.* **2014**, 1147-1150.
[31] F. Reinscheid, M. Schmidt, H .Abromeit, S. Liening, G. K. E. Scriba, U. M. Reinscheid, *J. Mol. Struct.* **2015**, submitted
[32] J. S. Lomas, *Magn. Reson. Chem*. **2014**, *52*, 745-754.

[33] M. Albrecht, J. Will, M. A. Suhm, *Angew. Chem. Int. Ed.* **2010**, *49*, 6203-6206.
[34] J. R. Avilés Moreno, F. Partal Urena, J. J. Lopez González, *Struct. Chem*. **2013**, *24*, 671-680.
[35] T. Egawa, M. Sakamoto, H. Takeuchi, S. Konaka, *J. Phys. Chem. A* **2003**, *107*, 2757-2762.
[36] J. L. McCann, **1998**, Dissertation, Department of chemistry, University of Calgary, Alberta, Canada
[37] D. Schmitz, V. A. Shubert, T. Betz, M. Schnell, *Front. Chem.* **2015**, *3*, 15
[38] Y. Senda, S. Imaizumi, *Tetrahedron* **1975**, *31*, 2905-2908.
[39] R. B. Jensen, *Act. Chem. Scand.* **1968**, *22*, 1271-1278.
[40] J. B. Paine III, Philipp Morris USA confidential **1997**, research center, Doc code P0622
[40a] JASCO application note, www.jascoinc.com/docs/application-notes/p-0002_e.pdf?sfvrsn=
[41] P. L. Polavarapu, *Chirality* **2006**, *18*, 348-356.
[42] Y. M. Grigor`ev, S. M. Morozov, O. V. Sverdlova, *J. appl. Spectrosc.* **1975**, *23*, 1362-1364.
[43] W. Hückel, H. Feltkamp, S. Geiger, *Liebigs Ann. Chem.* **1960**, *637*, 1-19.
[44] D. Voisin, B. Gastambide, *Bull. Soc. Chim.* **1971**, *7*, 2643-2651.
[45] J. B. Hendrickson, *J. Am. Chem. Soc.* **1964**, *86*, 4854-4866.
[46] J. Read, W. J. Grubb, *J. Chem. Soc.* **1934**, 313-317.
[47] W. Hückel, S Gupte, *Chimia* **1966**, *20*, 276.
[48] A. R. H. Cole, P. R. Jefferies, *J. Chem. Soc.* **1956**, 4391-4397.
[49] R. J. Abraham, E. J. Chambers, W. A. Thomas, *J. Chem. Soc., Perkin Trans.* 2 **1993**, 1061-1066.
[50] R. J. Abraham, T. A. D. Smith, W. A. Thomas, *J. Chem. Soc., Perkin Trans*. 2 **1996**, 1949-1955.
[51] T. Tominaga, S. Tenma, H. Watanabe, *J. Chem. Soc. Faraday Trans*. **1996**, *92*, 1863-1867.
[52] H. Feltkamp, N. C. Franklin, *Tetrahedron* **1965**, *21*, 1541-1546.
[53] P. R. de Oliveira, L. Tasic, S. A. Rocco, R. Rittner, *Magn. Reson. Chem.* **2006**, *44*, 790-796.
[54] G. Gill, D. M. Pawar, E. A. Noe, *J. Org. Chem.* **2005**, *70*, 10726-10731.
[55] J. Firl, G. Kresze, T. Bosch, V. Arndt, *Liebigs Ann. Chem.* **1978**, 87-97.
[56] M. C. Schopohl, K. Bergander, O. Kataeva, R. Fröhlich, S. R. Waldvogel, *Synthesis* **2003**, *17*, 2689-2694.
[57] D. A. de Vekki, V. M. Uvarov, A. N. Reznikov, N. K. Skvortsov, *Russ. Chem. Bull. Int. Ed.* **2008**, *57*, 349-357.
[58] Y. Zhou, J. Dong, F. Zhang, Y. Gong, *J. Org. Chem.* **2011**, *76*, 588-600.
[59] Y. Zhou, Y. Gong, *Eur. J. Org. Chem.* **2011**, 6092-6099; Y. Zhou, Q. Liu, Y. Gong, *Org. Biomol. Chem.* **2012**, *10*, 7618-7627; H. Yuan, J. Hu, Y. Gong, *Tetrahedron: Asymmetry* **2013**, *24*, 699-705; Y. Zhou, Y. Zhu, S. Yan, Y. Gong, *Angew. Chem. Int. Ed.* **2013**, *52*, 10265-10269; Y. Zhou, Q. Liu, Y. Gong, *Tetrahedron Lett.* **2013**, *54*, 3011-3014.
[60] P. Jumaryatno, K. Rands-Trevor, J. T. Blanchfield, MJ Garson, *Arkivoc* **2007**, 157-166.
[61] J. Read, G. J. Robertson, *J. Chem. Soc.* **1927**, 2168-2174.
[62] D. Galisteo, M. E. González-Vadillo, J.A. López Sastre, M. H. Martinez Garcia, J. F. Rodriguez Amo, *J. Mol. Struct.* **1994**, *326*, 239-247.
[63] J. Read, W. W. Cuthbertson, *Rec. Chim. Pays-Bas* **1950**, *69*, 539-544.
[64] H. Feltkamp, F. Koch, T. N. Thanh, *Liebigs Ann. Chem.* **1967**, *707*, 78-86.
[65] Origin ™, version 6, Microsoft, **1999**
[66] R. K .Kondru, P. Wipf, D. N. Beratan, *J. Phys. Chem. A* **1999**, *103*, 6603-6611.
[67] M. D. Kundrat, J. Autschbach, *J. Am. Chem. Soc.* **2008**, *130*, 4404-4414.

[68] J.-H. Lii, N. L. Allinger, *J. Phys. Chem.* A **2008**, *112*, 11903-11913.
[69] P. L. Polavarapu, D. K. Chakraborty, *Chem. Phys*. **1999**, *240*, 1-8.
[70] R. Núnez Miguel, J. A. Lopez Sastre, D. Galisteo, A. Diez Martin, A. Gordaliza Ramos, *J. Mol. Struct.* **2000**, *522*, 219-231.
[71] L. D. Barron, L. Hecht, S. M. Blyth, *Spectrochim. Acta* **1989**, *45A*, 375- 379.
[72] M. Biczysko, P. Panek, G. Scalmani, J. Bloino, V. Barone, *J. Chem. Theory Comput.* **2010**, *6*, 2115-2125.
[73] D. R. Moore, A. D. Kossoy, *J. Chem. Ed.* **1961**, *33*, 1437.
[74] A. K. Bose, S. Harrison, L. Farber, *J. Org. Chem.* **1963**, *28*, 1223-1225.
[75] N. G. Kozlov, T. I. Pekh, T. K. Vyalimyaé, *Chem. Nat. Compounds,* **1982,** *17*, 238-243.
[76] J. Read, R. A. Storey, *J. Chem. Soc.* **1930**, 2761-2769.

Table of Contents

The complete series of menthol and menthylamine (base and protonated/HCl form) isomers has been investigated concerning their conformation and configuration. Using experimental and calculated optical rotation data it was possible to successfully assign the absolute configuration for all 12 compounds.

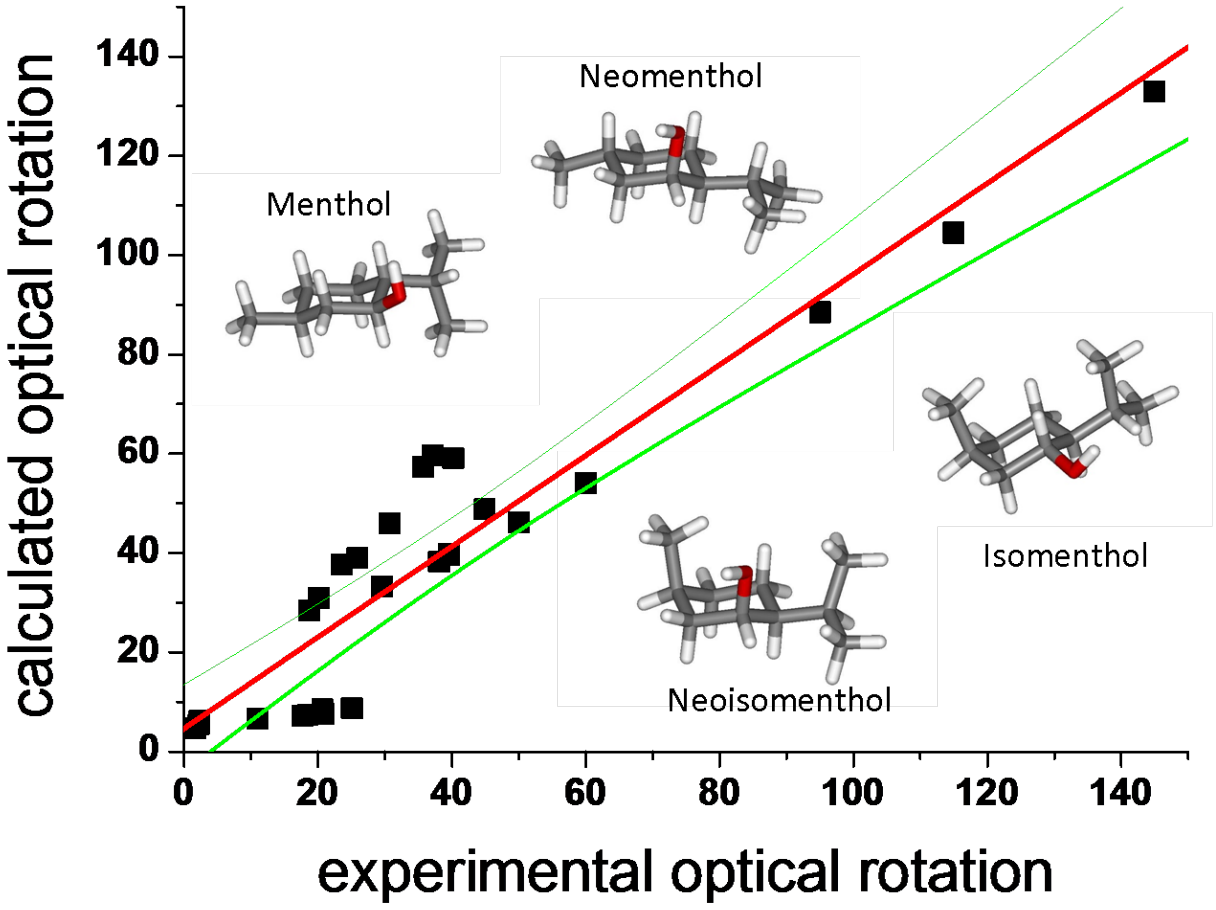

10. Supporting informations

Supporting information

Stereochemical analysis of (+)-limonene using theoretical and experimental NMR and chiroptical data

F. Reinscheid[a], U.M. Reinscheid*[a]

Table S1: Calculated isotropic shielding constants of (+)-limonene (theory level 1: mpw1pw91/cc-pvdz; IEF-PCM using chloroform as solvent)

atom number	conformer 1	conformer 2	conformer 3
C2	73.02	72.35	72.66
C3	161.69	164.75	163.16
C4	154.14	153.72	150.32
C5	167.13	163.87	166.54
C6	163.71	162.82	163.78
C1	59.39	59.92	59.84
H2	25.81	25.75	25.79
H3 pro*R*	29.11	29.59	29.67
H3 pro*S*	29.81	29.16	29.22
H4	29.6	29.65	29.24
H5 pro*S*	29.73	29.5	29.93
H5 pro*R*	29.95	30.37	29.92
H6 pro*R*	29.38	29.36	29.38
H6 pro*S*	29.54	29.55	29.57
C7	171.28	171.28	171.11
C7 protons	29.76	29.76	29.77
C8	42.74	43.89	43.15
C10	171.91	171.73	177.69
C9	87.46	87.14	84.39
C10 protons	29.62	29.60	29.73
H *trans* (H-C9-C8-C4)	26.46	26.4	26.53
H *cis* (H-C9-C8-C4)	26.55	26.49	26.39

Table S2: Calculated isotropic shielding constants of (+)-limonene (theory level 2: B3LYP/6-311+g(d,p); IEF-PCM using chloroform as solvent)

atom number	conformer 1	conformer 2	conformer 3
C2	54.41	53.79	54.04
C3	145.49	149.54	147.35
C4	138.1	137.98	133.79
C5	151.83	147.8	150.57
C6	148.09	146.94	148.22
C1	37.87	38.43	38.3
H2	26.06	25.99	26.04
H3 pro*R*	29.26	29.84	29.9
H3 pro*S*	30.09	29.42	29.45
H4	29.76	29.83	29.46
H5 pro*S*	29.98	29.69	30.19
H5 pro*R*	30.18	30.62	30.12
H6 pro*R*	29.57	29.52	29.58
H6 pro*S*	29.73	29.73	29.76
C7	157.01	157.04	156.84
C7 protons	29.99	30.0	30.0
C8	18.04	19.18	18.06
C10	157.33	157.25	163.43
C9	72.45	72.24	69.13
C10 protons	29.86	29.83	30.0
H *trans* (H-C9-C8-C4)	26.84	26.79	26.91
H *cis* (H-C9-C8-C4)	26.95	26.93	26.78

Table S3: Calculated isotropic shielding constants of (+)-limonene (theory level 3**:** PBEPBE /cc-pvtz; IEF-PCM using chloroform as solvent)

atom number	conformer 1	conformer 2	conformer 3
C2	57.38	56.78	56.99
C3	145.47	149.36	147.33
C4	137.83	137.73	133.55
C5	152.34	148.44	151.36
C6	148.17	146.9	148.32
C1	41.79	42.39	42.31
H2	25.49	25.44	25.48
H3 pro*R*	28.59	29.22	29.3
H3 pro*S*	29.55	28.82	28.87
H4	29.14	29.18	28.79
H5 pro*S*	29.33	29.04	29.59
H5 pro*R*	29.64	30.12	29.56
H6 pro*R*	29.03	28.97	29.04
H6 pro*S*	29.11	29.12	29.15
C7	157.57	157.58	157.37
C7 protons	29.5	29.5	29.5
C8	22.62	23.98	23.09
C10	158.1	158.05	164.55
C9	74.96	74.74	71.47
C10 protons	29.34	29.31	29.48
H *trans* (H-C9-C8-C4)	26.3	26.24	26.38
H *cis* (H-C9-C8-C4)	26.35	26.33	26.23

Figure S4A: Linear regression of calculated (mpw1pw91/cc-pvdz; IEF-PCM: chloroform) ^{13}C shieldings with experimental chemical shifts of (+)-limonene; red line: predicted by linear regression; black dots: five data pairs; Selection of five resonances with calculated shielding variation of =< 1.15 ppm among the three conformers; the arithmetic mean of the three conformers was taken

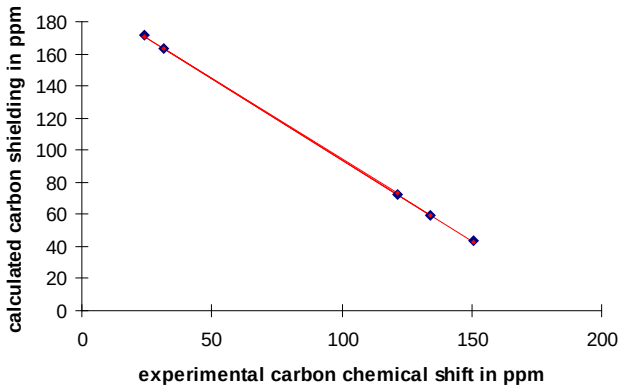

Figure S4B: residuals for the linear regression of the calculated isotropic ^{13}C shielding constants versus experimental ^{13}C chemical shifts of (+)-limonene (theory level 1: mpw1pw91/cc-pvdz; IEF-PCM using chloroform as solvent)

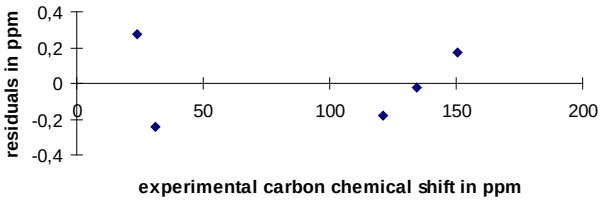

Figure S4C: Experimental ^{13}C chemical shifts in $CDCl_3$ (Skakovskii et al., 2010) and in acetone-d6 (Lukacs and Neszmelyi, 1981)

Carbon number	Skakovskii et al. (2010) $CDCl_3$	Lukacs and Neszmelyi (1981) acetone-d6
C1	134,3	133,3
C2	121,3	121,2
C3	31,5	31,0
C4	41,8	41,6
C5	28,6	28,4
C6	31,3	31,3
C7	24,1	23,6
C8	150,8	149,6
C9	109,1	108,9
C10	21,5	20,8

Figure S5A: Experimental ORD values of (+)-limonene at four wavelengths (corrected by using the methanol value (Rule and Chambers, 1937) which was itself corrected using the homogenous value comparison with Wilson et al. (2005)) and calculated ORD values (mpw1pw91/cc-pvdz, IEFPCM (methanol); In black: population mix 39:31:30; In blue: conformer 1; In green: conformer 2; In orange: conformer 3

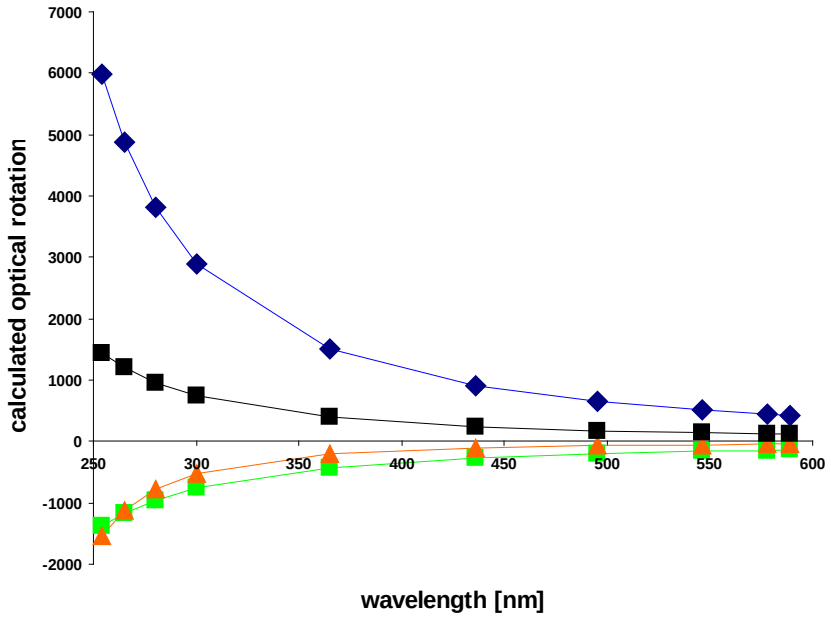

Table S5B: experimental (chloroform, 22.4 mg/ml, 20.4°C) and calculated ORD values of (+)-limonene (mpw1pw91/cc-pvdz, IEFPCM (methanol)) with a population mix of 39:31:30

wavelength [nm]	experimental	calculated
589	113.8	112.4
546	132.8	135.4
495	153.8	171.9
436	221.9	237.9

Table S5C: Experimental (Wilson et al., 2005) and calculated (mpw1pw91/cc-pvdz, in vacuo, population mix of 39:31:30) ORD values of (+)-limonene

wave-length [nm]	experimental	conformer 1	conformer 2	conformer 3	population mix with 39:31:30
633	62.1	388.29	-174.69	-35.38	86.7
355	315.5	1684.31	-689.26	-218.69	377.6

The same levels of theory as in the main text were used for calculation of UV/Vis and ECD spectra of (+)-limonene (IEFPCM using ethanol as solvent).

level of theory	functional	basis set
A	mpw1pw91	cc-pvdz
B	mpw1pw91	aug-cc-pvdz
C	mpw1pw91	cc-pvtz
D	mpw1pw91	aug-cc-pvtz
E	B3LYP	cc-pvdz
F	B3LYP	aug-cc-pvdz
G	B3LYP	cc-pvtz
H	B3LYP	aug-cc-pvtz
I	B3LYP	6-311++g(2d,2p)

Figures S6 A-I: Calculated ECD spectra of (+)-limonene at different levels of theory for conformer 1 (on the x-axis: wavelengths in nm, on the y-axis: Δε [Mol*l^{-1}*cm^{-1}]

A

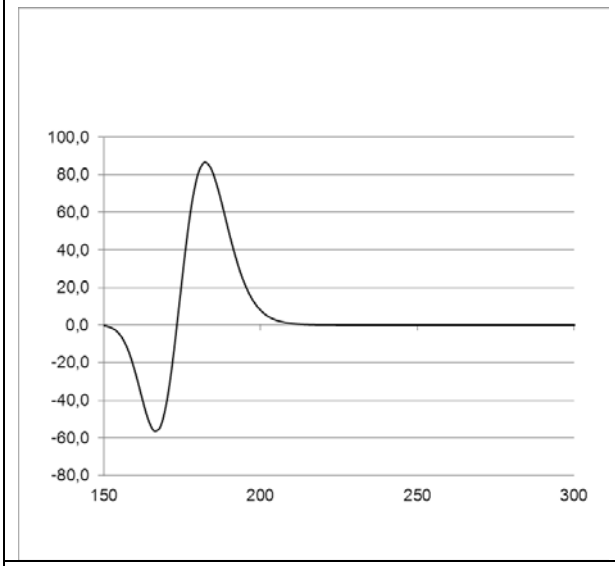

B

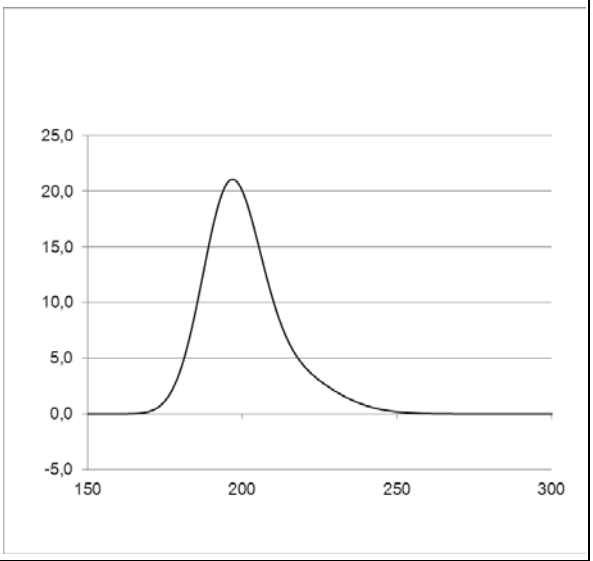

C

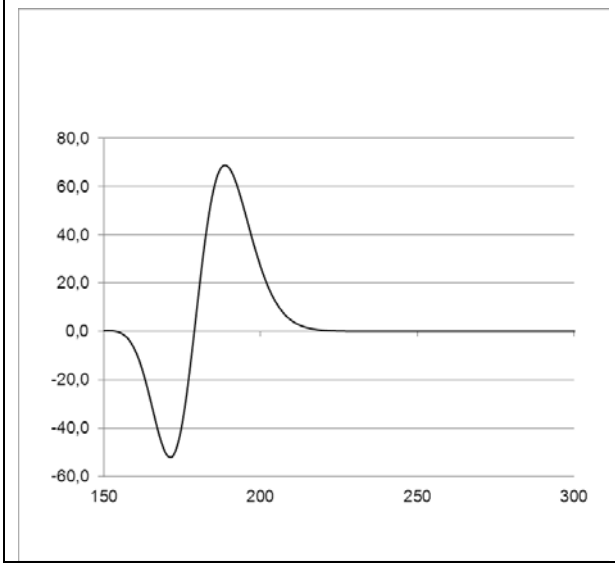

D

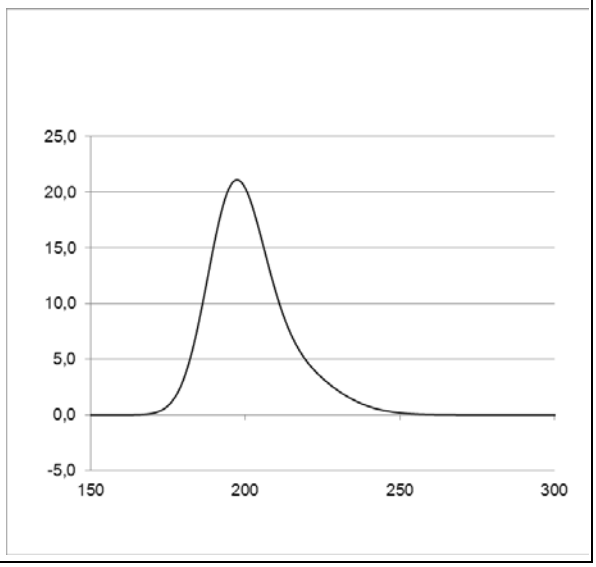

E

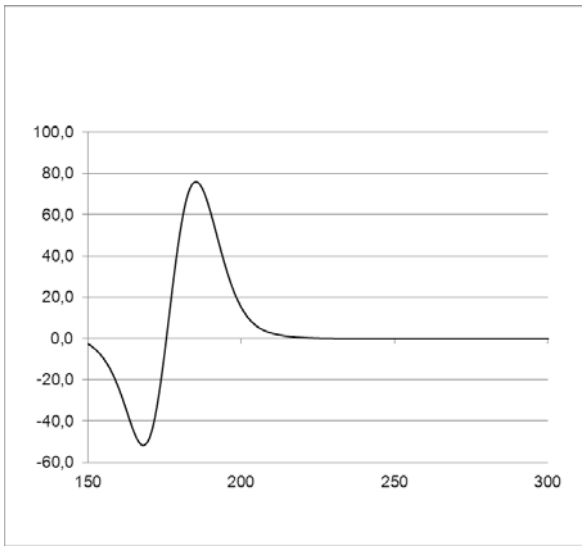
100,0
80,0
60,0
40,0
20,0
0,0
-20,0
-40,0
-60,0
150
200
250
300

F

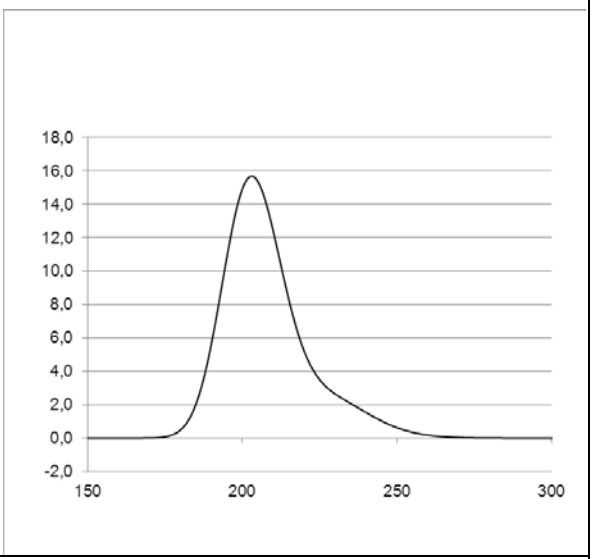
18,0
16,0
14,0
12,0
10,0
8,0
6,0
4,0
2,0
0,0
-2,0
150
200
250
300

G

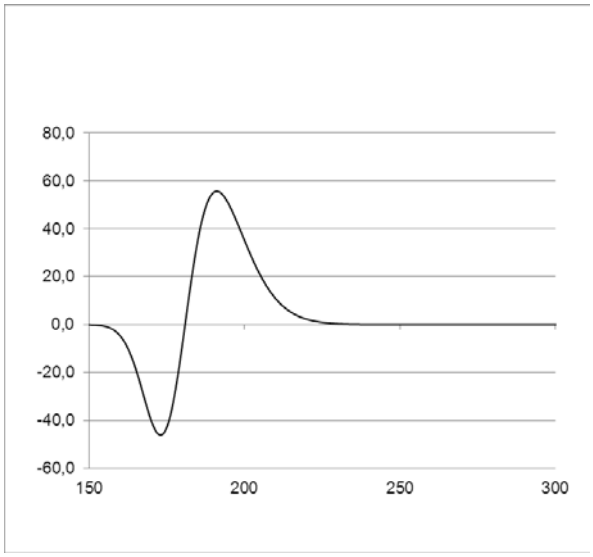
80,0
60,0
40,0
20,0
0,0
-20,0
-40,0
-60,0
150
200
250
300

H

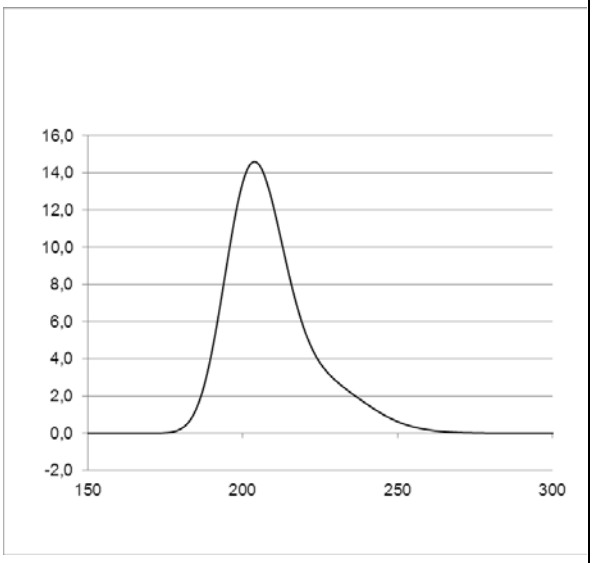
16,0
14,0
12,0
10,0
8,0
6,0
4,0
2,0
0,0
-2,0
150
200
250
300

I

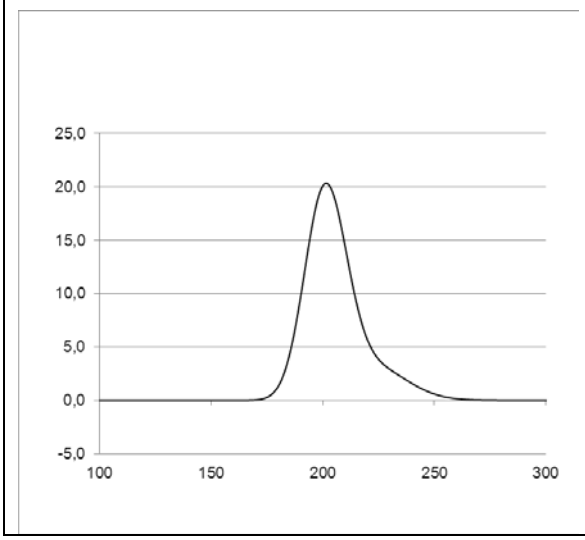
25,0
20,0
15,0
10,0
5,0
0,0
-5,0
100
150
200
250
300

Figures S7 A-I: Calculated ECD spectra of (+)-limonene at different levels of theory for conformer 2 (on the x-axis: wavelengths in nm, on the y-axis: Δε [Mol*l^{-1}*cm^{-1}]

A

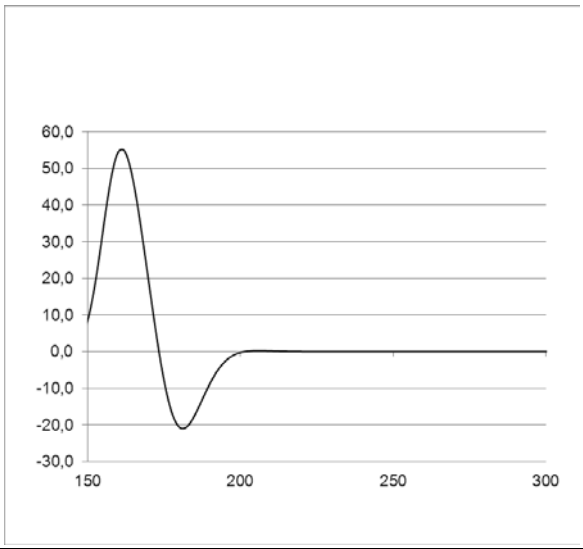

B

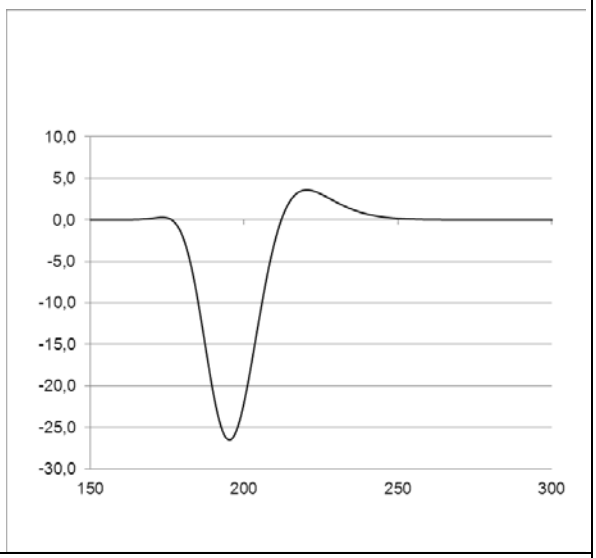

C

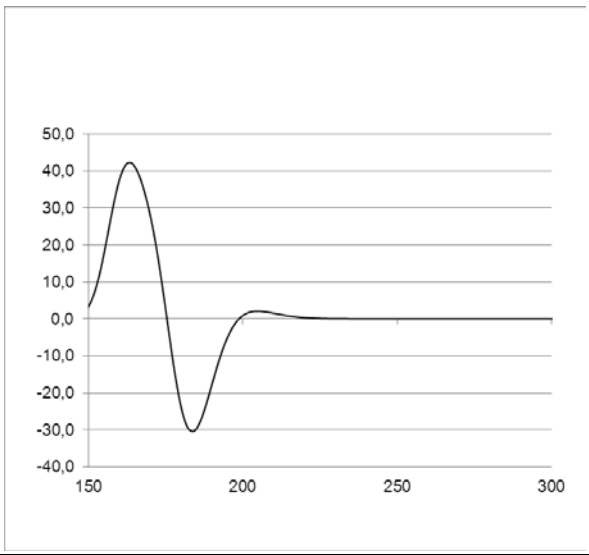

D

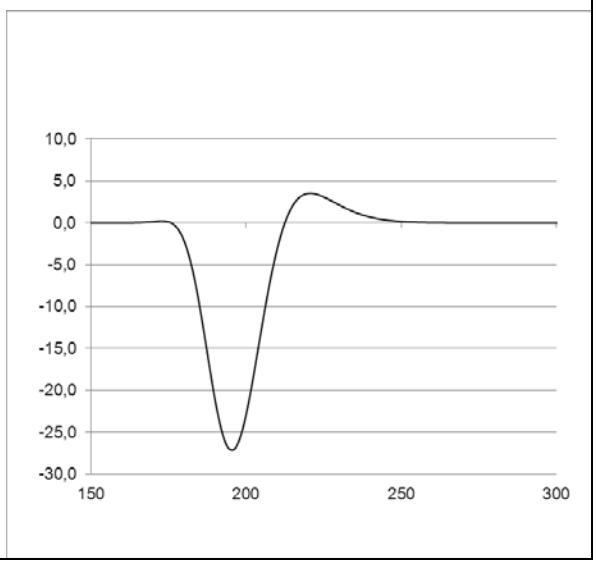

E

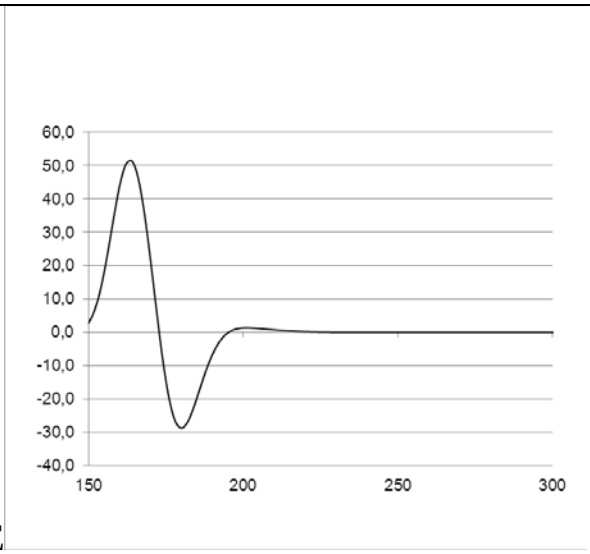
60,0
50,0
40,0
30,0
20,0
10,0
0,0
-10,0
-20,0
-30,0
-40,0
150
200
250
300

F

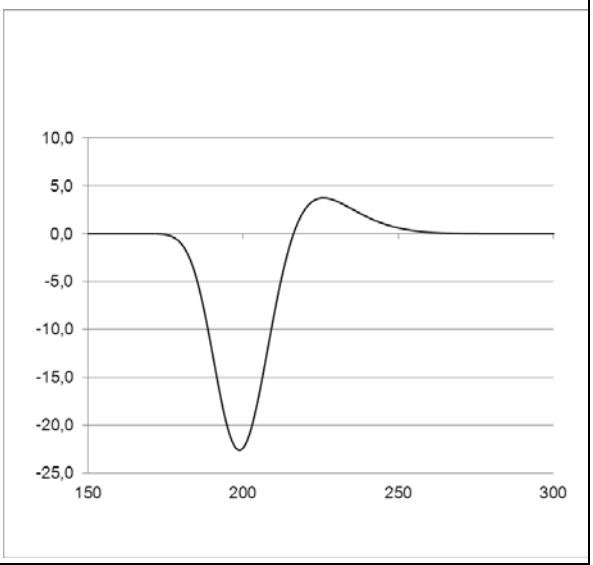
10,0
5,0
0,0
-5,0
-10,0
-15,0
-20,0
-25,0
150
200
250
300

G

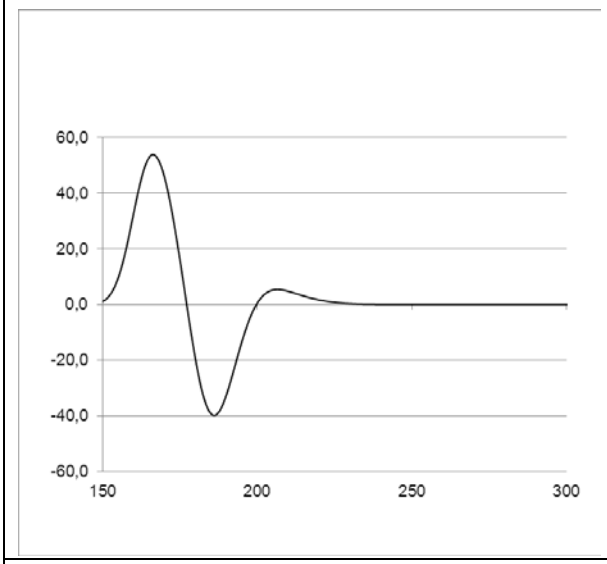
60,0
40,0
20,0
0,0
-20,0
-40,0
-60,0
150
200
250
300

H

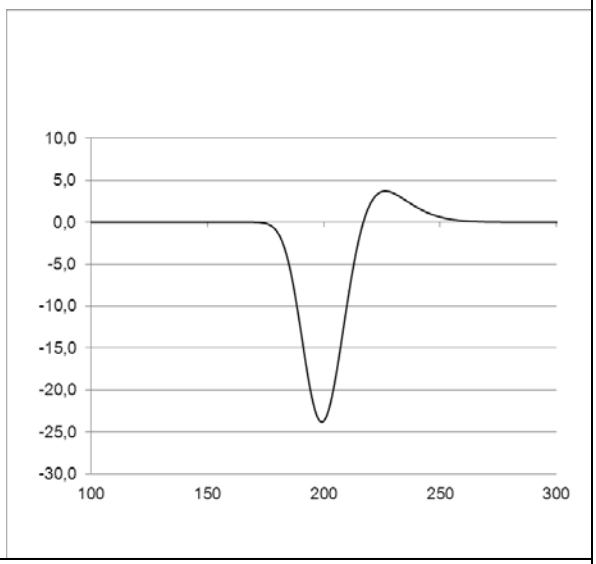
10,0
5,0
0,0
-5,0
-10,0
-15,0
-20,0
-25,0
-30,0
100
150
200
250
300

I

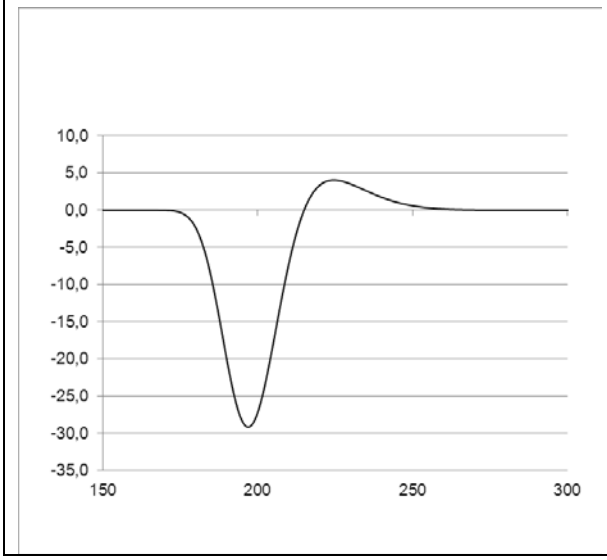
10,0
5,0
0,0
-5,0
-10,0
-15,0
-20,0
-25,0
-30,0
-35,0
150
200
250
300

Figures S8 A-I: Calculated ECD spectra of (+)-limonene at different levels of theory for conformer 3 (on the x-axis: wavelengths in nm, on the y-axis: Δε [Mol*l^{-1}*cm^{-1}]

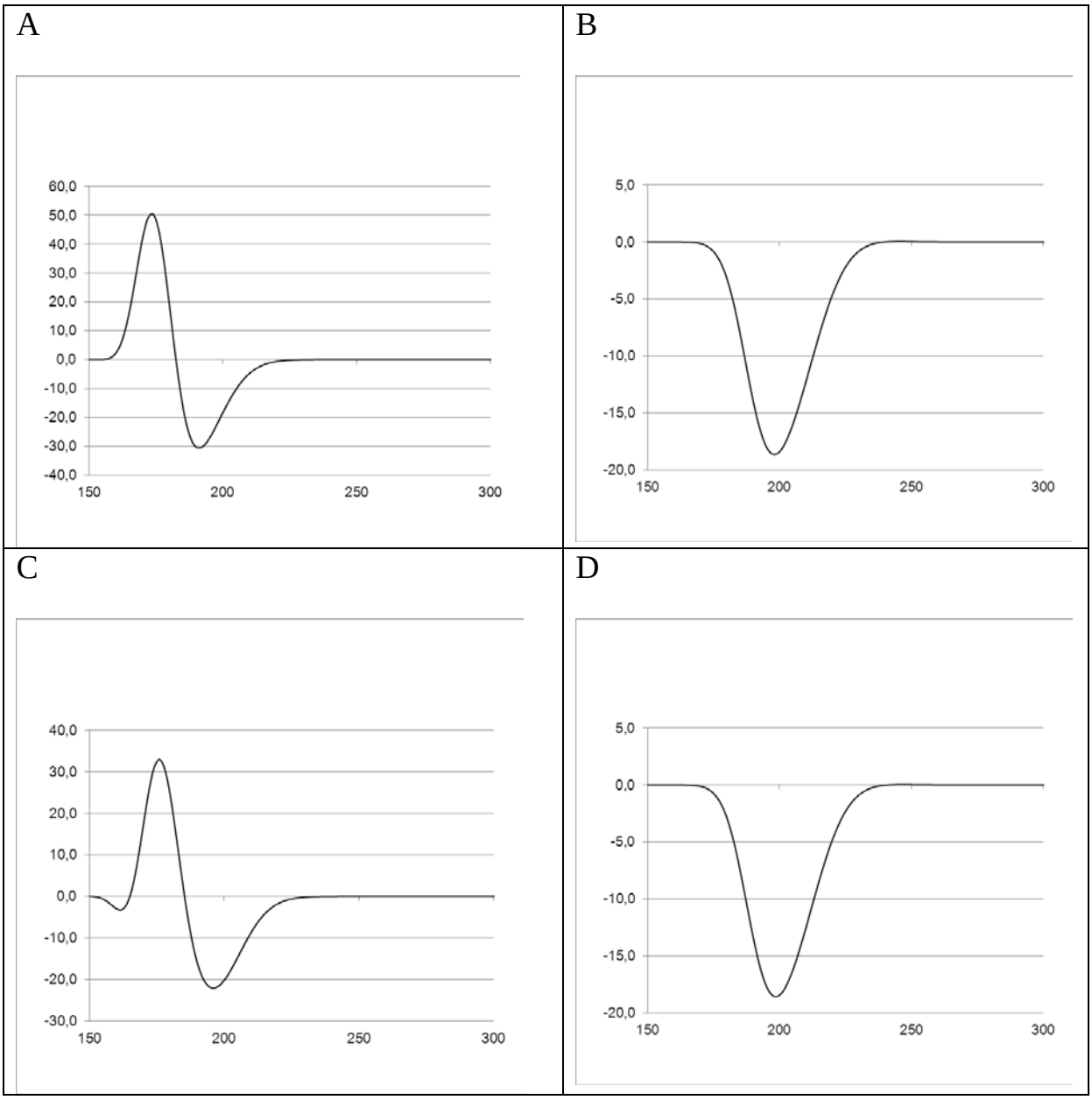

E

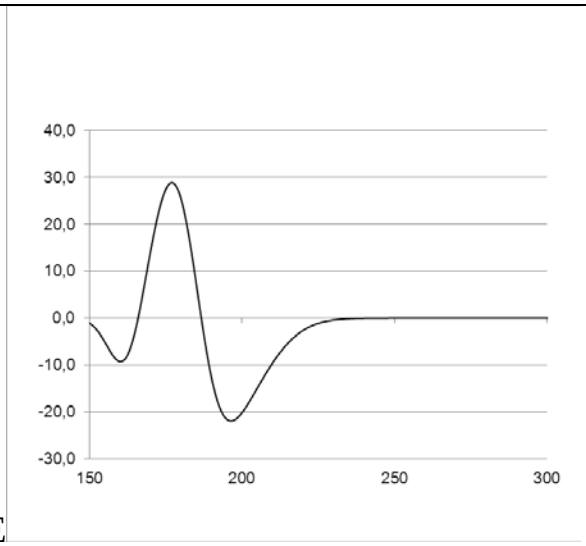
40,0
30,0
20,0
10,0
0,0
-10,0
-20,0
-30,0
150
200
250
300

F

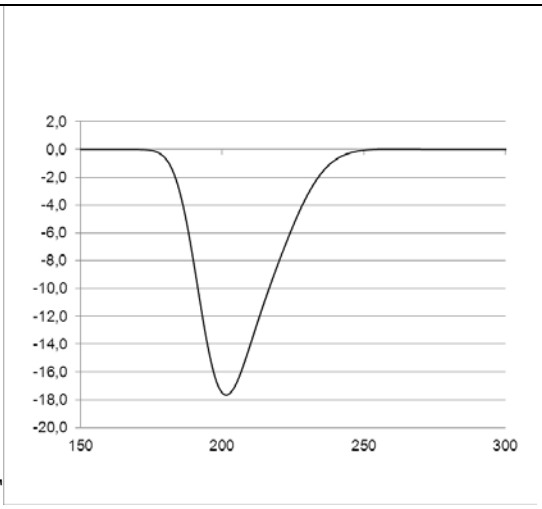
2,0
0,0
-2,0
-4,0
-6,0
-8,0
-10,0
-12,0
-14,0
-16,0
-18,0
-20,0
150
200
250
300

G

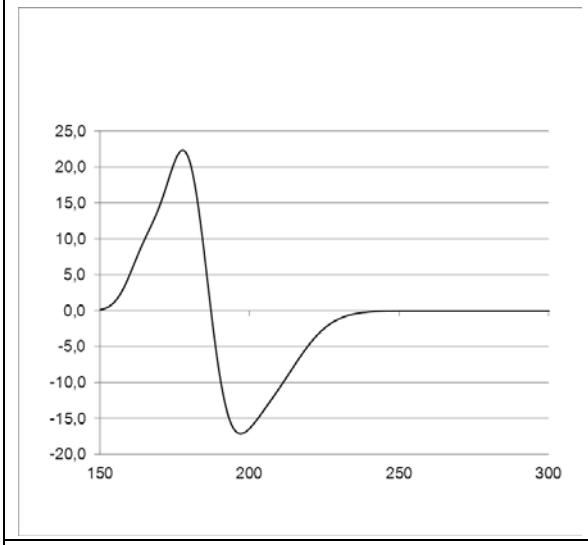
25,0
20,0
15,0
10,0
5,0
0,0
-5,0
-10,0
-15,0
-20,0
150
200
250
300

H

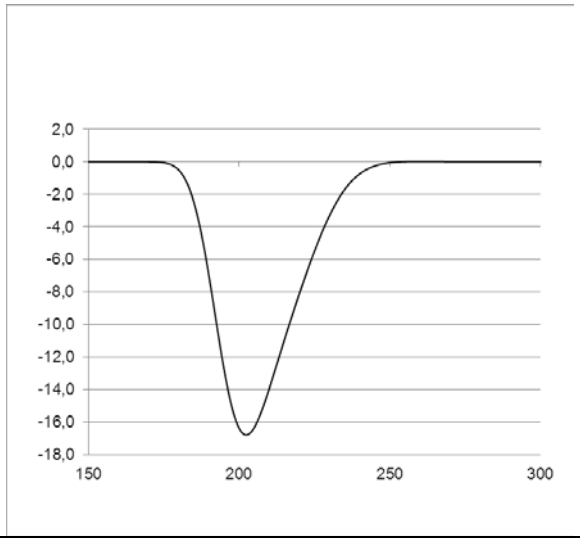
2,0
0,0
-2,0
-4,0
-6,0
-8,0
-10,0
-12,0
-14,0
-16,0
-18,0
150
200
250
300

I

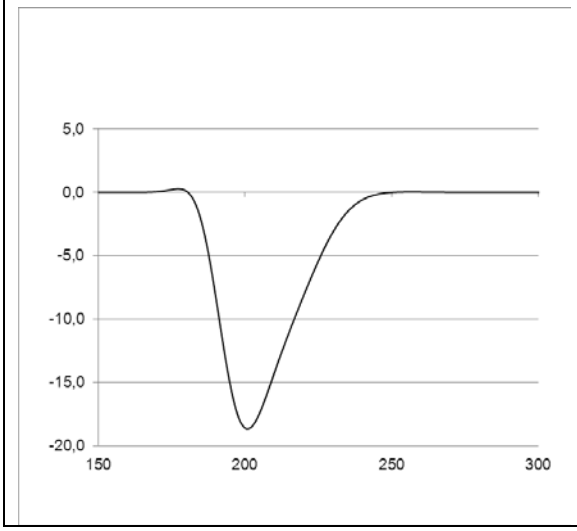
5,0
0,0
-5,0
-10,0
-15,0
-20,0
150
200
250
300

Figure S9 A-D: Basis set and population dependence of calculated ECD spectra of (+)-limonene:

A and B: mpw1pw91/cc-pvdz; C and D: mpw1pw91/aug-cc-pvdz (on the x-axis: wavelengths in nm, on the y-axis: Δε [Mol*l^{-1}*cm^{-1}]

A

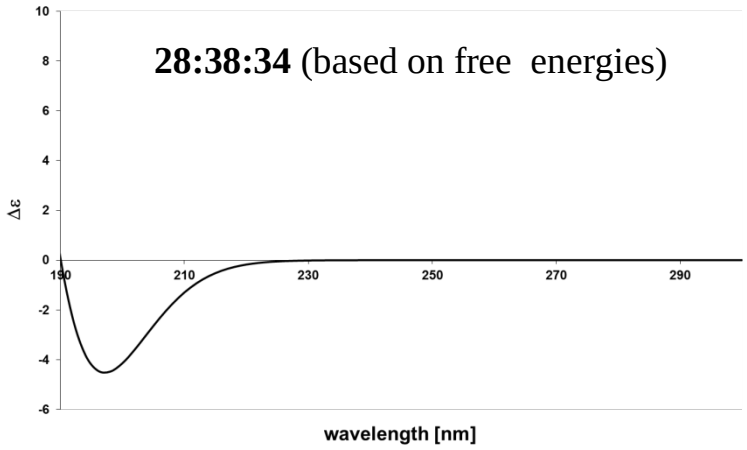

B

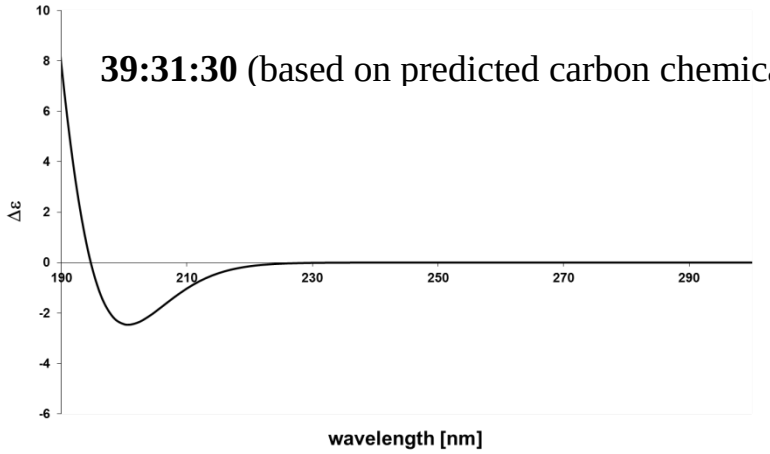

C

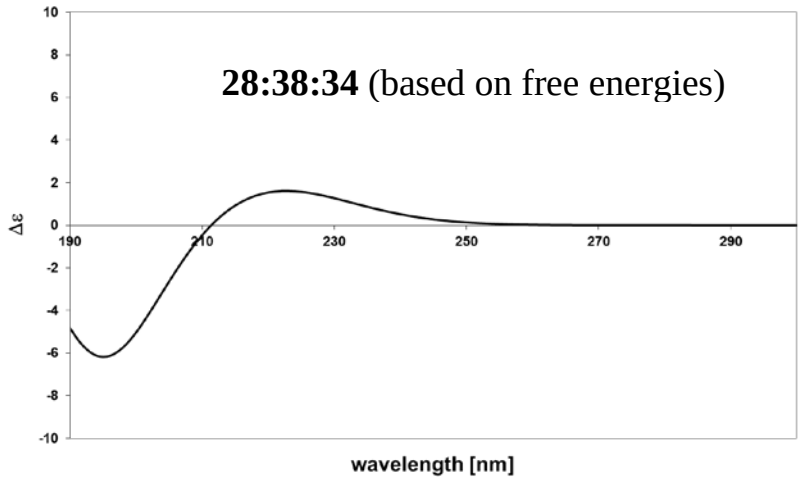
28:38:34 (based on free energies)
Δε
wavelength [nm]

D

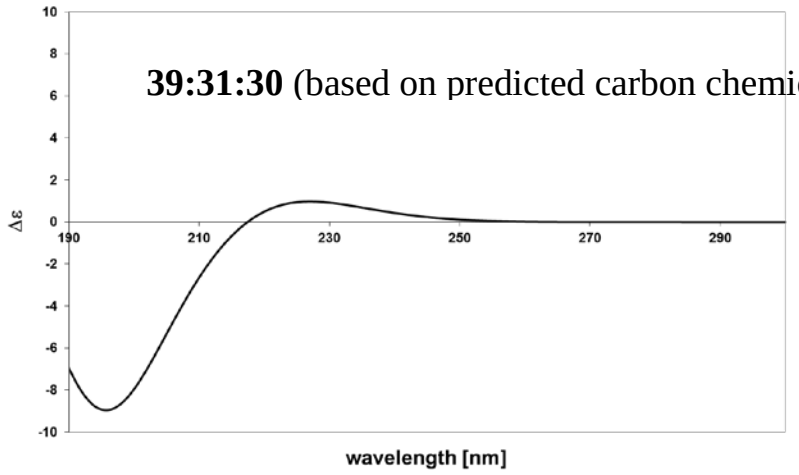
39:31:30 (based on predicted carbon chemical shifts)
Δε
wavelength [nm]

Figure S10 A-I: Calculated UV-Vis spectra of (+)-limonene at different levels of theory for conformer 1 (on the x-axis: wavelengths in nm, on the y-axis: ε [Mol*l^{-1}*cm^{-1}]

A

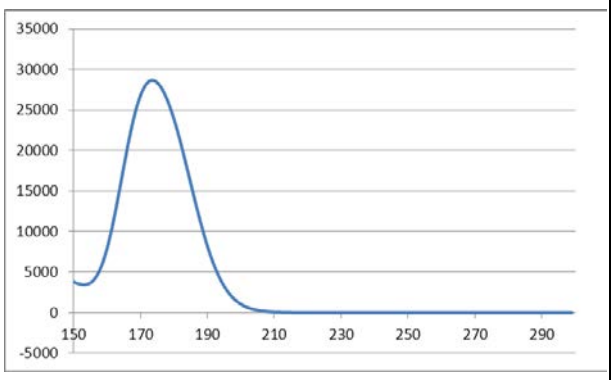

B

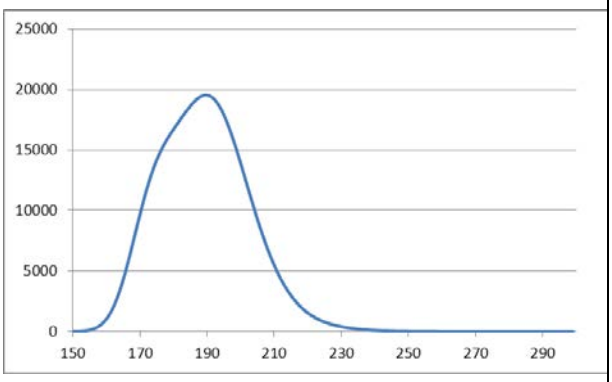

C

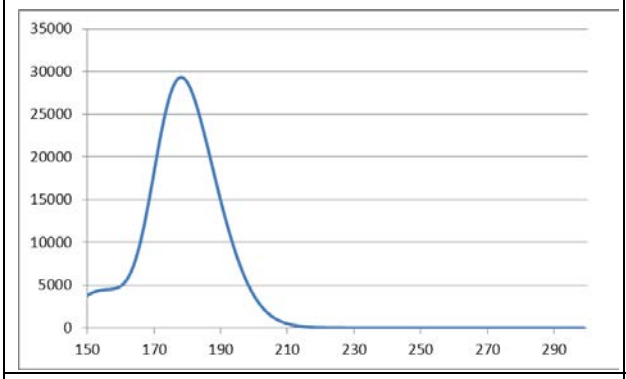

D

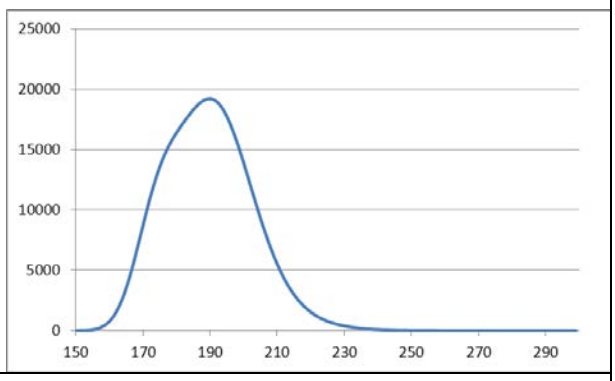

E

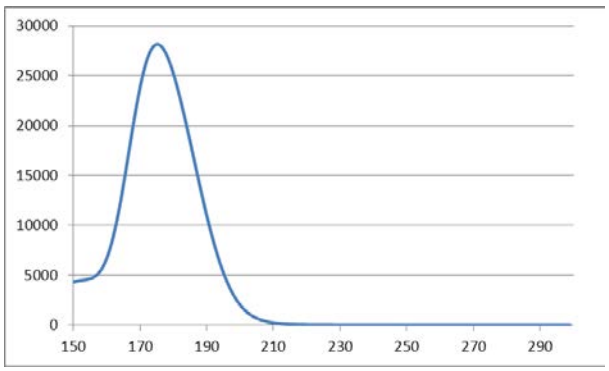

F

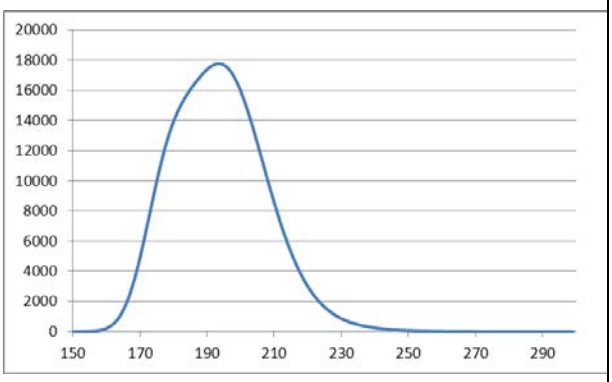

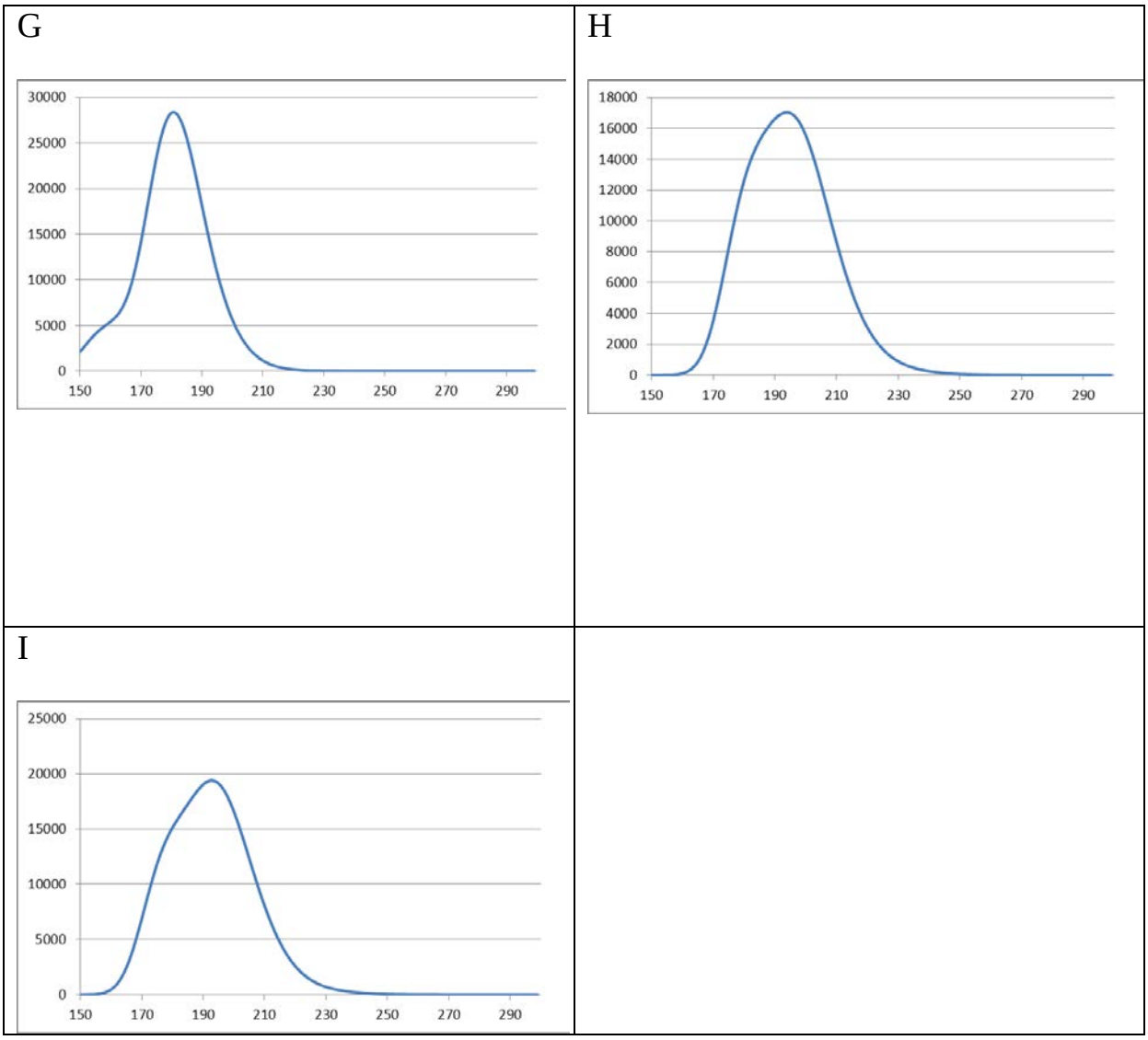

Figure S11 A-I: Calculated UV-Vis spectra of (+)-limonene at different levels of theory for conformer 2 (on the x-axis: wavelengths in nm, on the y-axis: ε [Mol*l^{-1}*cm^{-1}]

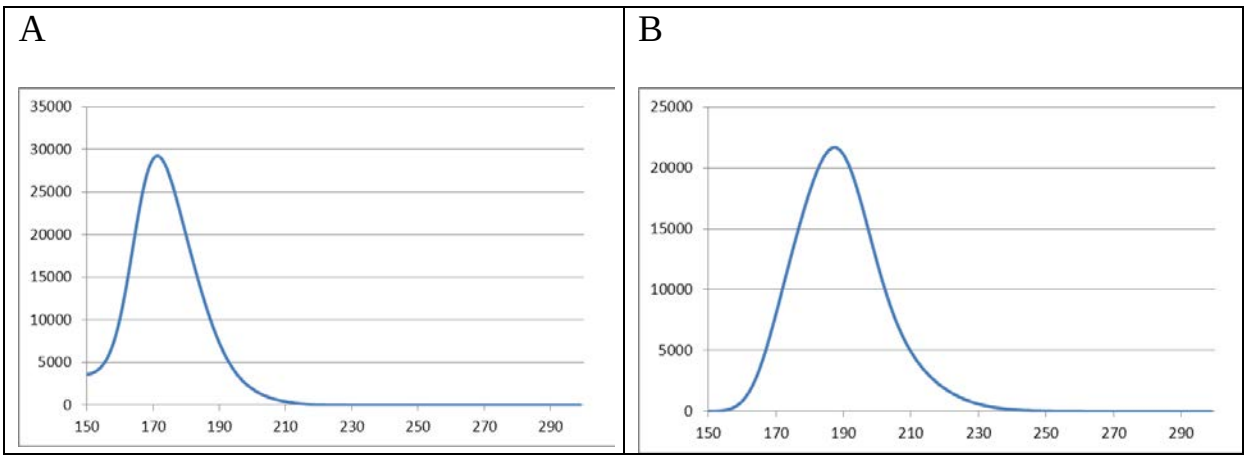

C

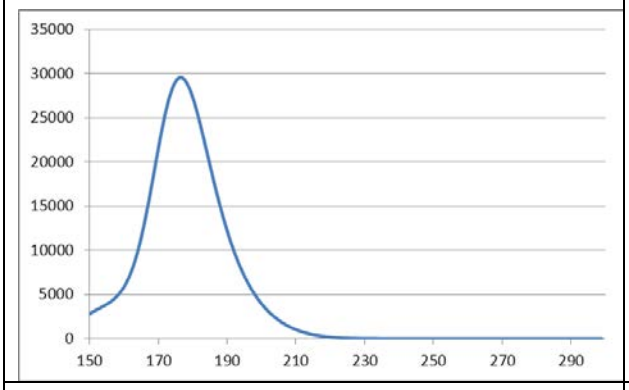
35000
30000
25000
20000
15000
10000
5000
0
150 170 190 210 230 250 270 290

D

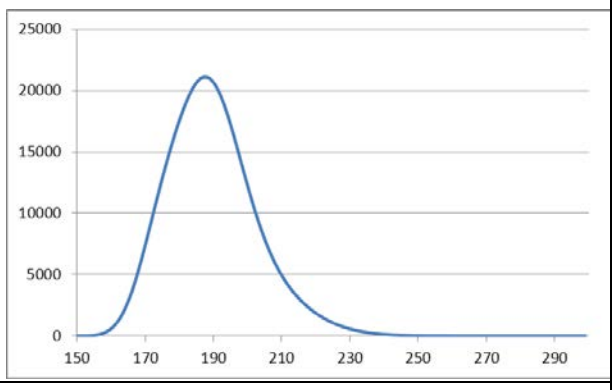
25000
20000
15000
10000
5000
0
150 170 190 210 230 250 270 290

E

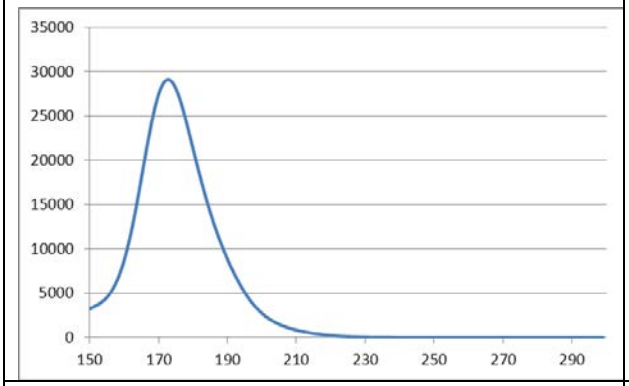
35000
30000
25000
20000
15000
10000
5000
0
150 170 190 210 230 250 270 290

F

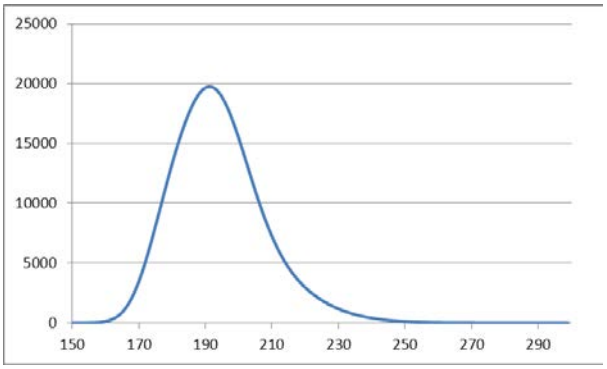
25000
20000
15000
10000
5000
0
150 170 190 210 230 250 270 290

G

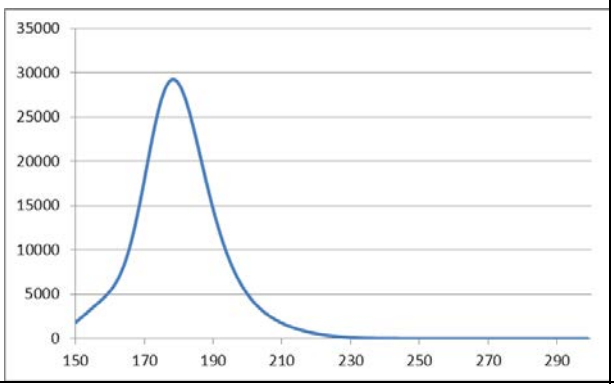
35000
30000
25000
20000
15000
10000
5000
0
150 170 190 210 230 250 270 290

H

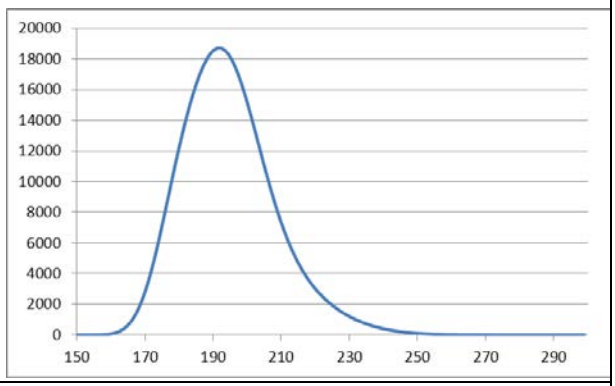
20000
18000
16000
14000
12000
10000
8000
6000
4000
2000
0
150 170 190 210 230 250 270 290

I

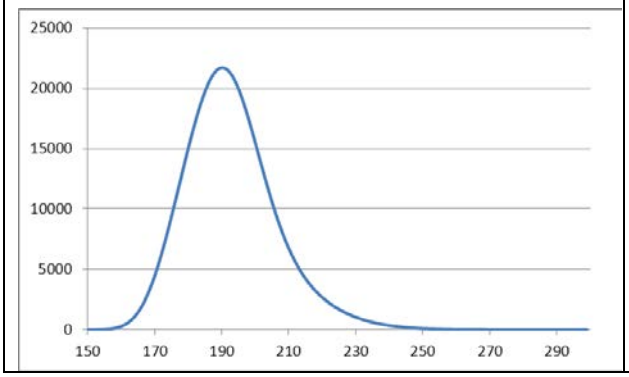
25000
20000
15000
10000
5000
0
150 170 190 210 230 250 270 290

Figure S12 A-I: Calculated UV-Vis spectra of (+)-limonene at different levels of theory for conformer 3 (on the x-axis: wavelengths in nm, on the y-axis: ε [Mol*l^{-1}*cm^{-1}]

A

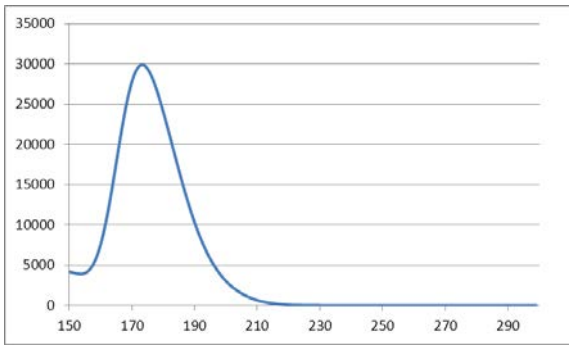

B

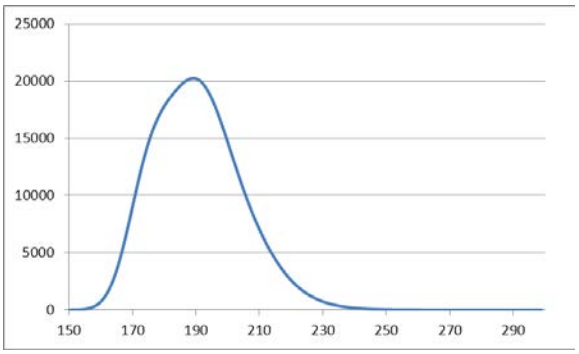

C

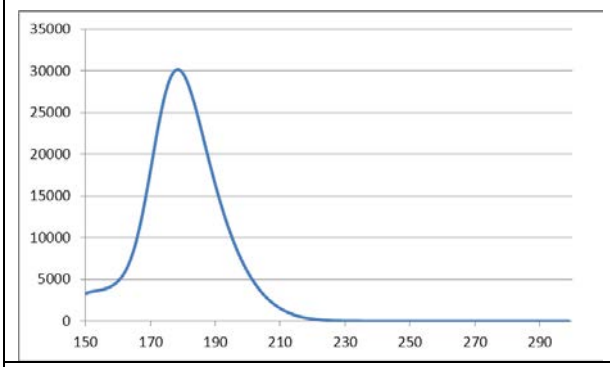

D

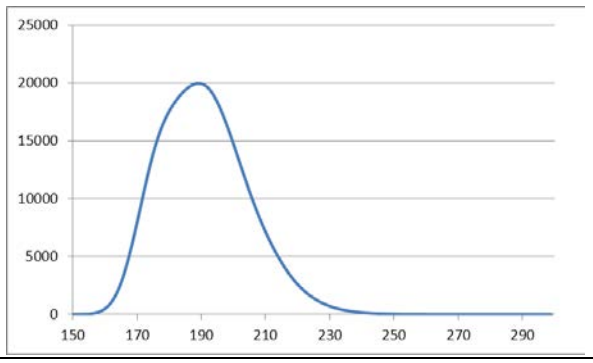

E

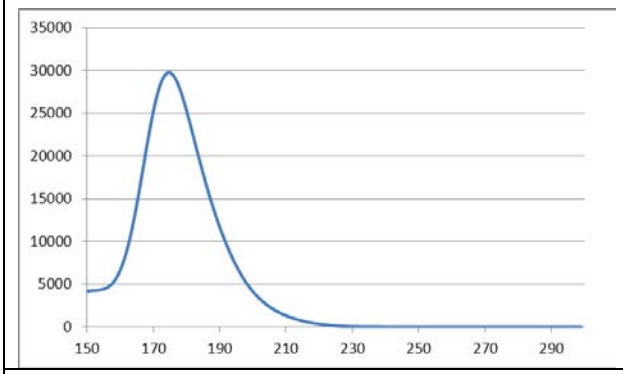

F

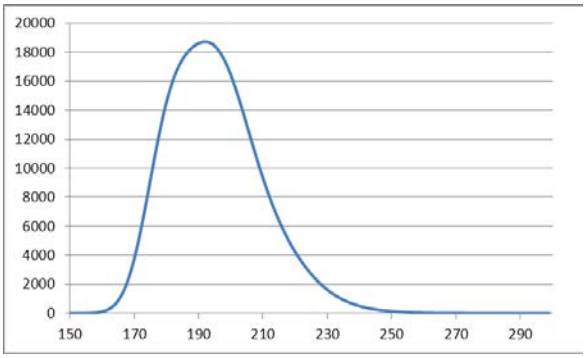

G

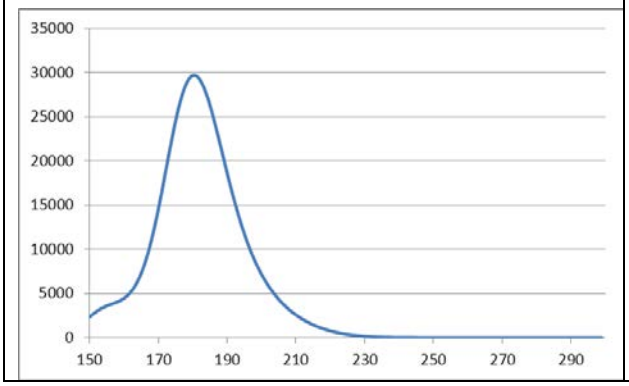

H

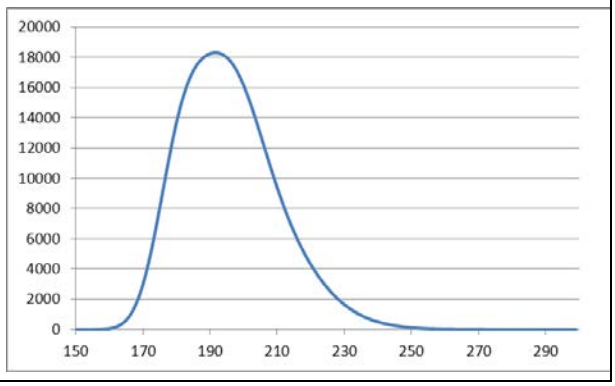

I

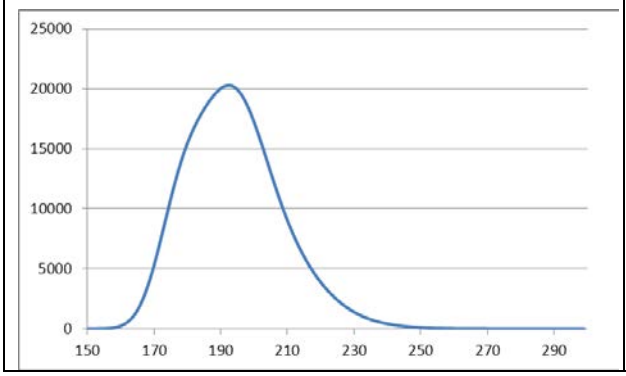

Figures S13 A-C:
Experimental UV spectra of (+)-limonene in methanol or ethanol at different concentrations (on the x-axis: wavelengths in nm, on the y-axis ε [Mol*l^{-1}*cm^{-1}]
A: 2.7 mg/ml in methanol; B: 0.1 mg/ml in methanol; C: 2.4 mg/ml in ethanol

A

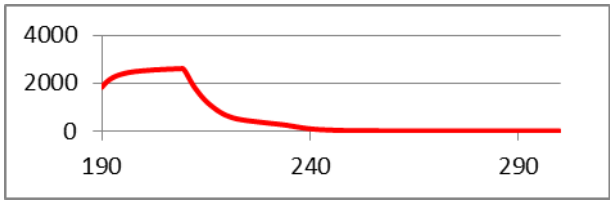

B

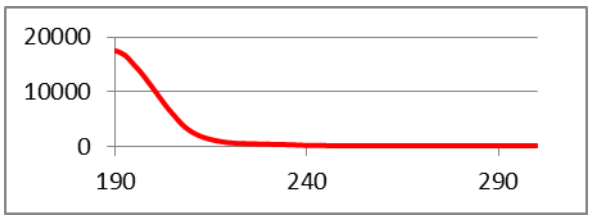

C

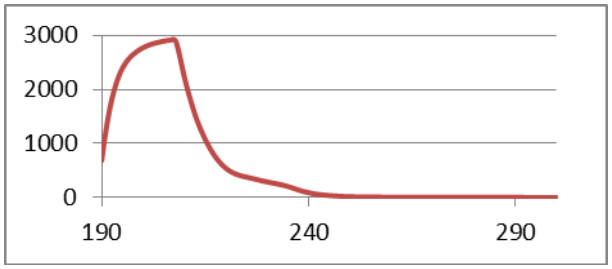

Figures S14 to S17 show the calculated VCD spectra of (+)-limonene for the other levels of theory. The same conclusions from above can be drawn so that the VCD analysis seems to be robust concerning the level of theory. Fig. S18 shows that an arithmetic mean of all spectra obtained at the various levels of theory still shows the enantiodiscriminative bands.

Figure S14: Calculated (level of theory b) VCD spectra of (+)-limonene of the three conformers 1,2 and 3 (A, B, and C); D: population weighted mix 39:31:30 (on the x-axis: wavenumbers in cm^{-1}, on the y-axis: $\Delta\varepsilon$ [$Mol*l^{-1}*cm^{-1}$]

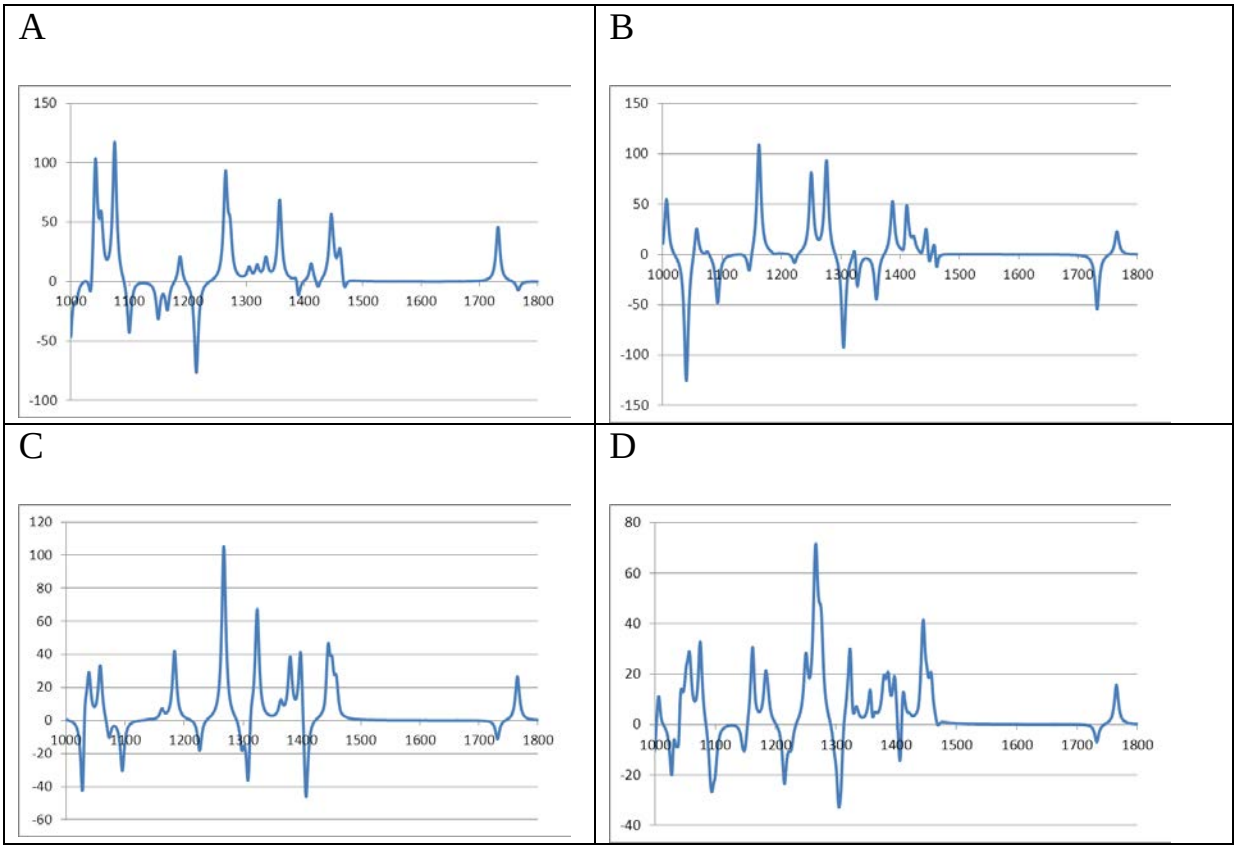

Figure S15: Calculated (level of theory c) VCD spectra of (+)-limonene of the three conformers 1,2 and 3 (A, B, and C); D: population weighted mix 39:31:30 (on the x-axis: wavenumbers in cm^{-1}, on the y-axis: $\Delta\varepsilon$ [$Mol*l^{-1}*cm^{-1}$]

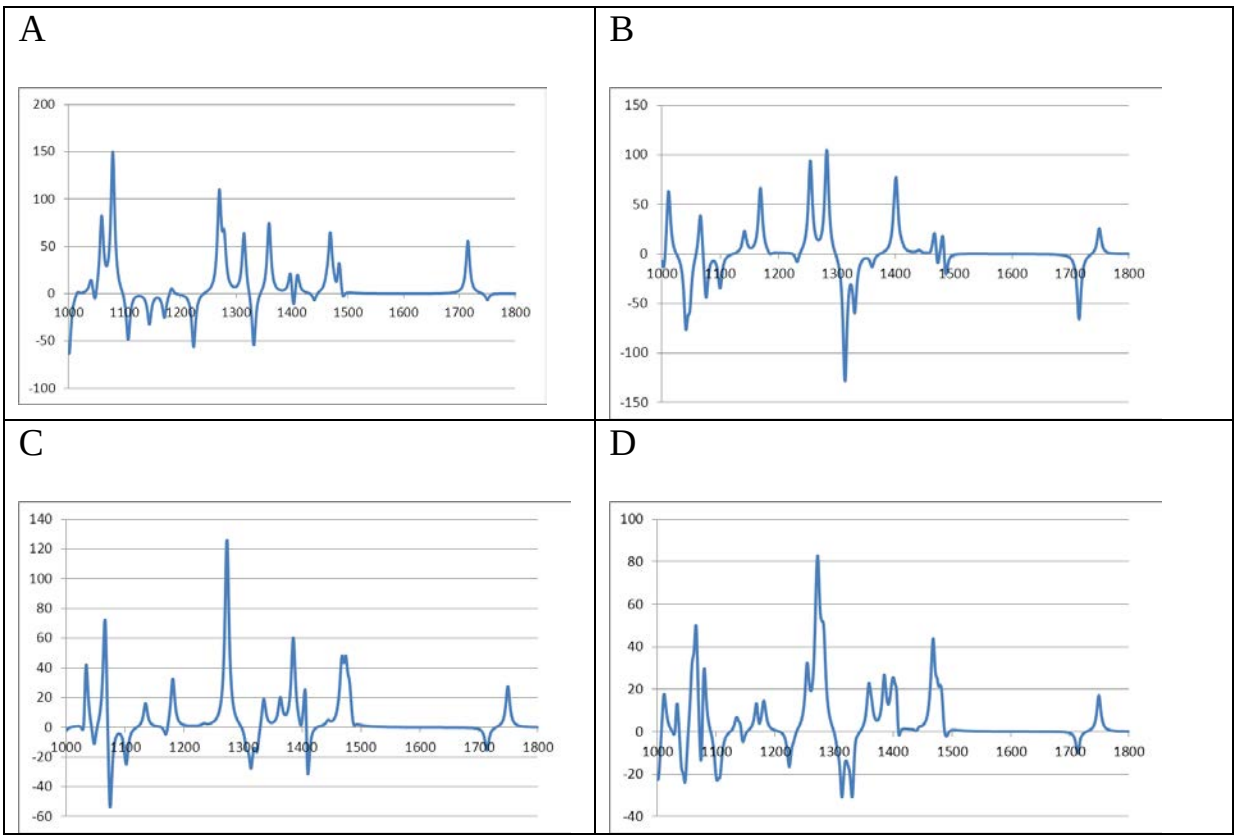

Figure S16: Calculated (level of theory d) VCD spectra of (+)-limonene of the three conformers 1,2 and 3 (A, B, and C); D: population weighted mix 39:31:30 (on the x-axis: wavenumbers in cm^{-1}, on the y-axis: $\Delta\varepsilon$ [$Mol*l^{-1}*cm^{-1}$]

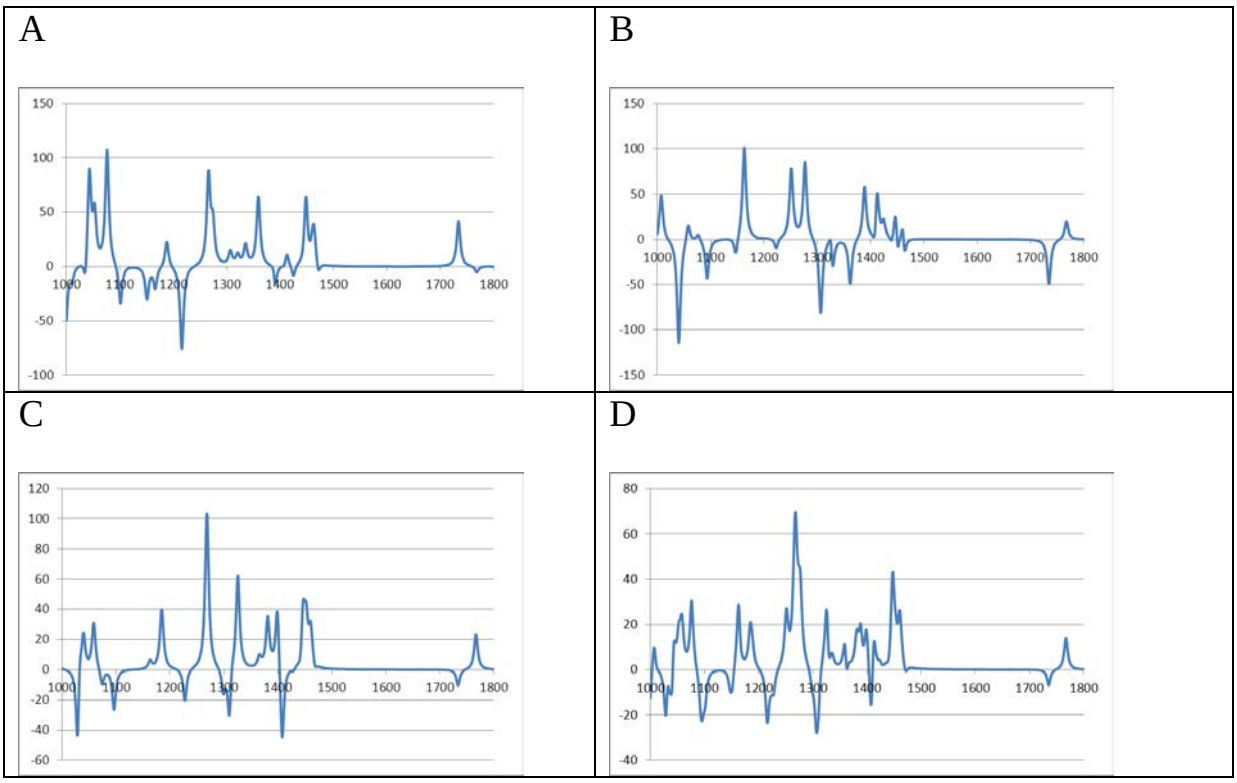

Figure S17: Calculated (level of theory e) VCD spectra of (+)-limonene of the three conformers 1,2 and 3 (A, B, and C); D: population weighted mix 39:31:30 (on the x-axis: wavenumbers in cm^{-1}, on the y-axis: $\Delta\varepsilon$ [$Mol*l^{-1}*cm^{-1}$]

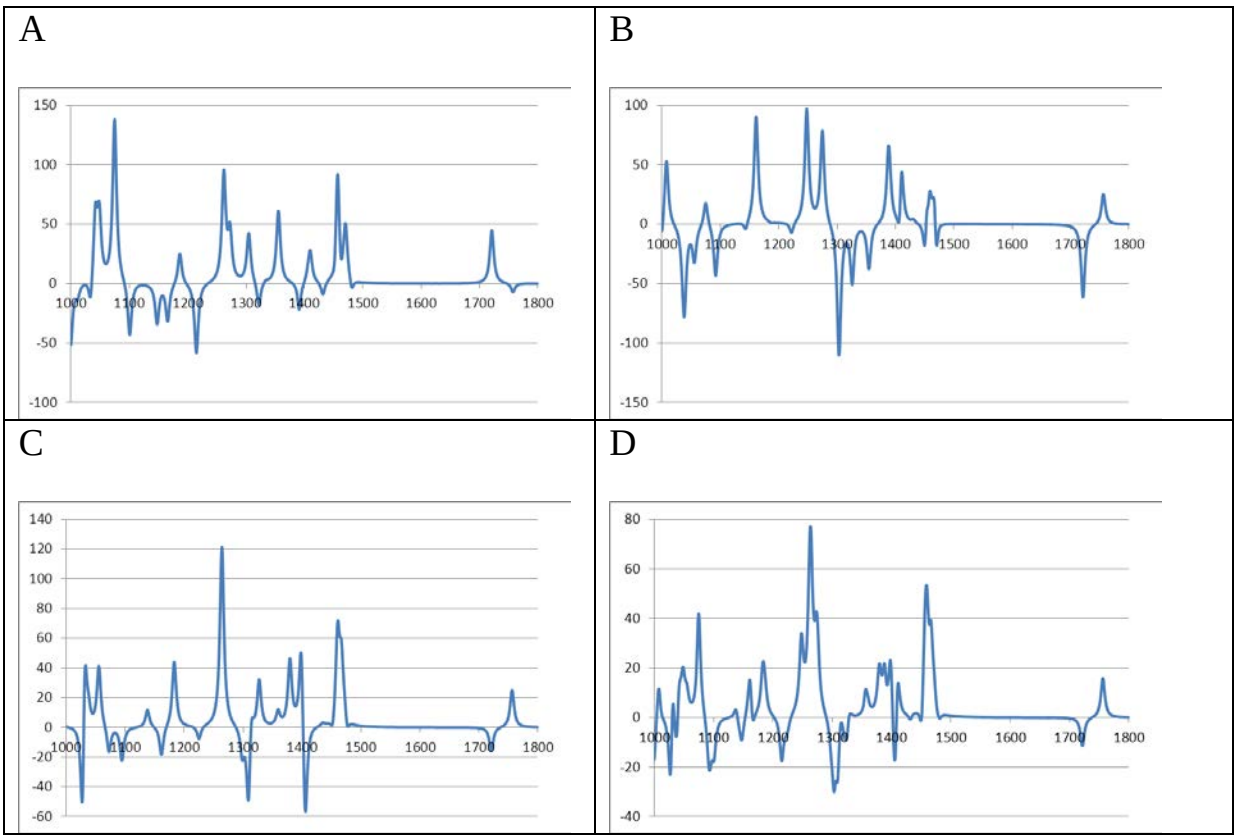

Figures S18 A and B: calculated VCD spectrum of (+)-limonene of arithmetic mean for the five levels of theory together with a population mix of 39:31:30 of the three conformers (on the x-axis: wavenumbers in cm^{-1}, on the y-axis: $\Delta\varepsilon$ [$Mol*l^{-1}*cm^{-1}$]

A: From 1800 cm^{-1} to 1000 cm^{-1}

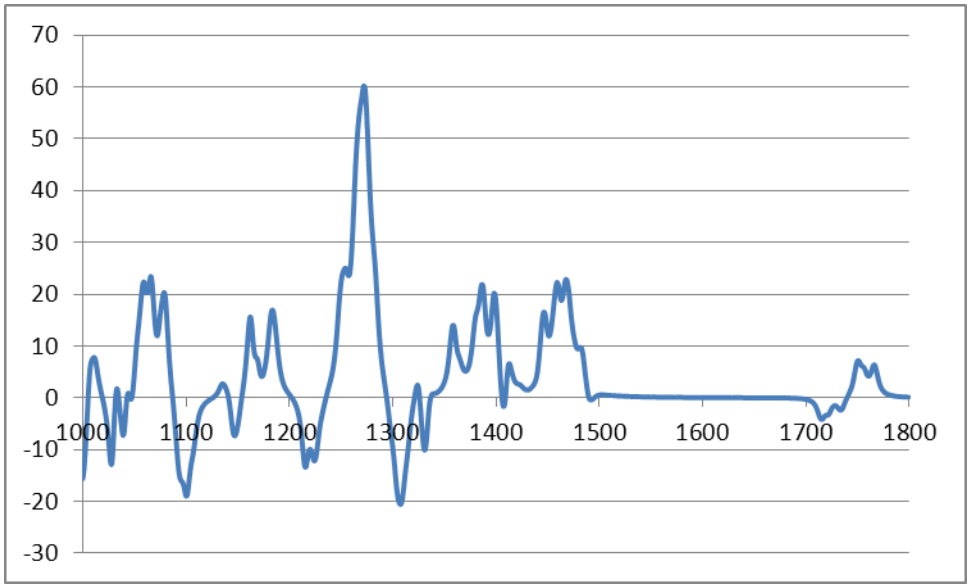

B: From 1420 cm^{-1} to 1000 cm^{-1}

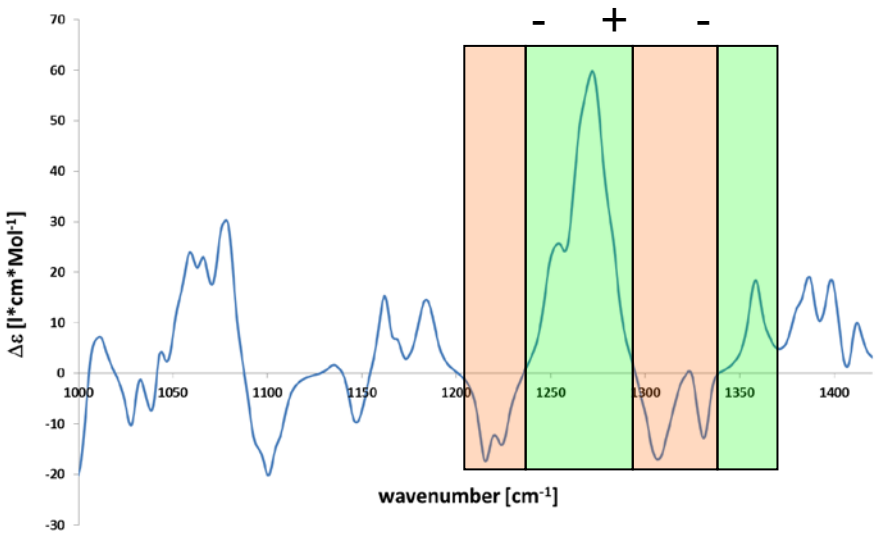

References

G Lukacs, A Neszmelyi (1981), Tetrahedron Lett., 22, 5053-5056

ED Skakovskii, WP Kiselev, LY Tychinskaya, AG Schutova, LW Gonsharova, EW Spiridowish, NA Bovdey, PA Kiselev, OA Gaidukevich, (2010), J. Appl. Spectrosc. 2010, 77, 329-334

Supporting information

Structural and chiroptical analysis of naturally occurring (−)-strychnine

F. Reinscheid[§], M. Schmidt[§], H. Abromeit[#], S Liening[#], G. K. E. Scriba[#], U.M. Reinscheid[§]

Concentration dependence of chemical shifts

Table S1: Proton resonances of (−)-strychnine base in $CDCl_3$

proton resonances	concentration of the sample: 2 mg/ml	concentration of the sample: 100 mg/ml	difference (2 mg/ml – 100mg/ml)
H4	8.09	8.05	0.04
H3	7.26	7.2	0.06
H1	7.18	7.12	0.06
H2	7.1	7.05	0.05
H22	5.95	5.85	0.1
H12	4.29	4.24	0.05
H23 pro*R*	4.16	4.1	0.06
H23 pro*S*	4.06	4.01	0.05
H16	4.01	3.89	0.12
H8	3.87	3.81	0.06
H20 pro*R*	3.75	3.65	0.1
H18 pro*R*	3.27	3.15	0.12
H14	3.17	3.1	0.07
H11 pro*S*	3.14	3.08	0.06
H18 pro*S*	2.9	2.82	0.08
H20 pro*S*	2.78	2.68	0.1
H11 pro*R*	2.67	2.62	0.05
H15 pro*S*	2.37	2.31	0.06
H17 pro*R* and pro*S*	1.92	1.84	0.08
H15 pro*R*	1.49	1.4	0.09
H13	1.29	1.22	0.07

Table S2: Proton resonances of (−)-strychnine HCl in methanol-*d3*

proton resonances	concentration of the sample: 2 mg/ml	concentration of the sample: 65 mg/ml	difference (2 mg/ml – 65 mg/ml)
H4	8.04	8.02	0.02
H1	7.41	7.45	-0.04
H3	7.35	7.33	0.02
H2	7.21	7.2	0.01
H22	6.43	6.43	0
H16	4.49	4.55	-0.06
H12	4.41	4.41	0
H23 pro*R*	4.27	4.28	-0.01
H23 pro*S*	not detected	4.21	
H20 pro*R*	4.23	4.24	-0.01
H20 pro*S*	3.58	3.57	0.01
H8	4.21	4.21	0
H18 pro*S*	3.85	3.88	-0.03
H18 pro*R*	3.41	3.39	0.02
H14	3.46	3.45	0.01
H11 pro*S*	3.09	3.07	0.02
H11 pro*R*	2.75	2.74	0.01
H15 pro*S*	2.6	2.61	-0.01
H15 pro*R*	1.76	1.73	0.03
H17 pro*R*	2.25	2.21	0.04
H17 pro*S*	2.07	2.08	-0.01
H13	1.5	1.48	0.02
H19	not detected	10.7	

Table S3: Proton resonances of (−)-strychnine HCl in methanol-*d3* (65 mg/ml) and in DMSO-*d6* (36 mg/ml)

proton resonances	methanol-*d3* (65 mg/ml)	DMSO-*d6* (36 mg/ml)	difference (methanol-*d3* – DMSO-*d6*
H4	8.02	7.94	0.08
H1	7.45	7.39	0.06
H3	7.33	7.31	0.02
H2	7.2	7.16	0.04
H22	6.43	6.33	0.1
H16	4.55	4.41	0.14
H12	4.41	4.36	0.05
H23 pro*R*	4.28	4.18	0.1
H23 pro*S*	4.21	4.13	0.08
H20 pro*R*	4.24	4.08	0.16
H20 pro*S*	3.57	3.5	0.07
H8	4.21	4.08	0.13
H18 pro*S*	3.88	3.71	0.17
H18 pro*R*	3.39	3.13	0.26
H14	3.45	3.32	0.13
H11 pro*S*	3.07	2.96	0.11
H11 pro*R*	2.74	2.65	0.09
H15 pro*S*	2.61	2.48	0.13
H15 pro*R*	1.73	1.59	0.14
H17 pro*R*	2.21	2.18	0.03
H17 pro*S*	2.08	1.85	0.23
H13	1.48	1.45	0.03
H19	10.7	12.01	-1.31

Table S4: ^{13}C resonances of (−)-strychnine HCl in methanol-*d3* and in DMSO-*d6*

13C resonances	methanol-*d3* (65 mg/ml)	DMSO-*d6* (36 mg/ml)	differences (methanol-*d3* – DMSO-*d6*)
C10	171.44	169.5	1.94
C5	143.23	142.3	0.93
C22	137.3	135	2.3
C21	133.73	133.6	0.13
C3	130.79	129.7	1.09
C6	130.62	130.1	0.52
C2	126.02	124.7	1.32
C1	123.76	123.3	0.46
C4	117.33	115.8	1.53
C12	77.95	76.5	1.45
C23	64.96	63.6	1.36
C16	63.66	61.3	2.36
C8	60.23	59	1.23
C20	53.22	51.4	1.82
C7	53.2	51.8	1.4
C18	52.22	50.7	1.52
C13	48.1	46.6	1.5
C11	42.7	41.7	1
C17	41.98	40.9	1.08
C14	31.58	30.1	1.48
C15	25.85	24.8	1.05

ORD

For (−)-strychnine base with the smaller basis set cc-pvdz the correct AC would have been predicted, however, with a worse match to experiment (Fig. S1). In contrast, the AC prediction for (−)-strychnine HCl would have failed with the smaller basis set (Fig. S2). In conclusion, the difference in [α] using the two basis sets cc-pvdz and

aug-cc-pvdz is large enough to switch the sign of the predicted value, and hence, would give the incorrect result in case of strychnine HCl. The difference between the two solvents DMSO and chloroform is much less (Fig. S3).

Figure S1: Calculated (mpw1pw91/ iefpcm: chloroform, major conformer; in blue: cc-pvdz, in red: aug-cc-pvdz) and experimental (in green, 2 % in chloroform) ORD curve of (−)-strychnine base based on four wavelengths (589, 546, 495, and 436 nm respectively)

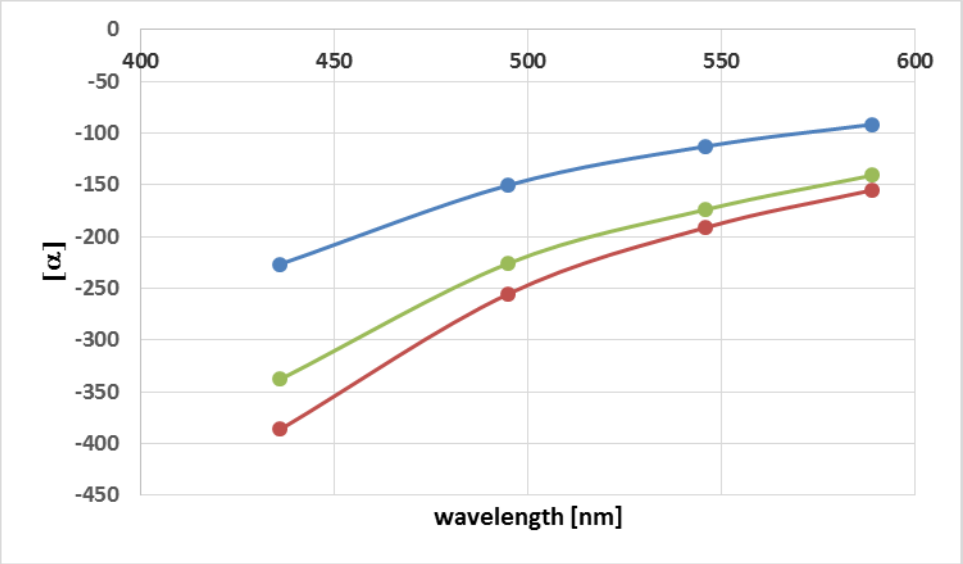

Figure S2: Calculated (mpw1pw91/ iefpcm: methanol, major conformer; in blue: cc-pvdz, in red: aug-cc-pvdz) and experimental (in green, 2 % in methanol) ORD curve of (−)-strychnine HCl/protonated strychnine based on four wavelengths (589, 546, 495, and 436 nm respectively)

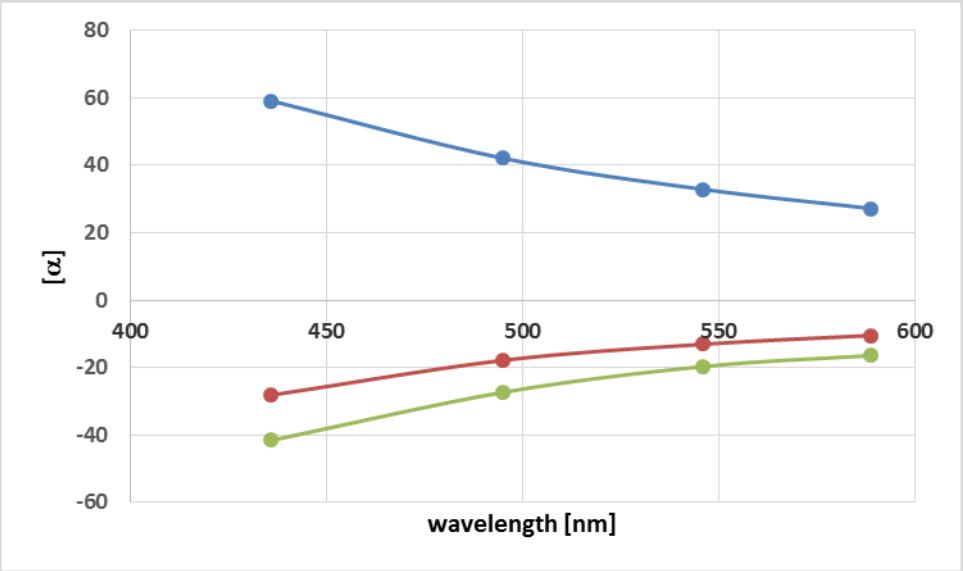

Figure S3: Calculated (mpw1pw91/cc-pvdz, iefpcm, major conformer; in blue: DMSO, in red: chloroform) and experimental (in green, 2 % in chloroform) ORD curve of (−)-strychnine base based on four wavelengths (589, 546, 495, and 436 nm respectively)

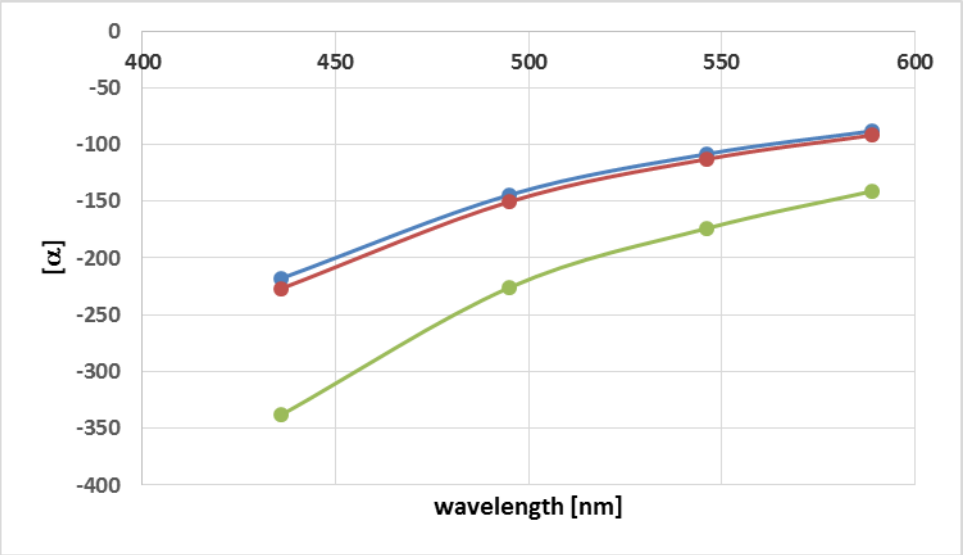

Calculated and experimental UV/Vis and ECD spectra

Solution phase calculations of n-π* transitions can be difficult as exemplified in the following. The gas phase and water phase n-π* transition of pyrimidine was correctly calculated using the PCM approach (Manzoni et al., 2010). The calculated values for gas and water phase (291 and 278 nm, respectively) match very well to the experimental values (298-292 nm, 271 nm). The two lowest energy transitions of uracil in the gas phase are n-π* followed by π-π*. However, in water the first one should show a blue shift while the latter one a red shift bringing the two transitions close in energy. So far, no experimental study could find a n-π* transition, most probably due to the overlaid strong π-π* transition. In a computational study Ludwig et al. (2007) showed that using 60 solute-solvent configurations with the explicit inclusion of 200 water molecules these solvatochromic shifts could be reproduced by quantum mechanical calculations. The authors suggest that the n-π* transition lies around 255 nm hidden by the intense and broad π-π* transition at 260 nm. Interestingly, the sign of the solvent-dependent shifts was also correctly reproduced by using only the PCM approach instead of the Monte Carlo/QM procedure from above. An even more complicated case is the blue shift of the lowest π-π* transition of phenol going from gas phase to water (Barreto et al., 2009). Depending if phenol is the proton-donor or –acceptor different shifts were observed and calculated: red shift versus blue shift, respectively. The overall blue shift was assigned to contributions of outer solvent water molecules (Barreto et al., 2009).

Figure S4: ECD spectrum of (−)-strychnine base in chloroform (0.049 mg/ml) at 25 °C

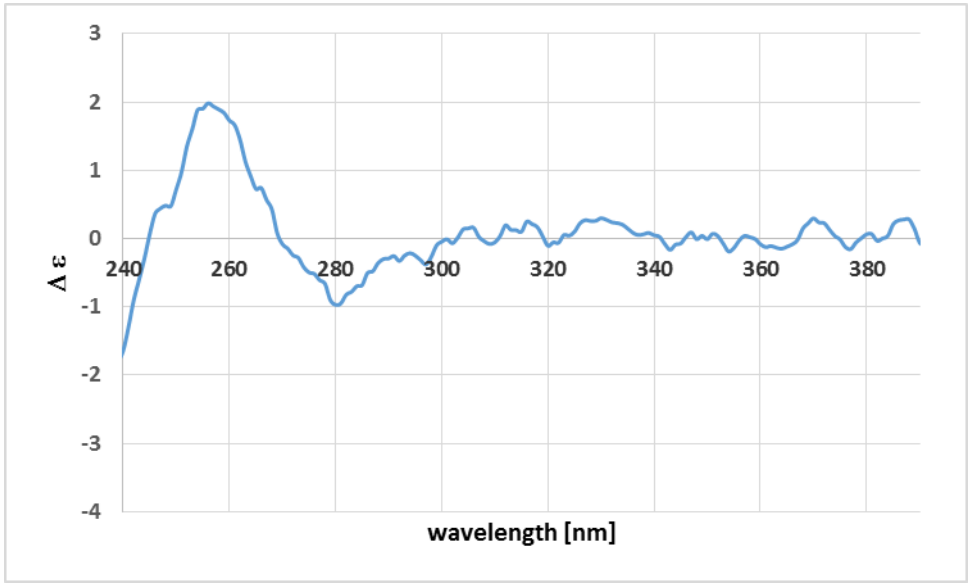

Figure S5: UV/Vis spectrum of (−)-strychnine base in chloroform (0.049 mg/ml) at 25 °C

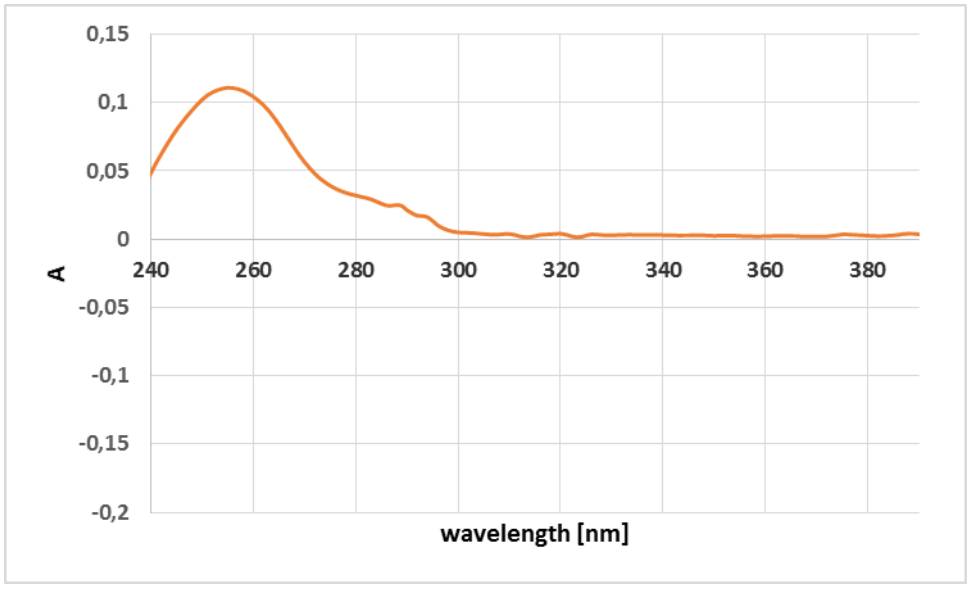

Figure S6: UV/Vis spectrum of (−)-strychnine base in acetonitrile (0.145 mg/ml) at 25 °C

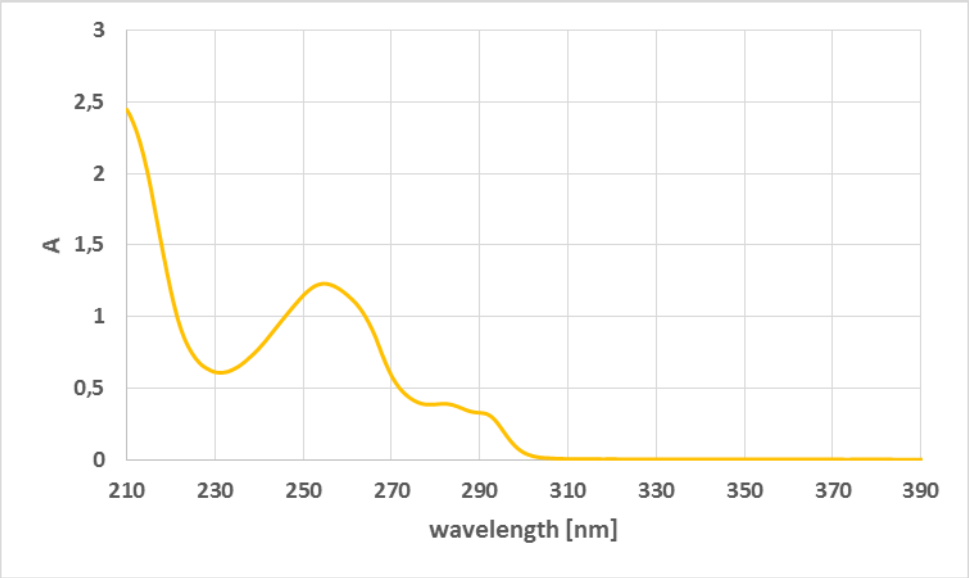

Figure S7: ECD spectrum of (−)-strychnine base in acetonitrile (0.029 mg/ml) at 25 °C

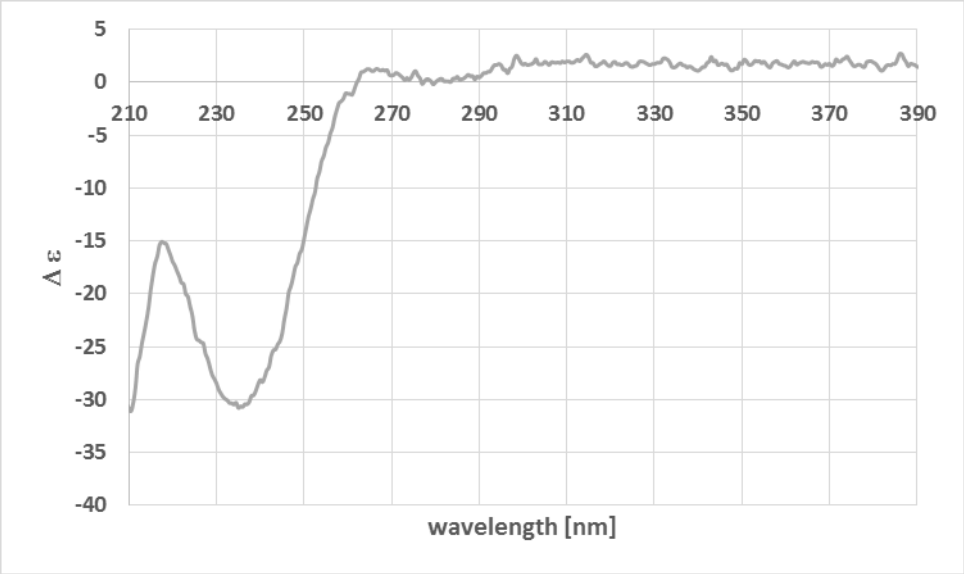

Figure S8: UV/Vis spectrum of (−)-strychnine base in acetonitrile (0.029 mg/ml) at 25 °C

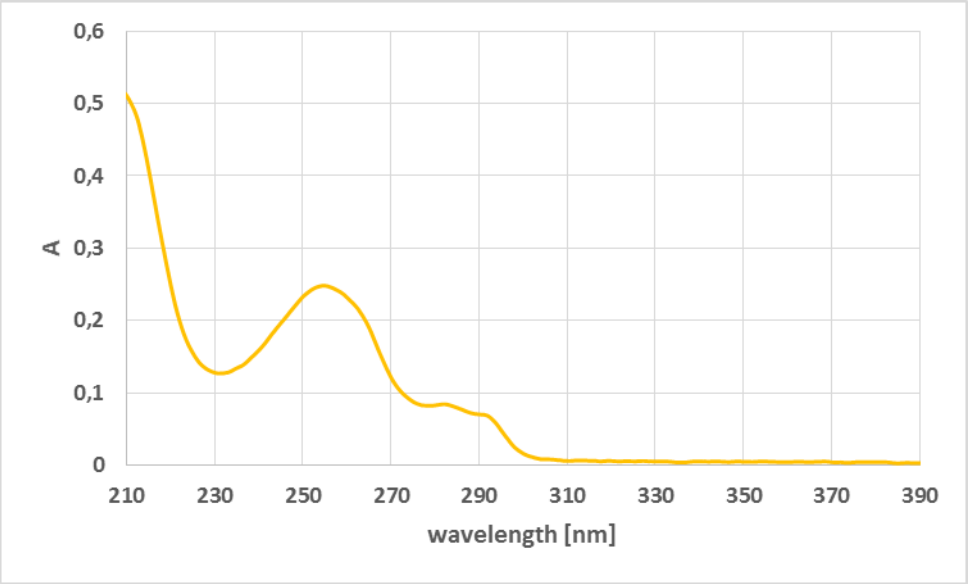

Figure S9: Experimental ECD spectrum of (−)-strychnine HCl (1.3 mg/ml) in methanol-*d3*

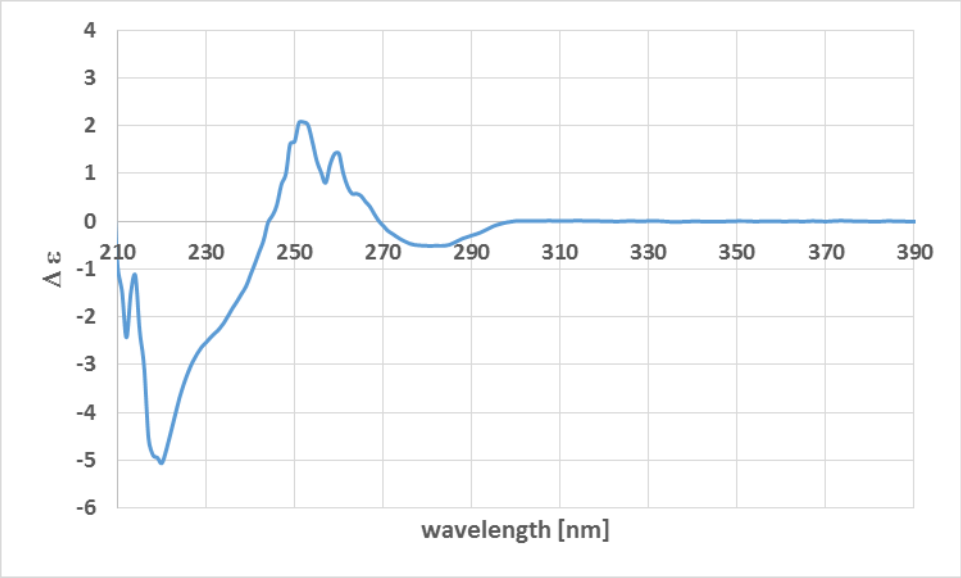

Figure S10: Experimental UV/Vis spectrum of (−)-strychnine HCl (1.3 mg/ml) in methanol-*d3*

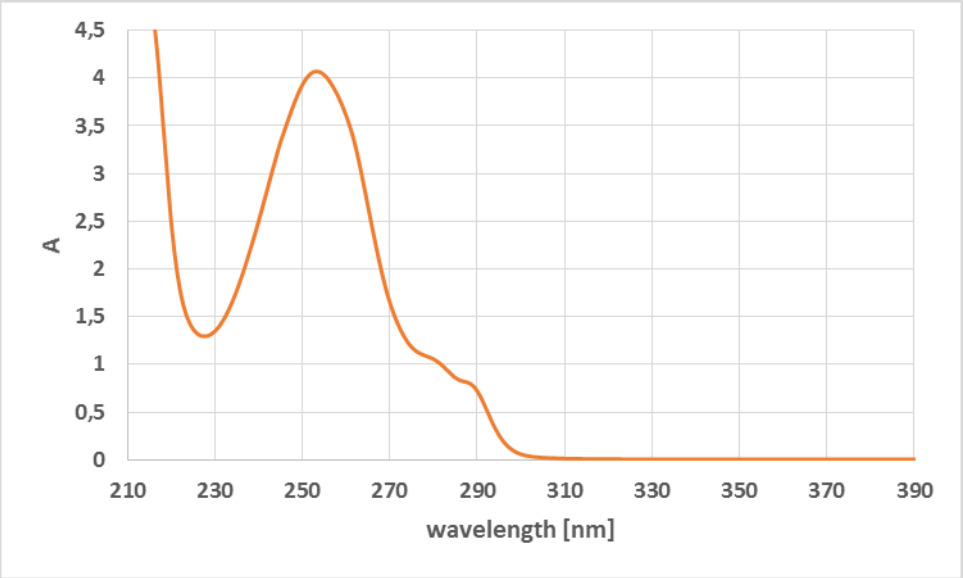

Table S5: Calculated rotational strengths of (−)-strychnine base (chloroform) and protonated (−)-strychnine (methanol) of the major conformer

Excitation frequency in nm	Rotational strength for strychnine base in cgs (10^{-40} erg esu cm/Gauss)	Excitation frequency in nm	Rotational strength for protonated strychnine in cgs (10^{-40} erg esu cm/Gauss)
260.17	-1.46	257.29	-7.36
256.24	-4.23	248.52	3.56
250.59	-28.25	243.07	15.93
247.84	7.76	234.84	-11.35
242.01	1.31	220.74	-12.76
235	-4.24	204.89	-5.7
225.58	-3	204.1	6.8
206.94	2.62	201.79	11.23
205.69	-4.26	200.18	-67.46
203.72	-17.2	198.47	-0.84
200.42	3	197.1	-5.4
199.92	-15.5	194.56	88.7
198.96	11.7	193.59	32.8

194.84	-6.2	190.27	-4.7
193.13	1.6	189.22	0.7
189.85	28.2	184.07	-16.8
188.55	-42.6	182.39	3.5
188.27	21.7	178.38	-10.2
185.43	29	175.24	-2.1
184.47	-2.4	173.45	-5.9
183.62	20.5	172.09	16.4
180.45	4.8	169.85	-16.6
178.55	-4.5	167.63	-32.2
175.21	-6.3	167.55	-37.4
174.15	-0.2	166.92	22.5
173.55	-25.8	165.2	-23.2
171.94	4.1	164.63	6.6
170.03	1.6	164.24	-28.5
169.68	-8	164.15	0.2
167.78	37.4	163.53	102.7

IR/VCD spectra

The calculated IR spectra for the major conformer of (−)-strychnine base and protonated (−)-strychnine are very similar (Figure S11), and only some of the bands in the VCD spectra are shifted (Figure S12). Concentrating on only few or only one band, in this case the amide stretch, there were no significant changes. In addition, the structural differences between the major and minor conformer do not change the IR and VCD spectra of (−)-strychnine base significantly (Figures S13 and S14) with some exceptions (e.g. the IR band at 1193 cm^{-1} of the major conformer shows a strong negative VCD band, whereas for the minor conformer almost no VCD band occurs in that region).

Figure S11: Calculated IR spectra of (−)-strychnine base (in orange) and protonated (−)-strychnine (in blue) of the major conformer (mpw1pw91/cc-pvdz, IEFPCM: chloroform and methanol, respectively)

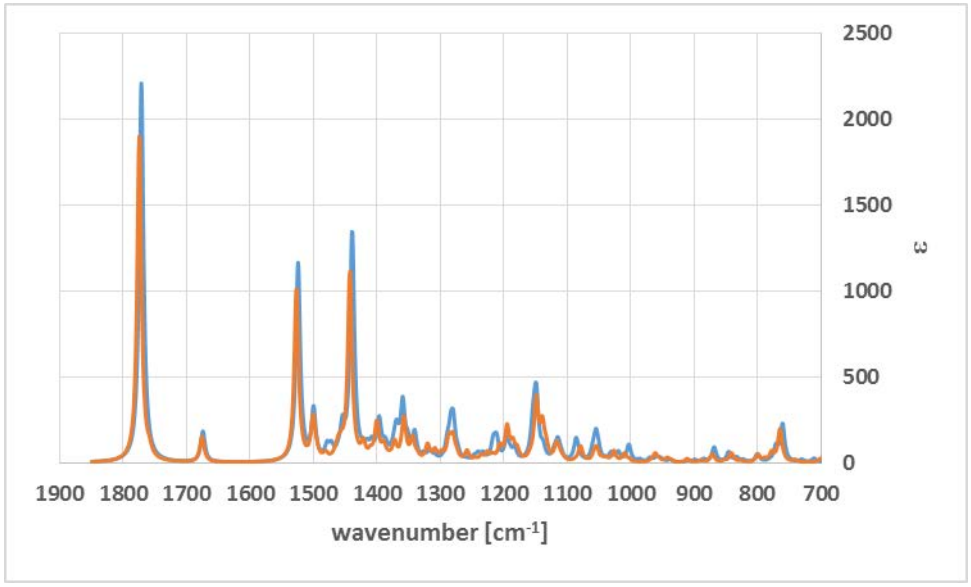

Figure S12: Calculated VCD spectra of (−)-strychnine base (in orange) and protonated (−)-strychnine (in blue) of the major conformer (mpw1pw91/cc-pvdz, IEFPCM: chloroform and methanol, respectively)

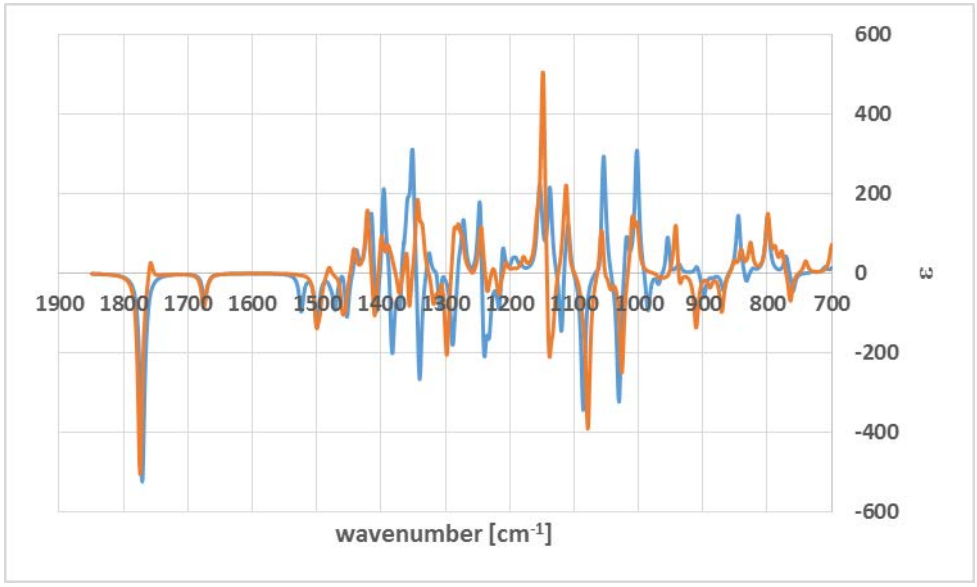

Figure S13: Calculated IR spectrum of (−)-strychnine base of the major (in blue) and minor conformer (in orange) (mpw1pw91/cc-pvdz, IEFPCM: chloroform)

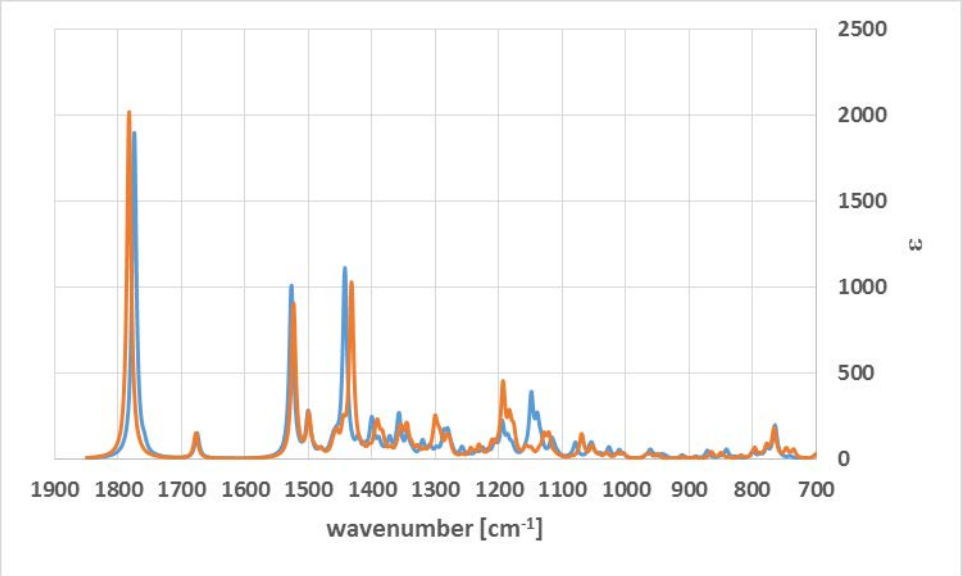

Figure S14: Calculated VCD spectrum of (−)-strychnine base of the major (in blue) and minor conformer (in orange) (mpw1pw91/cc-pvdz, IEFPCM: chloroform)

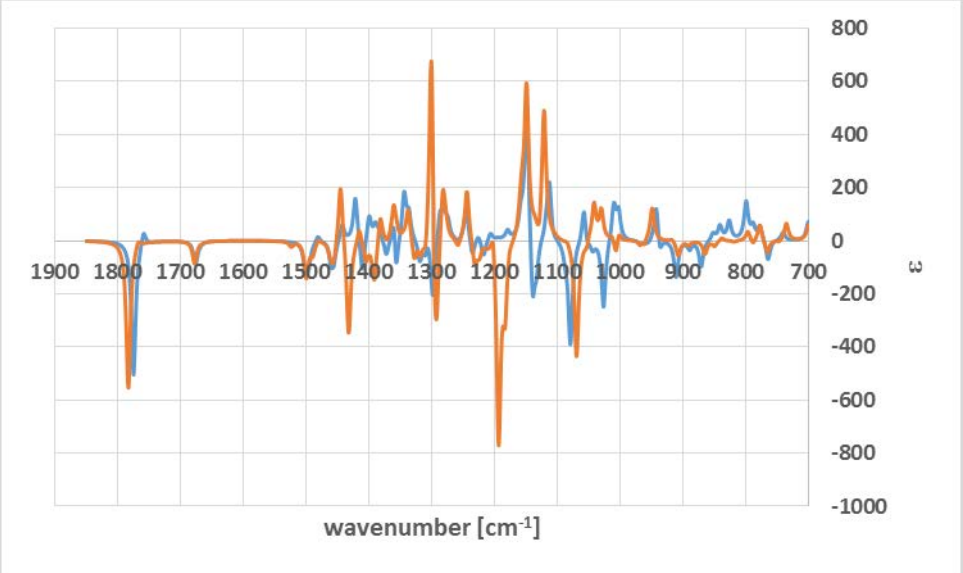

References

RC Barreto, K Coutinho, HC Georg, S Canuto, 2009, PhysChemChemPhys, 11, 1388-1396
V Ludwig, K Coutinho, S Canuto, 2007, PhysChemChemPhys, 9, 4907-4912

G09 files (.mol) of the nitrogen inverted major and minor conformers

Major Conformer of protonated (−)-strychnine (geometry optimized on the mpw1pw91/cc-pvdz (IEFPCM: methanol) level of theory, inverted nitrogen

```
Title Card Required

Created by GaussView 5.0.8
 48 54  0  0  0  0  0  0  0  0  0    0
    2.3583    0.4936    0.1492 C   0  0  0  0  0  0  0  0  0  0  0  0
    2.0618   -0.8634   -0.0372 C   0  0  0  0  0  0  0  0  0  0  0  0
    3.6345    0.9972   -0.0975 C   0  0  0  0  0  0  0  0  0  0  0  0
    3.0415   -1.7398   -0.4871 C   0  0  0  0  0  0  0  0  0  0  0  0
    4.6068    0.1049   -0.5542 C   0  0  0  0  0  0  0  0  0  0  0  0
    4.3207   -1.2464   -0.7541 C   0  0  0  0  0  0  0  0  0  0  0  0
    1.2095    1.1876    0.5750 N   0  0  0  0  0  0  0  0  0  0  0  0
    0.0433    0.3013    0.5010 C   0  0  0  0  0  0  0  0  0  0  0  0
    0.6492   -1.1441    0.3953 C   0  0  0  0  0  0  0  0  0  0  0  0
   -1.7128   -0.2271   -1.3992 C   0  0  0  0  0  0  0  0  0  0  0  0
   -0.2784   -1.9762   -0.4904 C   0  0  0  0  0  0  0  0  0  0  0  0
    1.0075    2.5486    0.4836 C   0  0  0  0  0  0  0  0  0  0  0  0
   -0.4494    2.9570    0.5671 C   0  0  0  0  0  0  0  0  0  0  0  0
   -0.7953    0.8040   -0.7029 C   0  0  0  0  0  0  0  0  0  0  0  0
   -1.4229    2.1499   -0.3149 C   0  0  0  0  0  0  0  0  0  0  0  0
   -2.9003   -0.7637   -0.5909 C   0  0  0  0  0  0  0  0  0  0  0  0
   -3.8476    0.0492   -0.1108 C   0  0  0  0  0  0  0  0  0  0  0  0
   -3.7520    1.5444   -0.2591 C   0  0  0  0  0  0  0  0  0  0  0  0
   -2.6175    2.0471    0.4414 O   0  0  0  0  0  0  0  0  0  0  0  0
   -2.7646   -2.1973   -0.1024 C   0  0  0  0  0  0  0  0  0  0  0  0
   -1.4034   -2.0901    0.5228 N   0  0  0  0  0  0  0  0  0  0  0  0
   -0.7435   -2.7985    1.6605 C   0  0  0  0  0  0  0  0  0  0  0  0
    0.5689   -1.9720    1.7322 C   0  0  0  0  0  0  0  0  0  0  0  0
    1.9227    3.3478    0.3711 O   0  0  0  0  0  0  0  0  0  0  0  0
   -0.5400    0.4170    1.4295 H   0  0  0  0  0  0  0  0  0  0  0  0
    2.8209   -2.7985   -0.6302 H   0  0  0  0  0  0  0  0  0  0  0  0
    5.0979   -1.9211   -1.1127 H   0  0  0  0  0  0  0  0  0  0  0  0
    5.6109    0.4787   -0.7580 H   0  0  0  0  0  0  0  0  0  0  0  0
    3.8484    2.0506    0.0562 H   0  0  0  0  0  0  0  0  0  0  0  0
   -0.7753    2.8065    1.6088 H   0  0  0  0  0  0  0  0  0  0  0  0
   -0.5055    4.0304    0.3618 H   0  0  0  0  0  0  0  0  0  0  0  0
   -1.6362    2.7051   -1.2448 H   0  0  0  0  0  0  0  0  0  0  0  0
   -4.6265    2.0285    0.1913 H   0  0  0  0  0  0  0  0  0  0  0  0
   -0.0508    1.0486   -1.4785 H   0  0  0  0  0  0  0  0  0  0  0  0
   -2.7505   -2.9787   -0.8692 H   0  0  0  0  0  0  0  0  0  0  0  0
   -3.5008   -2.4456    0.6677 H   0  0  0  0  0  0  0  0  0  0  0  0
    1.4348   -2.6395    1.8001 H   0  0  0  0  0  0  0  0  0  0  0  0
    0.5837   -1.3144    2.6100 H   0  0  0  0  0  0  0  0  0  0  0  0
   -0.5929   -3.8483    1.3925 H   0  0  0  0  0  0  0  0  0  0  0  0
   -1.3723   -2.7278    2.5526 H   0  0  0  0  0  0  0  0  0  0  0  0
   -3.7142    1.8450   -1.3211 H   0  0  0  0  0  0  0  0  0  0  0  0
   -4.6573   -0.3586    0.4987 H   0  0  0  0  0  0  0  0  0  0  0  0
   -2.1089    0.2546   -2.3059 H   0  0  0  0  0  0  0  0  0  0  0  0
    0.1105   -2.9916   -0.6383 H   0  0  0  0  0  0  0  0  0  0  0  0
   -0.7946   -1.3808   -1.7809 C   0  0  0  0  0  0  0  0  0  0  0  0
   -1.3130   -2.1432   -2.3751 H   0  0  0  0  0  0  0  0  0  0  0  0
    0.0573   -1.0359   -2.3813 H   0  0  0  0  0  0  0  0  0  0  0  0
   -1.4904   -1.1480    0.9184 H   0  0  0  0  0  0  0  0  0  0  0  0
  1  2  4  0  0  0  0
  1  3  4  0  0  0  0
```

```
 1  7  1  0  0  0  0
 2  4  4  0  0  0  0
 2  9  1  0  0  0  0
 3  5  4  0  0  0  0
 3 29  1  0  0  0  0
 4  6  4  0  0  0  0
 4 26  1  0  0  0  0
 5  6  4  0  0  0  0
 5 28  1  0  0  0  0
 6 27  1  0  0  0  0
 7  8  1  0  0  0  0
 7 12  4  0  0  0  0
 8  9  1  0  0  0  0
 8 14  1  0  0  0  0
 8 25  1  0  0  0  0
 9 11  1  0  0  0  0
 9 23  1  0  0  0  0
10 14  1  0  0  0  0
10 16  1  0  0  0  0
10 43  1  0  0  0  0
10 45  1  0  0  0  0
11 21  1  0  0  0  0
11 44  1  0  0  0  0
11 45  1  0  0  0  0
12 13  1  0  0  0  0
12 24  2  0  0  0  0
13 15  1  0  0  0  0
13 30  1  0  0  0  0
13 31  1  0  0  0  0
14 15  1  0  0  0  0
14 34  1  0  0  0  0
15 19  1  0  0  0  0
15 32  1  0  0  0  0
16 17  2  0  0  0  0
16 20  1  0  0  0  0
17 18  1  0  0  0  0
17 42  1  0  0  0  0
18 19  1  0  0  0  0
18 33  1  0  0  0  0
18 41  1  0  0  0  0
20 21  1  0  0  0  0
20 35  1  0  0  0  0
20 36  1  0  0  0  0
21 22  1  0  0  0  0
21 48  1  0  0  0  0
22 23  1  0  0  0  0
22 39  1  0  0  0  0
22 40  1  0  0  0  0
23 37  1  0  0  0  0
23 38  1  0  0  0  0
45 46  1  0  0  0  0
45 47  1  0  0  0  0
```

Minor Conformer of protonated (−)-strychnine (geometry optimized on the mpw1pw91/cc-pvdz (IEFPCM: methanol) level of theory, inverted nitrogen

```
Title Card Required

Created by GaussView 5.0.8
 48 54  0  0  0  0  0  0  0  0  0    0
    2.2952    0.5259    0.2053 C   0  0  0  0  0  0  0  0  0  0  0  0
    2.0504   -0.8254   -0.0889 C   0  0  0  0  0  0  0  0  0  0  0  0
    3.5522    1.0951    0.0165 C   0  0  0  0  0  0  0  0  0  0  0  0
    3.0688   -1.6256   -0.5908 C   0  0  0  0  0  0  0  0  0  0  0  0
    4.5630    0.2782   -0.4953 C   0  0  0  0  0  0  0  0  0  0  0  0
    4.3304   -1.0632   -0.8025 C   0  0  0  0  0  0  0  0  0  0  0  0
    1.1130    1.1457    0.6593 N   0  0  0  0  0  0  0  0  0  0  0  0
   -0.0071    0.2304    0.4505 C   0  0  0  0  0  0  0  0  0  0  0  0
    0.6502   -1.1884    0.3293 C   0  0  0  0  0  0  0  0  0  0  0  0
   -1.7270   -0.2895   -1.4278 C   0  0  0  0  0  0  0  0  0  0  0  0
   -0.2796   -2.0502   -0.5358 C   0  0  0  0  0  0  0  0  0  0  0  0
    0.8427    2.5004    0.6683 C   0  0  0  0  0  0  0  0  0  0  0  0
   -0.6445    2.8086    0.6092 C   0  0  0  0  0  0  0  0  0  0  0  0
   -0.7321    0.7150   -0.8255 C   0  0  0  0  0  0  0  0  0  0  0  0
   -1.2811    2.1464   -0.6310 C   0  0  0  0  0  0  0  0  0  0  0  0
   -2.8348   -0.7280   -0.4593 C   0  0  0  0  0  0  0  0  0  0  0  0
   -3.5690    0.1294    0.2629 C   0  0  0  0  0  0  0  0  0  0  0  0
   -3.5008    1.6255    0.2672 C   0  0  0  0  0  0  0  0  0  0  0  0
   -2.6925    2.2407   -0.7086 O   0  0  0  0  0  0  0  0  0  0  0  0
   -2.7706   -2.1919   -0.0341 C   0  0  0  0  0  0  0  0  0  0  0  0
   -1.3678   -2.1815    0.5198 N   0  0  0  0  0  0  0  0  0  0  0  0
   -0.6621   -2.8997    1.6233 C   0  0  0  0  0  0  0  0  0  0  0  0
    0.6296   -2.0350    1.6619 C   0  0  0  0  0  0  0  0  0  0  0  0
    1.7151    3.3512    0.6936 O   0  0  0  0  0  0  0  0  0  0  0  0
   -0.6661    0.2994    1.3309 H   0  0  0  0  0  0  0  0  0  0  0  0
    2.8909   -2.6779   -0.8160 H   0  0  0  0  0  0  0  0  0  0  0  0
    5.1368   -1.6779   -1.2019 H   0  0  0  0  0  0  0  0  0  0  0  0
    5.5541    0.7034   -0.6570 H   0  0  0  0  0  0  0  0  0  0  0  0
    3.7229    2.1411    0.2548 H   0  0  0  0  0  0  0  0  0  0  0  0
   -1.1162    2.4372    1.5322 H   0  0  0  0  0  0  0  0  0  0  0  0
   -0.7668    3.8959    0.5856 H   0  0  0  0  0  0  0  0  0  0  0  0
   -0.9712    2.7328   -1.5049 H   0  0  0  0  0  0  0  0  0  0  0  0
   -3.2190    1.9403    1.2910 H   0  0  0  0  0  0  0  0  0  0  0  0
    0.0726    0.8022   -1.5732 H   0  0  0  0  0  0  0  0  0  0  0  0
   -2.8512   -2.9421   -0.8257 H   0  0  0  0  0  0  0  0  0  0  0  0
   -3.4714   -2.4249    0.7731 H   0  0  0  0  0  0  0  0  0  0  0  0
    1.5168   -2.6766    1.6931 H   0  0  0  0  0  0  0  0  0  0  0  0
    0.6552   -1.3861    2.5463 H   0  0  0  0  0  0  0  0  0  0  0  0
   -0.4932   -3.9412    1.3352 H   0  0  0  0  0  0  0  0  0  0  0  0
   -1.2611   -2.8551    2.5376 H   0  0  0  0  0  0  0  0  0  0  0  0
   -4.5109    2.0321    0.1056 H   0  0  0  0  0  0  0  0  0  0  0  0
   -4.2744   -0.2735    0.9971 H   0  0  0  0  0  0  0  0  0  0  0  0
   -2.1785    0.1602   -2.3218 H   0  0  0  0  0  0  0  0  0  0  0  0
    0.1324   -3.0553   -0.6904 H   0  0  0  0  0  0  0  0  0  0  0  0
   -0.8711   -1.4917   -1.8110 C   0  0  0  0  0  0  0  0  0  0  0  0
   -1.4455   -2.2688   -2.3301 H   0  0  0  0  0  0  0  0  0  0  0  0
   -0.0581   -1.1996   -2.4878 H   0  0  0  0  0  0  0  0  0  0  0  0
   -1.4121   -1.2475    0.9377 H   0  0  0  0  0  0  0  0  0  0  0  0
  1  2  4  0  0  0  0
  1  3  4  0  0  0  0
  1  7  1  0  0  0  0
  2  4  4  0  0  0  0
  2  9  1  0  0  0  0
```

```
 3  5  4  0  0  0  0
 3 29  1  0  0  0  0
 4  6  4  0  0  0  0
 4 26  1  0  0  0  0
 5  6  4  0  0  0  0
 5 28  1  0  0  0  0
 6 27  1  0  0  0  0
 7  8  1  0  0  0  0
 7 12  4  0  0  0  0
 8  9  1  0  0  0  0
 8 14  1  0  0  0  0
 8 25  1  0  0  0  0
 9 11  1  0  0  0  0
 9 23  1  0  0  0  0
10 14  1  0  0  0  0
10 16  1  0  0  0  0
10 43  1  0  0  0  0
10 45  1  0  0  0  0
11 21  1  0  0  0  0
11 44  1  0  0  0  0
11 45  1  0  0  0  0
12 13  1  0  0  0  0
12 24  2  0  0  0  0
13 15  1  0  0  0  0
13 30  1  0  0  0  0
13 31  1  0  0  0  0
14 15  1  0  0  0  0
14 34  1  0  0  0  0
15 19  1  0  0  0  0
15 32  1  0  0  0  0
16 17  2  0  0  0  0
16 20  1  0  0  0  0
17 18  1  0  0  0  0
17 42  1  0  0  0  0
18 19  1  0  0  0  0
18 33  1  0  0  0  0
18 41  1  0  0  0  0
20 21  1  0  0  0  0
20 35  1  0  0  0  0
20 36  1  0  0  0  0
21 22  1  0  0  0  0
21 48  1  0  0  0  0
22 23  1  0  0  0  0
22 39  1  0  0  0  0
22 40  1  0  0  0  0
23 37  1  0  0  0  0
23 38  1  0  0  0  0
45 46  1  0  0  0  0
45 47  1  0  0  0  0
```

Supporting information

Stereochemical analysis of menthol and menthylamine isomers using calculated and experimental optical rotation data

F. Reinscheid[a], U.M. Reinscheid*[a]

Senda and Imaizumi (1975) and Bohlmann (1975) assigned the ^{13}C resonances of neoisomenthol incorrectly. Therefore, the correct data for the menthols from Lanfranchi et al. (2008) were used as experimental values.

Menthol

Table S1: Calculated shieldings [ppm] of the three OH rotamers (isopropyl group: *gauche*$^+$; mpw1pw91/cc-pvdz/IEFPCM: acetonitrile as solvent) and experimental chemical shifts [ppm] of the ^{13}C resonances of (+)-menthol in $CDCl_3$ (Lanfranchi et al., 2008)

Carbon number	Calc. OH *trans*	Calc. OH *gauche*$^+$	Calc. OH *gauche*$^-$	Calc. population-weighted	Exp. chemical shifts
1	161.56	162.12	162.48	162.01	31.66
2	149.41	152.56	149.29	150.15	45.06
3	125.63	125.54	126.11	125.77	71.51
4	142.57	143.24	145.09	143.59	50.13
5	171.34	172.19	171.91	171.74	23.12
6	160.22	160.14	160.22	160.20	34.56
7	172.31	172.29	172.39	172.33	22.23
8	167.82	167.43	167.98	167.78	25.8
9	179.83	180.46	180.06	180.06	16.07
10	173.54	172.42	173.64	173.30	21.03

(+)-(1*R*,3*S*,4*S*)-Neomenthol

For (+)-neomenthol, the conformational search delivered the OHax chair with a *trans* orientation of the isopropyl group as dominant conformer (Table S2). This is supported by the findings of Pekh et al. (1980) using low-temperature NMR and CD_2Cl_2 as solvent. We calculated the three OH rotamers of the dominant chair (OHax). Based on these conformers we calculated a $^3J_{OH}$ coupling constant of 3.2 Hz. Due to overlap, no experimental value is available. The predicted $^3J_{isopropyl}$ value for neomenthol is 6.6 Hz which poorly matches the experimental value of 9.2 Hz in $CDCl_3$ (Härtner and Reinscheid, 2008).

Table S2: Calculated parameters of the OH rotamers of the OHax chair of (+)-(1*R*,3*S*,4*S*)-neomenthol (mpw1pw91/cc-pvdz, IEFPCM: acetonitrile) with a *trans* orientation of the isopropyl group

	eq/ax/eq; *trans*/ g$^-$	eq/ax/eq; *trans*/ g$^+$	eq/ax/eq; *trans*/trans
H8-C8-C4-H4	+171.2	+175.1	+174.4
H-O-C3-H3	–62.4	+63.8	+175.4
$[\alpha]_{589}$	+21.98	-30.92	+15.80
$[\alpha]_{578}$	+22.95	-32.25	+16.47
$[\alpha]_{546}$	+26.16	-36.66	+18.67
rel. free energy (kcal/mole)	0	0.37	0.26
population (%)	45.9	24.7	29.4
$^3J_{OH}$ [Hz]	0.57	0.53	9.65
$^3J_{isopropyl}$ [Hz]	6.48	6.84	6.58
$[\alpha]_{589}$ (solvent: CS_2)	+25.91	-32.17	+16.09

In agreement, Albrecht et al. (2010) found by IR spectroscopy in the gas phase a chair conformation in which the OH group is axial in neomenthol. The OH dihedral was determined as g$^-$ for (+)-neomenthol which fits our calculations with the g$^-$ rotamer as highest in population. Likewise, the dominant isopropyl dihedral was determined as *trans* for (+) neomenthol by Albrecht et al. (2010). This fits our results for (+)-neomenthol in solution. The energy differences (electronic energy including harmonic zero point correction of the OH *gauche*$^-$ rotamer minus the OH *trans* rotamer) were determined as +0.29 kcal/mole and +0.36 kcal/mole at the B3LYP/6-311+G* and the MP2/6-311+G* level of theory, respectively. This does not fit our result at the mpw1pw91/cc-pvdz (IEFPCM: acetonitrile) level of theory: 0 kcal/mole – 0.26 kcal/mole = -0.26 kcal/mole with a dominant OH *gauche*$^-$ rotamer (Table S2). It is likely, that using the continuum model with acetonitrile is responsible for this different ordering of the conformer populations. No data for the OH *gauche*$^+$ conformer were presented by Albrecht et al. (2010).

In agreement with our results, Senda and Imaizumi (1975) predicted a chair with 100% OHax. Likewise, Jensen (1968) assumed 100% of the axial OH group for neomenthol based on the bandwidth measurements of the H3 resonance, presumably in CCl_4 as solvent.

Based on the populations of the three conformers (Table S2) derived from free energies, we predicted a $[\alpha]_{589}$ value of +7.1 which roughly fits the experimental value of +17.685 of neat compound (20.0 °C) (Paine III, 1997) (Table S3). The $[\alpha]_D$ value of a neomenthol sample changed from +19.57, to +19.62 and +19.72 when going from 4.5°C to 18°C and 29.5°C (Pickard and Littlebury, 1912). This might be due to the increase of the (+)-contributing OH rotamers, and/or a larger contribution of other conformers at higher temperature. However, the changes are too small to be used for a conformational analysis. From Table S2 it can be seen that using CS_2 as solvent in the ORD calculation (using population-weighted conformers with acetonitrile as solvent) only slightly changes the $[\alpha]_{589}$ value to 8.7. Both experimental and calculated ORD curves are monosignate (Table S3).

Table S3: Calculated (acetonitrile) and experimental (as neat compound, Paine III, 1997) ORD values of (+)-(1*R*,3S,4*S*)-neomenthol

wavelength [nm]	$[\alpha]_{exp}$	$[\alpha]_{calc}$
589	+17.685	+7.1
578	+18.474	+7.4
546	+20.698	+8.4

(–)-(1*S*,3*R*,4*S*)-Isomenthol

For (–)-isomenthol, the conformational search delivered two chair forms of similar energies with the OHeq chair dominant and the indicated isopropyl rotamers (Table S4). Likewise, Pekh et al. (1980) determined two chairs of isomenthol in CCl_4 as solvent (assuming that no differences in the chemical shifts of the individual conformers exist between the two solvents CCl_4 and CD_2Cl_2) with a ratio of 72.2:27.8 for OHeq:OHax. We calculated data for the three OH rotamers of the OHeq chair with a g^- dihedral of the isopropyl group, and of the OHax chair with a *trans* dihedral of the isopropyl group (Table S4). Similar to menthol, the calculated values differ to literature data obtained in vacuo (Table S5) (Egawa et al., 2003).

Table S4: Calculated OH rotamers of the OHeq (g^- of the isopropyl group) and OHax (*trans* of the isopropyl group) chairs of (–)-(1*R*,3*S*,4*S*)-isomenthol (mpw1pw91/cc-pvdz, IEFPCM: acetonitrile)

chair	ax/eq/eq			eq/ax/ax		
	g^-/g^-	g^-/g^+	g^-/ *trans*	*trans*/ *trans*	*trans*/ g^+	*trans*/ g^-
H8-C8-C4-H4	-64.7	-67.2	-70.2	-169.6	-168.2	-170.0
H-O-C3-H3	-49.5	+60.1	+178.6	177.6	+65.7	-66.3
$[\alpha]_{589}$	-4.64	-70.2	-53.6	-20.4	-18.9	+32.1
rel. free energy (kcal/mole)	0.58	0.22	0	1.04	0.83	0.93
popu-lations (%)	14.0	25.6	37.1	6.4	9.2	7.7
$^3J_{OH}$ [Hz]	2.21	0.9	9.77	9.56	0.32	0.29
$^3J_{isopropyl}$ [Hz]	1.84	1.75	1.49	7.39	7.34	7.13

Based on the calculated free energies of the six conformers the two chairs are in a ratio of 77:23 (OHeq:OHax) which fits very well to the experimental value for CCl_4 (Pekh et al., 1980).

Table S5: Literature data converted to (−)-isomenthol, isopropyl and OH dihedral indicated, energy differences in kcal/mole

chair ax/eq/eq isopropyl/OH dihedral	this report mpw1pw91/ cc-pvdz (IEFPCM: acetonitrile	RHF/6-31G*, in vacuo (Egawa et al., 2003)	B3LYP/6-31G*, in vacuo (Egawa et al., 2003)
g^-/g^-	0.58	-	-
g^-/g^+	0.22	0	0
g^-/*trans*	0.0	-	-
g^+/g^+	-	0.75	0.52
trans/g^+	-	2.4	
chair eq/ax/ax isopropyl/OH dihedral			
trans/*trans*	1.04	-	-
trans/g^+	0.83	0.53	0.41
trans/ g^-	0.93	-	-
g^-/g^+	-	3.36	-
g^+/g^+	-	3.61	-

Using the calculated populations from Table S3 we predicted a $[\alpha]_{589}$ value of –39.0 which fits roughly to the experimental value for the (+) enantiomer of isomenthol of $[\alpha]_{589}$= +25.9 (c=2.0305, 17°C, ethanol) (Paine III, 1997). The OHeq conformers contribute –38.4, and the OHax conformers –0.6. This means that the higher the OHeq:OHax ratio, the more negative the calculated optical rotation will be. Solvents stabilizing the OHeq chair will therefore give more negative (in case of the (–)-enantiomer), or more positive values (in case of the (+)-enantiomer).
Using the OHeq:OHax 72.2:27.8 ratio based on low-temperature NMR of ^{13}C resonances in CD_2Cl_2 compared to resonances in CCl_4 at room temperature (Pekh et al., 1980) as a factor with which the populations are corrected, a specific optical rotation of –36.5 was determined which fits slightly better to experiment. Experimental and calculated ORD curves are monosignate and allow a safe AC assignment of isomenthol (Table S6).

Table S6: Experimental ORD values of (+)-(1*R*,3*S*,4*R*)-isomenthol and calculated ORD values of (–)-(1*S*,3*R*,4*S*)-isomenthol (mpw1pw91/cc-pvdz, IEFPCM: acetonitrile)

wavelength [nm]	$[\alpha]_{exp}$ [a]	$[\alpha]_{exp}$ [b]	$[\alpha]_{calc}$
656	+20.1	+18.5	-31.0
589	+25.9	+22.6	-39.0
546	+30.7	+27.2	-45.9
486	+40.2	-	-59.1

[a]: ethanol (c=2.0305, 17°C); Read et al. (1933) [b]: CCl_4, c=4.064, 20°C, Hückel and Niggemeyer (1939)

In Table S7 the optical rotation of (+)-isomenthol in a large number of solvents taken from Hückel and Niggemeyer (1939) is presented. The data for acetic acid were neglected since at the very high concentration of 4% isomenthol (ca. 0.3 M) an acetylation reaction cannot be excluded. The ORD values at 546 nm increase from 22.78 (nitrobenzene) to 33.85 (diethylether), indicating a solvent dependence on the population mix and/or the ORD values of the individual conformers. The experimental ORD values differ less than 1.4 units between the two concentrations tested for benzene and ethanol (4% and 8%, w/V).
With the assumption that the chair ratio is the relevant factor, the increased optical rotation from nitrobenzene to diethylether is interpreted as increasing stabilization of OHeq and/or destabilization of OHax. It can be partly rationalized using the polarizability parameter SP of Catalán (2009). A regression was performed for the $[\alpha]_{546}$ values resulting in the following parameters: y = 46.567-24.166*SP, R^2=0.729, n=11. This wavelength was chosen because the optical rotation is larger for all solvents at this wavelength compared to longer wavelengths. The solvent dependent behaviour can easily be attributed to a shift of the chair ratio: with increasing polarizability, the OHax is more stabilized than the OHeq form. The polarizability parameter was derived from the mixed dipolarity/polarizability SPP parameter which also contained dipolar contributions, SdP (Catalán, 2009). Both are based on the solvatochromic behaviour of two compounds. Likewise, the solvent acidity (SA) describes the solvent H-bond donating acidity and the solvent basicity (SB) parameter the solvent H-bond accepting basicity determined by the solvent-induced shift of the UV/Vis absorption of two other test molecules with respect to a reference (Catalán et al., 1996).
At the high concentrations used for the optical rotation measurements it is clear that the menthol isomers are aggregated at least in apolar solvents. Therefore, the changing optical rotation could also be due to the solvent-dependent stability of these aggregates. Self-aggregation of cyclohexanol comes into play at concentration ≥ 10 mM in $CDCl_3$, and ≥ 1mM in CCl_4, protic solvents having the largest aggregate disintegrating capacity (Abraham et al., 1993).
For neoisomenthol H-bond donor solvents stabilize the OHeq chairs better than the OHax forms, and the increasing dipolarity stabilizes the neoisomenthol OHeq forms even more (vide infra). This behaviour can easily explained by the arguments put forward by Abraham et al. (1993, 1996). However, isomenthol obviously does not fit into this scheme which could be explained by the existence of dimers which were stabilized/destabilized by different solvents thereby changing the OHeq:OHax ratio. In fact, it is not clear which precise effect the solvents have for the conformers of isomenthol and the very difficult question of a molecular static and dynamic picture of polar, H-bonding compounds (Nagy, 2014) such as the menthol isomers in H-bonding solvents cannot be answered yet.

Table S7: $[\alpha]$ values of (+)-(1*R*,3*S*,4*R*)-isomenthol at 20°C in different solvents (Hückel and Niggemeyer, 1939), and polarizability parameter SP (Catalán, 2009)

solvent	concentration[a]	$[\alpha]_{656}$	$[\alpha]_{589}$	$[\alpha]_{546}$	SP	$[\alpha]_{546}$ by linear regression[b]
Nitrobenzene	4.016	+16.18	+19.67	+22.78	0.891	+25.04
Chlorobenzene	4.074	+17.18	+20.99	+24.54	0.833	+26.44
CS_2	4.048	+17.29	+21.12	+25.07	1	+22.40
anisole	4.094	+17.83	+21.71	+25.64	0.82	+26.75
CCl_4	4.064	+18.45	+22.63	+27.18	0.768	+28.01
benzene	4.084	+18.98	+23.73	+28.03	0.793	+27.40
benzene	8.076	+19.00	+23.77	+28.04	0.793	+27.40
1,4-dioxane	4.076	+20.24	+24.53	+28.58	0.683	+28.76
cylcohexane	4.044	+21.01	+25.22	+29.54	0.783	+30.06
chloroform	4.064	+20.92	+25.22	+29.52	0.633	+27.65
ethanol	4.056	+20.83	+26.38	+30.70	0.617	+31.27
ethanol	8.032	+20.85	+26.39	+30.75	0.617	+31.27
diethylether	4.032	+22.69	+28.52	+33.85	0.833	+31.66

[a]: g/100 ml; [b]: y=46.567-24.166*SP, R^2 = 0.729, n = 11

Based on the six conformers of Table S3 we calculated a $^3J_{OH}$ coupling constant of 4.8 Hz. This fits perfect to the experimental value of 4.9 Hz in DMSO (Kartha et al., 1976). The predicted $^3J_{isopropyl}$ value amounts to 3.0 Hz which poorly fits the experimental value of 5.5 obtained in $CDCl_3$ as solvent (Härtner and Reinscheid, 2008). So far, the reasons for this discrepancy are unclear.
Senda and Imaizumi (1975) predicted a population of 87 % for the equatorial position of the OH group. Likewise, Jensen (1968) assumed 69 % of OHeq for isomenthol based on the bandwidth measurements of the H3 resonance, presumably CCl_4 as solvent.
The OHeq chair of (+)-isomenthol was predicted to be slightly dominant in $CDCl_3$ (55 +/- 8: 45 +/- 8) (Feltkamp and Franklin, 1965; Firl et al., 1978). The estimate was based on empirical rules for the dependence of ^{13}C chemical shifts on the position of substituents. It is in contrast to the ratio of 90:10 which was based on proton resonances (Feltkamp et al., 1967).
Similarly, Egawa et al. (2003) using gas electron diffraction and computations concluded that (+)-isomenthol exists in a 68:32 mixture at 298 K of equatorial to axial position of the OH group. However, the range was 68% +30%/-40% indicating a very low precision. The isopropyl dihedral was determined as *gauche*$^+$ for the equatorial form and *trans* for the axial form which is similar to our results for (–)-isomenthol (OHeq: g^-, OHax: *trans*). Lomas (2014) calculated a 80:20 ratio of the OHeq:OHax chairs of (–)-isomenthol in $CDCl_3$. However, the assignment of the methyl protons turned out to be difficult since with all combinations the RMSD remained high (0.10 ppm) compared to 0.07 ppm for menthol.

Neoisomenthol

Table S8: Calculated shieldings [ppm] of four conformers, population mix of 30.8:36.2:18.2:14.8 (OHax,tg$^+$/OHax,tg$^-$/OHeq,tg$^+$/OHeq,tg$^-$) (mpw1pw91/cc-pvdz/IEFPCM: acetonitrile as solvent) and experimental chemical shifts [ppm] of the ^{13}C resonances of (–)-(1*S*,3*S*,4*S*)-neoisomenthol in $CDCl_3$ at room temperature (Lanfranchi et al., 2008) and in CD_2Cl_2 at 193 K (Pekh et al., 1975)

Carbon number	OHeq t/g+	OHeq t/g-	OHax t/g+	OHax t/g-	Population-weighted shieldings	Exp. chemical shifts (Lanfranchi et al.)	Exp. chemical shifts (Pekh et al.) OHax	Exp. chemical shifts (Pekh et al.) OHeq
1	161.73	162.05	166.2	166.25	164.79	28.33	26.5	32.0
2	158.12	154.5	157.91	154.9	156.35	39.02	38.6	37.8
3	120.73	121.18	128.15	128.39	125.85	70.77	66.2	73.4
4	147.64	150.76	145.59	146.38	147.01	47.43	48.2	44.7
5	166.59	166.23	174.12	173.64	171.41	22.01	19.2	27.7
6	166.03	165.54	162.21	162.23	163.41	30.97	32.2	29.1
7	172.37	172.42	174.08	174.22	173.57	21.49	20.4	24.5
8	168.73	168.66	164.17	163.31	165.35	27.5	28.3	24.5
9	171.22	170.53	173.87	173.94	172.92	21.85	21.5	22.7
10	173.32	173.68	175.3	175.04	174.61	21.49	20.8	22.2

Table S9A: Calculated ^{13}C shieldings [ppm] (mpw1pw91/cc-pvdz, IEFPCM: ethanol) of the OHeq chair of (–)-(1*S*,3*S*,4*S*)-neoisomenthol

shorthand Isopropyl dihedral	g+	g-	t	g+	g-	t	g+	g-	t
shorthand OH dihedral	g+	g+	g+	g-	g-	g-	t	t	t
C1	161.74	161.89	161.73	161.91	162.17	162.05	161.03	161.23	160.31
C2	156.39	156.85	158.12	153.24	153.31	154.5	153.6	153.66	155.37
C3	121.82	123.22	120.73	122.02	123.92	121.18	121.72	123.51	120.01
C4	150.85	150.05	147.64	153.09	152.33	150.76	151.87	150.99	148.67
C5	160.46	170.84	166.59	160.11	170.68	166.23	160.04	170.58	165.59
C6	164.04	163.33	166.03	164.08	163.19	165.54	164.02	162.99	165.68
C7	172.25	172.19	172.37	172.35	172.29	172.42	172.29	172.22	172.36
C8	156.91	168.8	168.73	156.89	169.32	168.66	157.29	168.34	167.21
C9	172.55	170.29	171.22	172.27	170.51	170.53	171.2	170.56	174.3
C10	166.75	172.86	173.32	167.34	172.91	173.68	167.58	173.16	171.26

Table S9B: Calculated ^{13}C shieldings [ppm] (mpw1pw91/cc-pvdz, IEFPCM: ethanol) of the OHax chair of (–)-(1*S*,3*S*,4*S*)-neoisomenthol

shorthand Isopropyl dihedral	g+	g-	t	g+	g-	t	g+	g-	t
shorthand OH dihedral	g+	g+	g+	g-	g-	g-	t	t	t
C1	165.39	165.49	166.2	165.52	165.54	166.25	166.22	166.4	166.88
C2	156.83	156.69	157.91	153.87	153.65	154.9	155.09	155.22	155.87
C3	127.84	120.74	128.15	127.69	121.14	128.39	127.56	120.81	128.12
C4	146.31	146.99	145.59	147.67	146.86	146.38	147.99	147.19	146.76
C5	171.76	178.3	174.12	172.26	178.76	173.64	173.64	180.02	175.26
C6	161.35	161.88	162.21	161.44	161.67	162.23	162.71	163.14	163.49
C7	173.3	174.28	174.08	173.85	173.75	174.22	173.22	173.18	173.6
C8	159.74	160.77	164.17	159.99	159.48	163.31	159.83	159.9	163.33
C9	173.49	176.08	173.87	173.84	176.74	173.94	173.85	176.98	174.2
C10	176.01	171.57	175.3	177	171.81	175.04	177.4	172.08	175.25

Table S9C: Calculated enthalpy differences among the conformers of the OHeq chair of (–)-(1*S*,3*S*,4*S*)-neoisomenthol

shorthand Isopropyl dihedral	g+	g-	t	g+	g-	t	g+	g-	t
shorthand OH dihedral	g+	g+	g+	g-	g-	g-	t	t	t
Enthalpy differences in KJ/mole	24.94	16.48	4.83	25.11	18.55	7.82	27.67	18.33	12.65

Table S9D: Calculated enthalpy differences among the conformers of the OHax chair of (–)-(1*S*,3*S*,4*S*)-neoisomenthol

shorthand Isopropyl dihedral	g+	g-	t	g+	g-	t	g+	g-	t
shorthand OH dihedral	g+	g+	g+	g-	g-	g-	t	t	t
Enthalpy differences in KJ/mole	14.02	11.42	3.36	8.41	6.70	0.00	14.25	13.36	6.51

(+)-(1*R*,3*S*,4*S*)-neomenthylamine base

The conformational search indicated that the NH_2ax chair with a *trans* and g^+ orientation of the isopropyl group is dominant. Likewise, Firl et al. (1978) estimated for (–)-neomenthylamine the *trans* rotamer of the isopropyl group as dominant conformer. The estimate was based on empirical rules for the dependence of ^{13}C chemical shifts on the position of substituents. The experimental data of Kulisch et al. (2011) (not assigned) follow the data of Firl et al. (1978) with differences of less than 1 ppm. Again, we calculated all three NH_2 rotamers of the dominant *trans* isopropyl rotamers (Table S10). Based on the populations using free energies, we predicted a $[\alpha]_{589}$ value of +25.1 which fits roughly to the experimental value of +8.7 (chloroform) (Read and Storey, 1930). ORD values are shown in Table S11. Kulisch et al. (2011) presented a slightly different experimental value of +11.6 at 589 nm (c=1.0, chloroform, 20 °C).

Table S10: Calculated parameters of the NH_2 rotamers of the NH_2ax chair with a *trans* and g^+ isopropyl dihedral of (+)-(1*R*,3*S*,4*S*)-neomenthylamine (mpw1pw91/cc-pvdz, IEFPCM: acetonitrile)

	trans/ g^-	*trans*/g^+	*trans/trans*
H8-C8-C4-H4	174.0	179.4	174.6
Hpro*R*-N-C3-H3	-58.3	57.9	178.7
$[\alpha]_{589}$	+14.87	-25.47	+65.76
$[\alpha]_{578}$	+15.48	-26.68	+68.65
$[\alpha]_{365}$	+42.88	-97.57	+217.94
rel. free energy (kcal/mole)	0.12	0.26	0
population (%)	33.2	26.1	40.7
$^3J_{isopropyl}$ [Hz]	6.82	6.79	6.62

Table S11: Calculated (mpw1pw91/cc-pvdz, IEFPCM: acetonitrile) and experimental ORD values of (+)-neomenthylamine

Wavelength in nm	$[\alpha]_{exp}$	$[\alpha]_{calc}$
589	+8.7[a]	+25.1
578	+11.7[b]	+26.1
365	+15[b]	+77.5

[a]: (+)-neomenthylamine, c=between 2 and 4, $CHCl_3$, Read and Storey (1930); [b]: Feltkamp et al., 1967

(–)-(1*S*,3*R*,4*S*)-isomenthylamine base

Based on the conformational search, two chairs were obtained: NH_2eq and NH_2ax. Since we expected that additional NH_2 rotamers are substantially populated we also calculated three rotamers for each dominant isopropyl rotamer (Table S12). A chair ratio of 88:12 was determined for NH_2eq:NH_2ax (Table S12).
Taking all 6 conformers into account and using populations based on free energies, the predicted $[\alpha]_{589}$ value is -33.2 for the (–) enantiomer which fits very well to the experimental value of +29.4 (c= 4, chloroform, 25 °C) for the (+) enantiomer (Table S13) (Read and Cuthbertson, 1950).
Two chair ratios with a different NH_2eq population were reported. Firl et al. (1978) estimated for (+)-isomenthylamine in $CDCl_3$ the NH_2eq as dominant chair (75 +/- 5: 25 +/- 5). The estimate was based on empirical rules for the dependence of ^{13}C chemical shifts on the position of substituents. A higher ratio (90:10) was reported based on proton resonances (Feltkamp et al., 1967). The predicted $^3J_{isopropyl}$ coupling constant amounts to 2.4 Hz.

Table S12: Calculated parameters of the NH_2 rotamers of the NH_2eq chair of (–)-(1*S*,3*R*,4*S*)-isomenthylamine (mpw1pw91/cc-pvdz, IEFPCM: acetonitrile) with a g^- and a *trans* isopropyl dihedral

	ax/eq/ax			eq/ax/ax		
	g^-/g^+	g^-/g^-	g^-/ *trans*	*trans*/ g^-	*trans*/ g^+	*trans*/ *trans*
H8-C8-C4-H4	–69.1	–60.6	–65.2	–167.3	–166.4	–169.2
H31proR-N-C3-H3	+62.2	–45.7	–172.8	–56.4	+63.2	–179.3
$[\alpha]_{589}$	–80.8	+27.5	–1.7	+35.5	–48.9	+35.9
rel. free energy (kcal/mole)	0	0.91	0.19	1.23	1.55	1.68
population (%)	45.4	9.8	32.9	5.8	3.4	2.7
$^3J_{isopropyl}$ [Hz]	1.6	2.3	1.9	7.1	7.3	7.1

Table S13: Calculated ORD values of (–)-(1*S*,3*R*,4*S*)-isomenthylamine (mpw1pw91/cc-pvdz, IEFPCM: acetonitrile) based on 6 conformers (Table 17 B) and experimental ORD values of (+)-isomenthylamine

Wavelength in nm	$[\alpha]_{exp}$	$[\alpha]_{calc}$
589	+29.6[a]	–33.2
578	+20.2[68]	–34.6
365	+34.0[68]	–97.3

[a]: (+)-isomenthylamine, c=between 2 and 4, $CHCl_3$, Read and Cuthbertson (1950)

(–)-(1*S*,3*S*,4*S*)-neoisomenthylamine base

Table S14 A: Calculated dihedrals and populations based on free energy differences weighted by the Boltzmann equation (mpw1pw91/cc-pvdz, IEFPCM: chloroform) and $[\alpha]_{589}$ values (mp1pw91/cc-pvdz, IEFPCM: chloroform) of the NH_2eq chair of (–)-(1*S*,3*S*,4*S*)-neoisomenthylamine

shorthand Isopropyl dihedral	g+	g-	t	g+	g-	t	g+	g-	t
shorthand NH_2 dihedral	g+	g+	g+	g-	g-	g-	t	t	t
isopropyl dihedral	80.9	-73.3	-151.4	82.6	-78.2	-161.4	82.7	-69.4	162.2
NH_2 dihedral	65.8	68.9	67.2	-60.1	-59.0	-57.6	-168.7	-165.9	-164.6
population [%]	0.07	4.00	7.77	0.19	2.76	19.47	0.09	1.82	1.44
$[\alpha]_{589}$	-80.88	-109.07	-106.82	1.58	-46.84	-25.48	13	0.34	-7.96

Table S14 B: Calculated dihedrals and populations based on free energy differences weighted by the Boltzmann equation (mpw1pw91/cc-pvdz, IEFPCM: chloroform) and $[\alpha]_{589}$ values (mp1pw91/cc-pvdz, IEFPCM: chloroform) of the NH_2ax chair of (–)-(1*S*,3*S*,4*S*)-neoisomenthylamine

shorthand Isopropyl dihedral	g+	g-	t	g+	g-	t	g+	g-	t
shorthand NH_2 dihedral	g+	g+	g+	g-	g-	g-	t	t	t
isopropyl dihedral	51.1	-83.6	179.6	48.8	-83.0	175.1	50.7	-79.2	174.5
NH_2 dihedral	49.0	54.5	52.4	-69.6	-69.9	-64.6	175.3	-178.1	175.1
population [%]	0.22	0.50	9.24	0.87	1.93	32.68	0.72	1.19	15.05
$[\alpha]_{589}$	47.76	24.91	17.31	62.87	21.17	23.19	132.57	67.16	114.01

Protonated (in experiment: HCl) (+)-menthylamine, (+)-neomenthylamine and (–)-isomenthylamine

Only for menthylamine HCl (Schopohl et al., 2003) and neomenthylamine HCl (Kulisch et al., 2011; one ^{13}C resonance is missing) experimental ^{13}C values are available in the literature. Like for menthol, the g^+ isopropyl dihedral dominates (Table S15). The calculated $[\alpha]$ values are adjusted to be comparable with experimental values obtained with the hydrochlorides (molecular weight differences). In Table S16 the calculated and experimental ORD values are listed.

Table S15: Calculated parameters of the conformers of (+)-(1*S*,3*S*,4*R*)-menthylamine protonated (ORD values adusted for HCl) (mpw1pw91/cc-pvdz, IEFPCM: acetonitrile) obtained by a conformational search and subsequent DFT optimization

compounds/ Isopropyl dihedral	(+)-menthyl-amine	(+)-neomenthyl-amine	(−)-isomenthyl-amine	(−)-isomenthyl-amine
	eq/eq/eq; g^+	eq/ax/eq; *trans*	ax/eq/eq; g^-	eq/ax/ax; *trans*
H8-C8-C4-H4	+64.2	-178.2	-66.5	-170.8
$[\alpha]_{589}$	+38.1	+28.4	-46.6	-8.6
$[\alpha]_{546}$	+44.9	+33.3	-54.9	-10.1
rel. free energy (kcal/mole)	-	-	0	0.7
population (%)	Set to 100	Set to 100	76.6	23.4
$^3J_{isopropyl}$ [Hz]	1.76	7.26	0.15	7.14

Table S16: Calculated, population weighted (protonated, IEFPCM: acetonitrile) and experimental (HCl) ORD values of (−)-menthylamine, (+)-neomenthylamine and (+)-isomenthylamine

	(+)-menthyl-amine	(−)-menthyl-amine	(+)-neo-menthyl-amine	(+)-neomenthyl-amine	(−)-isomenthyl-amine	(+)-isomenthyl-amine
λ in nm	$[\alpha]_{calc}$	$[\alpha]_{exp}$ [c]	$[\alpha]_{calc}$	$[\alpha]_{exp}$ [a]	$[\alpha]_{calc}$	$[\alpha]_{exp}$ [b]
589	+38.1	−38.1	+28.4	+18.7	−37.7	+23.5
578	+39.7	−39.6	-	-	-	-
546	+48.8	−44.9	-	-	−44.4	-
436	+73.4	−74.2	-	-	-	-
365	+110.2	−112.6	-	-	-	-

[a]: c=1.01, chloroform, 20 °C, Kulisch et al. (2011)
[b]: c=2, water, Read and Cuthbertson (1950)
[c]: c=0.99, methanol, 20 °C, Schopohl et al. (2003)

Table S17: Calculated ^{13}C shieldings [ppm] (mpw1pw91/cc-pvdz/IEFPCM: water as solvent) of protonated (+)-menthylamine and experimental chemical shifts [ppm] of (–)-menthylamine HCl in DMSO (Schopohl et al., 2003) (regression between calculated shieldings (NH_3^+eq/isopropyl g^+) and experimental chemical shifts: y=196.33 ppm – 1.071*chemical shifts [ppm], standard errors of intercept and slope: 1.73 ppm and 0.053 ppm, respectively, R^2 = 0.981, n=10)

Carbon number	NH_3^+eq Isopropyl g^+	Exp. chemical shifts
1	162.03	30.9
2	156.26	39.7
3	139.89	51.0
4	148.57	45.4
5	171.95	22.5
6	161.62	33.8
7	173.09	22.1
8	166.12	25.0
9	180.86	15.6
10	173.95	21.1

Table S18: Calculated ^{13}C shieldings (mpw1pw91/cc-pvdz/IEFPCM: water as solvent) of protonated (+)-neomenthylamine (NH_3^+ax), and experimental chemical shift of (+)-neomenthylamine in $CDCl_3$ (20 % solution) (Firl et al., 1978) (regression between calculated shieldings of the NH_3^+ax/isopropyl *trans* conformer and experimental chemical shifts: y=194.557 ppm – 0.9666*chemical shifts [ppm], standard errors of intercept and slope: 3.2 ppm and 0.096 ppm, respectively, R^2 = 0.927, n=10)

Carbon number	NH_3^+ax Isopropyl *trans*	Exp. chemical shifts
1	167.78	25.7
2	158.08	43.3
3	142.49	47.4
4	149.83	48.2
5	171.33	24.0
6	161.33	35.5
7	173.1	22.6
8	164.73	29.3
9	175.4	20.7
10	174.03	21.4

Table S19: Calculated ^{13}C shieldings (mpw1pw91/cc-pvdz/IEFPCM: water as solvent) of protonated (–)-isomenthylamine and experimental chemical shifts (Firl et al., 1978) (regression between calculated shieldings (population-weighted) and experimental chemical shifts: y=194.42 ppm – 0.966*experimental chemical shifts [ppm], standard errors of intercept and slope: 2.9 ppm and 0.09 ppm, respectively, R^2 = 0.935, n=10)

Carbon number	NH_3^+eq Isopropyl g-	NH_3^+ax Isopropyl *trans*	Calculated shieldings with a 76.6:23.7 ratio based on calc. free energies	Exp. Chemical shifts (20 % solution in $CDCl_3$)
1	165.21	166.89	165.60	27.6
2	158.03	162.9	159.17	41.5
3	143.19	141.54	142.80	47.0
4	147.58	151.17	148.42	50.8
5	176.92	172.61	175.91	19.0
6	164.33	166.84	164.92	31.2
7	177.79	172.82	176.63	19.7
8	165.98	166.58	166.12	26.4
9	180.43	174.08	178.94	17.2
10	174	174.9	174.21	21.4

Table S19a: Calculated ^{13}C shieldings [ppm] (mpw1pw91/cc-pvdz/IEFPCM: water as solvent) of the two dominating conformers of protonated (–)-neoisomenthylamine; calculated shieldings [ppm] and chemical shifts [ppm] (based on the regression of protonated menthylamine /menthylamine HCl) using a population mix adjusted to a sum of 100 % (experimental chemical shifts are not available)

Carbon number	NH_3^+eq Isopropyl *trans*	NH_3^+ax Isopropyl *trans*	Calculated shieldings with a **57.2/42.8** ratio based on calc. free energies (adjusted to a sum of 100 %)	Calculated chemical shifts based on calculated shieldings and the regression for protonated menthylamine
1	160.39	168.16	163.72	30.45
2	161.94	160.85	161.47	32.54
3	135.08	141.88	137.99	54.47
4	152.79	149.41	151.34	42.00
5	165.31	176.28	170.01	24.58
6	167.01	164.58	165.97	28.34
7	173.11	174.45	173.68	21.14
8	167.55	164.61	166.29	28.04
9	175.25	175.79	175.48	19.46
10	172.14	173.95	172.91	21.86

ORD

Literature ORD values of the menthol isomers

Paine III (1997, Philipp Morris confidential) measured optical rotations at 20.0°C, with bath temperature variations of less than 0.2°C (Table S20). The accuracy of the polarimeter was determined as +/- 0.001°. The principal sources of error were expected to come from the sample preparation (temperature dependent volumes, accuracy of volumetric equipment). Starting material was menthol measured in toluene (c=10.315) as: +46.09, +48.24, and +54.39 at 589, 578, and 546 nm, respectively.

Table S20: Optical rotation data from Paine III (1997)

compound	589 nm	578 nm	546 nm	samples
(+)-(1*S*,3*S*,4*R*)-menthol	+48.13	+50.39	+56.81	toluene, c=10.05
(+)-(1*R*,3*S*,4*S*)-neomenthol	+17.685	+18.474	+20.698	neat
(+)-(1*R*,3*S*,4*R*)-isomenthol	+24.2	+25.32	+28.48	Not indicated (probably neat)
(+)-(1*R*,3*R*,4*R*)-neoisomenthol[a]	+0.406	+0.425	+0.473	Neat, 99.3% pure by GC[a]
(+)-(1*R*,3*R*,4*R*)-neoisomenthol[a]	+0.137	+0.140	+0.148	Neat, 99.6% pure by GC[a]

[a]: two different preparations

Yoshida et al. (1965) measured the following values for $[\alpha]_{589}$: menthol: -50.0, c=10, ethanol; neomenthol: +16.8, homogenous; isomenthol: +27.1, c=10, ethanol), indicating that for these three isomers the solvent influence on the $[\alpha]_{589}$ values is small. Likewise, only a small concentration dependence on optical rotation was found for the menthol isomers (Hückel and Niggemeyer, 1939). For neoisomenthol the literature values are: $[\alpha]_{656}$ = +1.7, $[\alpha]_{589}$ = +2.2 and $[\alpha]_{546}$ = +2.3 (16°C, c=2, ethanol) and for the neat compound: $[\alpha]_{656}$ = +0.07, $[\alpha]_{589}$ = +0.14 and $[\alpha]_{546}$ = +0.15 at 16°C by Read and Grubb (1934) (Table S21). For isomenthol Read et al. (1933) presented an optical rotation of +40.2 at 486 nm (ethanol, c=2.0305, 17°C).
Unfortunately, some studies contain insufficient information about the measurement conditions (solvent, temperature, concentration). This has severe consequences in the case of compounds such as neoisomenthol with an intrinsically small specific optical rotation (< 5). Even conformationally rigid compounds such as menthol, show differences of up to almost 2 units dependent on the solvent.
Nevertheless, from these data some conclusions can be drawn: 1) A comparison between Ueda and Mitsui (1954) (Table S22) and Read and Grubb (1934) (Table S21) showed that the change of solvents for isomenthol from hexane to ethanol did not alter the measured value much (difference of 1.1); 2) a slightly lower value was found for neomenthol as homogenous sample, compared to ethanol as solvent (difference of 2.9); 3) The value for homogenous neoisomenthol was higher compared to the value of Read and Grubb (1934), but is still very small (1.04).
Yamana (1961) presented $[\alpha]_D$ literature values for menthol, neomenthol, and isomenthol at 20°C (-49.6, +19.6, -25.2) with menthol and isomenthol in chloroform, and for neomenthol no solvent was indicated. In the Tables S23 and S24, additional literature values are presented.

Table S21: Specific optical rotation presented by Read and Grubb (1934)

compound	$[\alpha]_{589}$	Solvent, temperature, concentration
menthol	-49.6	ethanol, 16°C, c=2
neomenthol	+20.7	ethanol, 16°C, c=2
isomenthol	+25.9	ethanol, 15°C, c=1,8
neoisomenthol	+2.2	ethanol, 16°C, c=2
neoisomenthol	+0.14	homogenous

Table S22: Specific optical rotation presented by Ueda and Mitsui (1954)

compound	$[\alpha]_D$	Solvent and temperature
menthol	-48.3	ethanol, temp. not indicated
neomenthol	+17.8	homogenous, 10°C
isomenthol	+27	n-hexane, 15°C
neoisomenthol	+1.04	homogenous, 15°C

Table S23: Specific optical rotation presented Bombicz et al. (1999), [a]: Oritani and Yamashita, (1973)

compound	$[\alpha]_D$	solvent	$[\alpha]_D$ of the antipode	solvent
menthol	48.3	ethanol	-50	chloroform
neomenthol	18	not indicated	-20.7	ethanol
isomenthol	25.9	chloroform	nd	
neoisomenthol	-3.8[a]	ethanol (99% purity of the analyte by GC)	nd	

nd: not determined

Table S24: Optical rotation data from Haut (1985)

compound	$[\alpha]_{589}$ at 20°C, c=2, ethanol	$[\alpha]_{546}$ at 20°C, c=2, ethanol	$[\alpha]_D$ (Weast (1979)	$[\alpha]_D$ (Dict. Organic chemicals (1982)
menthol	-50.1	-52.3	-49.2 (20°C, c=2.5, ethanol)	-50.0 (20°C, c=2, $CHCl_3$)
neomenthol	+20.1	+20.9	+19.6 (20°C, ethanol)	+18.02 (10°C, neat)
isomenthol	+25.3	+26.2	+25.5 (20°C, c=4, ethanol)	+25.9 (20°C, c=1.56, $CHCl_3$)
neoisomenthol	+1.77	+1.85	+2.2 (15°C, c=2, ethanol)	+3.8 (18°C, c=6, $CHCl_3$)

Literature ORD values of the menthylamine isomers

The data from Read and Storey (1930), and Read and Grubb (1934) and Read and Cuthbertson (1950) were taken for the menthylamine isomers as base and hydrochlorides (Table S25).

Table S25: Specific optical rotation at 589 nm for menthylamine isomers as bases (homogenous or in chloroform, c=from 2 to 4) and hydrochlorides (in water, concentration c=2) and at 546 nm for the menthylamine isomers as bases

compound	[d] $[\alpha]_{589}$	compound	[a] homo-genous $[\alpha]_{589}$	[b] $CHCl_3$ $[\alpha]_{589}$	[b] homo-genous $[\alpha]_{546}$	[b] $CHCl_3$ $[\alpha]_{546}$
Menthyl-amine HCl	−36.5	Menthylamine	-44.53	-38.0	-53.21	-45.3
Neomenthyl-amine HCl	+21.4	Neomenthyl-amine	+15.12	+8.7	+17.42	+10.0
Isomenthyl-amine HCl	+23.5	Isomenthyl-amine	+28.96	+29.6	+34.06	+34.6
Neoiso-menthyl-amine HCl	+20.9[c]	Neoiso-menthyl-amine	+2.32	+11.0	+2.66	+12.4

[a]: Read and Grubb (1934); [b]: Read and Storey (1930); [c]: $[\alpha]_D$ = +18.9 at 15°C, c=1.78 in water (McNiven and Read, 1952); [d]: Read and Cuthbertson (1950)

McNiven and Read (1952) presented optical rotation data for menthylamine salts in water which differ slightly: the hydrobromide (c=1.88) gave -26.9 units and the hydrochloride (c=2.74): - 32.4 units. Both values were measured at 11°C. Since both concentrations are similarly high, we attribute the difference to an anion effect. This difference for a salt in a polar (water) solvent amounts to 5.5.

Tutin and Kipping (1904) presented optical rotation data for menthylamine HCl in water and chloroform, respectively: -36.6 and -45.4 (concentrations in both solvents: 500 mg in 20 ml). The temperature was not indicated. The difference of 8.6 can be taken as a measure for solvent effects on dissolved salts.

Galisteo et al. (1994) presented literature values (Table S26) of optical rotation data for the series of menthylamine isomers as bases that are based on the data from Read and Storey (1930) and Pickard and Littlebury (1912) from above.

Schopohl et al. (2003) presented optical rotation data for menthylamine as base and hydrochloride (menthylamine as base, 20°C, c=1.39, $CHCl_3$: $[\alpha]_{589}$ = -35.7, $[\alpha]_{578}$ = -37.1, $[\alpha]_{546}$ = -41.9, $[\alpha]_{436}$ = -67.6, $[\alpha]_{365}$ = -98.9; menthylamine HCl, 20°C, c=0.99, methanol: $[\alpha]_{589}$ = -38.1, $[\alpha]_{578}$ = -39.6, $[\alpha]_{546}$ = -44.9, $[\alpha]_{436}$ = -74.2, $[\alpha]_{365}$ = -112.6). The data remain essentially the same (Welschoff and Waldvogel, 2010) at slightly different concentrations of menthylamine $[\alpha]_{589}$ = -36.1 (20°C, c=0.5, $CHCl_3$). Kulisch et al. (2011) recently added further information about neomenthylamine as base (c=1.0, $CHCl_3$: $[\alpha]_{589}$ at 20°C = +11.6) and hydrochloride (c=1.01, $CHCl_3$: $[\alpha]_{589}$ at 20°C = +18.7). De Vekki reported a $[\alpha]_{589}$ value of -27.1 at 20°C (c=0.15, ethanol) for (-)-menthylamine HCl which might be due to a lower enantiomeric excess compared to the data from Schopohl et al. (2003).

Interestingly, a recent publication (Zhou et al., 2011) reported a different value for menthylamine: $[\alpha]_{589}$ at 25°C: +5.4 (c=0.6, $CHCl_3$) and cited a value of 6.5 from literature (Jumaryatno et al., 2007). In our opinion, these values are wrong. The reasons for it are discussed in the main text.

In a study by Feltkamp et al. (1967) ORD values for the menthylamine isomers as bases are presented, however without indicating solvent, temperature, and concentration (Table S27). Since no AC assignment was conducted it is unclear which enantiomer was taken as neoisomenthylamine. The other three isomers can be reliably assigned (vide infra). Importantly, values at 366 nm were measured that indicate a monosignate curve for all menthylamine isomers. However, the value for neoisomenthylamine at 578 nm seems to be too large so that impurities might be present. Since no quantitative information about the purity of the samples was given, this possibility cannot be ruled out and we prefer to use the values of Table S25.

Table S26: Specific optical rotation and molar optical rotation values of the menthylamine isomers (Galisteo et al., 1994), based on literature values

compound	methyl	NH_2	isoprop	$[M]_D$	$[\alpha]_D$
(+)-Menthylamine	*S*	*S*	*R*	+69	+44.1
(-)-Neomenthyl-amine	*S*	*R*	*R*	-23	-14.7
(+)-Isomenthyl-amine	*R*	*S*	*R*	+45	+28.8
(+)-Neoisomenthyl-amine	*R*	*R*	*R*	+3.6	+2.3

Table S27: Optical rotation values for the menthylamine isomers at 578 nm and 366 nm (Feltkamp et al., 1967)

compound	$[\alpha]_{578}$	$[\alpha]_{366}$
(-)-menthylamine	-29.5	-86.2
(+)-neomenthylamine	+11.7	+15.0
(+)-isomenthylamine	+20.2	+34.0
(+)-neoisomenthylamine	+15.4	+24.1

References

M Albrecht, J Will, MA Suhm, Angew. Chem. Int. Ed. 2010, 49, 6203-6206
F Bohlmann, R Zeisberg, E Klein, 1975, Org. Magn. Reson., 7, 426-432
P Bombicz, J Buschmann, P Luger, N Xuan Dung, C Ba Nam, 1999, Z. Kristallogr., 214, 420-423
J Catalán, C Diaz, V López, P Perez, GLG. de Paz, JG Rodriguez, Liebigs Ann. 1996, 1785-1794
J Catalán, J. Phys. Chem. B 2009, 113, 5951-5960
DA de Vekki, VM Uvarov, AN Reznikov, NK Skvortsov, 2008, Russ. Chem. Bull., Int. Ed., 57, 349-357
Dictionary of Organic chemicals, Chapman and Hall, New York, 1982, Vol. 5, p. 3442
T Egawa, M Sakamoto, H Takeuchi, S Konaka, J. Phys. Chem. A 2003, 107, 2757-2762
H Feltkamp, NC Franklin, Angew. Chem. 1965, 77, 798-807
H Feltkamp, F Koch, TN Thanh, 1967, Liebigs Ann. Chem., 707, 78-86
H Feltkamp, NC Franklin, F Koch, TN Thanh, Liebigs Ann. Chem. 1967, 707, 87-94
J Firl, G Kresze, T Bosch, V Arndt, 1978, Liebigs Ann. Chem., 87-97
D Galisteo, ME González-Vadillo, JA López Sastre, MH Martinez Garcia, JF Rodriguez Amo, 1994, J. Mol. Struct., 326, 239-247
J Härtner, UM Reinscheid, J. Mol. Struct. 2008, 872, 145-149
SA Haut, 1985, J. Agric. Food Chem., 33, 278-280
W Hückel, H Niggemeyer, 1939, Ber. Dtsch. Chem. Ges., 72, 1354-1358
RB Jensen, Act. Chem. Scand. 1968, 22, 1271-1278
P Jumaryatno, K Rands-Trevor, JT Blanchfield, MJ Garson, 2007, Arkivoc, 157-166
G Kartha, KT Go, AK Bose, MS Tibbetts, J. Chem. Soc. Perkin II 1976, 717-723
J Kulisch, M Nieger, F Stecker, A Fischer, SR Waldvogel, 2011, Angew. Chem. Int. Ed., 24, 5564-5567
DA Lanfranchi, M-C Blanc, M Vellutini, P Bradesi, J Casanova, F Tomi, 2008, Magn. Reson. Chem., 46, 1188-1194
JS. Lomas, Magn. Reson. Chem. 2014, 52, 745-754
NL McNiven, J Read, 1952, J. Chem. Soc., 153-158
PI Nagy, Int. J. Mol. Sci. 2014, 15, 19562-19633
T Oritani, K Yamashita, 1973, Agr. Biol. Chem., 37, 1695-1700
JB Paine III, 1997, Philipp Morris USA confidential, research center, Doc code P0622
TI Pehk, ET Lippmaa, V I Lysenko, II Bardyshev, Russ. J. Org. Chem. 1980, 1694-1703
RH Pickard, WO Littlebury, 1912, J. Chem. Soc., 101, 109-127
J Read, RA Storey, 1930, J. Chem. Soc., 2761-2769
J Read, WJ Grubb, D Malcolm, 1933, 170-173
J Read, WJ Grubb, 1934, J. Chem. Soc, 313-317
J Read, WW Cuthbertson, 1950**,** Rec. Chim. Pays-Bas**,** 69, 539-544
MC Schopohl, K Bergander, O Kataeva, R Fröhlich, SR Waldvogel, 2003, Synthesis, 17, 2689-2694
Y Senda, S Imaizumi, 1975, Tetrahedron, 31, 2905-2908
F Tutin, FS Kipping, 1904, J. Chem. Soc., 85, 65-78
H Ueda, T Mitsui, 1954, J. Agric. Chem. Soc. Japan, 12, 945-950
RC Weast, 1979, Ed., "Chemical Rubber Handbook, 60th edition, CRC Press, Boca Raton, FL
N Welschoff, SR Waldvogel, 2010, Synthesis-Stuttgart, 21, 3596-3601
S Yamana, 1961, Bull. Chem. Soc. Japan, 34, 1414-1418
T Yoshida, A Komatsu, M Indo, 1965, Agr. Biol. Chem., 29, 824-831
Y Zhou, J Dong, F Zhang, Y Gong, 2011, J. Org. Chem., 76, 588-600